Investigation of the Expression Pattern and Functional Importance of the *Gnasxl*-encoded XLαs protein of the Imprinted *Gnas* Locus

Thesis submitted in accordance with the requirements of the University of Liverpool for the degree of Doctor of Philosophy

By

Katie Louise Burton

May 2012

ABSTRACT

XLαs is a NH_2-terminal splice variant of the stimulatory G-protein α-subunit G_sα. Both are encoded by the imprinted *Gnas* locus. Similar to G_sα, XLαs can couple 7-TM receptors to adenylate cyclase in cultured cells. Previously, a knock-out mouse specific for the *Gnasxl* transcript was generated (*Gnasxl*$^{m+/p-}$) (PLAGGE *et al.* 2004). This mouse model exhibits a lean, hypermetabolic phenotype with elevated sympathetic nervous system (SNS) activity (XIE *et al.* 2006). Changes in phenotype between neonatal and adult stages (e.g. mortality; failure to thrive as neonates vs. healthy but hypermetabolic adults) are not yet fully understood. More recently a conditional gene trap knock-out mouse line (*XLlacZGT*) was established. Immunohistochemistry, XGal and immunofluorescence data were collected to document the changes in expression pattern of XLαs and determine possible signalling pathways affected by lack of XLαs in the brain; histological analysis of the *lacZ*-containing genetrap line revealed new sites of XLαs expression.

A comparison of neonatal and adult brain expression patterns revealed that the lateral hypothalamus (LH), dorsomedial hypothalamus (DMH), arcuate nucleus (Arc), locus coeruleus and ventrolateral medulla express XLαs in both stages; the laterodorsal tegmental nucleus, hypoglossal and facial nucleus (motor nuclei important for feeding) express XLαs only in neonates; and expression in the amygdala and preoptic area are only found in adult brain.

Colocalisation studies in the brain for XLαs, neuropeptides and other markers related to regulation of food intake and energy expenditure. Orexin partly colocalised with XLαs in the LH and DMH (22% orexin neurons XLαs positive); tyrosine hydroxylase/dopaminergic neurons colocalised with XLαs in the Arc (60% TH neurons XLαs positive); and phosphorylated S6, a component of the leptin signalling pathway, colocalised with XLαs in the Arc (30% XLαs neurons pS6 positive). MCH and CRF did not colocalise with XLαs. Changes in pS6/S6K1 and the indicators of ghrelin signalling in knock-out Arc neurons did not reach statistical significance.

Analysis of the *lacZ*-genetrap line at neonatal stages revealed that XLαs is also expressed in spinal cord and peripheral tissues e.g. skeletal muscle, tongue muscle and blood vessel smooth muscle cells. Expression in muscle tissues, including blood vessel smooth muscle cells is silenced in adults, but the spinal cord remains positive for XLαs.

XLαs expression pattern changes in the brain and peripheral tissues concur with changes in phenotype seen between neonatal and adult mice. pS6 is a good indicator of S6K1 activity, which influences leptin and insulin signalling. A decrease of S6K1 activity in *Gnasxl*$^{m+/p-}$ mice might explain their leptin sensitivity (Frontera *et al.* in prep). XLαs colocalises with orexigenic peptides – including orexin and NPY/AgRP neurons (Frontera *et al.* in prep) – in the hypothalamus; however, the function of XLαs in energy expenditure and SNS activity remains elusive.

ACKNOWLEDGEMENTS

Firstly I would like to thank my supervisor Dr Antonius Plagge, without whom this project would not have been possible. I would also like to thank Nic Nunn and Stefan Krechowec for their help carrying out experiments in this project. I would also like to thank Anna Newlaczyl who completed an MRes project alongside my PhD project and carried out experiments which assisted in this project. I would like to thank Bettina Wilm and John Quayle for antibodies against blood vessel markers used in fluorescence experiments.

Mum and Dad, thank you for always supporting me in my decision to carry on in further education and always encouraging me to do my best in whatever I choose. My little sister Kristy thanks for always making me laugh and being there when I need a chat. Karl, thank you for being there when I am feeling low and disheartened, thank you for listening to my problems and for helping me to pick myself up and carry on.

I would also like to thank the Medical Research Council for supporting the project financially.

LIST OF FIGURES

LIST OF TABLES

ABBREVIATIONS

α-MSH	alpha melanocyte-stimulating hormone
α-SMA	alpha smooth muscle actin
βGal	beta galactosidase
3V	third ventricle
5-HT	serotonin
7N	facial nucleus
12N	hypoglossal nucleus
A5	noradrenergic cell group
A7	noradrenergic cell group in the pons
A12	dopaminergic neurons of the arcuate nucleus of the hypothalamus
A13	dopaminergic neurons of the zona incerta
A14	dopaminergic neurons of the periventricular nucleus
A20	*Gnasxl* second exon
ABC	avidin biotin complex
AC	adenylyl cyclase
aca	anterior commisure
ACC	acetyl-coenzymeA carboxylase
ACTH	adrenocorticotrophic hormone
ADP	anterodorsal preoptic nucleus
AF	alexa fluorophore
Ag	agonist
AgRP	agouti-related protein
AHO	Albright's hereditary osteodystrophy
Amb	ambiguus nucleus
Amp	ampicillin
AMPK	adenosine monophosphate-activated protein kinase
Amy	amygdala
Akt	serine/threonine protein kinase
APS	ammonium persulphate
Arc	arcuate nucleus of the hypothalamus
AS	Angelman syndrome

ATP	adenosine -5'-triphosphate
BAT	brown adipose tissue
BCA	bicinchoninic acid
BCIP	5-bromo-4-chloro-3-indolyl phosphate
BLAST	basic local alignment search
BMI	body mass index
bp	base pair
BSA	bovine serum albumin
BST	bed nucleus of the stria terminalis
BSTMA	bed nucleus of the stria terminalis medial anterior part
BSTVA	bed nucleus of the stria terminalis ventral anterior part
BWS	Beckwith-Wiedemann syndrome
cAMP	cyclic adenosine monophosphate
CART	cocaine- and amphetamine-regulated transcript
CeA	central nucleus of the amygdala
cDNA	complimentary deoxyribonucleic acid
CHAPS	3-[(3-cholamidopropyl) dimethylammonio]-1-propane-sulfonate
ChAT	choline acetyltransferase
CMV	cytomegalovirus
CNS	central nervous system
Cre	Cre recombinase
CRH	corticotropin releasing hormone
CRHR1	corticotropin releasing hormone receptor 1
CRHR2	corticotropin releasing hormone receptor 2
CSF	cerebrospinal fluid
DAPI	4', 6'-diamino-2-phenylindole
dATP	deoxyadenosine triphosphate
DBH	dopamine beta hydroxylase
dCTP	dioxycytidine triphosphate
ddH_2O	double distilled water
DEPC	diethyl pyrocarbonate
dGTP	deoxyguanine triphosphate
DIG	digoxigenin

DMH	dorsomedial hypothalamus
Dmnt	DNA methyltransferase
DMR	differentially methylated region
DMSO	dimethylsulfoxide
DNA	deoxyribonucleic acid
dNTP	dioxyribonucleotide triphosphate
DTT	dithiothreitol
dTTP	deoxythymidine triphosphate
dUTP	deoxyuradine triphosphate
E	embryonic day
ECL	enhanced chemiluminescence
E. coli.	Escherichia coli
EDTA	ethylene diamine tetraacetic acid
EGTA	ethylene glycol tetraacetic acid
ESC	embryonic stem cell
EtBr	ethidium bromide
EtOH	ethanol
FAA	food anticipatory activity
FANTOM	functional annotation of mouse clones
Floxed	loxP-flanked
Flpe	flippase recombination enzyme
Frt	flippase recognition target
GABA	gamma-aminobutyric acid
Gad67	glutamate decarboxylase; molecular weight 67 kDa
GAP	GTPase activating protein
GAPDH	Glyceraldehyde 3-phosphate dehydrogenase
GHSR	growth hormone secretagogue receptor
Gi	gigantocellular reticular nucleus of the medulla oblongata
GPCR	G-protein coupled receptor
$G_s\alpha$	stimulatory G-protein alpha subunit
HRP	horse radish peroxidase
ICR	imprinting control region
i.c.v.	intracerebroventricular

IF	immunofluorescence
IHC	immunohistochemistry
IML	intermediolateral
InsR	insulin receptor
i.p.	intraperitoneal
ISH	*in situ* hybridiastation
IRS	insulin receptor substrate
Jak2	Janus kinase 2
kDa	kilo Dalton
kbp	kilo base pair
KO	knock-out
lacZ	lacZ structural gene encoding βgalactosidase in E.Coli
LB	Luria-Bertani
LC	locus coeruleus
LDTg	laterodorsal tegmental nucleus
LepR	leptin receptor
LH	lateral hypothalamus
LHA	lateral hypothalamic area
LoxP	locus of chromosomal crossover (x) in the bacteriophage P1
LSV	lateral septal nucleus
mA	milli-amperes
MC3R	melanocortin-3 receptor
MC4R	melanocortin-4 receptor
MCH	melanin concentrating hormone
MCH1R	melanin concentrating hormone receptor 1
ME	median eminence
MeOH	methanol
MnPO	medial preoptic nucleus
Mo5	motor trigeminal nucleus
mRNA	messenger ribonucleic acid
MRt	medullary reticular area
mTOR	mammalian target of rapamycin
mTORC1	mammalian target of rapamycin complex 1

NA	noradrenaline
NBT	nitroblue tetrazolium
NCBI	National Center for Biotechnology Information
NDS	normal donkey serum
Nesp	neuroendocrine secretory protein
NGS	normal goat serum
NP-40	nonidet P40
NPY	neuropeptide Y
NRS	normal rabbit serum
NTS	nucleus of the solitary tract
ob	obese gene
OD	optical density
Oed-Sml	oedematous-small
ORF	open reading frame
OX_1R	orexin receptor 1
OX_2R	orexin receptor 2
pACC	phosphorylated acetyl-coenzymeA carboxylase
pAMPK	phosphorylated adenosine monophosphate-activated protein kinase
PB	phosphate buffer
PBS	phosphate-buffered saline
PCR	polymerase chain reaction
PDK1	phosphoinositide dependent protein kinase-1
PFA	paraformaldehyde
PGCs	primordial germ cells
PH	pleckstrin homology
PHP-Ia	pseudohypoparathyroidism – type 1
PHP-Ib	pseudohypoparathyroidism – type 2
PI3K	phosphatidylinositol 3-kinase
PIP_3	phosphatidylinositol (3,4,5)-triphosphate
PK	proteinase K
PMSF	phenylmethylsulfonyl fluoride
PNS	parasympathetic nervous system

POA	preoptic area
polyA	polyadenylated
POMC	proopiomelanocortin
pS6	phosphorylated ribosomal protein S6
PTg	anterior pons peduncle
PTH	parathyroid hormone
PVDF	polyvinylidene fluoride
PVN	paraventricular nucleus of the hypothalamus
PWS	Prader-Willi syndrome
qPCR	quantitative reverse transcriptase polymerase chain reaction
R	G-protein-coupled t-transmembrane receptor
Rheb	Ras homolog enriched in brain
RIPA	radio-immunoprecipitation assay
RPa	raphe pallidus
RNA	ribonucleic acid
ROb	raphe obscurus
RT	reverse transcriptase
RT-PCR	reverse transcriptase-polymerase chain reaction
S6	ribosomal protein S6
S6K1	ribosomal p70-S6 kinase 1
SA	splice acceptor
SCN	suprachiasmatic nucleus
SDS	sodium dodecyl sulphate
SDS-PAGE	sodium dodecyl sulphate polyacrylamide gel electrophoresis
SEM	standard error of the mean
SH2B	a SH2 and PH domain containing adaptor protein
SNS	sympathetic nervous system
SOC	super optimal broth with catabolite repression
SPN	sympathetic preganglionic neuron
SSC	sodium chloride-sodium citrate
SubC	subcoeruleus
TAE	tris-acetate-EDTA
TBS	tris-buffered saline

TE	tris-EDTA buffer
TEMED	N,N,N',N'-Tetramethylethylenediamine
TENS	Tris, EDTA, NaOH, SDS
TH	tyrosine hydroxylase
TOPO	topoisomerase
TPBS	tween phosphate-buffered saline
Tris	tris(hydroxymethyl)aminomethane
TTBS	tween tris-buffered saline
TSC1/2	tuberous sclerosis protein1/2
UCP1	uncoupling protein 1
UV	ultraviolet
V	voltage
v/v	volume by volume
vGAT	vesicular GABA transporter
VMH	ventromedial hypothalamus
VMN	ventral motor neurons
VP	ventral pallidum
vWF	von Willebrand Factor
w/v	weight by volume
WAT	white adipose tissue
WT	wild type
XGal	5-bromo-4-chloro-3-indolyl b-D-galactopyranoside
XLαs	alternative extra-large stimulatory G-protein alpha subunit
XL-βGal	XLα*s*-Beta galactosidase fusion protein
XLlacZGT	conditional knock-out mouse line containing lacZ fused to *Gnas* exon2 splice acceptor site
XLN1	truncated XLαs protein containing N1 exon
ZI	zona incerta

CHAPTER 1. INTRODUCTION

1.1. GENOMIC IMPRINTING

1.1.1. WHAT IS GENOMIC IMPRINTING?

Offspring inherit two copies of an allele, one from each parent, for any given gene. However, it has been established that the parental genomes do not always contribute equally to gene expression. Genomic imprinting is an epigenetic phenomenon that is defined as the parent-of-origin-specific silencing of an allele. It is the result of a complex interaction of mechanisms, which create control regions within a gene locus for the implementation of genomic imprinting (in specific ways for specific genes). This phenomenon has only been observed in eutherian/placental mammals, marsupials and plants.

There are approximately 100 known imprinted genes in humans and mice (some conserved, others not) although there is now evidence to suggest there are many more than this that have yet to be described fully (GREGG *et al.* 2010). These are located in imprinting regions throughout the genome, many in clusters (for example the *Gnas* locus*),* but others are single imprinted genes isolated from any other imprinted gene (Figure 1.1). Imprinted genes have a variety of functions (some examples are outlined in Table 1.1). A comprehensive database of known imprinted genes in mice has been compiled (WILLIAMSON *et al.* 2011). Many methods have been used to try and identify genomically imprinted genes within the mouse and human genomes, including genome-wide analyses and surveys as well as transcriptome sequencing (BABAK *et al.* 2008). There are a wide variety of imprinting effects that can occur if these imprinted genes are expressed incorrectly, these include behavioural abnormalities, growth defects and lethality (PETERS and BEECHEY 2004).

Figure 1.1. Imprinted genes in the Mouse Genome from Mouse Book

From the MRC Harwell Mousebook (WILLIAMSON *et al.* 2011)

A schematic of the mouse chromosomes that have imprinted genes, showing the maternally expressed genes (red), the paternally expressed genes (blue), the maternally expressed small nucleolar RNAs and microRNA gene (red dot) and paternally expressed nucleolar RNAs (blue dot).

Yellow blocks indicate regions of abnormal imprinting phenotypes with maternal duplication or paternal duplication.

Function	Imprinted genes
Transporters	*Slc22a2*, *Slc22a3*, *Slc38a4*, *Copg2*, *Tssc5*, *Obph1*
Ubiquitin- related pathways	*Ube3*, *Usp29*
Cell cycle control	*Zac1(Plagl1)*, *Cdkn1c*
Transcription	*Zim1*, *Mash2*
G-Protein-coupled receptor signalling	*Gnas*, *Calcr*, *Htr2a*
Intracellular signalling cascades	*Asb4*, *Rasgrf1*, *Grb10*, *Gnas*
Creatine synthesis	*Gatm*
Pre- and post-natal growth and development development	*Ins1*, *Ins2*, *Igf 2*, *Igf 2r*, *Rasgrf1*, *Grb10*, *Gnas*

Table 1.1. Some examples of imprinted genes and their functions (PETERS and BEECHEY 2004)

1.1.2. THE EVOLUTION OF GENOMIC IMPRINTING

Imprinting makes genes more vulnerable to mutation. If a mutation occurs on the allele which is not silenced then the effects of the mutation will appear immediately, as there is no possibility of a compensatory effect from the parental allele which is silenced. There are several possible routes of evolution for genomic imprinting. One is the parental-conflict hypothesis (WILKINS and HAIG 2003). This theory for the evolution of genomic imprinting is based upon the idea that the paternal and maternal genomes each want different things for their potential offspring. The father's genome wants to promote resource acquisition from the mother in embryonic/neonatal offspring carrying his alleles, while the maternal allele wants to limit the acquisition of a particular offspring so that the resources available to her can be distributed equally to all of her offspring (CHARALAMBOUS *et al.* 2007; CONSTANCIA *et al.* 2004). In some cases genes that are maternally imprinted promote the acquisition of resources (i.e. paternally expressed transcripts such as the *Gnasxl* transcript). When these paternally expressed genes are disrupted they tend to result in adult phenotypes of hypermetabolism and leanness (XIE *et al.* 2006). The opposite can also be true, maternal disruption of the paternally-imprinted genes can result in opposite phenotypes, producing offspring that are obese or overgrown (e.g. *Grb10*) in adulthood with reduced energy expenditure (CHEN *et al.* 2005; SMITH *et al.* 2007). However, not all imprinted genes fit this theory for example, there are maternally expressed genes that have a positive influence on nutrient acquisition while some imprinted genes do not affect postnatal growth.

Transposable elements are segments of DNA which are mobile and use the cellular machinery to replicate (ZAMUDIO and BOURC'HIS 2010).

Approximately half of the genomes of mice and humans are made up of transposable elements. It is necessary to control these transposable elements at a transcriptional level in order for the mammalian genome to tolerate their presence. DNA methylation, a mechanism that controls gene expression, might have originally evolved at the promoters of transposable elements to silence their transcription (YODER *et al.* 1997). If these transposable elements were inserted within or close to the promoters of genes they might have been affected by the silencing of the transposable element. It might then have been an advantage to maintain the silencing of the gene in order to control the expression level of that gene.

Recent research has shown genomic imprinting in mice has a complex pattern (WOLF *et al.* 2008). The imprinting is not just on the maternal or paternal allele but can also manifest as partial imprinting, where the expression level of the gene is reduced on one allele but not completely removed. Genomic imprinting can also be tissue-specific with some genes expressing biallelically in some tissues while only expressing from a single allele in another tissue, for example *Gnas* (WILKINS and HAIG 2003). There is also evidence to suggest that many more genomically imprinted genes have yet to be discovered (WOLF *et al.* 2008).

1.1.3. EPIGENETIC CONTROL OF GENOMIC IMPRINTING

There are several epigenetic modifications that can control genomic imprinting, such as DNA methylation, histone modification and siRNAs. DNA methylation in mammals is targeted to CpG dinucleotides. The group of enzymes called DNA methyltransferases (Dnmts) are responsible for the transfer of a methyl group onto the DNA. These enzymes are essential for

viability and fertility. There are several types of Dnmt: Dnmt1 is the most abundant in mammalian cells and is responsible for the maintenance of methylation after DNA replication. It has been found that homozygous deletion of Dmnt1 in mice results in embryonic lethality (LI *et al.* 1992). Dnmt3a and Dnmt3b work in conjunction to establish methylation patterns by *de novo* methylation. Knock-outs of these Dnmts result in male sterility and embryonic lethality.

Dnmt3-like (Dnmt3L) cannot mediate methylation on its own, but is a co-factor of Dnmt3a and is involved in de novo methylation. Dnmt3L is essential for maternal methylation establishment. Loss of Dnmt3L results in male sterility and biallelic expression of genes which are normally silenced on the maternal allele (ZAMUDIO and BOURC'HIS 2010).

Imprinted genes contain differentially methylated regions of DNA (DMRs). These areas have DNA methylation, which differs between the maternal and paternal allele and results in silencing of the methylated allele. Methylation is erased in the embryo then re-established in early development in the appropriate way for the sex of the offspring – this would be maintained throughout life (CONSTANCIA *et al.* 1998).

DNA methylation occurs by the addition of a methyl group to the 5 position on a cytosine residue. It is particularly prevalent in areas of DNA with a high cytosine guanine percentage (CpG islands). This is known as CpG methylation.

Methylation can prevent the expression of a transcript, as in the *Gnas* locus, where areas of methylation silence the maternal or paternal allele (depending on the location of the methylation). The maternal allele is

methylated on the *Gnasxl* promoter, while *Gnas* imprinting is not caused by a DMR, but is possibly due to transcription of *Gnas* exon 1A blocking the transcription through the *Gnas* exon. It has been shown that disruption of *Gnas* exon 1A results in biallelic expression of $G_s\alpha$ in all tissues (Figure 1.2) (WILLIAMSON *et al.* 2004; WILLIAMSON *et al.* 2006).

In pre-implantation embryos the parental methylation is almost completely erased in the somatic cells of the embryo, imprinted genes maintain their methylation (REIK 2007; REIK and WALTER 2001). The paternal genome is actively demethylated, while the maternal genome passively loses methylation. The passive loss of methylation occurs when Dnmt1 is excluded from the nucleus of the cell and so cannot maintain the methylation pattern on new strands of DNA created during replication (MERTINEIT *et al.* 1998).

The imprint marks are erased in the primordial germ cells (PGCs) of the offspring and then re-established in the correct pattern for the sex of that offspring (ROSSANT 1993). The de-methylation of both male and female PGCs is completed by embryonic day (E) 14. Re-methylation begins at E16 in the male PGCs (BRANDEIS *et al.* 1993; KAFRI *et al.* 1992). For oocytes, their arrested development at E13.5 halts re-methylation, which is not restarted until after birth, during oocyte growth periods and when there is a high level of Dmnt available (MERTINEIT *et al.* 1998).

Imprinted genes have, within their gene locus, control areas for the correct imprinting of a gene. Imprinting control regions (ICR) are areas along the locus which are important for correct DNA methylation. *Nesp* deletion in the *Gnas* locus results in a disruption of the ICR (CHOTALIA *et al.* 2009). There are also differentially methylated regions (DMRs) located on the loci. The *Gnas* locus

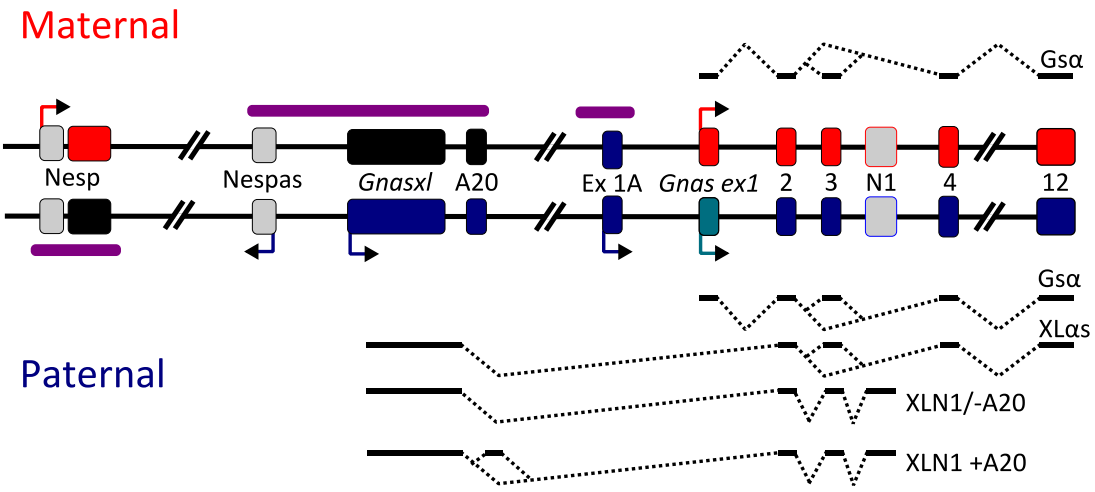

Figure 1.2. Schematic of the complex *Gnas* locus

The *Gnas* locus is a complex imprinted locus on mouse chromosome 2. There are five main transcripts expressed from this locus (2 non-coding and 3 coding). From the main *Gnas* transcript the G-protein alpha subunit, $G_s\alpha$, is produced. This protein is expressed biallelically in most tissues but is imprinted in some tissues, being expressed only from the maternal allele. The second transcript is derived from the *Gnasxl* exon 1, expression from this transcript is only from the paternal allele and can result in two proteins. The main protein is XLαs; this is an extra-large version of $G_s\alpha$. This protein is identical to $G_s\alpha$ apart from the extra large first exon, splicing onto exons 2 through 12. The second protein expressed from this transcript is XLN1. This is a truncated form of XLαs, This protein splices onto exons 2, 3 then N1 which results in the truncation due to a stop codon in the N1 exon. It has been indicated that splicing can occur onto exon A20. The imprinting of the gene locus is controlled by imprinting control regions (indicated in purple). There are three imprinting control regions on the *Gnas* locus, two on the maternal allele across the *Gnasxl* promoter and a second across exon 1A. The third is expressed from the paternal allele across the Nesp exons. The DNA methylation in these regions prevents expression from the allele.

Adapted from (PLAGGE *et al.* 2004)

has several DMRs. These are located at specific positions on the locus to achieve silencing of the appropriate allele (e.g. the *Nespas* DMR on the maternal allele; *Gnas exon 1A* on the maternal allele (Figure 1.2)).Methylation is essential for correct imprinting of genes but the way in which these imprinting methylation marks are established is not fully understood. There have been several suggestions for when the DMRs are established in offspring. The first is that the marks are erased in the offspring and re-established in accordance with the sex of the embryo (CONSTANCIA *et al.* 1998).

DNA methylation is one of the mechanisms by which imprinting occurs, and these methylation marks can be used to identify imprinted genes. DMRs occur at specific sites on the genome and prevent transcription (PETERS and BEECHEY 2004) (Figure 1.2). There is evidence to show that transcription through the DMRs is essential for germ line methylation marks to be established (CHOTALIA *et al.* 2009). Another mechanism, known to have a role in the establishment of the imprinting marks of genes, is known as histone modification. This is likely to have an instructive role in the establishment of imprints (FERGUSON-SMITH 2011).

1.1.4. FUNCTIONS OF IMPRINTED GENES.

Many imprinted genes have been associated with embryonic development but more recent research has determined that some imprinted genes have a function in postnatal development (CHARALAMBOUS *et al.* 2007; CONSTANCIA *et al.* 2004; CURLEY *et al.* 2005; FRONTERA *et al.* 2008; GARFIELD *et al.* 2011; KOZLOV *et al.* 2007; WILKINSON *et al.* 2007).

Many of these imprinted genes continue to be expressed in adulthood – not only in the central nervous system (CNS) but also in peripheral tissues

associated with metabolism (CHARALAMBOUS *et al.* 2007; FRONTERA *et al.* 2008; WILKINSON *et al.* 2007).

Dysfunctions of these imprinted genes can have serious implications resulting in abnormal development and usually severe phenotypes – many associated with embryonic lethality. There have been some disorders associated with imprinted genes in both mice and humans. Some of these include Beckwith-Wiedemann syndrome, Prader-Willi syndrome/Angelman syndrome and transient neonatal diabetes.

1.1.5. DISORDERS INVOLVING IMPRINTED GENES

Many human disorders occur as a result of genetic defects in imprinted genes. These include Beckwith-Wiedemann Syndrome (BWS), Prader-Willi syndrome (PWS), Angelman Syndrome (AS), and Albright's Hereditary Osteodystrophy (AHO).

PWS and AS are two rare genetic disorders associated with disruption of imprinted genes on human chromosome 15, in a 2 MB imprinted domain (LEDBETTER *et al.* 1981). Two of the imprinted genes in this cluster are magel2 and Necdin. PWS, associated with mutations in SNRPN, is defined by a phenotype of hypotonia, hypogonadism, hyperphagia (resulting in obesity), short stature and behavioural problems (psychosis, lying, stealing and aggressive behaviour) (CASSIDY *et al.* 1997). Neonates also exhibit difficulty feeding, defined as a failure to thrive in infancy (ROBERTSON 2005). PWS is commonly the result of a deletion of the SNRPN/SNURF first exon and promoter (ROBERTSON 2005). AS has a phenotype of mental retardation, speech impairment as well as behavioural abnormalities and is the result of the loss of maternally expressed UBE3A which is imprinted in the brain (ROBERTSON 2005).

Transient neonatal diabetes is associated with imprinted genes (*PLAGL1/ZAC1* and *HYMAI*). These are located on human chromosome 6 (ROBERTSON 2005).

BWS is associated with disruption of human chromosome 11. It is known to affect growth. It has a phenotype of placental and embryonic overgrowth, macroglossia, examphalos, and a predisposition to childhood tumours. *IGF2* and *CDKN1C* are the two imprinted genes associated with BWS, with the two main causes being uniparental disomy and point mutations. Over-expressing *IGF2* is associated with overgrowth while the deficiency of *CDKN1C* is more likely to cause abdominal wall defects (WALTER and PAULSEN 2003).

Neurological defects associated with imprinting disorders include those seen in AS (NICHOLLS 2000).

Imprinting also has a role to play in early development of the embryo as well as other functions such as placental development (GEORGIADES *et al.* 2001). It has been suggested that genomic imprinting has a role to play in the social behaviour of mice in the bonding of the mother with her offspring, as well as influencing adult social interactions (ISLES *et al.* 2006).

1.2. THE COMPLEX IMPRINTED *GNAS* LOCUS

1.2.1. TRANSCRIPTS OF THE *GNAS* LOCUS

The imprinted *Gnas* locus, located on mouse distal chromosome two, encodes five distinct transcripts: *Gnas, Gnasxl, Gnas1A, Nespas* and Nesp. These encode several proteins (Figure 1.2). The locus is highly conserved between the mouse and human genome, thus it is possible to study human disorders in *GNAS* with mouse models and several mouse models have been established to study the locus.

The *Gnas* transcript of the *Gnas* locus codes for the stimulatory alpha-subunit ($G_s\alpha$) of the G-protein signalling complex. It is associated with the βγ subunit and can stimulate adenylyl cyclase (AC) to produce the second messenger cAMP (Figure 1.3). This transcript is biallelically expressed in most tissues (HAYWARD *et al.* 1998a; HAYWARD *et al.* 1998b). However, in some tissues (for example the renal proximal tubules, anterior pituitary, ovary, thyroid gland, and paraventricular nucleus of the hypothalamus) it is imprinted and expressed solely from the maternal allele (Figure 1.2) (CHEN *et al.* 2010; GERMAIN-LEE *et al.* 2002; GERMAIN-LEE *et al.* 2005; HAYWARD *et al.* 2001; MANTOVANI *et al.* 2002). In adipose tissues there is evidence for transient imprinting of $G_s\alpha$ (CHEN *et al.* 2010; CHOTALIA *et al.* 2009; WILLIAMSON *et al.* 2004). Homologous knock-out of $G_s\alpha$ is always embryonically lethal (CHEN *et al.* 2005; GERMAIN-LEE *et al.* 2005; YU *et al.* 1998). This is indicative of the importance of $G_s\alpha$ in development. XLαs, the protein derived from the *Gnasxl* exon, like other α-subunits, binds to the plasma membrane through post translational lipid modifications as well as binding to the G-protein βγ-complex (UGUR and JONES 2000). It has been located in cells with constitutive and regulated protein secretion pathways (KEHLENBACH *et al.* 1994) and is also known to be a cholera toxin substrate (UGUR and JONES 2000).

XLαs is identical to the $G_s\alpha$ protein except for its start exon where the *Gnas* exon 1 (47 amino acids) is replaced by the significantly larger *Gnasxl* exon (347 amino acids; Figure 1.4) (KEHLENBACH *et al.* 1994; LI *et al.* 2000) (Figure 1.4). The expression of this protein has been shown to be restricted mainly to neuroendocrine tissues (KEHLENBACH *et al.* 1994; PASOLLI *et al.* 2000) with some expression in adipose tissue at neonatal day 4 (PLAGGE *et al.* 2004). Similarly to $G_s\alpha$, *in vitro* studies have shown stimulation of AC, however, *in vivo* this has not

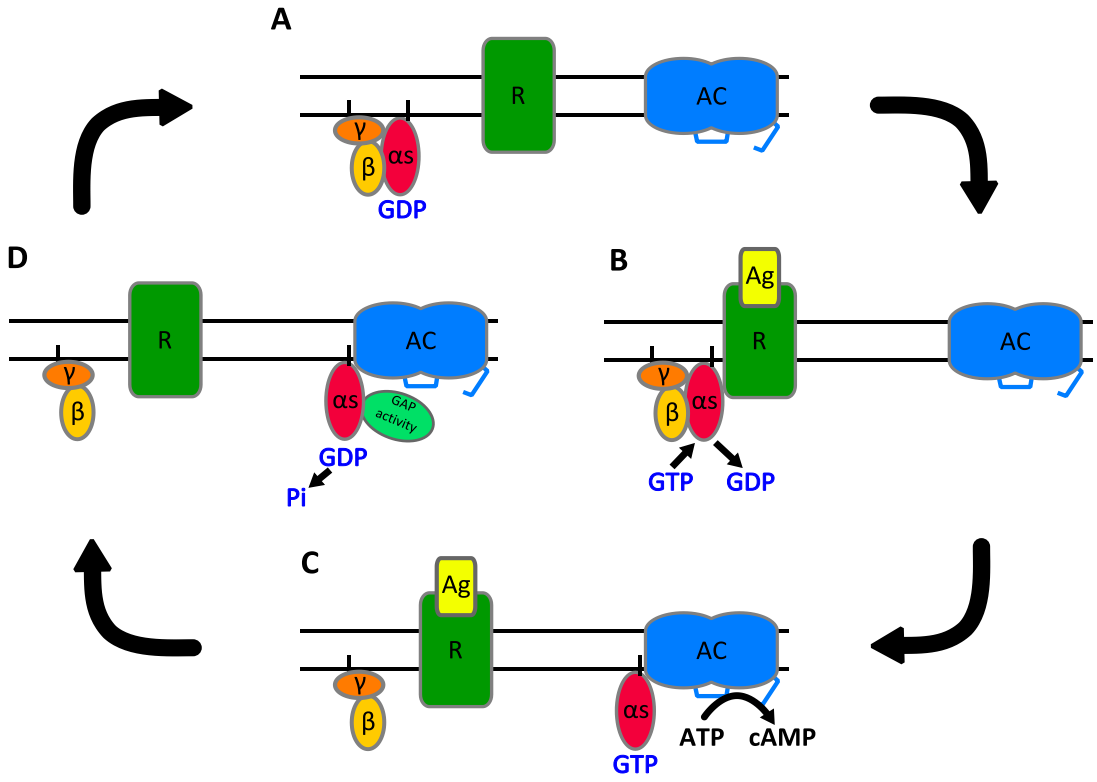

Figure 1.3. Stimulatory G-Protein Stimulation of cAMP

(A) The inactive G-protein complex, with the alpha subunit ($G_s\alpha$ or XLαs) in its GDP bound conformation

(B) When an agonist (Ag) binds to the G-protein coupled 7-transmembrane receptor (R) the GDP is replaced by a GTP. This leads to a conformational change and activation of the alpha subunit which dissociates from the beta/gamma subunit.

(C) The GTP-bound alpha-subunit, now in its active form, can now interact with the adenylyl cyclase (AC) which increases the production of the second messenger cyclic AMP (cAMP).

(D) Binding of GTPase activating proteins (GAP) stimulates the GTP hydrolysis activity of alpha-subunits. This results in the alpha-subunit becoming inactive and rebinding to the beta/gamma subunit.

Adapted from (PLAGGE *et al.* 2008)

Figure 1.4. The protein domains encoded in the *Gnasxl* and *Gnas* first exons.

The α_s and $\beta\gamma$ binding portion of the exons are conserved between the *Gnas* and *Gnasxl* first exons. This allows XLαs to perform the same signalling role as $G_s\alpha$. The XL-domain is specific to the *Gnasxl* exon 1. This domain contains a cysteine rich region (C) and a proline rich region (P) (Pasolli 2000).

been clearly established (BASTEPE *et al.* 2002; KLEMKE *et al.* 2000; XIE *et al.* 2006).

1.2.2. KNOCK-OUT MOUSE LINES OF THE *GNAS* LOCUS

Several knock-out mouse lines have been generated which result in the heterozygous removal of $G_s\alpha$. The *Gnas* exon 2 knock-out line could disrupt either the maternal allele ($E2^{m-/+}$) or the paternal allele ($E2^{+/p-}$) (YU *et al.* 1998). It was discovered that the E2 mutation would disrupt the alternative transcripts of the locus, *Gnasxl* and *Nesp*, as well as $G_s\alpha$. The $E2^{+/p-}$ mice have narrow bodies, increased glucose tolerance, increased insulin sensitivity, decreased body weight and decreased serum leptin as well as poor suckling ability and inactivity (YU *et al.* 1998). The $E2^{m-/+}$ mice have wide bodies, subcutaneous oedema and increased body weight as well as neurological defects and resistance to parathyroid hormone (PTH) (YU *et al.* 1998).

A second mouse line was developed, which disrupts the first exon of *Gnas* with either maternal ($E1^{m-/+}$) or paternal ($E1^{+/p-}$) transmission, each resulting in different phenotypes (CHEN *et al.* 2005). $E1^{+/p-}$ mice have a normal phenotype as opposed to the lean phenotype seen in both the $E2^{+/p-}$ and the XLαs specific knock-out mice (PLAGGE *et al.* 2004; YU *et al.* 1998).

Maternal transmission of the E1 mutation resulted in mice with increased body weight and a significant increase in adipose tissue but no change in lean mass. They also showed no difference in food intake but had a small, significant decrease in metabolic rate (CHEN *et al.* 2005). The neonatal mice showed subcutaneous oedema and 50% lethality shortly after birth; adults are obese and insulin resistant (CHEN *et al.* 2005). $E1^{+/p-}$ showed an opposite phenotype to the E2 paternal disruption mice, suggesting the $E2^{+/p-}$ phenotype is due to the removal of XLαs, which shares exons 2 through 12 with $G_s\alpha$.

A point mutation in exon 6 of the *Gnas* locus, converting a valine to a glutamine, resulted in the Oedematous-Small line (Oed-Sml); maternal transmission of this point mutation results in subcutaneous oedema and obesity in adulthood (Oed), while paternal transmission results in growth retardation (Sml) (CATTANACH *et al.* 2000; KELLY *et al.* 2009; SKINNER *et al.* 2002). The *Oed* phenotype mirrors the phenotype of the *Gnas* knock-out line while the *Sml* phenotype is the same as the *Gnasxl*$^{m+/p-}$ mice (CHEN *et al.* 2005; XIE *et al.* 2006).

A paternal knock-out (*Gnasxl*$^{m+/p-}$) of the *Gnasxl* exon 1 removed XLαs, Alex (a protein generated from an alternate open reading frame of the *Gnasxl* transcript) and the truncated XLαs isoform, XLN1, which is missing much of the functional domain downstream of exon 3, as exon 4 is replaced by the N1 exon (PLAGGE *et al.* 2004) (Figure 1.1). *Gnasxl*$^{m+/p-}$ mice show several physiological differences to wild type mice. They exhibit reduced adiposity due to increased energy expenditure, increased metabolic rate with increased lipid metabolism in adipose tissue, as well as increased glucose tolerance and insulin sensitivity (XIE *et al.* 2006). Neonatal mice have difficulties suckling and inertia as well as severe lethality, however these are overcome in adult survivors (PLAGGE *et al.* 2004; XIE *et al.* 2006). Brown adipose tissue has increased mitochondrial content in *Gnasxl*$^{m+/p-}$ (XIE *et al.* 2006). They are thought to be lean due to an increase in lipid mobilization and oxidation however there are some changes in expression of genes that regulate metabolism in other tissues, such as an increase of Glut4 in muscles which might contribute to the insulin sensitivity (XIE *et al.* 2006). There are several indicators that suggest XLαs is involved in sympathetic nervous system activity regulation including increased urine norepinephrine levels. In male mice there is an increase in urine epinephrine

suggesting an increase in activity of the adrenal medulla; there is also an increase in sympathetic nervous system (SNS) controlled gene expression in adipose tissue which would result in increased lipolysis (XIE *et al.* 2006).

In adult *Gnasxl*$^{m+/p-}$ mice, there is an increase in energy expenditure (these mice eat more food per body weight than their wild type counterparts but remain lean) (XIE *et al.* 2006). They also exhibit hypoleptinaemia which contributes further to the idea of XLαs' involvement in the SNS (XIE *et al.* 2006) along with the finding that XLαs is expressed in the sympathetic trunk of the central nervous system (PASOLLI and HUTTNER 2001; PLAGGE *et al.* 2004). The increased glucose tolerance and decreased insulin levels seen in *Gnasxl*$^{m+/p-}$ mice is not likely to be related to an impairment of the secretion of insulin by the β cells. This hypoleptinaemia is caused by the low lipid stores in white adipose tissue (WAT). Insulin sensitivity might be due to increased insulin clearance but this is quite likely a secondary effect to a decrease in tissue triglyceride content which is a result of chronically increased lipid oxidation and energy expenditure (CHEN *et al.* 2009a). There may also be a contribution to hypoleptinaemia from a decrease in the expression of hepatic lipogenic genes (XIE *et al.* 2006).

The fact that G_sα-knock-out and XLαs-knock-out mice have opposite metabolic phenotypes (G_sα being obese and XLαs being lean) suggests that these two proteins, although almost identical, act in distinct pathways in the cell to control energy (XIE *et al.* 2006). There is a very specific distribution of XLαs expression in the postnatal brain tissue (PLAGGE *et al.* 2004). There has been little information collected about its distribution within the adult mouse brain. Changes in the expression pattern of XLαs/*Gnasxl* might account for the change

in phenotype from pre-weaning to post-weaning in *Gnasxl*$^{m+/p-}$ mice and this is currently under investigation.

1.2.3. DISORDERS ASSOCIATED WITH THE *GNAS* LOCUS

In humans, mutations of *GNAS* result in several severe phenotypes. The first is Albright hereditary osteodystrophy (AHO). This disorder is a result of mutations in *Gnas* that can be paternally or maternally inherited and result in a 50% reduction in the expression of *Gnas*. The disorder exhibits as mental retardation and subcutaneous ossification. This subcutaneous ossification is also observed in mice (HUSO *et al.* 2011; SAKAMOTO *et al.* 2009).

Maternal transmission of *Gnas* mutations results in AHO with the addition of hormonal resistance is several tissues, including the thyroid, kidney and gonads, as a result of the loss of imprinted *Gnas*. This is called pseudo-hypoparathyroidism type-Ia (PHP-Ia). Hormone resistances include parathyroid hormone signalling in kidney and thyroid stimulating hormone (GERMAIN-LEE *et al.* 2002; LEVINE *et al.* 1983; WEINSTEIN *et al.* 2001).

PHP-Ib is caused by the loss of the methylation on the maternal allele at exon 1A on the *Gnas* locus. This would silence the expression of $G_s\alpha$ in tissues that have monoallelic expression of $G_s\alpha$. The phenotype associated with $G_s\alpha$ mutations is characterised by renal PTH resistance (JÜPPNER *et al.* 2006), a mild TSH resistance and in some cases AHO-like symptoms (LIU *et al.* 2003; MANTOVANI *et al.* 2007).

1.3. CNS REGULATION OF ENERGY HOMEOSTASIS

With several imprinted genes having an impact on neonatal feeding behaviours and being expressed in areas of the brain which control food intake regulation and energy expenditure, it is interesting to investigate the control of

energy homeostasis by these imprinted genes.

One of the fastest growing medical problems in the western world is obesity. This is defined as a body mass index (BMI) above 30. Obesity is associated with many other health problems, being a predicting factor for diseases such as type 2 diabetes mellitus and heart disease. To tackle the growing number of overweight individuals it is important to understand how energy homeostasis is controlled. It is well established that having a higher calorific intake than energy expenditure is how people become overweight. Having a clear picture of how the body processes nutrient signals and how they might be manipulated to manage weight is currently an important area of research.

Energy homeostasis is a finely tuned balance of many complex and interacting signalling pathways. To maintain this homeostasis, energy expenditure and food intake must be balanced to avoid a negative energy balance (i.e. decreased calorific intake compared to the calories burned) resulting in body weight loss, or – perhaps more importantly for medical researchers today – a positive energy balance (i.e. increased calorific intake compared to energy burned) resulting in body weight gain and, if left unchecked, obesity. Although many pathways have been established as having a role in energy homeostasis, the exact mechanisms and functions of each in these complex and interacting pathways have yet to be clarified.

Many of the pathways that control energy balance involve neuropeptides in the brain that are activated by nutrient signalling from the gut via nerves such as the vagus. One of the best-known regulators of energy metabolism is leptin signalling. This will be discussed further in Chapter 7.

1.4. AIMS OF THE PHD

This project set out to investigate several aspects of *Gnasxl* expression patterns.

Firstly, to establish a suitable position for placement of a gene trap into the intron, after the *Gnasxl* exon 1, splice variants of *Gnasxl*-derived proteins were analysed.

Secondly, to investigate the possible causes of a phenotypic change from neonatal to adult phases of development, the expression pattern of XLαs was analysed in the brain of neonatal mice and compared to the expression pattern of XLαs in adult mouse brain. This analysis of XLαs expression pattern was continued in peripheral tissues of neonatal and adult mice.

Finally, the project addressed the significance of XLαs in signalling pathways and the importance of XLαs removal. This was investigated through colocalisation studies and immunoblotting.

CHAPTER 2. MATERIALS AND METHODS

2.1. CHEMICALS AND REAGENTS

CD1 (wild type mice) were obtained from Charles River, UK. Electrophoresis grade reagents for PAGE gels and Western blotting were purchased from National Diagnostics except the broad-spectrum protein ladder, which was purchased from Fermentas. For histology, normal donkey serum was obtained from Sigma or Vector Laboratories. Vectastain Elite kits, normal goat serum and normal rabbit serum were purchased from Vector Laboratories. Histoclear was obtained from National Diagnostics and the TritonX100 and Eukitt hard-mounting medium were from Fluka. From Sigma was purchased PFA, PBS tablets, Tris, sucrose, sodium citrate and DAB tablets. From Thermo Scientific were obtained the Superfrost and Polylysine slides and the Shandon Cyromatrix. Fluorogel mounting medium was purchased from Electron Microscopy Sciences. For Western blotting, Pierce® BCA protein assay kits, Amersham ECL Plus Western blotting detection system and Amersham Hybond-P PVDF membrane were purchased from GE Healthcare (through Thermo Scientific). The PhosSTOP phosphatase inhibitor tablets were purchased from Roche. Protease inhibitors, PMSF, Kodak fixative and developer solutions as well as Kodak X-Ray film were provided by Sigma. Reagents for PCR reactions were obtained from Qiagen (HotStar Taq) or Promega (Go Taq Hotstart Polymerase). TOPO cloning kits were bought from Invitrogen along with the Alexa Fluorophore- (AF-) conjugated secondary antibodies. Restriction enzymes were purchased from Promega, Fermentas and New England Biolabs. For Southern blotting and *in situ* hybridisation DNA and RNA probe labelling kits were obtained from Roche, along with blocking reagent and the alkaline phosphatase-conjugated anti-DIG-Fab fragments. The ProbeQuant G-50 Sephadex columns

and Amersham Hybond N^+ nylon membrane were obtained from GE Healthcare. DEPC, single stranded DNA from salmon testes, phenol: chloroform: isoamyl (25:24:1), chloroform: isoamyl (24:1), agarose, LB broth, ampicillin, agar, Tween20, NBT and BCIP were all purchased from Sigma. The DNA extraction kit was bought from Geneflow. The 1 kb DNA ladder was obtained from New England Biolabs. Antibodies were purchased from Santa Cruz, Jackson ImmunoResearch Laboratories, Abcam, Cappel, Cell Signalling Technology, Invitrogen, Millipore, Lifespan Biosciences, Acris Antibodies and Alpha Diagnostics.

2.2. BUFFERS AND SOLUTIONS

2.2.1 TISSUE COLLECTION

Fixative stock. 4 % (w/v) paraformaldehyde (PFA); 1 x PBS. This was heated to 50°C for up to 1 hour until dissolved then aliquoted into 50 mL tubes and stored at -20°C.

2.2.2. HISTOLOGY

Cryoprotectant Sucrose. 30% (w/v) sucrose; 1 x PBS. Sterile filtered and stored at 4°C.

10x Tris-Buffered Saline (TBS). 100 mM Tris-HCl, pH7.5; 150 mM NaCl. This solution was diluted to 1 x concentration with ddH_2O for washing steps. To make Tween TBS (TTBS), 0.1% (v/v) Tween20 (Sigma) was added to 1 x dilution of TBS stock. This solution can be stored at room temperature.

10x PBS stock. 50 PBS tablets (Sigma) were dissolved in 1 L of ddH_2O and then autoclaved. This gave the following concentrations of the tablet components: 0.1 M phosphate buffer; 2.7 mM KCl_2; 1.37 M NaCl. This stock was diluted with ddH_2O to 1 x concentration for washing and antibody solutions. For Tween PBS (TPBS) 0.1% (v/v) Tween20 was added to 1 x dilution of the stock. This solution can be stored at room temperature.

1 M Sodium Citrate for Antigen Retrieval. 147.1 g sodium citrate was diluted in 0.5 L ddH_2O. This was diluted to 10 mM for antigen retrieval protocols.

DAB Colour Substrate. 1 DAB tablet (Sigma) was dissolved in 15 mL 1 x PBS. This was sterile filtered and stored as 500 µL aliquots at -20°C. Before use aliquots were thawed (one aliquot per slide) and 1.67 µL 30% H_2O_2 (Final concentration 0.1% (v/v)) was added. This produces a brown colour substrate; to change the colour of the precipitate metal salts can be added (nickel

chloride).

50% Nickel Chloride. 50% (w/v) nickel chloride was dissolved in ddH_2O. Long term storage was at -20°C but it was stored at room temperature for shorter periods. This solution was added in a 1:100 dilution to thawed DAB aliquots. This produces a black/purple colour precipitate.

Vectastain Elite ABC Solution. 2% (v/v) solution A; 2% (v/v) solution B; PBS. 500 µL was prepared per slide to be stained (i.e. 10 µL A; 10 µL B; 480 µL PBS)

Normal Serum for Blocking. 10% (v/v) normal serum (donkey, rabbit or goat; Sigma or Vector Laboritories); 1 x PBS.

Antibody Dilution Solution. 10 % (v/v) normal serum (donkey, rabbit or goat); 0.25% (v/v) TritonX100; 1 x PBS

ISH Blocking Solution. 1 x PBS; 20% (v/v) sheep serum (Sigma); 5% (w/v) milk powder; 0.05% (v/v) Tween20.

Cryoprotectant. 50 mM phosphate buffer; 30% (w/v) sucrose; 1% (w/v) polyvinylpyrolidone; 30% (v/v) ethylene glycol; ddH_2O

XGal Solution for Detection of lacZ in Tissues. 0.1 % (v/v) XGal; 2 mM $MgCl_2$; 0.01% (v/v) Na-deoxycholate; 0.02 % (v/v) NP-40; 5 mM potassium ferric cyanide; 5 mM potassium ferrous cyanide; 0.02 M NaH_2PO_4; 0.08 M Na_2HPO_4; H_2O. Potassium ferrous cyanide and potassium ferric cyanide were made up as fresh stocks before the XGal solution was prepared. The final XGal solution was pre-warmed to 37°C before applying to tissues.

0.1 M Phosphate Buffer. 0.02 M NaH_2PO_4; 0.08 M Na_2HPO_4

2.2.3. PAGE GELS

RIPA Lysis Buffer. 25 mM $NaPO_4$, pH 7.5; 25 mM NaF; 25 mM β-Glycerolphosphate; 100 mM NaCl; 5 mM EGTA; 0.5 % (w/v) Deoxycholate; 0.5

% (w/v) NP-40 (Igepal CA 630); 0.1 % (w/v) SDS; 0.01 % (w/v) Sodium azide. This solution was stored at 4°C. Before use in lysates PMSF (1:1000), protease inhibitors (1:100) and phosphatase inhibitors (1:10) were added to the required amount of RIPA lysis buffer.

20 % SDS stock. 20 % SDS (w/v); ddH20

PMSF stock. Final concentration of 0.5 M PMSF dissolved in DMSO. This was used at 1:1000 (0.5 mM) in protein lysates and stored at 4°C for up to 1 month.

Protease Inhibitor Stock. 104 mM 4-2-(aminoethyl)benzenesulphonyl fluoride; 80 µM aprotinin; 4 mM bestatin; 1.4 mM E-64; 2 mM leupeptin; 1.5 mM pepstatin A in DMSO. To be used at 1:100 dilution

Phosphatase Inhibitor Stock (PhosSTOP). 1 PhosSTOP tablet (Roche) dissolved into 1 mL ddH_2O. This was used at a 1:10 dilution in protein lysates. 1 PhosSTOP tablet contains 5.6 % sodium molybdate; 3.7 % Sodium orthovanadate; 0.4 % catheridine.

10% APS (10 mL). 1 g APS dissolved in 10 mL ddH_2O. This was stored as 500 µL aliquots, after thawing it was stored on ice while making PAGE gels and discarded at the end of the experiment.

5 x SDS-PAGE Electrophoresis buffer. 125 mM Tris base; 1.25 M Glycine; 0.5% SDS (w/v).

2x Laemmli buffer for SDS-PAGE gels. 100 mM Tris-HCl, pH 6.8; 20 % (v/v) glycerol; 4 % SDS (w/v); 200 mM DTT; 0.2% (w/v) bromphenol blue.

Transfer buffer. 25 mM Tris, pH 8.3; 192 mM Glycine; 20% (v/v) MeOH. This solution was pre-cooled to 4°C for several hours before use in transfers.

Stripping buffer. 100 mM β-mercaptoethanol; 2 % (w/v) SDS; 62.5 mM Tris-HCl pH 6.7.

10% Resolving Gel. 10 % (v/v) Accugel (30% stock; 29:1 Acrylamide:Bisacrylamide); 390 mM 1 M Tris-HCl, pH 8.8; 0.1 % (w/v) SDS. For polymerisation of the gel to occur 0.1 % APS and 0.04 % TEMED are added to the mixture. For native-PAGE gels SDS was omitted from the recipe and replaced with ddH_2O.

Stacking Gel. 5 % Accugel (30 % stock; 29:1 Acrylamide:Bisacrylamide); 100 mM Tris-HCl, pH 6.8; 0.1 % SDS. For polymerisation of the gel to occur 0.1 % (v/v) APS and 0.1 % (v/v) TEMED are added to the mixture. For native-PAGE gels SDS was omitted from the recipe and replaced with ddH_2O.

Ponceau S Staining Solution (1 L): 10 g Ponceau S; 30 g Trichloroacetic acid; 1 L ddH_2O.

Developer Solution (1 L). 218 mL Kodak developer solution (Sigma) made up to 1 L with ddH_2O. This solution was kept in the dark to avoid degradation.

Fixative Solution (1 L).). 218 mL Kodak fixative solution (Sigma) made up to 1 L with ddH_2O. This solution was kept in the dark to avoid degradation.

2.2.4. SOUTHERN BLOTTING AND *IN SITU* HYBRIDISATION

Hybridisation Buffer for Southern Blotting and* in situ *hybridisation. 5 x SSC; 1 x blocking reagent; 0.1 % (w/v) N-Lauroylsarcosine; 0.02 % (w/v) SDS. This solution was stored at -20°C. Salmon sperm DNA may be added to reduce background staining from probes.

10x blocking reagent. 5 g blocking reagent (Roche). made to 50 mL with DIG buffer 1. This stock was stored at -20°C.

DIG synthesis mix stock. 2mM dATP; 2mM dCTP; 2mM dGTP; 1.3 mM dTTP; 0.7 mM DIG-11-dUTP, alkali-labile; pH 7.0

NBT stock sol. 75 mg/mL in 70 % Dimethylformamide. This was aliquoted into

1 ml tubes and kept at -20°C. For colour reaction 45 µL NBT was added per 10 mL DIG buffer 3.

BCIP stock sol. 50 mg/ml in 70% Dimethylformamide. This was aliquoted into 1 ml tubes and kept at -20°C. For colour reactions 35 µL BCIP was added per 10 mL DIG buffer 3.

0.25 M HCl Solution for Gel preparation before Southern Blotting (2 L). 42 mL 37 % HCl; ddH_2O

Neutral solution for Gel preperation before Southern Blotting (2 L). 1 M ammonium acetate in ddH_2O [154 g NH_4COOH; ddH_2O].

Denaturing Solution for Gel preperation before Southern Blotting (2L). 0.5 M NaOH; 1.5 M NaCl in ddH_2O [40 g NaOH; 175.3 g NaCl; ddH_2O]

DIG Buffer 1. 0.1 M Maleic acid; 0.15 M NaCl; pH 7.5. This solution was dissolved on a hot plate and autoclaved before use.

DIG Buffer 3. 0.1 M Tris-HCl, pH 9.5; 0.1 M NaCl; 0.05 M $MgCl_2$

2.2.5. ELECTROPHORESIS

TAE (50x) buffer for Gel Electrophoresis. 2 M Tris base; 1 M acetic acid; 50 mM EDTA, pH 8.0. Diluted to 1 x for gel electrophoresis and agarose gel preparation.

Agarose gel preparation. 0.8, 1.2 or 2% gels were prepared by dissolving the appropriate percentage w/v agarose into the required volume of 1x TAE for the size of gel needed (50 mL, 100 mL or 200 mL). This mixture was heated in the microwave until all the agarose had dissolved. 1 µL ethidium bromide per 50 mL of agarose gel was added and the gel was poured into a gel tray to set.

2.2.6. CLONING

Luria-Bertani (LB) medium. 1 % (w/v) Tryptone; 0.5 % (w/v) Yeast extract; 1 % (w/v) NaCl. The solution was autoclaved and cooled to 55°C and 50 µg/mL

ampicillin was added. This was stored at 4°C.

LB Agar Plates. Prepared as for LB medium but 15 g/L agar was added before autoclaving. After cooling to 55°C, 50 µg/mL ampicillin was added and the LB/agar mix poured into 10 cm plates. These were allowed to air dry and then stored at 4°C.

TE buffer. 10 mM Tris, pH 8.0; 1 mM EDTA

TENS buffer. 10 mM Tris, pH 8.0; 1 mM EDTA; 0.1 M NaOH; 0.5% (w/v) SDS.

S.O.C. medium. 2 % (w/v) Tryptone; 0.5 % (w/v) Yeast extract; 10 mM NaCl; 2.5 mM KCl; 10 mM $MgCl_2$: 10 mM $MgSO_4$; 20 mM glucose

1x TAE buffer for gel electrophoresis. 40 mM Tris; 20 mM acetic acid; 1 mM EDTA.

Tail Lysis Buffer. 100 mM Tris; 5 mM EDTA; 200 mM NaCl; 0.2 % (w/v) SDS.

dNTPs. 2 mM dATP, 2 mM dTTP, 2 mM dGTP, 2 mM dCTP.

Ampicillin Stock. 50 mg/ml ampicillin. This was used at a 1:1000 dilution.

2.3. MICE

Mice carrying the global *Gnasxl* mutation (strain: XL3G5) (PLAGGE *et al.* 2004) were maintained on a CD1 out-bred genetic background (Charles River, UK) via crosses of female mutation carriers to wild type males, resulting in phenotypically normal *Gnasxl*$^{m-/p+}$ offspring. For analysis of the *Gnasxl*-deficient phenotype, male mutation carriers were crossed with wild type CD1 females, resulting in *Gnasxl*$^{m+/p-}$ offspring.

The conditional gene trap line – *XLlacZGT* – was generated in the University of Liverpool Transgenic Unit. Founder chimera mice were bred to *Flpe*-transgenic mice (RODRIGUEZ *et al.* 2000) to remove the frt-flanked neomycin^{r}-cassette, which can cause unexpected disruption of transcripts. In following generations, *XLlacZGT* female mice were crossed with CD1-background males to maintain the line with loss of the *Flpe*-transgene. The *XLlacZGT* line has a mixed background of 129/C57BL/6J/CD1. Cre crosses were carried out with Nestin-Cre (TRONCHE *et al.* 1999) and CMV-Cre (SCHWENK *et al.* 1995) females and *XLlacZGT* males to generate mice lacking *Gnasxl* in specific or all tissues, respectively.

CHAPTER 3. ANALYSIS OF EXON A20 SPLICING IN PROTEINS DERIVED FROM THE *GNASXL* TRANSCRIPT: XLAS VS.XLN1

3.1. INTRODUCTION

3.1.1. ALTERNATIVE SPLICING IN *GNASXL*: XLN1, EXON A20 AND EXON 3

XLN1 is a truncated form of the paternally expressed, extra-large variant of the stimulatory G-protein-signalling alpha subunit XLαs (Figure 1.2). This protein is found in neural tissue, expressed mainly in the brain stem and the hypothalamic area; it is also found in the pituitary and adrenal medulla, and is formed of the *Gnasxl* domain, the shared *Gnas* exons 2 and 3 and the XLN1-specific exon N1 (CRAWFORD *et al.* 1993; PASOLLI *et al.* 2000); splicing onto exon N1 results in a premature stop codon. The mRNA produced has a polyadenylated (poly A) tail that results in the termination of transcription; thus it does not splice onto the functional exons 4 through 12 (CRAWFORD *et al.* 1993). XLN1 protein has no known function, and as it lacks the functional exons of the full-length XLαs protein, a function seems unlikely. It might, however, be the case that the protein acts as an antagonist to $G_s\alpha$ and/or XLαs by preventing or limiting binding to receptors thus interfering with the signalling of the full-length functional proteins. XLαs/XLN1 has been detected in the rat embryonic brain from embryonic day 10 onwards (PASOLLI and HUTTNER 2001). In rat brain, XLN1 has been detected as a proportion of protein detectable from the *Gnasxl* transcript by an antibody that is specific for the N-terminal region of the full-length XLαs protein that is determined by *Gnasxl* exon 1 (PASOLLI and HUTTNER 2001; PASOLLI *et al.* 2000). It has also been observed that *Gnasxl* exon 1 can splice directly onto *Gnasxl* exon A20 – a small 95 bp exon downstream of the large *Gnasxl* exon 1 – in humans and in mice (Figure 1.2); however, there has not been a systematic or quantitative analysis of splicing onto exon A20 in either species (HAYWARD *et al.* 1998a; HOLMES *et al.* 2003).

It has been shown that there is alternative splicing of the 45 bp exon 3 in the full-length $G_s\alpha$ protein (KOZASA *et al.* 1988). This alternative splicing does not affect functionality of $G_s\alpha$ (LEVIS and BOURNE 1992; MATTERA *et al.* 1989). This would also apply to any other transcripts splicing onto exons 2 through 12 in the same manner as $G_s\alpha$, including XLαs and Nesp.

3.1.2. AIMS

The aim of this work was to carry out a systematic analysis of exon A20 splicing in the mouse to determine when it is included in splicing (XLN1 and/or the full-length XLαs), and what this might mean in terms of protein composition, as previous data collected from humans discovered a frame-shift when exon A20 was included in these proteins (HAYWARD *et al.* 1998a).

If the inclusion of exon A20 into a protein results in a frame-shift, and probable non-functionality of the protein, it was thought this might be an interesting area to insert a gene trap cassette to establish an XLαs conditional knock-out mouse line. The localisation of an exon, which results in splicing in the endogenous locus in this region of the *Gnas* locus and in a non-functional protein, is an interesting possibility for insertion of the conditional gene trap cassette. Placing the gene trap in a similar position would eliminate the uncertainty of splicing ability that would be associated with inserting the gene trap further into the intron. The fact that the protein produced from this splicing would appear to be non-functional is important, as the removal of the A20 exon should not produce a phenotype.

3.2. MATERIALS AND METHODS

3.2.1. TISSUE COLLECTION

Wild type mice were killed by Schedule One procedure and relevant tissues were quickly removed and frozen down on dry ice. Hypothalami were separated from the rest of the brain tissue by dissection for analysis of this brain region. It is particularly important the tissues are frozen down immediately to maintain RNA integrity. Tissues were stored at -80°C and used for RNA extraction.

3.2.2. RNA EXTRACTION

RNA was extracted from 40 mg hypothalamic tissue samples using the Stratagene RNA extraction kit following the protocol for tissue extraction. This included homogenization of tissue samples with 600 µL lysis buffer containing 4.2 µL β-Mercaptoethanol. Homogenate was added, 700 µL at a time, to a pre-filter spin-cup in a 2 mL receptacle tube and centrifuged for 5 minutes. The filtrate was added to an equal volume of 70% EtOH and mixed thoroughly. From the filtrate/EtOH mixture, 700 µL was transferred to an RNA-binding spin-cup and centrifuged for 1 minute, the filtrate was discarded and the rest of the mixture added to the spin-cup and centrifuged for 1 minute.

If RT-PCR was to be performed on the RNA extracts, 600 µL 1 x low salt buffer was added to the spin-cup and centrifuged for 1 minute. The cup was retained and replaced in the receptacle tube (the filtrate was discarded), 50 µL RNAse-free DNAse digestion buffer and 5 µL reconstituted RNAse-free DNAse I was pipetted onto the fibre matrix and incubated for 15 minutes at 37°C. 600 µL 1 x high salt wash buffer was added to the spin-cup and centrifuged for 1 minute. The filtrate was discarded and the spin-cup replaced in the receptacle

tube. 600 µL 1 x low salt wash buffer was added and the tube centrifuged for 1 minute. Again the spin-cup was retained and the filtrate discarded. 300 µL 1 x low salt buffer was added and the tube centrifuged for 2 minutes. The spin-cup was transferred to a fresh 1.5 mL tube and 30 µL elution buffer was added to the fibre matrix of the spin-cup, incubated for 2 minutes at room temperature and centrifuged for 1 minute. The elution step was repeated, giving a final volume of 60 µL eluate. These RNA extracts were stored at -80°C.

3.2.3. REVERSE TRANSCRIPTION-PCR (RT-PCR)

For each sample 1 µg total RNA was required. Hexamer stock (0.6 µL of a 500 ng/µL) was added and the volume made up to 13.7 µL with RNAse-free water. This was incubated at 65°C for 5 minutes then cooled slowly to room temperature (20°C). To each reaction 2 µL 10x AffinityScript™ RT buffer; 2 µL 100 mM DTT; 0.8 µL 10 mM dNTP mix; 0.5 µL RNAse inhibitor (20U); and 1 µL AffinityScript™ Multiple Temperature Reverse Transcriptase (Stratagene) were added. The reaction was mixed gently, incubated at 25°C for 10 minutes; 42°C for 1 hour; 70°C for 15 minutes and cooled to 37°C. 1 µL RNAseH was added and the reactions were incubated at 37°C for 20 minutes. The cDNA obtained was stored at -20°C.

PCR reactions consisted of 1 µL cDNA, 22 µL ddH_2O, 3 µL PCR buffer, 3 µL dNTPs, 0.5 µL forward primer, 0.5 µL reverse primer and 0.25 µL Taq polymerase. PCR reactions were run on the following thermocycler programme: heated lid at 111°C, 15 minute denaturation at 95°C, this was followed by 30 cycles of 45 seconds at 95°C (denaturation), 45 seconds at 56°C (annealing) and 1 minute at 72°C (extension). PCR products were stored at 4°C until required.

3.2.4. Ligation and Cloning into competent E. coli

Equimolar amounts of supercoiled, uncut plasmid (~50 ng) and PCR products were used in a total volume of 25 µL along with 12.5 µL H_2O; 1 x Ligation buffer; 0.2 mM dNTP, 1U SmaI restriction enzyme; 1 U T4 DNA Polymerase; and 3U T4 DNA ligase. This was left at room temperature overnight. One third of the reaction was transformed into competent E. coli (Strain: DH5α). Bacteria were grown on LB + Ampicillin (Amp) plates at 37°C overnight.

3.2.5. Cloning of PCR products using the TOPO TA Cloning® kit (Invitrogen)

A TOPO TA Cloning® kit was used to clone PCR products into competent bacterial cells. Two LB + Amp plates per cloning reaction to be performed were pre-warmed to 37 °C. 4 µL amplified PCR product to be cloned into bacteria was added to 1 µL salt solution (1.2 M NaCl; 0.06 M $MgCl_2$) and 1 µL 10 ng/µL pCR® 2.1-TOPO vector and incubated at room temperature for 5 minutes. To transform the vector into bacterial cells, 2 µL of the TOPO TA cloning ® reaction mixture was added to one vial of thawed, one-shot TOP10 cells and incubated on ice for 30 minutes. The TOP10 cells were then heat-shocked for 30 seconds at 42°C and immediately placed on ice. 250 µL SOC medium was added to the TOP10 cells in a mini-culture tube. This was left at 37°C for 1 hour with constant agitation. These were then plated out in 50 µL and 200 µL aliquots onto the pre-warmed LB + Amp plates and incubated at 37°C overnight.

3.2.6. Preparation of Bacterial Mini-cultures

Individual colonies were selected from cloning experiment LB + Amp plates and grown overnight in individual mini-culture tubes containing 2 mL LB

+ Amp broth at 37°C with constant agitation. After overnight incubation these were stored at 4°C and could be used to re-grow colonies of interest if necessary.

3.2.7. TENS Mini-Prep for Extraction of DNA from Bacterial Mini-cultures

Overnight bacterial mini-cultures were tipped into 1.5 mL tubes and spun in the centrifuge for 30 seconds at full speed. The supernatant was discarded, leaving a small amount (~50 µL) in the centrifuge tube for resuspension of the pellet. 300 µL of TENS buffer was added to lyse cells. Samples were placed on ice for 5 minutes. 150 µL of 3 M sodium acetate, pH 5.0, was added and mixed immediately by inverting. The samples were returned to ice for 5 minutes then centrifuged at maximum speed for 5 minutes. The supernatant was transferred to a separate tube containing 900 µL 100% EtOH, mixed and placed at -20°C for 30 minutes. Samples were spun for 5 minutes and the supernatant was removed. Pellets were washed twice with 700 µL 70% EtOH with a 1 minute spin. The EtOH was removed and the pellets allowed to dry for 10 minutes at 37°C then resuspended in 30 µL 1 x TE + RNAseA. These were stored at 4°C.

3.2.8. Determination of colonies containing PCR product insertions by EtBr agarose gel electrophoresis

Mini-prep DNA was digested using restriction enzymes to cut out the PCR product insert; 5 µL digested mini-prep DNA was run on 2% agarose gels containing EtBr. Colonies that were deemed to contain fragments of interesting size after visualisation on the gel doc were sent for sequencing by DBS Genomics (University of Durham). Sequences were returned and compared to

the full-length sequence to determine exon splicing of the fragment using NCBI BLAST.

3.3. RESULTS

3.3.1. ANALYSIS OF ALTERNATIVE SPLICING OF *GNASXL* EXON A20 IN FULL-LENGTH XLAS AND XLN1 PROTEIN

Using RT-PCR the splice variants of each of the different cDNA variations produced from the *Gnasxl* exon 1 were analysed. Alternative splicing of *Gnas* exon 3 is known to exist in the $G_s\alpha$ protein (KOZASA *et al.* 1988). This was taken into account when the splice variants were being analysed as alternative splicing of exon 3 would result in products differing in size by 45 bp, therefore at least two products were expected for each primer combination to be used. Unique sequences were selected as primers: a single forward primer for the *Gnasxl* domain (XL-FL1) was designed along with reverse primers for exon N1 (XLN1-R6) showing splicing in XLN1 protein and, as a positive control for full-length XLαs, a reverse primer for exon 5 (Exon5-R1) (Appendix Table 1). These pairings were expected to result in markedly different fragment sizes of 357 bp and 312 bp for the XL-FL1/XLN1-R6 combination and 468 bp and 423 bp for the XL-FL1/Exon5-R1 combination resulting from the alternative splicing of exon 3 (Figure 3.1 A; Table 3.1). This would allow the use of both reverse primers in the same PCR with the XL-FL1 forward primer. However, test PCRs for the individual reverse primers with the XLαs-specific forward primer resulted in exon N1 fragments which were larger than expected but distinguishable from the exon 5 control pairing (Figure 3.1 B and 3.2 A; Table 3.1).

To establish the cause of these larger than expected fragments, PCR was performed using the XLN1-R6 and Exon5-R1 reverse primers with the XL-FL1 forward primer as before. The separate bands for each combination were cut out of 2% agarose gels and the PCR product extracted. The extracted products

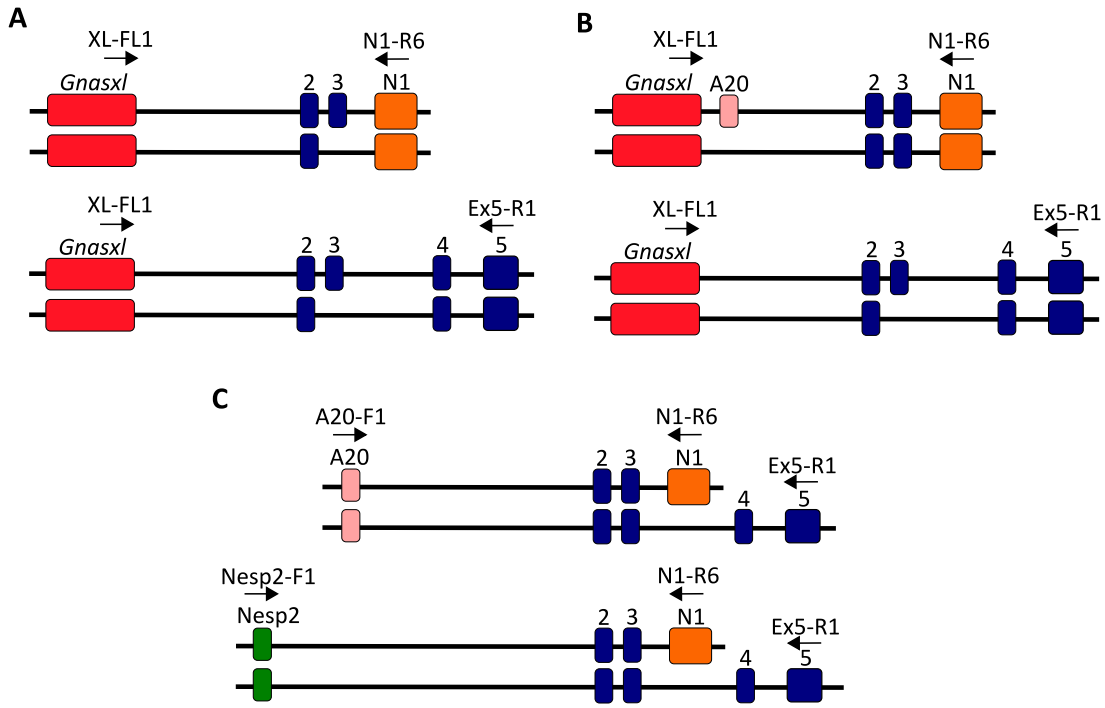

Figure 3.1. PCR products expected and observed in PCR for alternative splicing in XLN1 protein.

(A) Schematic of expected alternative splicing of exon 3 using *Gnasxl*-specific forward primer (XL-FL1) in PCRs with reverse primers for exon N1 (N1-R6) and exon 5 (Exon5-R1).

(B) Schematic of observed fragments for alternative splicing of exon A20 and exon 3 in XLN1 and XLαs full length respectively. There was no alternative splicing of exon 3 in XLN1 protein but this was replaced with alternative splicing of A20. In full-length XLαs protein there was only alternative splicing of exon3.

(C) Fragments expected from A20 (A20-F1) and Nesp2 (Nesp2-F1) forward primers. These were used to assess the splicing of A20 in full-length XLαs and Nesp.

Arrows indicate location of primers.

		XL-FL1 N1-R6	XL-FL1 Exon5-R1	A20-F1 N1-R6	A20-F1 Exon5-R1	Nesp2-F1 N1-R6	Nesp2-F1 Exon5-R1
A20	Exon3	452 bp U, O	563 bp U, N	218 bp E, O	329 bp U, N	272 bp U, N	383 bp U, N
A20	No Exon3	407 bp U, N	518 bp U, N	173 bp U, N	284 bp U, N	227 bp U, N	338 bp U, N
No A20	Exon3	357 bp E, O	468 bp E,O			177 bp E, O	288 bp E, O
No A20	No Exon3	312 bp E, N	423 bp E, O			132 bp U, N	243 bp U, N

Table 3.1. Expected and observed fragments for alternative splicing of *Gnasxl* Exon A20 and *Gnas* Exon 3.

Values indicate the size of a PCR product containing the exons on the left (A20 or exon3) when the PCR primer pairings along the top are used.

U – unexpected; O – observed; E – expected; N – not observed.

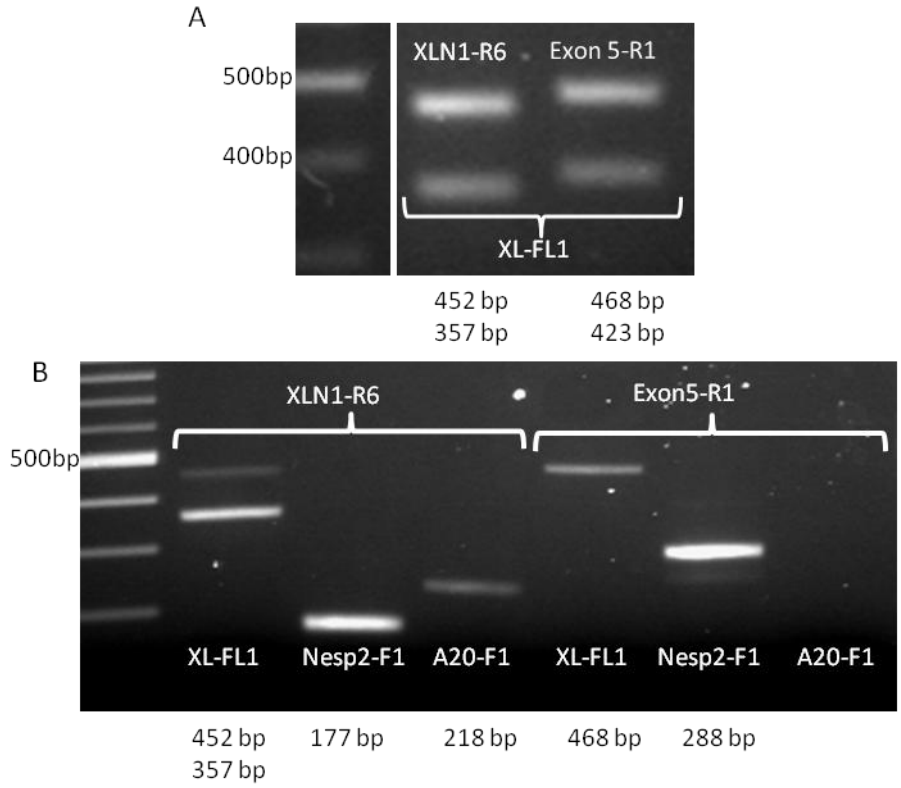

Figure 3.2. PCR of cDNA from hypothalamic lysates revealed unexpected alternative splicing of *Gnasxl* exon A20.

(A) PCR using XLN1 (XLN1-R6) and Exon 5 (Exon5-R1) reverse primers with the *Gnasxl* exon 1 (XL-FL1) forward primer resulted in PCR products of unexpectedly similar size.

(B) RT-PCR products showing alternative splicing of exon A20 in the XLN1 transcript but not in the full-length XLαs or Nesp proteins using forward primers for *Gnasxl* (XL-FL1), Nesp exon 2 (Nesp 2-F1) and exon A20 (A20-F1) in combination with reverse primers for XLN1 (XLN1-R6) and Exon 5 (Exon5-R1). Bands from each combination of forward and reverse primer were sent for sequencing. Where combinations of primers resulted in more than one band, these were extracted, cloned and sequenced separately.

(A-B) DNA ladder is 100 bp ladder and product sizes are indicated below the associated lanes.

were cloned in separate cloning reactions into competent E. coli cells. Between 10 and 15 colonies from each reaction were selected to be grown in mini-culture and mini-prep DNA was collected from them. Colony mini-prep DNA was digested with appropriate restriction enzymes and colonies deemed positive for the extracted PCR product were sent for sequencing (Figure 3.3). Using the TOPO TA cloning kit more positive clones were produced compared to standard ligation into pBluescript SK (-). BLAST analysis of the returned sequences established that there was consistent alternative splicing of *Gnasxl* exon A20 in the XLN1 protein but no alternative splicing of exon 3 (Figure 3.1 B, Table 3.1). Further analysis with forward primers in the A20 exon itself and the Nesp2 exon was used to assess splicing in all transcripts (Appendix Table 1). Exon A20 is not included in either of these proteins on a regular basis (Figure 3.1 B-C and 3.2 B). The alternative splicing of exon A20 into XLN1 also produced a frame-shift resulting in a premature stop codon in exon 2, further truncating the XLN1 protein (Figure 3.4).

3.3.2. SUMMARY

In summary the following combinations of splicing were observed. XLN1 always contained exon 3 and could be plus or minus exon A20. Full-length XLαs rarely contained exon A20, and could be plus or minus exon 3. Nesp was always minus A20 and contained exon 3. In conclusion, if splicing of exon A20 occurs then exon 3 is always spliced.

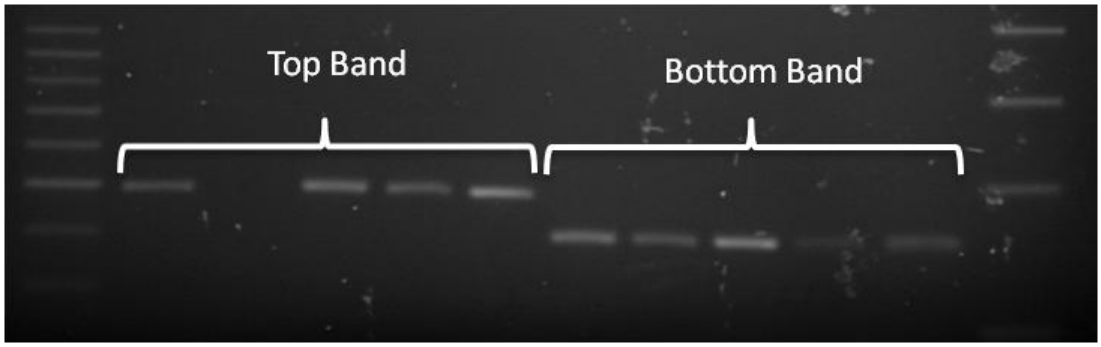

Figure 3.3. Restriction digest of mini-prep DNA to check for PCR product insertion.

Representative image of restriction enzyme analysis of mini-prep DNA for PCR product (XL-FL1 and Exon5-R1) insertion into plasmid. The gel shows mini-prep DNA made from two separate bands with the same primer combination. Only one does not contain the PCR insert. Restriction digests run on a 2% agarose gel.

MEITRPLLEIGRASIGVDDDTAVNMDSPPIASDGPPIEVSGAPDKSECAERPPVE
REAAEMEGSPTTATAVEGKVPSPERGDGSSTQPEAMDAKPAPAAQAVSTGSDA
GAPTDSAMLTDSQSDAGEDGTAPGTPSDLQSDPEELEEAPAVRADPDGGAAP
VAPATPAESESEGSRDPAAEPASEAVPATTAESASGAAPVTQVEPAAAAVSATLA
EPAARAAPITPKEPTTRAVPSARAHPAAGAVPGAPAMSASARAAAARAAYAGP
LVWGARSLSATPAARASLPARAAAAARAASAARAVAAGRSASAAPSRAHLRPP
SPEIQVADPPTPRPPPRPTAWPDKYERGRSCCRYEASSGICEIESSSDESEEGATG
CFQWLLRRNRRPGLPRSHTVGSNPVRNFFTRAFGSCFGLSECTRSRSLSPGKAK
DPMEERRKQMRKEAIEMREQKRADKKRSKLIDKQLEEEKMDYMCTHRLLLLG
RKVVPSDTEGRYRPEASASASDRRLDRRGREVLESLAKAPL*

Figure 3.4. Amino acid sequence resulting from splicing of exon A20.

The inclusion of exon A20 into either XLN1 or the full length XLαs protein would result in a frame-shift that had been previously described in humans (HAYWARD *et al.* 1998a) and a premature stop codon in exon 2. *Gnasxl* exon1 - Black; *Gnasxl* exonA20 - Blue; exon2 - red; * - stop codon

3.4. DISCUSSION

3.4.1. ALTERNATIVE SPLICING OF *GNASXL* EXON A20

The alternative splicing of the *Gnasxl* exon A20 in the XLN1 protein of mice is in concurrence with the data collected for human XLN1 (HAYWARD *et al.* 1998a), but has never been fully documented in mice – although this splicing has been detected using FANTOM clones (HOLMES *et al.* 2003). The implications of this splicing have never been fully understood. It has now been shown that the inclusion of exon A20 would cause a severe truncation of any protein it might be spliced into. It has also been established in this project that splicing of exon A20 is regularly observed only in the XLN1 protein and not in the full-length XLαs. Given the phenotype observed in *Gnasxl*$^{m+/p-}$ mice, this is unsurprising considering the serious implications of the premature termination codon in exon 2, which would result in the further truncation of both the XLN1 protein and in full-length XLαs. It has been suggested that XLN1 might interfere with cAMP signalling. The further truncation of the XLN1 protein, with the addition of exon A20 occurring on a regular basis, indicates it is unlikely to have a function *in vivo*.

3.4.2. PLACEMENT OF THE *XLLACZGT* GENE TRAP

The data obtained from the analysis of exon A20 splice variants were used in another project within our laboratory. This project established a conditional knock-out mouse line by insertion of a gene targeting cassette into the locus, which allowed the deletion of XLαs in specific or all tissues when crossed with specific Cre-recombinase- (Cre-) carrying mice. However, the established method of simply flanking the *Gnasxl* exon 1 with lox sites could not be applied due to the *Nespas/Gnasxl* ICR situated in this region of the locus (Figure 1.2). It

was therefore necessary to develop a novel targeting strategy that would insert a gene targeting cassette in a position which could disrupt the protein expression of XLαs but would not disturb the regulatory regions of the *Gnasxl* exon 1. A function for XLN1 was deemed to be more unlikely than previously thought due to the regular inclusion of exon A20 in XLN1 and the resulting truncation of the protein. The exon A20 position in the locus was deemed to be ideal for placement of a gene trap cassette as splicing spontaneously occurs at this location and inclusion of exon A20 was thought to be unimportant in transcripts.

The gene trap cassette deleted approximately 950 bp, which covered an area downstream of the *Gnasxl* exon, across the A20 exon and within the intron (Figure 3.5 A). This was replaced with a lox flanked cassette containing a frt-flanked neomycin and a cassette which consisted of an exon 2 splice acceptor site and a lacZ cassette with a polyA tail, flanked by two different pairs of lox sites (loxP and lox2272) in a head-to-head orientation (Figure 3.5 B). The bacterial gene lacZ produces the protein βGalactosidase. This is the enzyme which converts lactose into the monosaccarides, glucose and sucrose; it can be used as a reporter of gene expression under the control of specific promoters – in this case *Gnasxl*. The gene trap cassette was inserted into the gene locus in an inactive orientation with the exon 2 splice acceptor site in a position where *Gnasxl* exon 1 could not splice onto it allowing XLαs to be produced normally in carrier mice (Figure 3.5 C). To avoid interference with expression the frt-flanked neo cassette was removed by crossing with Flpe mice (Figure 3.5 D). Crosses of male gene trap carrier mice with female Cre-expressing mice result in inversion of the gene trap cassette. Litters were born in the expected

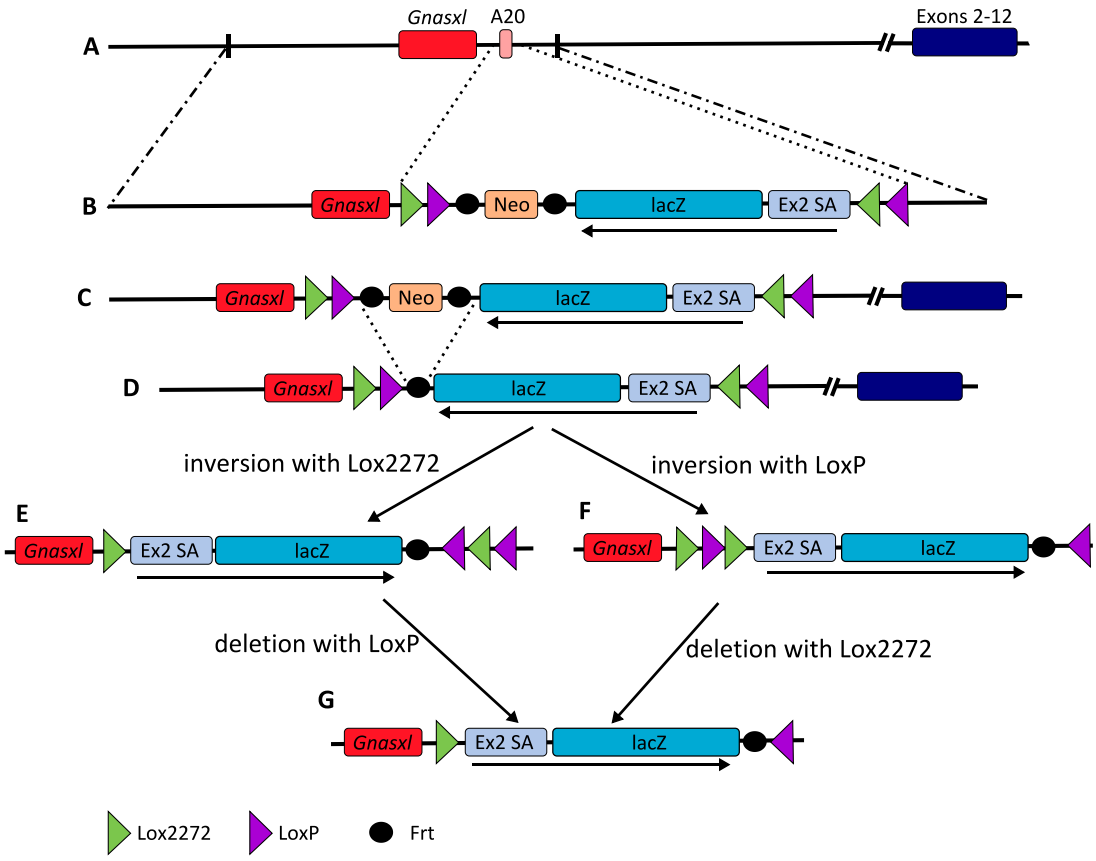

Figure 3.5. Schematic of gene targeting strategy for insertion and inversion of the gene trap cassette into *Gnas* gene locus.

(A) Shows a simplified scheme of the *Gnas* locus focussing on the *Gnasxl* domain indicating *Gnasxl* exon A20 (A20) location downstream of *Gnasxl* exon 1 (*Gnasxl*).

(B) Indicates the structure of the gene-targeting cassette flanked by Lox2272 and LoxP containing a frt-flanked neomycin cassette (Neo), a lacZ cassette and an exon 2 splice acceptor site (Ex2 SA). The arrow indicates the direction of the cassette orientation opposing the normal direction of splicing.

(C) The gene trap cassette inserted into the locus at the position of the A20 exon

(D) The Neo cassette could potentially cause some problems with the correct expression of the full-length XLαs protein in the active gene trap so it was removed by crossing with Flpe mice.

(E) Crossing with Cre mice resulting in the non-permanent inversion of the LacZ-Ex2 SA cassette into the inactive orientation with the Lox2272 sites so there are three lox sites on one side of the gene trap and one on the other side of the cassette

(F) Crossing with Cre mice resulting in the non-permanent inversion of the LacZ-Ex2 SA cassette into the active orientation with the LoxP sites so there are three lox sites on one side of the gene trap and one on the other side of the cassette.

(G) After inversion with the Lox sites deletion occurs at the two excess sites with the opposite lox site in order to lock the gene trap cassette into the active orientation.

Mendelian ratio. Only mice expressing the gene trap on the paternal allele along with Cre would have the required inversion and activation of the gene trap. This could occur between either of the pairs of lox sites (Figure 3.5 E and Figure 3.5 F).

The gene trap cassette is locked in to the active orientation by deletion between the two identical lox sites, leaving only an incompatible pair of lox sites flanking the gene trap cassette (Figure 3.5 G). This produces the XL-βGal fusion protein, in which XLαs functionality is lost, but βGalactosidase activity is retained in place of the XLαs full-length protein as the *Gnasxl* exon 1 splices onto the splice acceptor site on the inverted and active gene trap.

CHAPTER 4. *GNASXL* EXPRESSION: A COMPARATIVE STUDY OF CHANGES BETWEEN NEONATAL AND ADULT DEVELOPMENTAL STAGES I. THE CENTRAL NERVOUS SYSTEM

4.1. INTRODUCTION

4.1.1. PREVIOUSLY DESCRIBED *GNASXL* EXPRESSION PATTERN IN THE CNS

The *Gnasxl* expression pattern has previously been described in brain tissue of neonatal wild type mice using *in situ* hybridisation at neonatal day 4 (PLAGGE *et al.* 2004). These data describe expression in many regions important for the control of energy metabolism and sympathetic outflow including areas of the raphe nuclei, reticular area of the medulla, the laterodorsal tegmental nucleus (LDTg), and the locus coeruleus (LC) (PLAGGE *et al.* 2004). However, there has been no systematic analysis of the adult expression pattern of *Gnasxl* in mouse brain.

A specific phenotype change in feeding behaviour was observed between neonatal and adult stages of development in *Gnasxl*$^{m+/p-}$ mice. It was hypothesised that this could be related to an expression pattern change in nuclei in the brain which innervate muscles required for correct feeding (orofacial motor nuclei). It was also of interest to fully analyse the expression pattern across the adult brain to investigate possible causes of the adult phenotype of increased SNS outflow (XIE *et al.* 2006). The regions of interest and their functions are described in the following sections.

4.1.2. THE HYPOTHALAMUS

The hypothalamus is located at the base of the brain on both sides of the third ventricle, below the thalamus, and between the optic chiasm and the midbrain (Figure 4.1). It is essential for homeostatic regulation and has functions in regulating hunger, thirst, sexual and mating behaviours, pleasures and the fight or flight response. It receives signals from many regions of the brain including the limbic system. The hypothalamus is divided into sub-regions

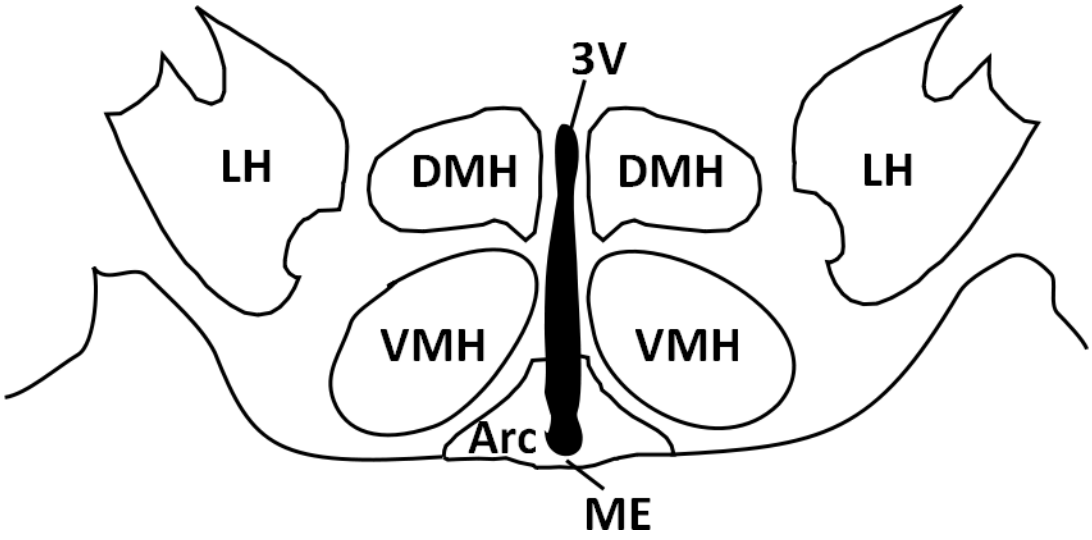

Figure 4. 1. Schematic of the hypothalamus in a coronal section of adult mouse brain.

Diagram showing the main areas of the hypothalamus; these include: the lateral hypothalamus (LH), the dorsomedial hypothalamus (DMH), the Arcuate nucleus (Arc) and the ventrolateral hypothalamus (VMH). The third ventricle (3V) demarks the midline of the brain, and the median eminence (ME) bridges the base of the 3V.

including: the lateral hypothalamus (LH); dorsomedial hypothalamus (DMH); ventromedial hypothalamus (VMH); arcuate nucleus (Arc); the paraventricular nucleus (PVN); and the preoptic area (POA).

4.1.2.1. The Arcuate Nucleus of the Hypothalamus

The Arc is an elongated nucleus – located on the ventral side of the brain and lateral to the third ventricle – containing subpopulations of neurons with differing roles including those involved in feeding and satiety (WILLIAMS *et al.* 2001). One population of neurons expresses both neuropeptide Y (NPY) and agouti-related protein (AgRP), while proopiomelanocortin (POMC-) and cocaine- and amphetamine-regulated transcript (CART-) expressing neurons occupy a second separate population (BROBERGER *et al.* 1998; ELIAS *et al.* 1998; HAHN *et al.* 1998; KRISTENSEN *et al.* 1998). These populations of neurons have opposite effects on food intake and have inhibitory effects on each other under the influence of leptin (NPY/AGRP neurons are orexigenic while POMC/CART neurons are anorexigenic) (Figure 4.2) (ELIAS *et al.* 1999). The Arc has many connections to other regions of the hypothalamus (LH, DMH, VMH and PVN) with information travelling in both directions regarding nutrient status (WILLIAMS *et al.* 2001). Molecules relaying energy status to the brain can be detected by the Arc in the third ventricle, which contains cerebrospinal fluid (CSF) (ELMQUIST *et al.* 1998). This region of the brain is also known to be GABAergic (VONG *et al.* 2011).

At the base of the third ventricle, connecting the two sides of the Arc, is the median eminence. This region is important for nutrient sensing; it is generally considered to be outside the blood-brain barrier and allows peptide hormones, like leptin, ghrelin and glucose, access to the Arc

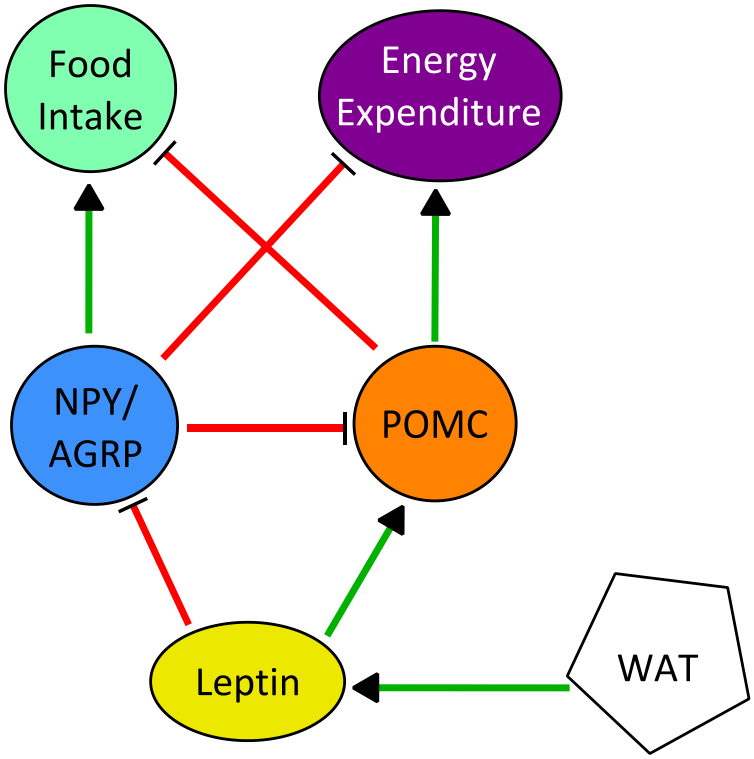

Figure 4.2. Schematic of leptin signalling influencing energy homeostasis through the Arc.
Leptin released from the white adipose tissue (WAT) has stimulatory effects on proopiomelanocortin (POMC)-expressing neurons which are anorexigenic and inhibit food intake and increase energy expenditure. Leptin has an inhibitory effect on neuropeptide Y (NPY)-/agouti-related protein (AgRP)-expressing neurons. NPY-/AgRP-expressing neurons promote food intake and inhibit energy expenditure. NYP/AgRP neurons also have an inhibitory effect on POMC neurons.

(BROADWELL and BRIGHTMAN 1976).

4.1.2.2. The Lateral and Dorsomedial Hypothalamic Nuclei

The LH/DMH region contains two distinct populations of neurons. One population expresses the neuropeptide orexin (also called hypocretin) while the other contains the neuropeptide melanin-concentrating hormone (MCH) (ABIZAID *et al.* 2006). These are both known to play roles in food intake regulation and energy homeostasis (ABIZAID *et al.* 2006; F. BRISCHOUX 2001). These populations will be discussed in greater detail in Chapter 7.

There are also many projections to this area from the NPY neurons in the Arc with reciprocal projections from orexin and MCH neurons, which contain NPY receptors (ELIAS *et al.* 1999; HU *et al.* 1996). Projections from the POMC neurons in the Arc have also been established to have an effect on orexin and MCH neurons in the LH (ELIAS *et al.* 1999). When this nucleus is stimulated, food intake is increased; in opposition to this, destruction of the LH results in weight loss and a decrease in food intake (NAMBU *et al.* 1999; WILLIAMS *et al.* 2001). Glucose-sensitive neurons are abundant in this region of the hypothalamus (BERNARDIS and BELLINGER 1996).

Moving further dorsal, the DMH has connections to the PVN, POA, LH and brainstem (ARMSTRONG 2004; YOSHIDA *et al.* 2009; ZHANG *et al.* 2011). Warm-sensing neurons in the POA have inhibitory effects on the DMH, controlling body temperature through brown adipose tissue (BAT) non-shivering thermogenesis via the sympathetic nervous system (SNS) (FAN *et al.* 2007). It is possible that the DMH and the PVN interact to control food intake and energy expenditure (CHRISTOPHE 1998). This region has been established as expressing XLαs in brain at neonatal day four along with the LH (PLAGGE *et al.* 2004).

4.1.2.3. The Paraventricular Hypothalamus

The PVN is located at the top of, and lateral to, the third ventricle. This region is important not only for integrating many energy homeostatic signals but also for SNS outflow. Many neurotransmitters are found in this region that are related to energy homeostasis including NPY, alpha-melanocyte-stimulating hormone (α-MSH), serotonin (5-HT), galanin, noradrenaline (NA) and opioid peptides (WILLIAMS *et al.* 2001). The PVN has corticotropin-releasing hormone (CRH) projections to the pituitary controlling the secretion of ACTH resulting in the secretion of cortisol (SIMMONS and SWANSON 2009).

4.1.2.4. The Ventromedial Hypothalamus

The VMH is located directly dorsal to the Arc in the hypothalamus. This area is known to inhibit food intake; however, lesioning of the region results in hyperphagia and body weight increases (STELLAR *et al.* 1954). This region has projections to and from the PVN, LH and DMH (ARMSTRONG 2004).

4.1.2.5. The Preoptic Area

The POA receives noradrenaline projections from the LC along with adrenergic projections from the ventrolateral medulla (ASTON-JONES 2004b). The ventrolateral POA has a role in sleep and waking (LU *et al.* 2000). In the POA are warm-sensing neurons and this area of the brain has been implicated in the control of BAT thermogenesis in response to cold (BOULANT and HARDY 1974). The POA is thought to have an inhibitory input onto the DMH and raphe pallidus (RPa). When the warm-sensing POA neurons are inhibited by GABA – released in response to skin cooling – the DMH and RPa neurons are disinhibited and thermogenesis proceeds (MCALLEN 2004; MORRISON and NAKAMURA 2011). MnPO neurons are required for BAT thermogenesis (MORRISON and NAKAMURA 2011). It has been shown that two separate populations of neurons in the POA project to

the DMH and RPa (YOSHIDA *et al.* 2009). The bed nucleus of the stria terminalis (BST) is formed of a fibre bundle which connects the amygdala with other regions of the brain.

4.1.2.6. The Suprachiasmatic Nucleus

The suprachiasmatic nucleus (SCh) is the body's internal clock. This nucleus projects both directly and indirectly to many nuclei in the brain including the DMH and PVN. This suggests that the SCh is not only important for wakefulness but other processes which fluctuate over the period of a day including SNS outflow (ARMSTRONG 2004; VRANG *et al.* 1997).

4.1.3. THE AMYGDALA

The amygdala is a nucleus located in the temporal lobe of the brain and is a part of the limbic system (CAMPBELL 2002). It is composed of several sub-regions: the basolateral complex, the centromedial nucleus (CeA) and the cortical nucleus (AMUNTS *et al.* 2005). There are several known functions of the amygdala. It is involved in arousal, emotion and fear responses as well as hormonal secretions. It is central to the creation and storage of memories as well as the recognition of emotions in facial expressions of other individuals (CAMPBELL 2002).

The amygdala has connections to the hypothalamus and it has been observed that stimulation or disruption of this area results in changes in feeding and drinking behaviours (MIÑANO *et al.* 1992). There are two major routes to the hypothalamus from the amygdala. The first is the stria terminalis: a compact bundle of fibres that originates from the medial, central and basomedial nuclei of the amygdala (MIGUELEZ *et al.* 2001). The second route is the ventral amygdalo-hypothalamic pathway; this arises from the piriform complex and

basolateral nucleus providing a diffuse network of efferent and afferent connections to the hypothalamus (MIGUELEZ *et al.* 2001). Hyperphagia occurs in rats given bilateral lesions at the postero-ventral border of the amygdala. Electrical stimulation of this region stops or greatly reduces food intake (HAN and JU 1990). Depending on the region of the amygdala there are varying numbers of GABA-expressing neurons: there is a high density in the CeA, but surrounding areas are less densely populated (VONG *et al.* 2011). Some diseases for which the amygdala has been investigated include: Alzheimer's disease, autism, schizophrenia, and bipolar disorder (CAMPBELL 2002). The amygdala receives projections which originate in the LC, NTS, and the ventral medulla (CLAYTON and WILLIAMS 2000; FALLON and MOORE 1978; ZARDETTO-SMITH and GRAY 1990; ZARDETTO-SMITH and GRAY 1995).

4.1.4. THE BRAIN STEM

4.1.4.1. The Raphe Nuclei (Figure 4.3)

The raphe nuclei are serotonergic and the main supplier of 5-HT to the brain. Clear links have been established between these nuclei and the medial POA (BERTON and NESTLER 2006; HOLLAND and GOADSBY 2009). These nuclei also have feedback projections to the SCh, indicating they have a role in circadian rhythms. These nuclei also receive efferent fibres from the NTS (NIEUWENHUYS *et al.* 2008).

There are several raphe nuclei and of particular interest are the raphe pallidus (RPa) and the raphe obscurus (ROb). The RPa has many MC4R-expressing neurons and receives projections from the POMC-expressing neurons of the Arc (LEI *et al.* 2008). It has also been established that the RPa neurons project to the sympathetic preganglionic neurons of the

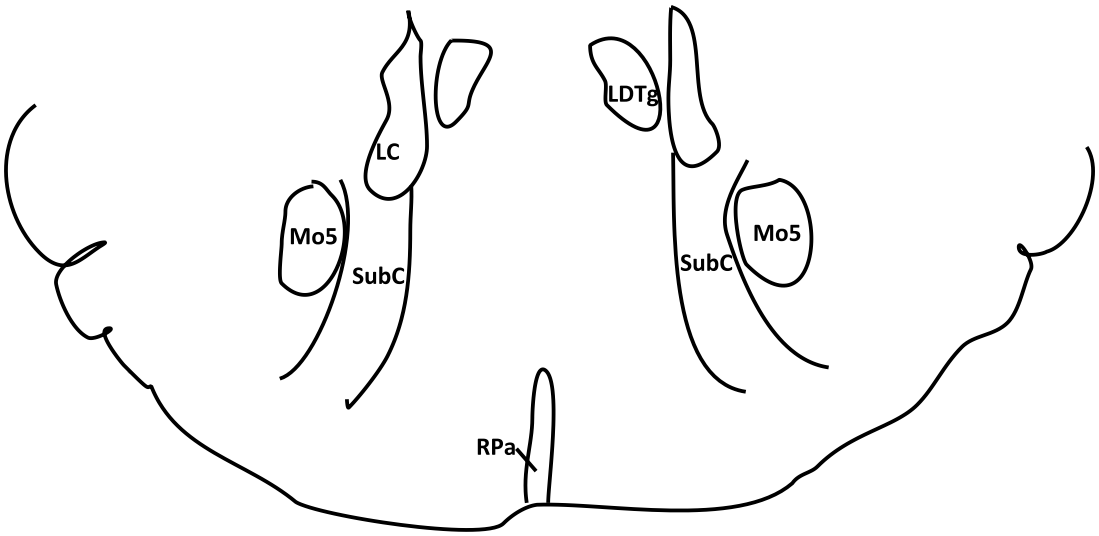

Figure 4.3. Schematic of the pons region of the adult mouse brain in a coronal section

Diagram of the pons region of the brain indicating the locus coeruleus (LC), the motor trigeminal nucleus (Mo5), the raphe pallidus (RPa), the laterodorsal tegmental nucleus (LDTg), and the subcoeruleus (SubC).

intermediolateral layer of the spinal cord (IML) (BACON *et al.* 1990; LOEWY and MCKELLAR 1981) and have implications in the control of BAT thermogenesis(BAMSHAD *et al.* 1999; MORRISON 2001a; MORRISON 2001b). The RPa receives afferent signals from the periaqueductal grey (PAG), PVN, DMH, LH, POA, the CeA, MnPO, Gi and the parvocellular reticular nucleus (HERMANN *et al.* 1997; HOSOYA 1985). It is possible that the RPa is constantly under GABAergic inhibition from the POA in the control of heart rate and BAT thermogenesis (MCALLEN 2004). The ROb has implications in the control of SNS outflow and autonomic motor outflow controlling the hypoglossal nerve (PEEVER *et al.* 2001).

4.1.4.2. The Locus Coeruleus (LC) and the Laterodorsal Tegmental Nucleus (LDTg) (Figure 4.3)

The LC is known to be important in alertness as well as stress response and is the main noradrenergic centre of the brain. It is located in the pons, dorsal to the ventricle. It has close proximity to the LDTg to which it is thought to have connections. These nuclei have a role in alertness and stress but their complete functional roles remain elusive.

Many neurotransmitters involved in alertness and stress are contained in the LC, including GABA, galanin, NPY, vasopressin, neurophysin, neurotensin, vasoactive intestinal peptide and atrial natriuretic factor (ASTON-JONES 2004a). Orexin stimulates the LC by decreasing the resting potassium conductance (HAGAN *et al.* 1999; HORVATH *et al.* 1999; IVANOV and ASTON-JONES 2000) – evidence that the LC is important for arousal and waking as these are affected by orexin (ASTON-JONES and BLOOM 1981a; SAKURAI 2007). There is also evidence that GABA inhibits the LC during sleep – further showing that this nucleus is involved in alertness and wakefulness (ASTON-JONES and BLOOM 1981a; ASTON-JONES and BLOOM 1981b).

Many receptors are found in the LC; these include leptin receptor (LepR) (HAY-SCHMIDT *et al.* 2001) as well as orexin receptors (SUNTER *et al.* 2001) and corticotropin-releasing hormone (CRH) receptors (MORIN *et al.* 1999). Although the presence of receptors does not always correspond to effects on the nucleus, it has been shown that CRH and serotonin have inputs to the nucleus (ASTON-JONES 2004b).

The LC has far-reaching projections in the brain as well as from many regions of the brain. Specific inputs have been observed from the medial POA (RIZVI *et al.* 1992) and the PAG (ENNIS *et al.* 1991). The LC is known to have projections to the POA (DUBOIS *et al.* 2006), the amygdala (CLAYTON and WILLIAMS 2000; FALLON and MOORE 1978) and the wall of the PVN (CUNNINGHAM and SAWCHENKO 1988).

LC neurons projecting to the spinal cord regulate sensory perception (FRITSCHY and GRZANNA 1990), as do LC neurons projecting to the brainstem (FRITSCHY and GRZANNA 1990; LEVITT and MOORE 1979). Interestingly, the LC's activity appears to be controlled by circadian rhythms produced by the SCh (ASTON-JONES *et al.* 2001). The SCh projects indirectly to LC via the DMH (ASTON-JONES *et al.* 2001).

The area surrounding the LC which includes the subcoeruleus (SubC) also has many inputs including the NTS (ENNIS and ASTON-JONES 1989a; ENNIS and ASTON-JONES 1989b; MANTYH and HUNT 1984; VAN BOCKSTAELE *et al.* 1996; WALLACE *et al.* 1989), the dorsal horn of the spinal cord (CECHETTO *et al.* 1985; STANDAERT *et al.* 1986) and the CeA (ASTON-JONES *et al.* 1986; VAN BOCKSTAELE *et al.* 1996). This region includes the A7 noradrenergic nucleus.

There is little functional data describing the LDTg. It is thought that the

nucleus has functions in controlling stress responses and alertness and the main studies into the region have been investigating this involvement.

The LDTg is a cholinergic nucleus with connections to the ventral tegmental area (VTA), which stimulates the limbic system (BLAHA *et al.* 1996; KIMURA *et al.* 1981; MESULAM *et al.* 1983; SHUTE and LEWIS 1967). The LDTg receives stimulatory innervations from orexin-expressing neurons and therefore has implications for sleep and wakefulness (BURLET *et al.* 2002; PEYRON *et al.* 1998). GABAergic and glutamatergic neurons have been detected in the nucleus contained in separate populations (CLEMENTS and GRANT 1990; WANG and MORALES 2009). Glutamate neurons are located in the rostral part of the nucleus, while the GABA-expressing neurons are in the caudal part (WANG and MORALES 2009). Ghrelin receptor (GHSR) and CRH-expressing neurons have also been identified in the neurons of this nucleus (ALON *et al.* 2009; ZIGMAN *et al.* 2006). The nucleus has projections to the thalamus, hypothalamus, substantia nigra, ventral tegmental nucleus and cortex. There are three known populations of neurons in the region: the first is the cholinergic neurons involved in both wakefulness and REM sleep (EL MANSARI *et al.* 1989); the second is involved in REM sleep only (EL MANSARI *et al.* 1989); and the third group are involved in wakefulness only (KAYAMA *et al.* 1992). The removal of XLαs in this nucleus has previously been suggested as a cause of the lethargy of XLαs-deficient mice (PLAGGE *et al.* 2004).

4.1.4.3. The Nucleus of the Solitary Tract (NTS) (Figure 4.4)

The NTS carries and receives vicsceral signals of sensation and taste from the facial, glossopharengeal and vagus nerves. This nucleus is long: stretching almost the entire length of the medulla oblongata, starting above the

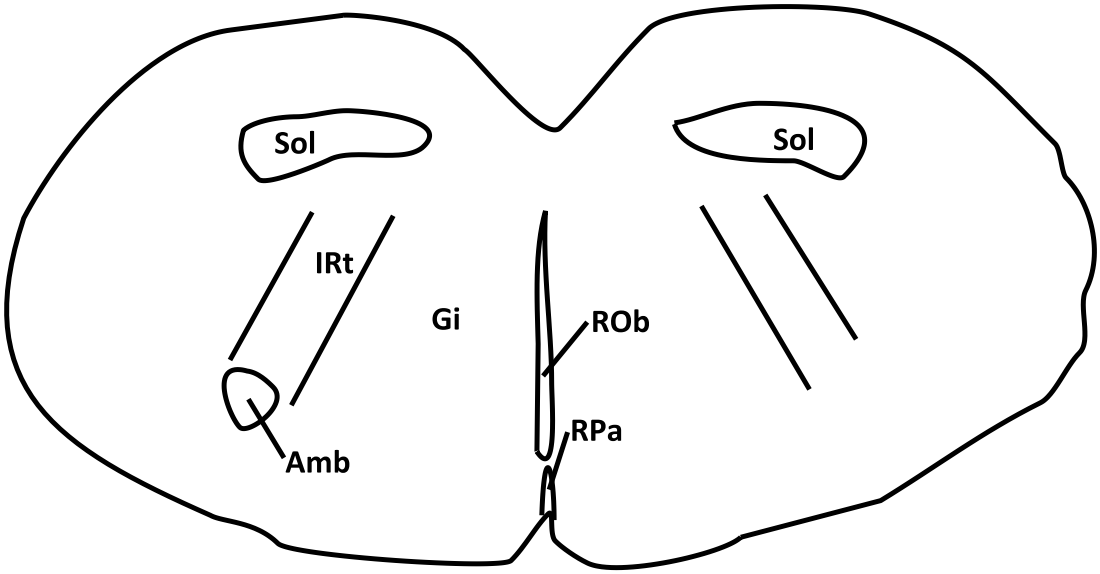

Figure 4. 4. Schematic of the medulla oblongata region of the mouse brain in a coronal section

Diagram of the medulla oblongata showing the main nuclei of the region including the nucleus of the solitary tract (Sol), the reticular area (IRt and Gi), the ambiguus nucleus (Amb), and the raphe nuclei (ROb and RPa)

central canal in the posterior brain stem and becoming more laterally positioned as it moves anterior. Medial NTS neurons are responsible for processing gastrointestinal vagal afferent signals coming from food intake and stimulation of the stomach and gut (HAYES and COVASA 2006; SCHWARTZ 2002; VRANG *et al.* 2003; WILLING and BERTHOUD 1997). In addition to nutrient signals, the NTS is also known to process afferent signals from the cardiovascular and respiratory systems (TAYLOR *et al.* 1999). The NTS, as part of the hindbrain circuitry, is likely to mediate the size of food intake inhibition signals (GRILL and HAYES 2009). Meal size is determined by gastrointestinal signals acting on the brainstem. This CNS system relays important information about nutrient status of the periphery to the brain. The main input of this system is through the NTS, which then relays information to other regions in the brain. It has been suggested that leptin acts upon the NTS through projections from the hypothalamus (SCHWARTZ 2002). However, it has been shown that the NTS possesses its own LepR and that leptin injection into the NTS reduces food intake (GRILL *et al.* 2002; MÜNZBERG *et al.* 2004). POMC-expressing neurons found in the NTS have a different role in signalling than the POMC-expressing neurons in the Arc (PERELLO *et al.* 2007). NTS neurons project to the hypothalamus but these neurons do not include those expressing POMC (GRILL 2006; GRILL and HAYES 2009; SCHWARTZ 2002).

4.1.4.4. Gigantocellular Reticular Nucleus of the Medulla (Gi) (Figure 4.4)

This nucleus is made up of giant neuronal cells and innervates the caudal hypoglossal nucleus by exciting the hypoglossal nerve. It is known to respond to glutamatergic stimuli. The diffuse region has inputs from the PAG, PVN, CeA and the parvocellular reticular nucleus (LOEWY *et al.* 1981). It is known to mediate

cardio-inhibition (SU *et al.* 1991). This nucleus innervates the neurons in the IML (LOEWY *et al.* 1981).

4.1.4.5. Ambiguus Nucleus (Figure 4.4)

The ambiguus nucleus (Amb) is located in the lateral part of the medulla and gives rise to the branchial efferent fibres of the vagus nerve. The external formation contains cholinergic preganglionic parasympathetic neurons for the heart. It acts with the dorsal motor nucleus of the vagus nerve to decrease cardiac activity in response to fast increase in blood pressure. The Amb strongly innervates the soft palate (STRUTZ *et al.* 1988).

4.1.4.6. Orofacial Motor Nuclei

The three orofacial motor nuclei – the motor trigeminal nucleus (Mo5), the hypoglossal (12N) and the facial nucleus (7N) – receive projections containing neurotransmitters and neuromodulating substances, which have both excitatory and inhibitory effects (TRAVERS 2004). Although the three nuclei are defined by individual characteristics, they have a co-ordinated influence on the stimulation of facial muscles during many behaviours including feeding, grooming and respiration (TRAVERS 2004).

The noradrenergic A7 and A5 cell groups are the main sources of noradrenaline to the Mo5 (GRZANNA *et al.* 1987; VORNOV and SUTIN 1983) (Figure 4.3). This nucleus is one of the important orofacial nuclei in the brainstem controlling facial muscles.

The 12N extends the length of the medulla located close to the midline below the central canal and is important for the control of the tongue (TRAVERS 2004). Many of the neurons in this nucleus express MCH1R (SAITO *et al.* 2001). The nucleus has been found to be a receiver of cholinergic and noradrenergic innervations (ALDES *et al.* 1992; CONNAUGHTON *et al.* 1986). It is known that the

SubC projects to the 12N and the SubC projections fall into the 12N in the same pattern as the noradrenergic neurons that are known in this region (TRAVERS 2004).

The 7N is involved in the control of facial muscles which are essential for suckling in neonates. Deletion of XLαs in this nucleus had previously been suggested as a possible cause of the suckling deficiency in the *Gnasxl*$^{m+/p-}$ neonates (PLAGGE *et al.* 2004). The 7N is another nucleus in which XLαs was shown to be highly expressed in neonatal tissue (PLAGGE *et al.* 2004).

4.1.5. SPINAL CORD

The spinal cord is the relay centre between peripheral tissues and the brain. There are many different types of neurons in separate populations in the spinal cord including the intermediolateral layer (IML), which contains sympathetic preganglionic neurons (SPNs) involved in SNS outflow to the periphery, including the adrenal glands (BACON and SMITH 1988). The ventral part of the spinal cord contains motor neurons (VMNs).

4.1.6. AIMS

To date, there has been no systematic analysis of *Gnasxl* expression in the brain in adult mice. As a comparison to the previously described neonatal expression pattern (PLAGGE *et al.* 2004), the aim of this project was to provide a comprehensive overview of staining in one-day old mice and adult tissue. Previously, neonatal staining was performed on four-day old mice using *in situ* hybridisation (PLAGGE *et al.* 2004). It was necessary to compare the two in a systematic way using more than one histological technique and to document changes between the two phases of development that might account for the phenotypic change that was previously described in *Gnasxl*$^{m+/p-}$ mice (PLAGGE *et*

al. 2004; XIE *et al.* 2006) and to establish any areas of the brain in which deletion of XLαs might result in the increased SNS outflow that has been described in *Gnasxl*$^{m+/p-}$ mice (XIE *et al.* 2006).

4.2. MATERIALS AND METHODS

4.2.1. TISSUE COLLECTION

For neonatal histology WT, *Nestin-Cre/+; +/XLlacZGT and CMV-Cre/+; +/XLlacZGT* brains were collected and placed in 4% PFA overnight and then placed in 30% sucrose until required. For adult histology WT, *Gnasxl*$^{m+/p-}$ and *CMV-Cre/+; +/XLlacZGT* mouse brains were collected by perfusion as described below.

4.2.2. ADULT MOUSE PERFUSION

Mice were deeply anaesthetised with an intraperitoneal (i.p.) injection of pentobarbitone. Once the mouse was deemed to be brain-dead, the chest was cut open and the right atrium of the heart punctured to allow blood to drain from the circulatory system. Mice were perfuse-fixed by injection of PBS then 4% PFA in PBS into the left ventricle of the heart. Relevant tissues were dissected out and the tissues placed in 4% PFA for appropriate times of fixation depending on technique (several minutes for XGal staining; overnight for cryosectioning). Tissues were transferred to 30% sucrose for 24-48 hours at 4°C to dehydrate and cryoprotect them. Tissues could then be processed for sectioning.

4.2.3. SECTIONING OF TISSUES

4.2.3.1. Cryosectioning

Perfuse-fixed tissues were mounted in Shandon Cryomatrix (Thermo Scientific) and serial frozen sections were cut using a Leica CM1950 cryostat (14 or 25 µm) onto SuperFrost* Plus slides (Thermo Scientific) in sets of ten. 14 and 25 µm sections were used for immunofluorescence and immunohistochemistry and required antigen retrieval (see below) for staining

to be clearly observed. These were used to visualise strongly-stained areas with immunohistochemistry and for colocalisation studies with immunofluorescence.

4.2.3.2. Microtome Sectioning

Tissues were mounted onto the Leica 2000R microtome stage, cryoprotected with 30% sucrose in PBS and allowed to freeze fully using dry ice. Serial sections of 80 µm were collected into 24-well plates filled with cryoprotectant (6 sections per well). These sections were used for immunohistochemistry only and did not require an antigen retrieval step. Thicker sections were used to visualise weakly-stained areas of tissue.

4.2.3.3. Vibratome Sectioning

After perfusion and brief fixation in 4% PFA, whole brains were washed four times in 1 x PBS for 10 minutes then trimmed back to create a flat surface for mounting. The cut edge was dried slightly then glued to the chuck with cyanoacrylate gel. The chuck and tissue were then fixed into the vibratome and submerged in PBS. Slices were cut at 300-500 µm using high vibration speeds and low cutting speeds. Cut sections were placed in 4% PFA in a 12-well plate for 5 minutes, washed twice with 1 x PBS, then used in XGal staining protocols.

4.2.4. ANTIBODIES

For immunohistochemistry the following primary antibodies were used: goat anti-XLαs (M14) (Santa Cruz; sc-18993; 1:200). The following secondary antibodies were used: Vectastain Elite biotin-conjugated rabbit anti-goat (Vector Laboratories; PK6105; 1:200) and Affinipure™ donkey anti-goat Biotin conjugated (Jackson ImmunoResearch Laboratories; 705-065-147; 1:3000).

For immunofluorescence the following primary antibodies were used: goat anti-ChAT (Millipore; AB144P; 1:100), chicken anti-βGalactosidase

(Abcam; ab9361; 1:500), and rabbit anti-βGalactosidase (Cappel; 55976; 1:2000). The following secondary antibodies were used: DAPI (Invitrogen; 1:1000), donkey anti-chicken Dylight 594 (Jackson ImmunoResearch Laboratories; 703-515-155; 1:3000), donkey anti-rabbit AF594 (Invitrogen; A21207; 1:1000) and donkey anti-goat AF488 (Invitrogen; A11055; 1:1000).

4.2.5. Antigen Retrieval

Sections were incubated with 10 mM sodium citrate (Sigma) at 60°C by heating in a microwave for 45 seconds. Sections were allowed to cool in solution for 1 minute before continuing with staining protocols.

4.2.6. Vectastain Elite Kit for Immunohistochemistry (Appendix 4)

14-80 µm sections were treated for antigen retrieval if necessary (see above) and washed three times in PBS for 5 minutes. A quenching step (1 minute in a solution of 0.03% H_2O_2 in 100% MeOH) was included to remove the endogenous horse radish peroxidise-like activity in blood vessels. Sections were washed three times for 5 minutes with PBS and incubated in 10% normal serum (Sigma or Vector Laboratories) in PBS for 1 hour at room temperature. These were transferred into primary antibody diluted in 10% normal serum in PBS overnight at 4°C. Sections were washed three times for 5 minutes in PBS and incubated with a biotin-conjugated secondary antibody in 10% normal serum in PBS for 1 hour at room temperature. After the secondary antibody was applied to sections, the avidin-biotin complex (ABC) solution was prepared. Sections were washed three times for 5 minutes and incubated with ABC solution from the Vectastain Elite Kit (Vector Laboratories) for 30 minutes at room temperature followed by washes in PBS and incubation with 3,3'-diaminobenzidine (DAB; Sigma) solution containing nickel chloride (1:100

dilution of 50% w/v stock). After washing with PBS and ddH_2O, sections were dehydrated with 70% EtOH, 90% EtOH, twice with 100% EtOH and finally cleared twice with Histo-clear™ (National Diagnostics) before being mounted with Eukitt® quick hardening mounting medium (Fluka).

80 µm free-floating microtome sections were carried through the above solutions in 24-well plates. After completion of the staining they were mounted from PBS onto polylysine slides (Thermo Scientific) and allowed to air-dry over night before being put through the dehydrating EtOH series and mounting with Eukitt®.

4.2.7. IMMUNOFLUORESCENCE (IF)

14 µm cryostat sections were treated for antigen retrieval (see above) then washed three times for 5 minutes with PBS, incubated for one hour with 500 µL blocking serum (10% donkey serum (Sigma); 1x PBS) then incubated in 500 µL primary antibodies diluted in blocking serum containing 0.25% TritonX100 (Fluka) overnight at 4°C. Primary antibody solutions were removed and the slides were washed three times for 15 minutes in PBS, incubated in 500 µL of a solution of secondary antibodies diluted in blocking serum containing 0.25% TritonX100. Antibody solutions were discarded and the slides washed three times in PBS for 15 minutes. Slides were mounted with Fluorogel (Electron Microscopy Sciences), allowed to air-dry, sealed and stored at 4°C.

4.2.8. XGAL STAINING

Whole mount tissues or 14 µm cryostat sections were fixed briefly with 4% PFA before being incubated with a pre-warmed solution (37°C) of XGal overnight at 37°C. Whole mount tissues were then fixed and stored in 4% PFA in PBS and cryostat sections were dehydrated and mounted with Eukitt®.

4.2.9. *IN SITU* HYBRIDISATION

4.2.9.1. Linearization of Probe

Using RNAse-free conditions, 10-20 μg of the plasmid containing the insert of more than 1 kbp was linearised by digestion with a 5'-overhang producing restriction enzyme that cuts at the 5'-end of the insert. This was run on a 1% agarose gel from which the linearised plasmid was extracted.

4.2.9.2. Gel Extraction (Geneflow)

Using RNAse-free conditions, gel fragments of the expected molecular weight were excised from the agarose gel. Gel pieces were weighed and equal volumes of binding buffer were added to the gel pieces. These were incubated at 65°C for 5-10 minutes with gentle vortexing at intervals until the agarose had dissolved. Equal volumes of binding buffer were added and then incubated at room temperature for 1 minute. The mixture was then added to a spin column supplied with the Geneflow kit and allowed to stand for 1 minute. The spin column was centrifuged for 1 minute and the flow-through discarded. 500 μL of wash solution I was added to the column. The column was centrifuged for 15 seconds and the flow-through discarded. This step was repeated. The column was spun for 1 minute to remove residual wash solution and then the column was transferred to a new 1.5 mL centrifuge tube. 30 μL of elution buffer was added onto the membrane in the column and it was incubated for 2 minutes at room temperature. Finally, the column was spun and the probe collected in the new tube. The extracted plasmid was EtOH precipitated and resuspended in a small volume to get a concentration of ~0.5-1.0 μg/μL.

4.2.9.3. EtOH Precipitation

To the sample from which DNA was to be extracted, either equal volumes of isopropanol (if sample buffers contained high salt levels) or 0.1 volume sodium acetate pH5.0 and 2.5 volumes EtOH (if buffers contained low salt

levels) were added. This was inverted until white strands of DNA could be seen precipitating out of the solution. This was centrifuged for 30 seconds to form a DNA pellet. The supernatant was removed and discarded and the DNA pellet was washed twice with 70% EtOH, centrifuging in between and removing the supernatant. The DNA pellets were air-dried at 37°C for 5-10 minutes and resuspended in an appropriate volume of 1 x TE with RNAse.

4.2.9.4. DIG-labelling of Antisense RNA Probe by In Vitro Transcription

The following components were incubated at 37°C for 2 hours: 12.5 µL RNAse-free water; 4 µL 5x transcription buffer; 2 µL 10x DTT; 2 µL 10x DIG-RNA labelling mix; 0.5 µL RNAse inhibitor (1 U/µL); 3µl (this is approximately 1 µg) linearised template plasmid; and 1 µL T7 RNA polymerase (1 U/µL). After 2 hours the following components were added to the reaction mix: 23 µL RNAse-free water; 5 µL 10x RNAse-free DNAse buffer; and 2 µL RNAse-free DNAse. This was incubated at 37°C for a further 30 minutes. To estimate final probe concentration 1 µL was removed from the reaction mixture and put into 20 µL 50% formamide.

4.2.9.5. Purification of DIG-Labelled RNA Probe

ProbeQuant G-50 Micro Sephadex Column (GE Healthcare) resin was resuspended and placed in a 2 mL support tube. This was spun at 735 g for 1 minute. Flow-through was discarded and the column returned to the support tube. 50 µL of *in vitro* transcription reaction was added to the column and spun again at 735 g for 1 minute; the flow-through contained the DIG-labelled RNA probe. For the gel estimation of concentration, 1 µL was removed and added to 20 µL 50% formamide. To the probe, 2 µL of RNAse inhibitor was added and it was stored at -20°C.

4.2.9.6. Gel Estimation of Probe

Before and after purification, probe samples were run on 1 % agarose gels with the λHinDIII and 1 kb DNA ladders (New England Biolabs) for comparison. Probe band strength was compared to bands of known DNA concentration in the ladders to determine the concentration of the probes.

4.2.9.7. Hybridisation of Adult Brain Sections

14 µm frozen sections were dried at 50°C. These were post-fixed in cold 4% PFA/PBS for 20 minutes then washed twice in PBS, followed by two 15-minute carbethoxylation washes in active 0.1% DEPC/PBS. The sections were equilibrated in DEPC-treated 5 x SSC for ~10 minutes, then pre-hybridised in hybridisation buffer (50% Formamide, 5 x SSC and 40 µg/mL salmon sperm DNA [heat denatured for 10 minutes]) for 2 hours at ~58°C. Hybridisation was carried out in the same buffer containing 0.4 µg/mL DIG-labelled RNA probe; slides were covered in parafilm and sealed in an airtight box overnight at 58°C. Parafilm was removed from slides and sections washed in: 2 x SSC at room temperature for 30 minutes; 2 x SSC at 65°C for 1 hour; 0.2 x SSC at 65°C for 1 hour; PBS/0.05% Tween20 at 65°C for 10 minutes; and PBS/0.05% Tween20 (Sigma) at room temperature for 10 minutes. Sections were blocked for 2 hours at room temperature with ~400 µL per slide blocking serum (0.05% Tween20, 5% sheep serum, 0.5-5% milk powder; 1 x PBS) and then incubated with the same solution containing alkaline phosphatase-conjugated anti-DIG-Fab fragments (Roche; 11093274910; 1:5000) at 4°C overnight. Sections were washed three times in TPBS for 30 minutes at room temperature, equilibrated for 5 minutes in alkaline phosphatase buffer (100 mM Tris-HCl, 100 mM NaCl, 50 mM $MgCl_2$, pH 9.5) and incubated with 400 µL of the same alkaline phosphatase buffer containing 45 µL NBT and 35 µL BCIP (for stocks see buffer

and solutions) per 10 mL alkaline phosphatase buffer overnight, in the dark, at room temperature. The reaction was stopped with PBS and post-fixed in 4% PFA/PBS for 20 minutes. Slides were washed with ddH_2O, dehydrated (with 2 minute incubations with 70%, 90%, 100%, 100% EtOH), cleared twice in Histo-clear™ for 2 minutes and mounted with Eukitt®.

4.2.10. IMAGING

Epifluorescence images were taken using a Zeiss Axioskop 40 microscope and Axioskop vision v4.6 software. Confocal images were taken using a Leica SP2 confocal microscope. Bright field images were taken using a Leica mz16 microscope for overview and whole mount images; higher magnification bright field images were taken using an inverted Leica DM IRB or an upright Leica Leitz DM RB microscope.

4.3. RESULTS

4.3.1. TISSUE PROCESSING FOR HISTOLOGY

The first method used to analyse the brain expression pattern of *Gnasxl*-derived proteins, was an antibody against a *Gnasxl* exon 1-encoded peptide. This antibody detects both XLαs and the truncated neural-specific XLN1 protein but not $G_s\alpha$. The specificity of the antibody was tested in the *Gnasxl*$^{m+/p-}$ mouse line along with a wild type sibling, under the same conditions, showing that the antibody was specific for the *Gnasxl*-derived proteins XLαs and XLN1 (Figure 4.5). In histology it is not possible to distinguish between the expression of these two proteins, and any expression described as XLαs protein would include both XLαs full-length and the truncated XLN1 in brain sections. The second method of detection used was XGal staining for the detection of XL-βGal fusion protein (XL-βGal) in *Cre/+; +/XLlacZGT* gene trap mice described in Chapter 3. The fusion protein was expressed in tissues where XLαs had been removed by crossing with specific Cre-expressing mice, for example *Nestin-Cre* (TRONCHE *et al.* 1999) or *CMV-Cre* (SCHWENK *et al.* 1995). *Nestin-Cre* is regarded as a brain-specific Cre-deleter, while *CMV-Cre* is an early embryonic general Cre-deleter.

Sections were made of neonatal and adult wild type brains at 14 or 80 μm for detection of XLαs protein in immunohistochemistry. Neonatal *Nestin-Cre/+; +/XLlacZGT* whole brains were used in XGal staining for XL-βGal and then sectioned on a freeze microtome at 80 μm after cryoprotection and dehydration in 30 % sucrose. Adult *CMV-Cre/+; +/XLlacZGT* brains were sectioned at 500 μm on a vibratome before being stained for the fusion protein with XGal.

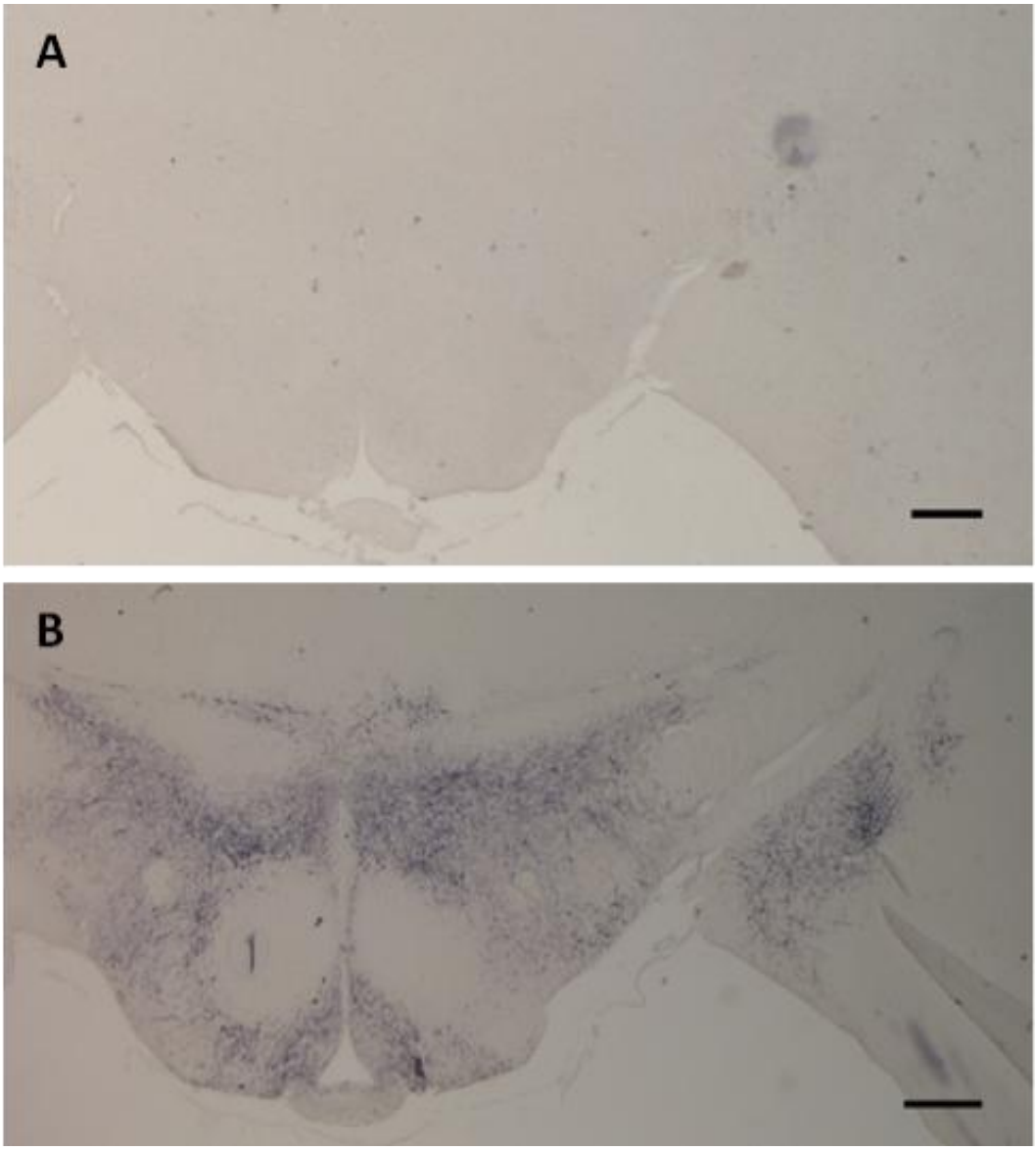

Figure 4.5. Control staining for XLαs in a *Gnasxl*$^{m+/p-}$ adult brain and a wild type littermate

(A) *Gnasxl*$^{m+/p-}$ mouse brain probed using anti-XLαs antibody showing no staining in the hypothalamus.

(B) Wild type sibling of the mouse in **(A)** showing clear staining of the hypothalamus. These tissues were stained using the anti-XLαs antibody at the same time under the same conditions.

14 µm coronal cryostat sections; 500 µm scale bar

4.3.2. *GNASXL* EXPRESSION IN THE NEONATAL HYPOTHALAMUS IS MAINTAINED AND BECOMES MORE WIDESPREAD IN ADULT TISSUE.

In the hypothalamus of neonatal tissue, expression of XLαs was observed in the LH, DMH and PVN (Figure 4.6 A). There was a small amount of staining in the Arc at neonatal day 1 (Figure 4.6 A). All of this staining was reproducible with XGal staining for XL-βGal fusion protein in neonatal *Nestin-Cre*/+; +/*XLlacZGT* mice (Figure 4.7 A and C). No XLαs was detected in the VMH with either mouse line (Figure 4.6 A; Figure 4.7 C). There was also clear staining in the POA of both wild type and *Nestin-Cre*/+; +/*XLlacZGT* mice (Figure 4.6 C; Figure 4.7 A). The SCh was positive for XLαs and XL-βGal (Figure 4.7 D). Blood vessel staining in neonatal tissue was not expected but was consistently observed with XGal staining in neonatal *Nestin-Cre*/+; +/*XLlacZGT* mice (Figure 4.7).

In adult tissue, the hypothalamic expression pattern remains largely the same as neonatal brain with more widespread staining in each of the nuclei that express XLαs. The LH, DMH and PVN all have more widespread staining (Figure 4.8; Figure 4.9 A and B). The Arc continues to develop after neonatal day 1 and in adult mice many neurons in this nucleus express XLαs in wild types as shown with IHC (Figure 4.8 A and C); in *CMV-Cre*/+; +/*XLlacZGT* mice there were few XL-βGal-positive neurons in the Arc (Figure 4.9 A; Figure 4.10 A). The SCh continues to be stained at adult stages of development with increased expression (Figure 4.8 D; Figure 4.9 D; Figure 4.10 A). The XLαs expression in the POA is also expanded in adults and can be defined as the BSTMA, LSV, ADP, MnPO; this staining can be confirmed with both IHC for XLαs (Figure 4.11) and XGal for XL-βGal fusion protein (Figure 4.10 A). Expression in the amygdala

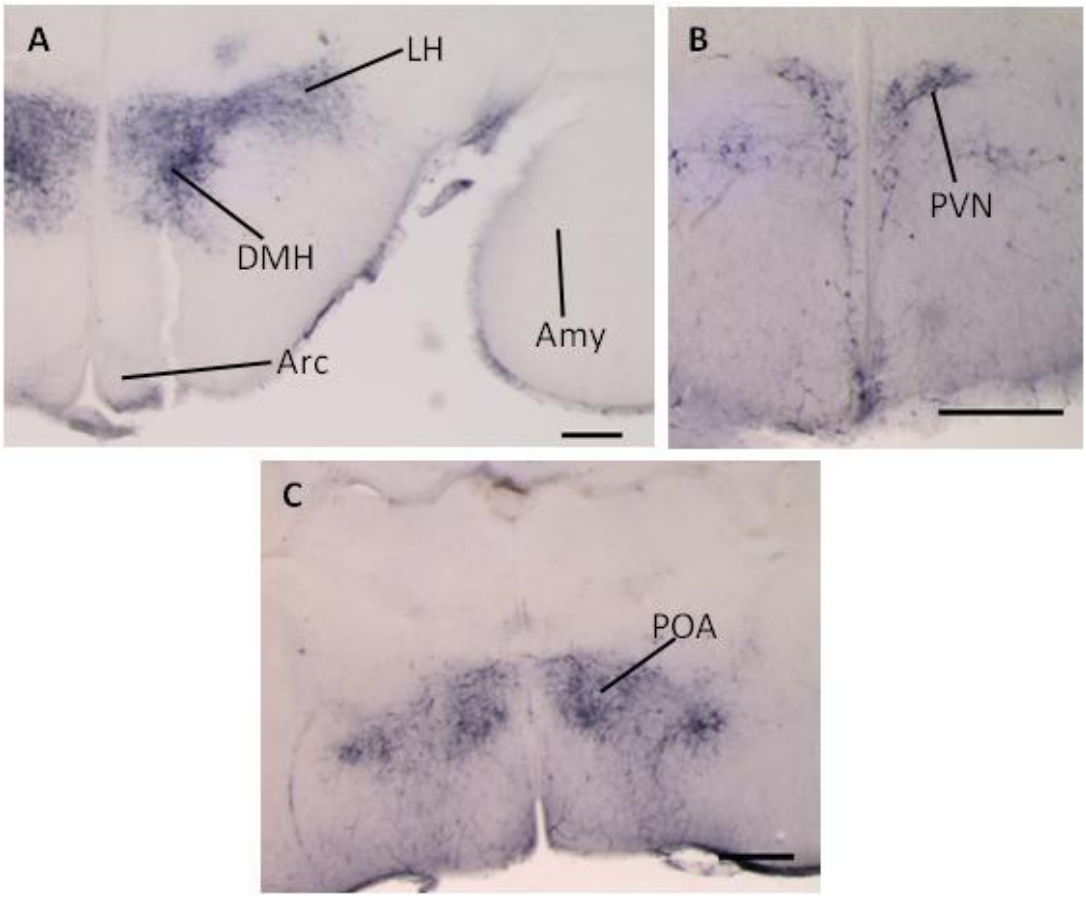

Figure 4.6. Neonatal expression of *XLαs* protein in the hypothalamus

(A) Neonatal wild type brain stained for XLαs protein showing the lateral hypothalamus (LH), the dorsomedial hypothalamus (DMH) and the arcuate nucleus (Arc). The amygdala does not show any XLαs expression at this stage.

(B) XLαs expression in the neonatal paraventricular nucleus (PVN).

(C) Neonatal wild type brain stained for XLαs protein showing the preoptic area (POA).

500 μm scale bars; 80 μm free floating coronal microtome sections

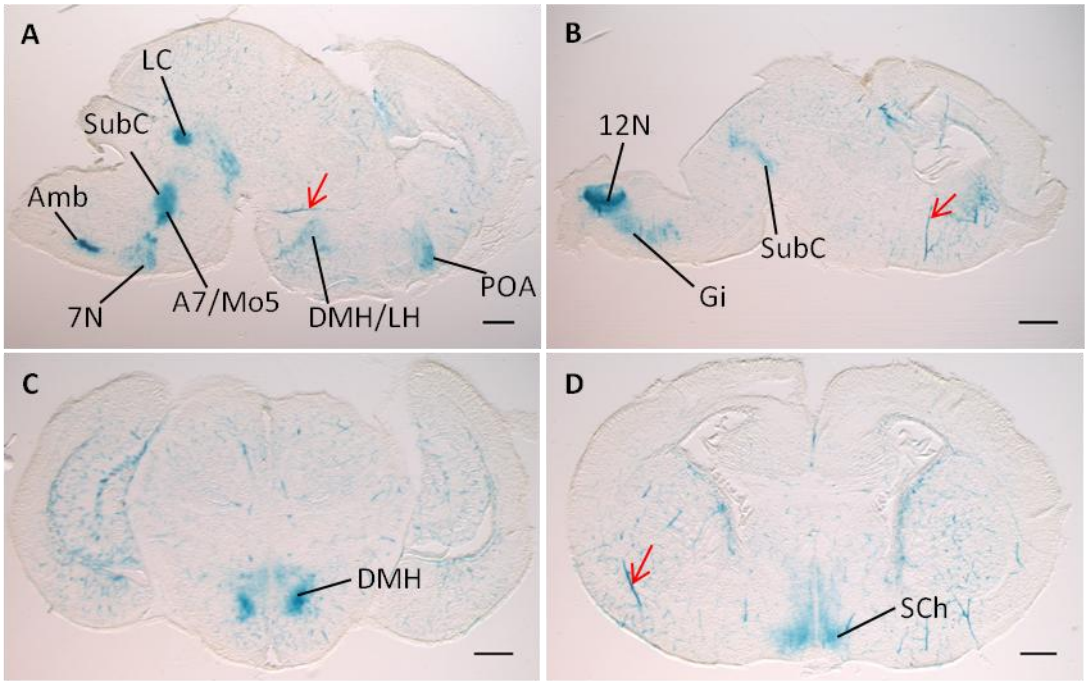

Figure 4.7. Sections of neonatal *Nestin-Cre/+; +/XLlacZGT* mice stained for XL-βGal with XGal

(A) Sagittal section of the neonatal brain stained for XL-βGal fusion protein using XGal showing the ambiguus nucleus (Amb), subcoeruleus (SubC), locus coeruleus (LC), facial nucleus (7N), motor trigeminal nucleus (Mo5), noradrenergic A7 nucleus (A7), dorsomedial hypothalamus (DMH), lateral hypothalamus (LH) and the preoptic area (POA).

(B) Sagittal section of neonatal brain stained for XGal showing the hypoglossal nucleus (12N), gigantocellular reticular nucleus (Gi) and the subcoeruleus (SubC).

(C) Neonatal *Nestin-Cre/+*; *+/XLlacZGT* coronal brain section stained for XL-βGal fusion protein with XGal showing the DMH.

(D) Coronal section of Neonatal *Nestin-Cre/+*; *+/XLlacZGT* anterior brain stained for XLαs showing the suprachiasmatic nucleus (SCh).

Red arrows indicate blood vessel staining; scale bars are 500 μm; crosses were performed with male *XLlacZGT*-carrying mice and female *Nestin*-Cre mice; 80 μm freeze microtome sections.

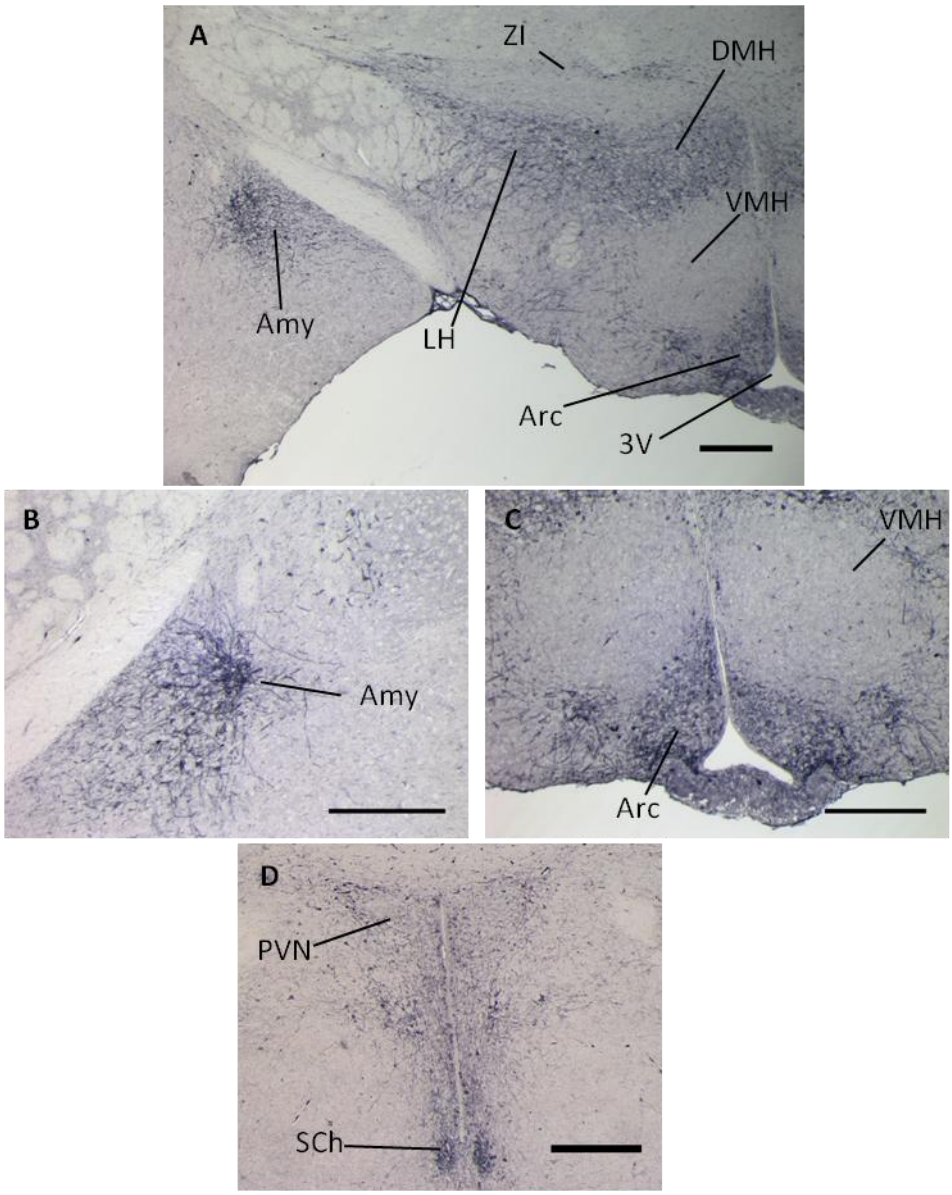

Figure 4.8. Adult hypothalamus stained for XLαs protein in wild type mice

(A) Overview of XLαs expression in the adult hypothalamus of wild type brain showing the amygdala (Amy), lateral hypothalamus (LH), zona incerta (ZI), dorsomedial hypothalamus (DMH) and arcuate nucleus (Arc) express XLαs. The ventromedial hypothalamus does not express XLαs. 3V third ventricle.

(B) Magnified image of amygdala expression of XLαs. Axonal staining can be clearly seen in this nucleus.

(C) Magnified image of Arc and VMH

(D) Expression of XLαs in the anterior hypothalamus of an adult wild type mouse showing XLαs is expressed in the paraventricular nucleus of the hypothalamus (PVN) and the Suprachiasmatic nucleus (SCh)

14 µm coronal cryostat sections; 500 µm scale bars

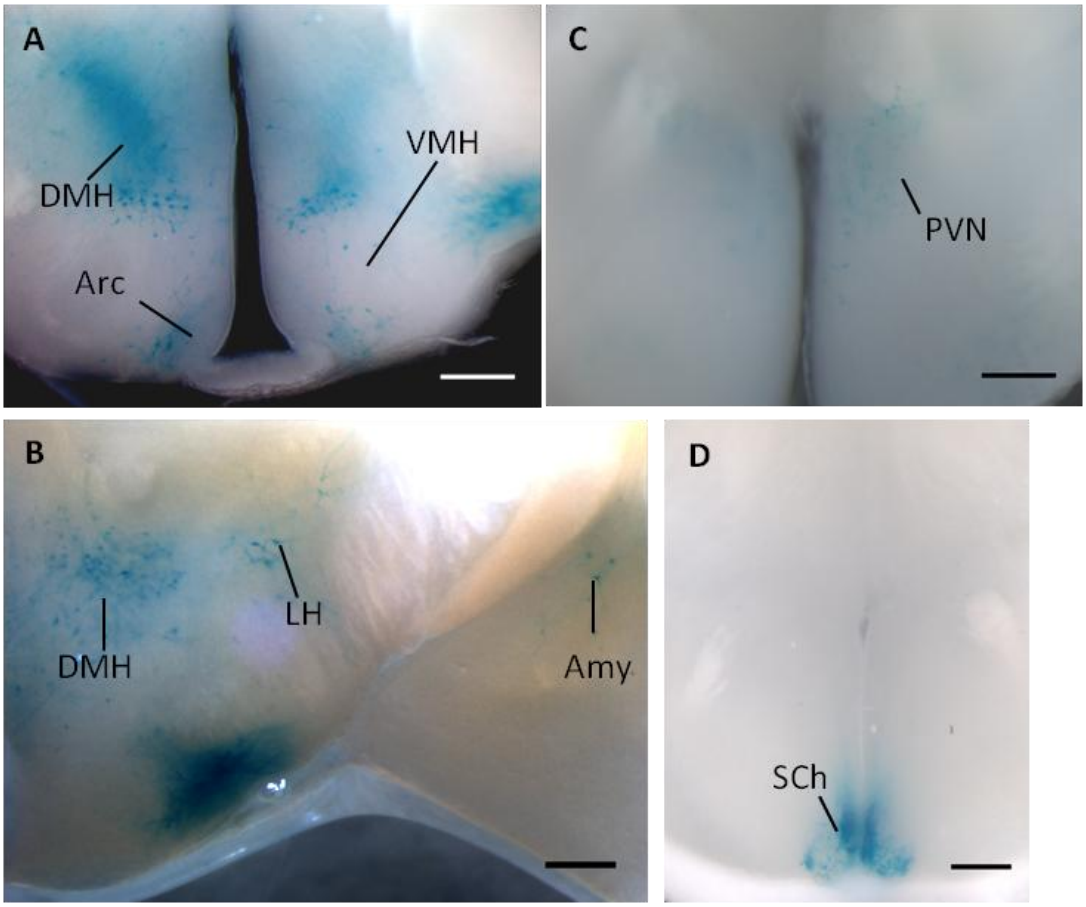

Figure 4.9. XGal staining for XL-βGal fusion protein in the hypothalamus of adult *CMV-Cre*/+; +/*XLlacZGT* brain

(A) XL-βGal expression in the hypothalamus of the adult *XLlacZGT* brain is not as strong as in IHC stained wild type brains but the DMH and Arc are clearly stained. The Arc staining was not as widespread as in IHC stained wild type brains.

(B) In the Amygdala (Amy) the XL-βGal staining is much reduced in adult brain compared to wild type Amy staining of XLαs.

(C) XL-βGal in the paraventricular nucleus of the hypothalamus (PVN) is less strong than in wild type brain.

(D) XL-βGal staining in the suprachiasmatic nucleus (SCh) is strong.

500 μm coronal vibratome sections; 500 μm scale bars

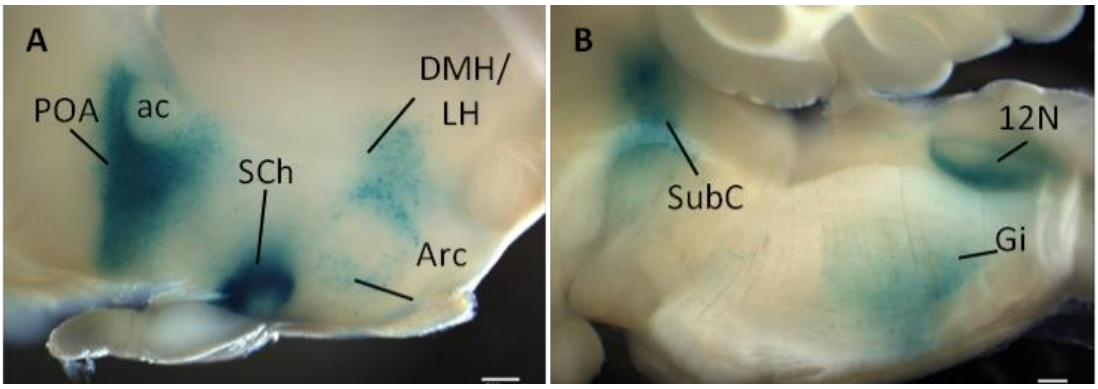

Figure 4.10. Sagittal sections of the adult *CMV-Cre*/+; +/*XLlacZGT* mouse brain stained for XL-βGal fusion protein with XGal

(A) Anterior part of the adult brain showing XL-βGal expression in the preoptic area (POA), suprachiasmatic nucleus (SCh), arcuate nucleus (Arc), lateral hypothalamus (LH) and the dorsomedial hypothalamus (DMH). The anterior commisure (ac) is not stained for XL-βGal.

(B) Hindbrain sagittal section showing staining of the subcoeruleus (SubC), gigantocellular nucleus (Gi) and the hypoglossal (12N).

500 µm Sagittal vibratome sections; 500 µm scale bars

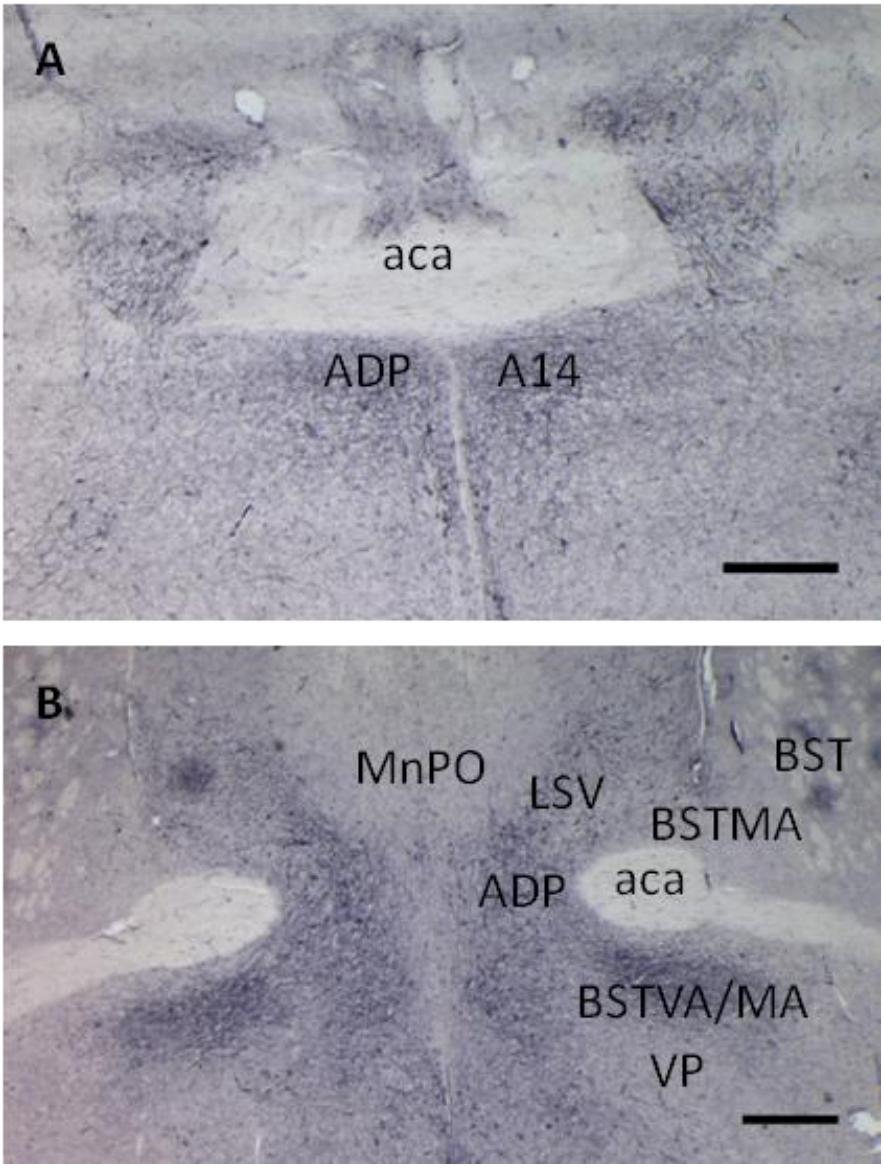

Figure 4.11. Adult XLαs expression pattern in the preoptic area of wild type mice.

(A) Posterior preoptic area shows expression in the anterodorsal preoptic nucleus (ADP) and the A14 noradrenergic neurons in this region. The anterior commisure (aca) does not express XLαs protein.

(B) The anterior preoptic area shows XLαs in the ADP, lateral septal nucleus (LSV) and bed nucleus of the stria terminalis (BSTMA; BSTVA). The medial preoptic nucleus (MnPO), aca and the ventral pallidum (VP) do not express XLαs.

14 μm coronal cryostat sections; 500 μm scale bars

develops in adult tissue (Figure 4.8 A and B). This nucleus is detected in *CMV-Cre*/+; +/*XLlacZGT* mice with XGal staining for XL-βGal; however, this is reduced compared to the staining seen in adult wild type mice (Figure 4.9 B). This finding concurs with the 90% reduction in expression levels seen by qPCR (KRECHOWEC *et al.* 2012). Adult brain sections did not show staining of blood vessels. This will be discussed further in Chapter 5.

4.3.3. *GNASXL* EXPRESSION IN THE BRAINSTEM IS ALTERED IN ADULT TISSUE COMPARED TO NEONATAL TISSUE

In neonatal wild type tissue, areas expressing XLαs protein include the raphe nuclei (RPa, ROb; Figure 4.12 A and B) and the Gi (Figure 4.12 B). The Amb also stains for XL-βGal fusion protein (Figure 4.12 D). The orofacial motor nuclei (7N and 12N) are strongly positive in both wild type and *Nestin-Cre*/+; +/*XLlacZGT* mice (Figure 4.7 A and B; 4.12 A and C.).

In adult medulla oblongata, the Gi stains for XLαs and XL-βGal (*CMV-Cre*/+; +/*XLlacZGT*) (Figure 4.13 A and D; Figure 4.10 B) as does the RPa (Figure 4.13 E.). The orofacial motor nuclei (7N and 12N) could not be detected in adult tissue with IHC for XLαs in wild type mice (Figure 4.13 C.) and *Gnasxl* expression was barely detectable with *in situ* hybridisation (Figure 4.14.); however, these nuclei were clearly detectable with XGal staining in 500 µm vibratome sections (Figure 4.10 B; Figure 4.14 A and B). Adult-specific staining was observed in the rostral part of the NTS, which was detected with IHC (Figure 4.13 A and B) and XGal (Figure 4.15 C).

In the neonatal pons the LC and LDTg nuclei were strongly positive for XLαs in wild type mice as well as XL-βGal in *Nestin-Cre*/+; +/*XLlacZGT* mice (Figure 4.16). In both mouse lines the SubC expressed the respective XL

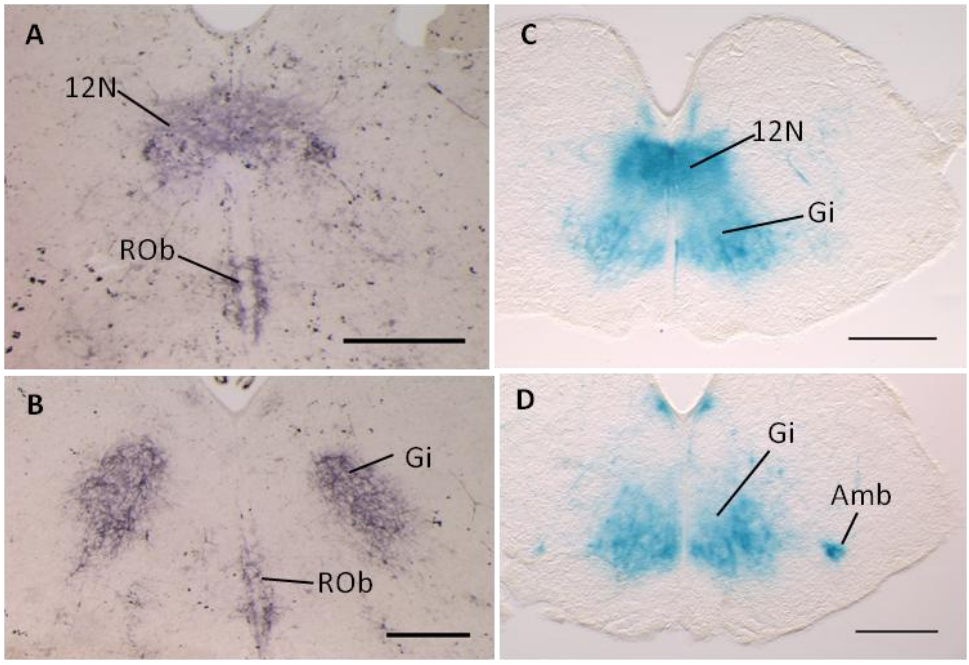

Figure 4.12. Neonatal expression of *Gnasxl* in the medulla oblongata

(A) XLαs expression in the hypoglossal (12N) and raphe obscurus (ROb) of wild type neonatal mice is strong

(B) XLαs expression in the gigantocellular reticular nucleus (Gi) and the ROb of wild type mice

(C) XL-βGal fusion protein expression in the 12N and Gi of *Nestin-Cre/+*; *+/XLlacZGT* mice stained with XGal

(D) XGal staining of XL-βGal fusion protein expression in the Gi and ambiguus nucleus (Amb) in *Nestin-Cre/+*; *+/XLlacZGT* mice

(A-B) 25 μm coronal cryostat sections; 500 μm scale bars

(C-D) 80 μm coronal cryostat sections; 500 μm scale bars

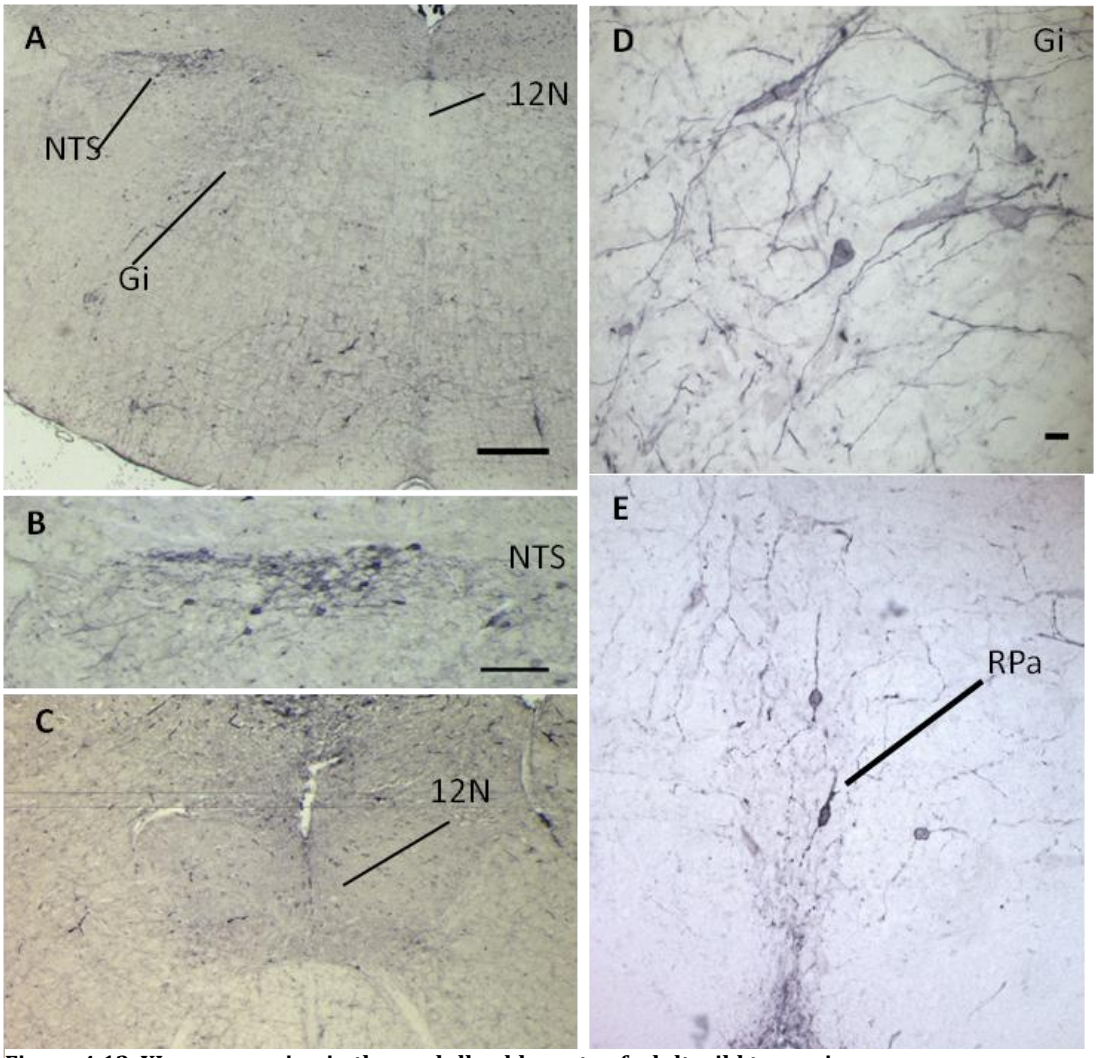

Figure 4.13. XLαs expression in the medulla oblongata of adult wild type mice

(A) Overview of XLαs protein expression in the medulla oblongata including the nucleus of the solitary tract (NTS), the gigantocellular reticular nucleus (Gi) and the hypoglossal (12N). 500 µm scale bar.

(B) Magnification of the NTS indicating cells and axonal staining. 200 µm scale bar.

(C) Magnification of the 12N showing no expression of XLαs using IHC. 500 µm scale bar.

(D) Magnification of the Gi. This image shows clear XLαs expression in neurons and the axonal projections from these neurons. 20 µm scale bar.

(E) XLαs is expressed in neurons and axons of the raphe pallidus (RPa). 200 µm scale bar.

14 µm coronal cryostat sections

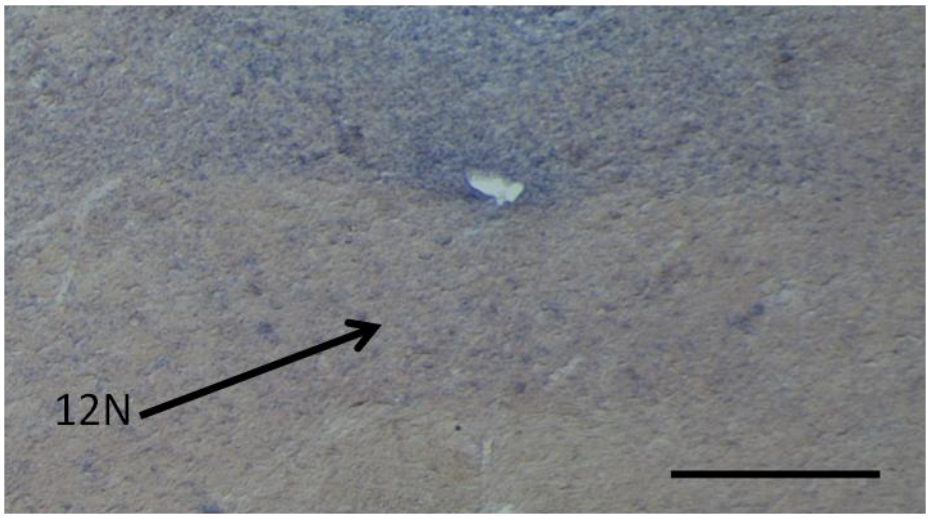

Figure 4.14. *in situ hybridisation* staining of *Gnasxl* expression in the hypoglossal of adult wild type mice

Expression of *Gnasxl* was barely detectable by *in situ hybridisation* in the hypoglossal (12N). This indicates that *Gnasxl* expression is reduced in adult mice. Confirming the lack of expression detected with the XLαs antibody in the 12N in wild type mice.

14 μm coronal cryostat section; 500 μm scale bar

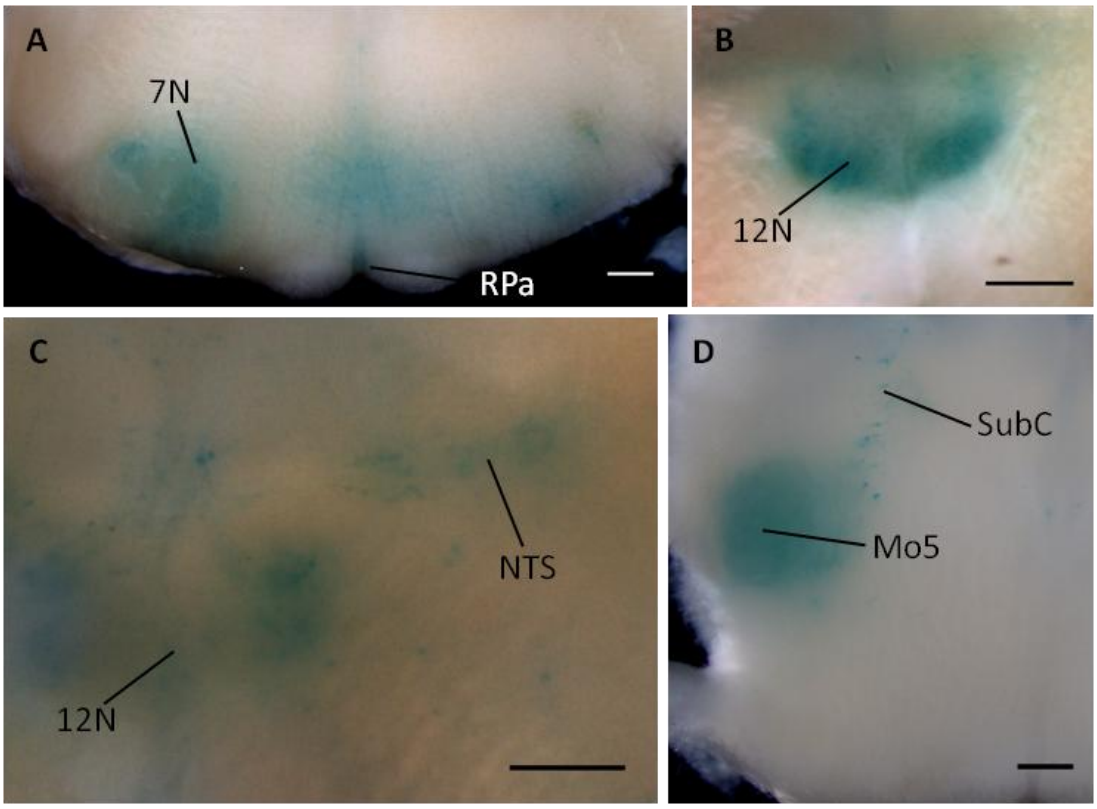

Figure 4.15. XL-βGal expression in the orofacial motor nuclei of adult *CMV-Cre*/+; +/*XLlacZGT* brains
(A) In the facial nucleus (7N) XL-βGal is expressed in a diffuse pattern. There is also expression in the raphe pallidus (RPa).
(B) XL-βGal fusion protein is expressed in the hypoglossal nucleus (12N).
(C) Staining in the medulla is seen in the 12N and the nucleus of the solitary tract (NTS). The NTS staining is weak compared to the staining of XLαs adult staining in wild type mice.
(D) In the pons the motor trigeminal nucleus (Mo5) is diffusely stained for XL-βGal fusion protein. The subcoeruleus (SubC) can also be seen.
500 μm coronal vibratome sections; 500 μm scale bars

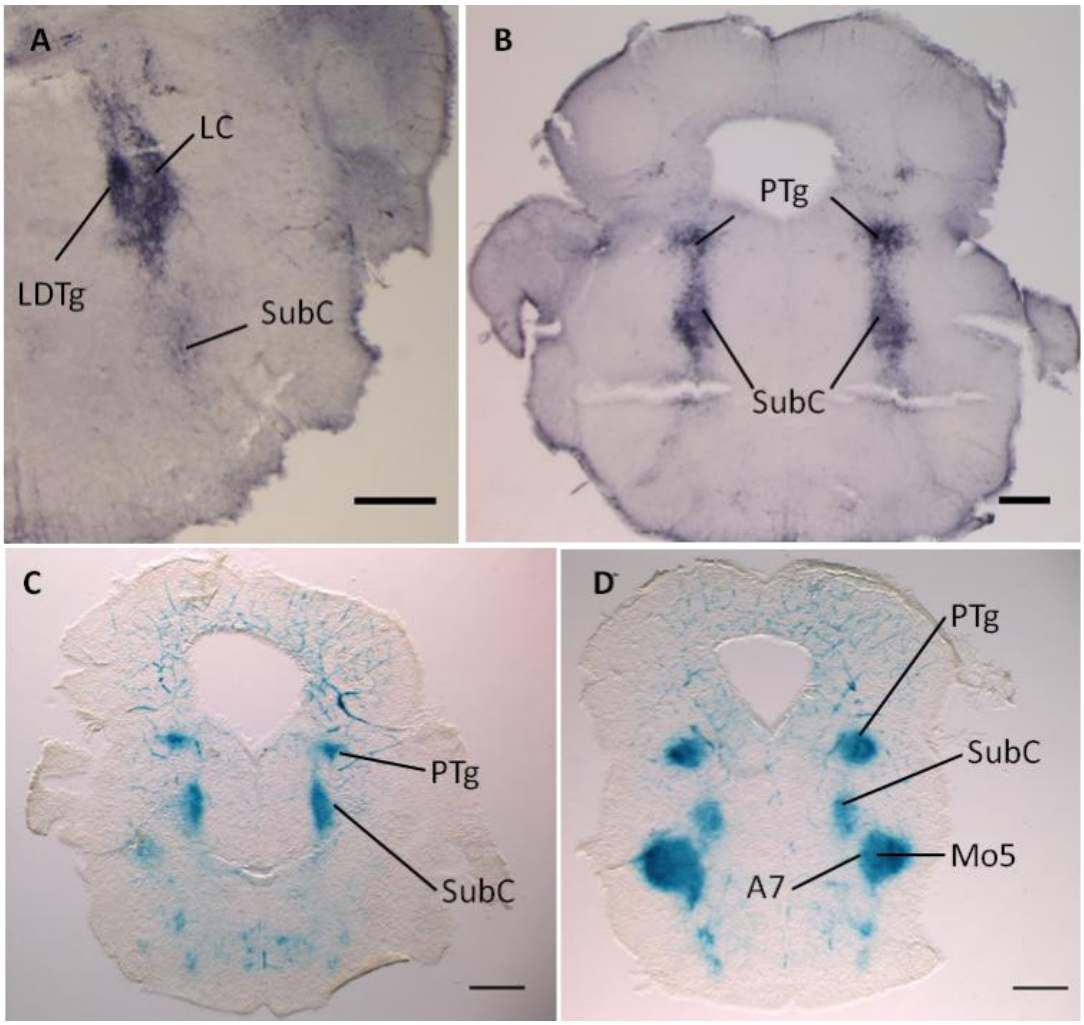

Figure 4.16. Neonatal *Gnasxl* expression pattern in the Pons

(A) XLαs expression in the laterodorsal tegmental nucleus (LDTg) and the locus coeruleus (LC) of wild type mice.

(B) XLαs expression pattern in the anterior pons peduncle (PTg) and the SubC of wild type mice.

(C) XL-βGal fusion protein expression in the PTg and the SubC of *Nestin-Cre*/+; +/*XLlacZGT* mice

(D) XL-βGal fusion protein expression in the PTg, SubC, A7 and Mo5 of *Nestin-Cre*/+; +/*XLlacZGT* mice

80 µm coronal freeze microtome sections; 500 µm scale bars

proteins (Figure 4.16). The Mo5 orofacial motor nucleus was also strongly positive for XL-βGal in *Nestin-Cre*/+; +/*XLlacZGT* neonates (Figure 4.7 A; Figure 4.16 D).

In the adult pons the expression pattern changed compared to neonates. The LC and SubC continued to express XLαs and XL-βGal (Figure 4.17; Figure 4.10 B). However, the LDTg region no longer expressed *Gnasxl* in either mouse line (Figure 4.17 B). The positive staining of the Mo5 orofacial motor nucleus was reduced, being undetectable with IHC and IF but diffusely stained with XGal (Figure 4.17 A; Figure 4.15 D).

4.3.4. XL-βGAL EXPRESSION IN THE SPINAL CORD

In *CMV-Cre*/+; +/*XLlacZGT* neonatal mouse spinal cord there was clear staining of XL-βGal fusion protein in the ventrolateral motor neurons (VMN) in the ventral part of the spinal cord. This clearly colocalised with a marker for cholinergic neurons: choline acetyl transferase (ChAT) (Figure 4.18 A and C). In the IML layer of the spinal cord there were many ChAT positive neurons; in this region ChAT denoted sympathetic preganglionic neurons (SPNs). These SPNs did not regularly colocalise with the few XL-βGal-expressing neurons in the IML that were observed (Figure 4.18 A and B). There were several XL-βGal-expressing neurons in the vicinity of the ChAT-expressing neurons in the IML layer (Figure 4.18 A and B).

In adult spinal cord, XL-βGal expression resulted in a more diffuse staining in the VMNs (Figure 4.19; Figure 20 A). There was still a considerable amount of colocalisation in this region between XL-βGal and ChAT in adult CMV-Cre/+; +/*XLlacZGT* spinal cord (Figure 4.20 A). In the IML layer there were

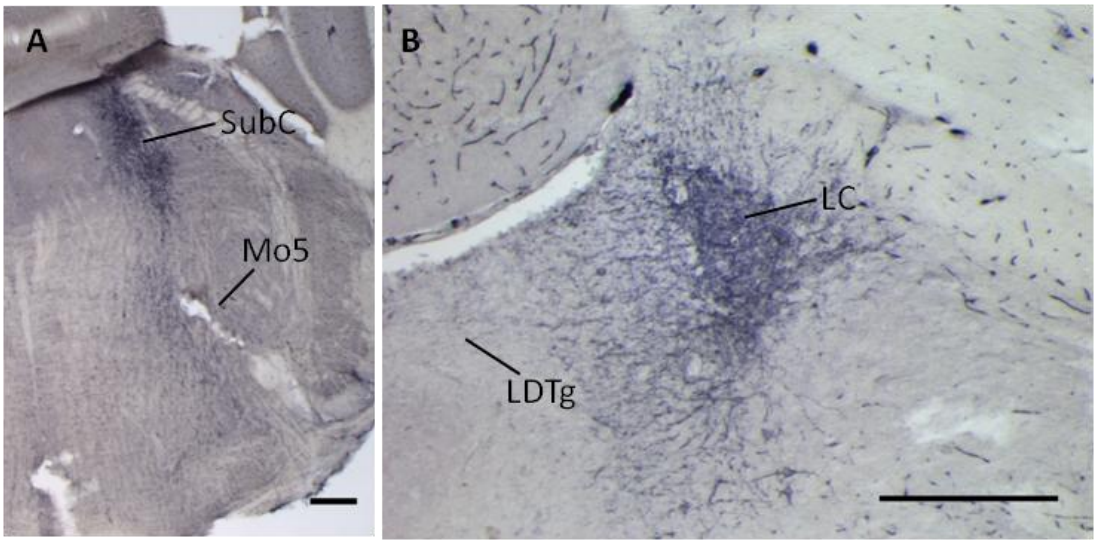

Figure 4.17. Staining in the adult wild type Pons

(A) XLαs expression in the SubC of the pons. The motor trigeminal nucleus (Mo5) is not visibly stained with the IHC technique. 80 μm coronal freeze microtome section.

(B) XLαs expression is observed strongly in the LC but no staining can be seen in the LDTg, a change from the neonatal expression pattern. 14 μm coronal cryostat section.

500 μm scale bars

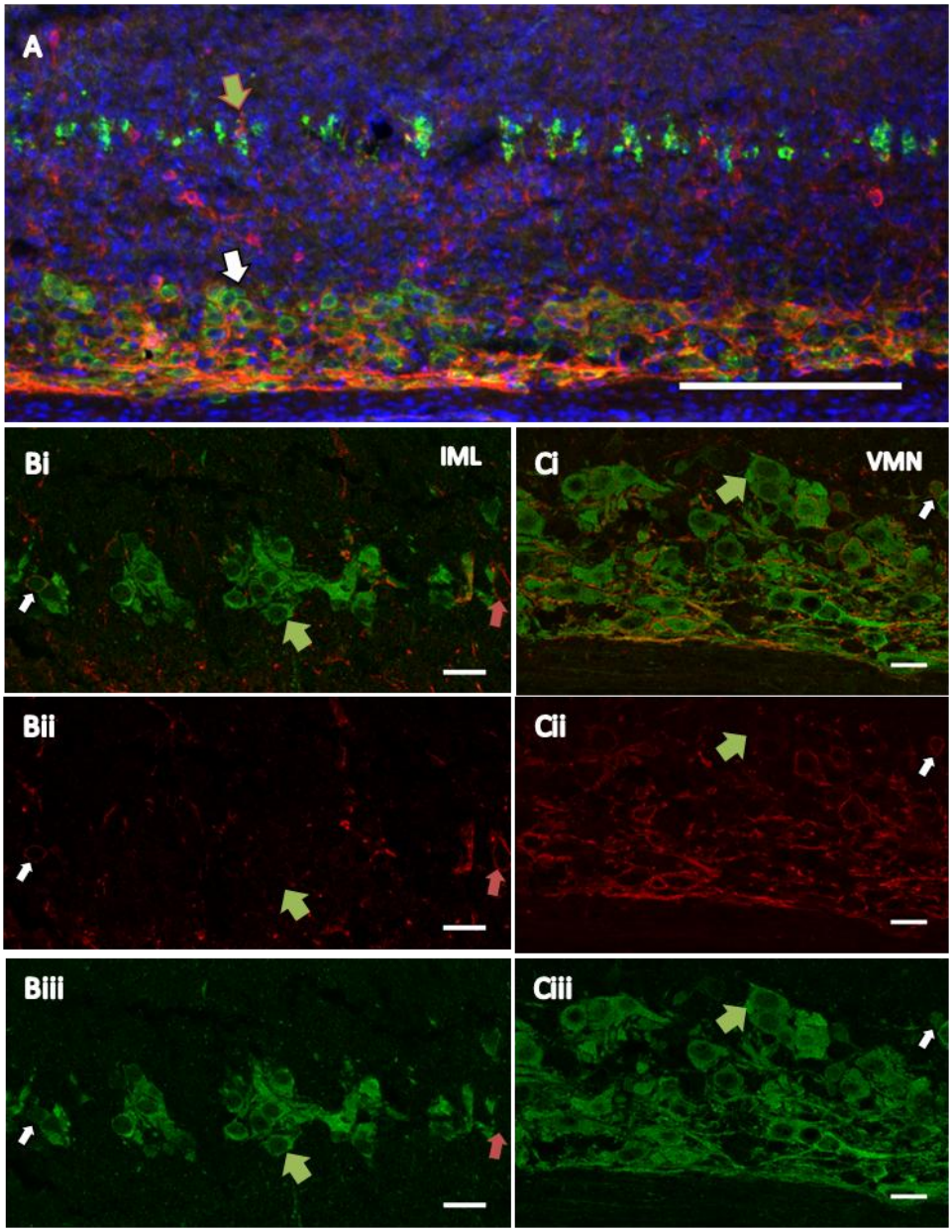

Figure 4.18. Confocal images of neonatal expression of XL-βGal fusion protein in the neonatal spinal cord of *CMV-Cre*/+; +/*XLlacZGT* mice

(A) Overview staining of the neonatal spinal cord shows two distinct layers of ChAT expressing neurons. The white arrow indicates the ventromedial layer neurons where there is a significant amount of colocalisation. 200 μm scale bar

(B) XL-βGal and ChAT staining in the intermediolateral layer of the spinal cord. White arrow indicates a colocalised cell. A green arrow indicates a singly stained ChAT cell. The red arrow indicates a singly stained XL-βGal neuron. Very few neurons express XL-βGal in this layer of the spine. (i) merged image (ii) XL-βGal only (iii) ChAT only.

(C) XL-βGal fusion protein expression in the VMN neurons shows some colocalisation in these neurons with ChAT. A green arrow indicate **(i)** merged image **(ii)** XL-βGal only **(iii)** ChAT only

(B-C) 20 μm scale bars

14 μm sagittal cryostat sections

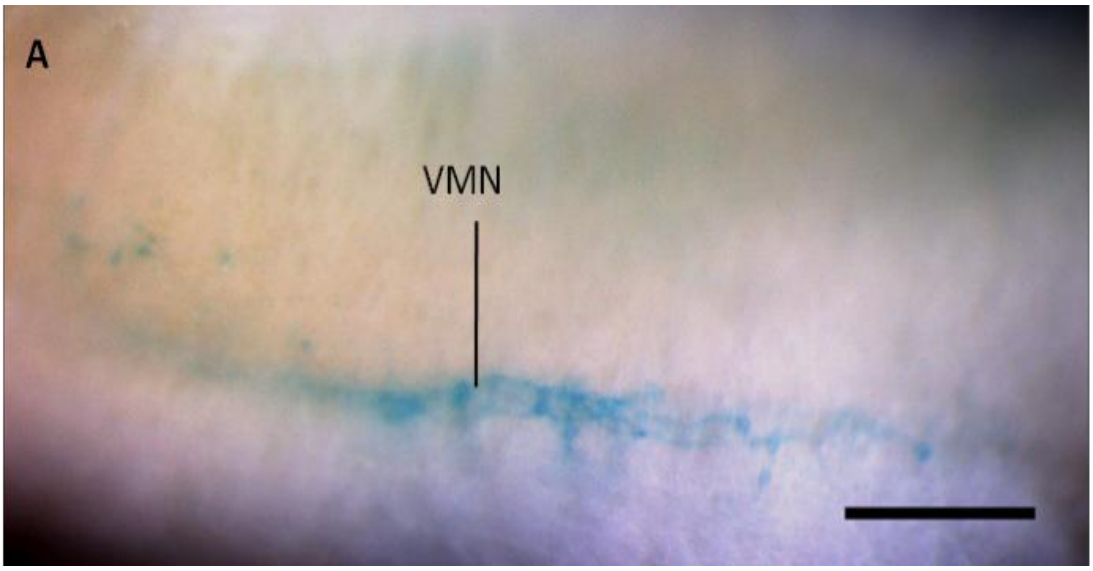

Figure 4.19. XGal staining for XL-βGal fusion protein expression in the spinal cord of adult *CMV-Cre*/+; +/*XLlacZGT mice*

(A) The XL-βGal fusion protein is expressed in the ventral motor neurons (VMNs) of the spinal cord. This tissue was dissected out, cut in half in a sagittal orientation and used in a whole mount staining protocol. 500 μm scale bar

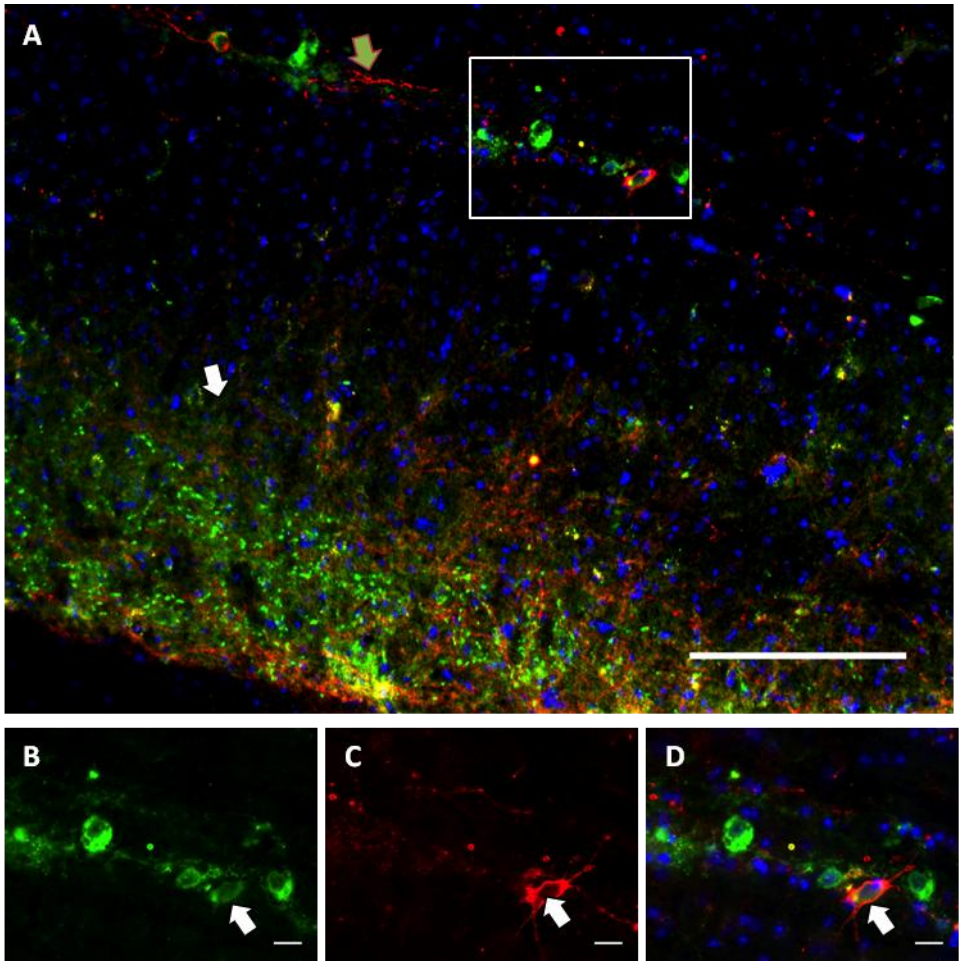

Figure 4.20. Transverse section of adult spinal cord stained for ChAT and XL-βGal fusion protein in *CMV-Cre*/+; +/*XLlacZGT* mice

(A) Overview image of adult transverse section of the spinal cord showing the VMN (white arrow) and the IML (green arrow). White square indicates the area magnified in (B-D). 200 μm scale bar.

(B) ChAT single stained section in the IML.

(C) βGalactosidase single stained section for XL-βGal fusion protein in the IML.

(D) Merged image of B and C showing one colocalised cell in the IML (white arrow)

(B-D) 20 μm scale bar

25 μm sagittal cryostat sections

several XL-βGal-positive neurons; these were mostly singly-stained with the occasional ChAT colocalised neuron (Figure 4.20; Figure 4.21). There were many more SPNs expressing ChAT in the IML layer than XL-βGal-expressing neurons (Figure 4.18; Figure 4.20; Figure 4.21). Neurons in the VMN were detectable with XGal staining in adult tissue (Figure 4.19).

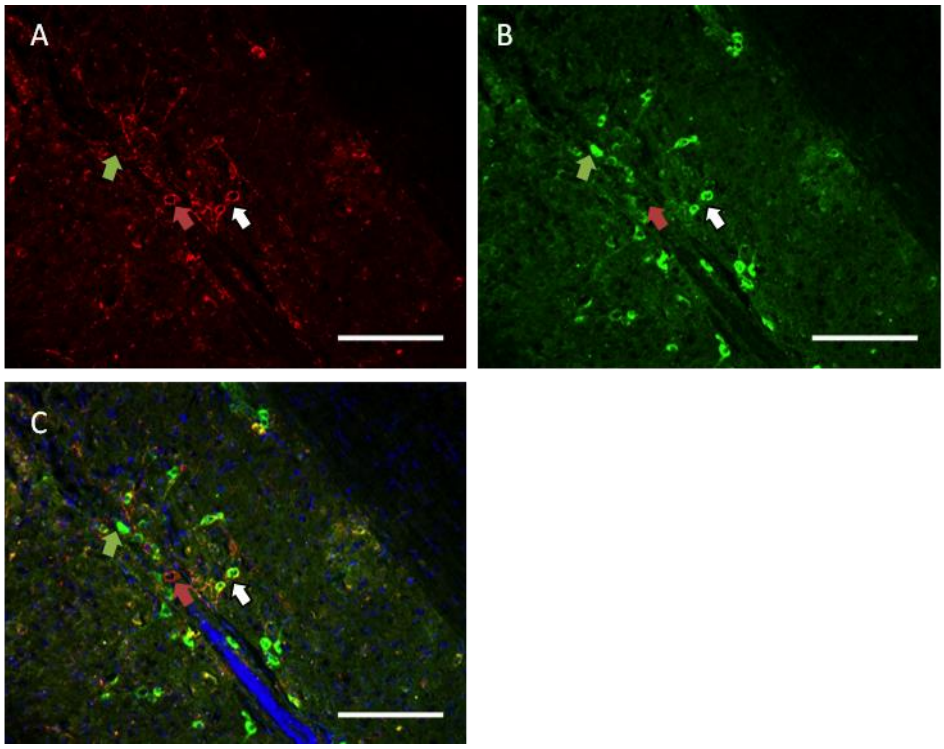

Figure 4.21. Horizontal section of *CMV-Cre*/+; +/*XLlacZGT* mouse spinal cord co-stained for XL-βGal fusion protein and the sympathetic preganglionic neuron marker choline acetyl transferase

(A) βGalactosidase IF of horizontally sectioned adult spinal cord showing clear XL-βGal expression in the inter medial lateral layer.

(B) Choline acetyl transferase (ChAT) expression in the same section.

(C) Merged image of (A) and (B) showing that there is little XL-βGal and ChAT coexpression in the IML

25 µm horizontal cryostat sections; 500 µm scale bar; red arrow indicates a single XL-βGal stained neuron; green arrow indicates a singly stained ChAT neuron; white arrow indicates a colocalised XL-βGal/ChAT co-expressing neuron.

4.4. DISCUSSION

4.4.1. EXPRESSION OF *GNASXL* IN REGIONS RESPONSIBLE FOR ENERGY HOMEOSTASIS

The hypothalamus is a well-described control centre for energy homeostasis. This is a region which has been described as having strong *Gnasxl* expression at neonatal day four (KRECHOWEC *et al.* 2012). This area of the hypothalamus continues to develop over the first neonatal days (BOURET *et al.* 2004; BOURET and SIMERLY 2004). The hypothalamic regions of the brain remain positive for XLαs from neonatal day one to adult phases of development. The XLαs expression in the LH, DMH and Arc continues to develop over the first neonatal days and is therefore unlikely to contribute to the lethargy and poor suckling phenotype seen in neonates that continues past neonatal day four (PLAGGE *et al.* 2004).

These regions show increased expression of XLαs in adult mice but this is unlikely to be the main contributing factor for the phenotypic difference between neonates and adults, although loss of XLαs in these neurons might have implications for the increased food intake and energy expenditure in adult mice.

A region of adult-specific XLαs expression is the amygdala – a region important not only for emotions and memories but also reward seeking behaviours and energy balance (CAMPBELL 2002; MIÑANO *et al.* 1992). This region could have wide-ranging effects although the exact impact of XLαs deletion in this nucleus remains to be elucidated. The CeA has many projections into parts of the brain involved in the regulation of energy homeostasis including the hypothalamus (it has reciprocal projections to orexin neurons in the DMH) (MIGUELEZ *et al.* 2001; MIÑANO *et al.* 1992).

4.4.2. *GNASXL* EXPRESSION IN REGIONS IMPORTANT FOR SNS OUTFLOW

The brain is integral to the correct functioning of the SNS. Many regions of the brain known to be centres for SNS outflow express *Gnasxl.* The PVN in adult tissues expresses XLαs clearly in the periphery of the nucleus. Neurons in this area of the PVN have been established as GABAergic (VONG *et al.* 2011) and it is possible that these neurons have inhibitory effects on the neurons expressing $G_s\alpha$ in the centre of the PVN (CHEN *et al.* 2009b) or other neurons in this central region. *Gnasxl*$^{m+/p-}$ mice show increased sympathetic activity (XIE *et al.* 2006) and this nucleus is also a well-known centre for SNS outflow. XLαs–expressing neurons might inhibit this in wild type mice – projecting onto the SNS mediating neurons in the centre of the nucleus.

It is also interesting that the POA projects to the DMH to control BAT thermogenesis through the SNS by inhibiting neurons (MCALLEN 2004; MORRISON and NAKAMURA 2011). However, both of these areas are stained in adults and have high *Gnasxl* expression at the day of birth suggesting they are not responsible for any changes in phenotype that have been noted. Loss of POA neurons inhibiting the DMH might have an impact on body temperature. The POA also has links to the amygdala through the BST; all of these regions contain *Gnasxl* expression.

The fact that XLαs expression continues to develop in these brain regions post-weaning indicates that this area is not a major contributor to the suckling behaviour of neonates observed from the day of birth, and therefore would not be a likely cause of the lethargy, feeding or mortality problems observed with the *Gnasxl*$^{m+/p-}$ neonatal mice (PLAGGE *et al.* 2004).

The observation that XLαs-expressing and ChAT-expressing neurons are

in mainly separate populations in the IML of the upper spinal cord suggests that XLαs is unlikely to directly affect the SPNs in this region; however, it is reasonable to hypothesise that XLαs neurons, with their close proximity to SPNs, might have a regulatory function on these SPN neurons.

Staining of the Amb was continuous throughout neonatal and adult developmental stages. This area is important for parasympathetic activity and it is possible that these XLαs-expressing neurons might act to inhibit SNS outflow, and deletion of XLαs in these neurons would result in the SNS over-activity seen in *Gnasxl*$^{m+/p-}$ mice (XIE *et al.* 2006).

4.4.3. *GNASXL* EXPRESSION IN NUCLEI RESPONSIBLE FOR MUSCLE INNERVATION

The orofacial motor nuclei (Mo5, 7N and 12N), with their strong XLαs expression even at neonatal day one that is reduced in adult tissue, could be important for the phenotype seen in neonatal mice. These regions are well-developed at birth and are extremely important for efficient suckling as they control not only the facial muscles but also the tongue (TRAVERS 2004).

It is interesting that the orofacial motor nuclei seem to be down-regulated towards adulthood in terms of their contribution to feeding. XLαs expression in these nuclei might be necessary for control of facial muscles during neonatal suckling but might not be required for adult feeding behaviours. This could be an explanation for the recovery of normal feeding behaviour in surviving *Gnasxl*$^{m+/p-}$ adults, which have increased food intake relative to their body weight when compared to wild type littermates. The fact that these nuclei could not be detected with IHC in adults might be due to the sensitivity of the IHC technique not detecting low levels of full-length XLαs protein compared to the XGal detection of the XL-βGal and the poor affinity of

the XLαs antibody compared to the anti-βGalactosidase antibody. It is also possible that the insertion of the gene trap into the exon A20 region of the gene locus could have disrupted something that controlled this expression – possibly an enhancer element or a developmental control region that has not been described previously . Analysis of the expression levels in the gene trap-carrying mice (inactive or active) showed that they have a 90% reduction in expression of the XLαs full-length (inactive) or the XL-βGal fusion protein (active gene trap) (KRECHOWEC *et al.* 2012). A new gene trap mouse model is in the process of being created; this gene trap will be inserted in a region of the intron much farther from the *Gnasxl* exon 1 and will not result in disruption of the full-length XLαs in mice carrying the non-active gene trap.

4.4.4. ALERTNESS AND SLEEP/WAKE NUCLEI EXPRESS *GNASXL*

In regions of the brain important for alertness, wakefulness and sleep (LDTg, LC, Gi) there is clear staining in neonatal brain using both IHC and XGal staining at neonatal day one. These areas were also positive at neonatal day four (PLAGGE *et al.* 2004). Previously it had been suggested that deletion of XLαs in these nuclei might be the cause of the lethargy seen in neonatal *Gnasxl*$^{m+/p-}$ mice (PLAGGE *et al.* 2004). In adult tissue the LDTg no longer expresses either full-length XLαs or the XL-βGal fusion protein, although both the Gi and the LC continue to express XLαs strongly. The loss of XLαs in the LDTg could partly explain the recovery of the lethargy seen in these *Gnasxl*$^{m+/p-}$ adult survivors as this nucleus is important for alertness and wakefulness and is only expressed at neonatal stages of development. Deletion of XLαs in the Gi and/or the LC might have a role in the phenotype, which is shared by the two developmental stages.

4.4.5. ADULT-SPECIFIC AREAS OF STAINING

The NTS, as a new area of adult-specific staining, is interesting: this region is the input centre in the brain for signals from the gut through the vagal nerve, transmitting satiety and hunger signals to the brain from the periphery (HAYES and COVASA 2006; SCHWARTZ 2002; VRANG *et al.* 2003; WILLING and BERTHOUD 1997). A disregulation of this nutrient-sensing system in *Gnasxl*$^{m+/p-}$ adult survivors might explain their increased food intake compared to their wild type siblings (XIE *et al.* 2006).

The amygdala is important for emotions and memory retention as well as energy homeostasis. It has connections with many regions of the brain including the DMH and the POA. It is possible that these areas have not fully developed at birth and as there is no expression found in these nuclei on the day of birth in wild type mice they are unlikely to contribute to the knock-out *Gnasxl* phenotype in neonates. The loss of XLαs signalling in these nuclei in adulthood might have implications for food intake and nutrient sensing.

4.4.6. DIFFERENCES BETWEEN ANALYSIS TECHNIQUES

The differences seen between expression patterns of XLαs protein with IHC and XL-βGal fusion protein using XGal or IF for βGalactosidase were interesting observations. There could be several possible explanations for this. Firstly, it could result from the insertion of the gene trap across the A20 region of the gene locus. There might be an enhancer or other control mechanism for expression in this location, which would be affected by the gene trap insertion. Secondly, it is possible that the two types of protein are processed differently in different regions of the brain *in vivo*. The shorter XL-βGal fusion protein could be quickly degraded in the amygdala and NTS. The cause of XL-βGal expression

detection in an area and no expression of XLαs full-length is likely to be a problem of antibody sensitivity. As we think these areas are down-regulated in adult brain it could be the case that the IHC detection of the full-length protein is not possible while the more sensitive XGal staining can still detect XL-βGal.

4.4.7. CONCLUSIONS

The *Gnasxl* expression pattern in the CNS alters from neonatal stages to adult stages of development (Table 4.1). Many regions of the brain maintain expression of *Gnasxl* while other regions are down-regulated or begin to produce *Gnasxl* once the brain is matured. Regions which strongly express *Gnasxl* on the day of birth but have down-regulated expression into adulthood appear to have functions which might explain not only the initial poor suckling phenotype observed in the neonatal mice but also why the surviving adult mice do not exhibit a feeding phenotype (Table 4.1).

Many regions which maintain expression are involved in the control of energy homeostasis (food intake and energy expenditure) and/or SNS control. This is in concurrence with the phenotype of an over-activity of the SNS in *Gnasxl*$^{m+/p-}$ mice (XIE *et al.* 2006).

New areas of *Gnasxl* expression in adult brain might be due to the continued development of the brain over the first weeks of life. These regions would be unlikely to have an effect on the neonatal phenotype but might have implications for the increased food intake and energy expenditure observed in adult survivor *Gnasxl*$^{m+/p-}$ mice (XIE *et al.* 2006).

Neonatal and Adult staining	Neonatal Specific staining	Adult Specific Staining
LH, DMH, PVN, Arc, VMN, IML, Mo5, 7N, 12N, RPa, Gi, LC, SubC, Amb, SCh, POA	LDTg	NTS, Amygdala

Table 4.1. Table of Brain areas in neonatal and adult tissues which show *Gnasxl* expression

CHAPTER 5. GNASXL EXPRESSION: A COMPARATIVE STUDY OF CHANGES BETWEEN NEONATAL AND ADULT DEVELOPMENTAL STAGES II. PERIPHERAL TISSUES

5.1. INTRODUCTION

5.1.1. PREVIOUS *GNASXL* EXPRESSION ANALYSIS IN NEONATES

XLαs expression has been partially described previously in peripheral tissues of both mice and rats using Northern blotting and *in situ* hybridisation (PASOLLI *et al.* 2000; PLAGGE *et al.* 2004). These data indicated that XLαs was expressed not only in the brain but also in the heart, BAT, white adipose tissue (WAT), pancreas, pituitary gland, adrenal gland and kidneys (PASOLLI *et al.* 2000; PLAGGE *et al.* 2004). These tissues are all important for the maintenance of energy homoeostasis and some are derived from the neural crest of the embryo (adrenal medulla), thus their expression of XLαs is unsurprising as they would simply be modified neurons. There has been no systematic analysis of *Gnasxl* expression pattern in these peripheral tissues.

5.1.2. THE PITUITARY GLAND

The pituitary gland is located at the base of the brain in contact with the median eminence via a portal vein. It is formed of two parts – the neurohypophysis (neural part) and the adenohypophysis. The neurohypophysis is derived from the diencephalic tissue and consists of the neural lobe, the pituitary stalk and median eminence (ARMSTRONG 2004). The neural lobe is supplied with catecholamines from the dopamine neurons in the NTS and rostral periventricular (GARTEN *et al.* 1989; KAWANO and DAIKOKU 1987). The main hormones released from the neurohypophysis are oxytocin and vasopressin. As well as catecholamines, both GABA and serotonin have been found in this lobe of the pituitary probably regulating hormone release (FALKE 1991).

The adenohypophysis consists of three parts - the anterior lobe, the

intermediate lobe and the pars tuberalis (ARMSTRONG 2004). The anterior lobe surrounds all but the dorsal part of the pituitary. The intermediate lobe, which is derived from the neural crest, is innervated by dopamine (BJÖRKLUND *et al.* 1973), serotonin (MEZEY *et al.* 1984) and GABA (TAPPAZ *et al.* 1983). This lobe is also known to produce POMC derived proteins including α-MSH (ARMSTRONG 2004).

5.1.3. THE ADRENAL GLANDS

The adrenal glands are located on the top of the kidneys and are endocrine glands. They release hormones in response to stress, for example they release corticosteroids such as cortisol and catecholamines such as epinephrine.

The adrenal medulla is the body's main source of the catecholamines: noradrenaline and adrenaline as well as some dopamine (TORTORA and GRABOWSKI 2003). They are stimulated through the thoracic spinal cord preganglionic fibres (MORRISON and CAO 2000). They release secretions directly into the blood. Medullary cells are derived from the neural crest, which means they are modified neuronal cells unlike the adrenal cortex, which is derived from the mesoderm. Norepinephrine released from the adrenal medulla activates the receptors in the vagal nerve, which in turn stimulates the NTS.

5.1.4. MUSCLE TISSUE

There are three main types of muscle tissue found in the body: skeletal muscle; smooth muscle; and cardiac muscle. The latter two are not under conscious control whilst the first can be controlled consciously (limb control) or unconsciously (breathing). Smooth muscle is contained in organs such as the gastrointestinal tract and blood vessels. The heart (cardiac muscle) was

previously described as having *Gnasxl* expression in wild type mice in four-day old mice Northern blot analyses (PLAGGE *et al.* 2004). This muscle type is controlled by SNS outflow from the brain. Its function has important implications in blood pressure and heart rate through sympathetic activation.

5.1.5. ADIPOSE TISSUE

There are two forms of adipose tissue, WAT and BAT, named for their colour; WAT is colourless to the naked eye while BAT has a distinctive brown coloration due to the high density of mitochondria in this tissue. The lean *Gnasxl*$^{m+/p-}$ mice have very little adipose tissue (BAT or WAT) although it has been indicated that *Gnasxl* is expressed in neonatal BAT and WAT by Northern blot and RT-PCR (PLAGGE *et al.* 2004; XIE *et al.* 2006).

WAT is located in the peritoneal cavity or subcutaneously (PAVELKA and ROTH 2010) and provides an important energy source in the form of triglycerides, which can be stored or metabolised depending on the energy status of an organism. Another important role of this tissue is its secretory function: WAT secretes leptin, along with other adipocytokines, as an indicator of adiposity (PAVELKA and ROTH 2010).

There are several BAT deposits located around the body, the main one being in the interscapular region. BAT cells contain fat in many small vacuoles, as opposed to the single large fat vesicle which demarks WAT (HULL and SEGALL 1966). BAT is important for non-shivering thermogenesis in the newborn mammal, although it is still present in adults. Non-shivering thermogenesis is induced by norepinephrine release and cold exposure. Several areas of the brain including the raphe pallidus, DMH and POA are involved in the SNS activation of non-shivering thermogenesis in BAT (CANNON and NEDERGAARD 2004).

Norepinephrine controls the cAMP production in BAT by binding to β_3-adrenergic receptors (a G_s-coupled receptor) to simulate cAMP production; it can also bind to α_2-adrenergic receptors (G_i-coupled receptors) inhibiting adenylyl cyclase and reducing cAMP production thus inhibiting thermogenesis (CANNON and NEDERGAARD 2004).

Heat is produced in the tissue by the uncoupling action of uncoupling protein 1 (UCP1), a BAT specific uncoupling protein, which is activated only in stimulated mature adipocytes and is the only uncoupling protein to mediate thermogenesis (CANNON and NEDERGAARD 2004). Other work has found an increase in UCP1 as well as an increased body temperature in adult *Gnasxl*$^{m+/p-}$ mice (XIE *et al.* 2006) (our unpublished data). It has also been observed that there is increased lypolysis in BAT and WAT of *Gnasxl*$^{m+/p-}$ mice, which is probably due to the global increase in SNS activity that is seen in these mice (XIE *et al.* 2006).

5.1.6. AIMS

The aim of this work was to confirm, on a histological level, the *Gnasxl* expression pattern in peripheral tissues using the *XLlacZGT* mouse line. For analysis of peripheral tissues crosses of *Nestin-Cre* (*Nestin-Cre*/+; +/*XLlacZGT)* and *CMV-Cre* (*CMV-Cre*/+; +/*XLlacZGT*) were performed with male *XLlacZGT* mice.

5.2. MATERIALS AND METHODS

5.2.1. TISSUE COLLECTION

Tissues were collected from neonatal and adult CMV-Cre/+; +/*XLlacZGT* and +/+; +/*XLlacZGT* mice as described in Chapter 4.

5.2.2. XGAL WHOLE-MOUNT STAINING

Protocols for immunofluorescence and whole mount staining with XGal were carried out as described in Chapter 4.

5.2.3. ANTIBODIES

Primary antibodies used for co-staining of XL-βGal and cellular markers in blood vessels were chicken anti-βGalactosidase (Abcam; 1:500; ab9361), mouse IgG2α anti-alpha Smooth Muscle actin (Sigma; 1:500; A2547) and rabbit anti-von Willebrand factor (Dako; 1:500; A0082).

Secondary antibodies used were donkey anti-chicken Dylight™ 594 (Jackson ImmunoResearch, 1:1000), Zenon direct labelling kit 488 (Invitrogen) and donkey anti rabbit AF488 (Invitrogen; 1:1000)

5.2.4. DIRECT LABELLING OF PRIMARY ANTIBODIES

Direct labelling was carried out according to the instructions for the mouse IgG2a AF488 kit. This consisted of the following steps: 1 µg antibody was pipetted into a 1.5 mL tube and 5 µL component A from the Zenon labelling kit was added, mixed carefully by pipetting and incubated in the dark for 5 minutes. 5 µL Component B was added, mixed by pipetting and incubated in the dark for 5 minutes. The directly labelled antibody was used in immunofluorescence co-localisation experiments by addition to the secondary and DAPI incubation solution of the immunofluorescence protocol described in Chapter 4.

5.2.5. IMMUNOFLUORESCENCE

This staining was carried out in the same way as described in Chapter 4.

5.2.6. HISTOLOGY OF XGAL STAINED WHOLE MOUNT TISSUES.

After XGal whole mount staining, tissues were prepared for microtome sectioning by dehydrating in an ethanol series and then incubating with Histoclear. Tissues were then embedded in paraffin, which was allowed to solidify before sectioning on a paraffin microtome at 7 μm. After mounting onto slides the sections could be rehydrated and counterstained with Eosin before a final dehydration and mounting with Eukitt® as described in Chapter 4.

5.3. RESULTS

5.3.1. TISSUE COLLECTION FOR ANALYSIS OF XL-βGAL EXPRESSION PATTERN IN THE PERIPHERAL TISSUES OF NEONATAL AND ADULT *XLLACZGT* MICE

To analyse the expression pattern of *Gnasxl* in the peripheral tissues of mice, tissues were collected from neonatal day one and adult *Cre*/+; +/*XLlacZGT* mice. These were processed for XGal staining as described in the methods section of Chapter 4. Litters of neonates were collected after schedule one killing while adult tissues were collected after perfusion fixation. Controls were performed on +/+; +/*XLlacZGT* littermates of *Cre*/+; +/*XLlacZGT* mice.

5.3.2. XL-βGAL IS EXPRESSED IN PERIPHERAL TISSUES

In the neonatal pituitary gland of *Cre*/+; +/*XLlacZGT* mice, staining was seen in the intermediate layer of the adenophysis (Figure 5.1. A). In the neonatal adrenal gland the XL-βGal staining was limited to the medullary tissues (Figure 5.1. B). Controls for the pituitary tissue determined that there was no βGalactosidase-like endogenous activity in this tissue (Figure 5.1. C). Both the intermediate layer of the pituitary and adrenal medulla expressed XL-βGal in adult tissue whole mount staining (Figure 5.2. A and B) and again in the pituitary of +/+; +/*XLlacZGT* mice there was no XGal staining (Figure 5.2. C).

5.3.3. XL-βGAL EXPRESSION IN ADIPOSE TISSUE IS FOUND IN BLOOD VESSELS

In the WAT of *CMV-Cre*/+; +/*XLlacZGT* neonatal mice staining of blood vessels was observed (Figure 5.3. A). This staining was not present in the +/+*;* +/*XLlacZGT* sibling mice (Figure 5.3. C). In BAT tissue staining was seen in the blood vessels only (Figure 5.3. B). Both *CMV-Cre*/+; +/*XLlacZGT* mice and their +/+; +/*XLlacZGT* siblings have very little adipose tissue similar to the *Gnasxl*$^{m+/p-}$ phenotype (XIE *et al.* 2006).

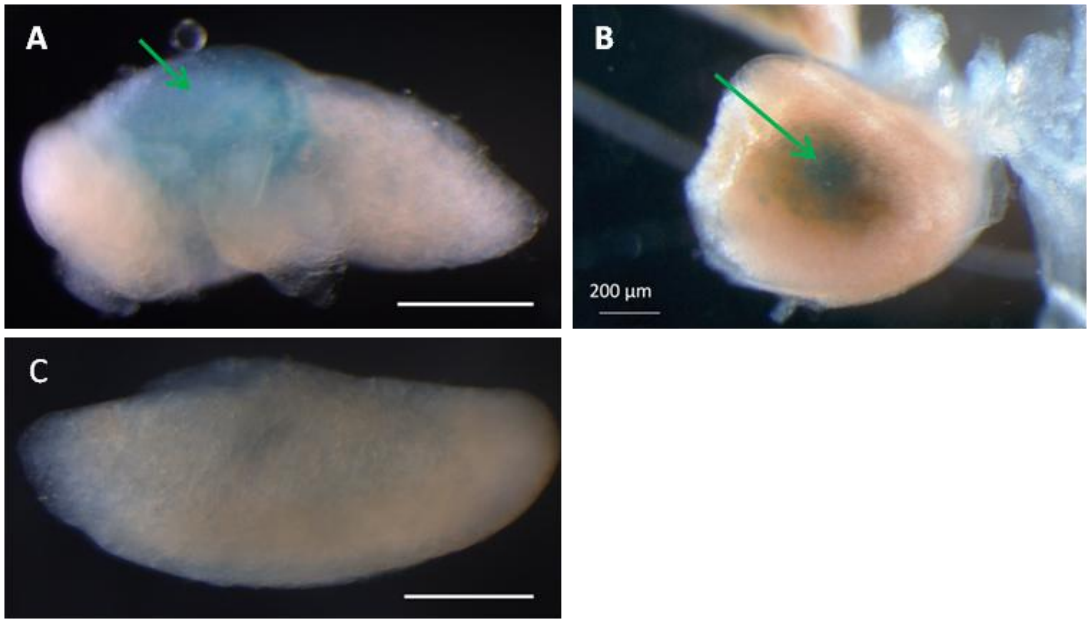

Figure 5.1. XL-βGal expression in whole mount neonatal tissues derived from the neural crest

(A) In the pituitary gland of neonatal *CMV-Cre*/+; +/*XLlacZGT* mice XL-βGal expression is confined to the intermediate layer of the gland

(B) XL-βGal expression in the adrenal gland of neonatal *CMV-Cre*/+; +/*XLlacZGT* tissue was limited to the adrenal medulla. No XGal staining of the adrenal cortex was observed (Staining performed by Stefan Krechowec).

(C) The intermediate layer of the pituitary gland in neonatal +/+; +/*XLlacZGT* mice does not stain for the XL-βGal fusion protein with XGal.

500 µm scale bars or as indicated

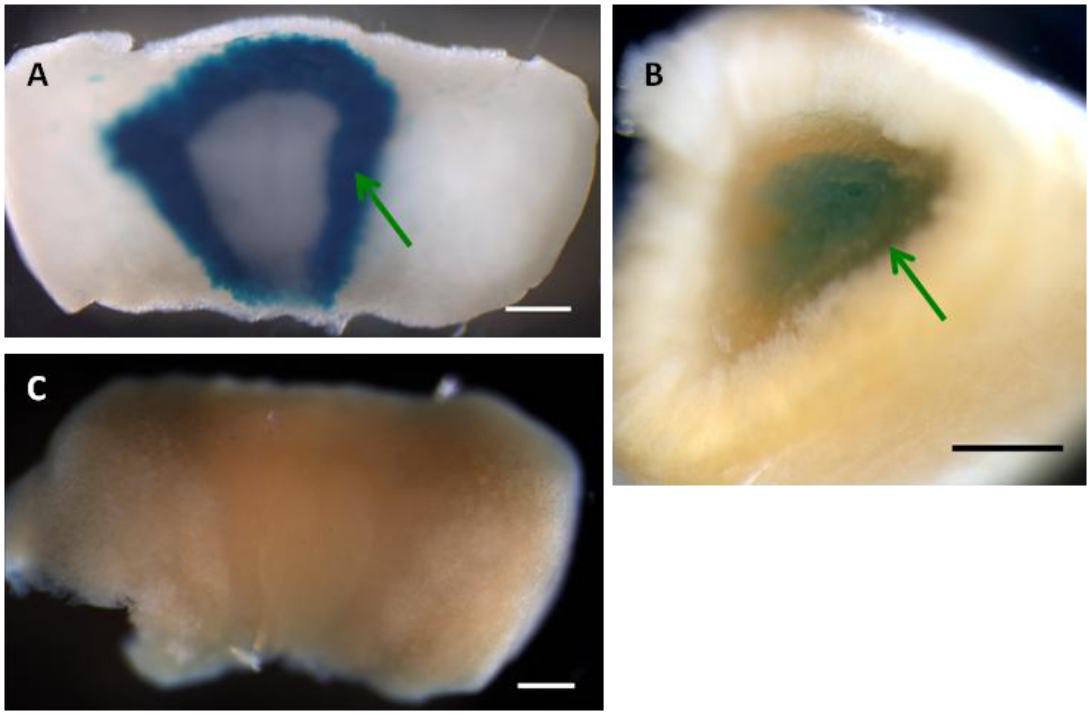

Figure 5.2. Whole mount XGal staining of adrenal and pituitary gland in adult mice

(A) The adult pituitary gland maintains expression in the intermediate layer (green arrow) of *CMV-Cre*/+; +/*XLlacZGT* mice.

(B) In adult *CMV-Cre*/+; +; +/*XLlacZGT* tissue XGal staining of XL-βGal is observed in the adrenal medulla (green arrow). The adrenal cortex does not express XL-βGal fusion protein.

(C) In The adult pituitary gland of +/+; +/*XLlacZGT* mice no XL-βGal was detected in the intermediate layer. 500 μm scale bars

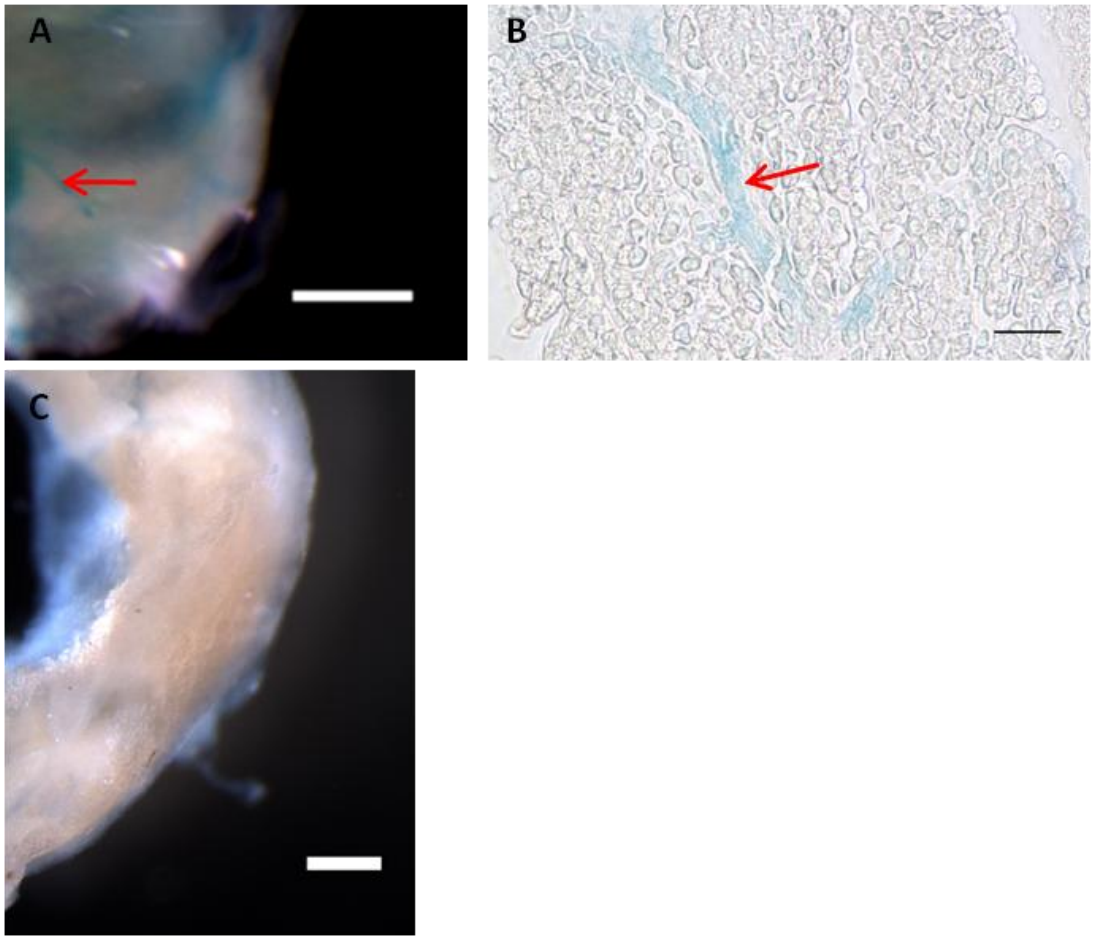

Figure 5.3. XL-βGal fusion protein expression pattern analysis in adipose tissue of neonatal mice using XGal staining

(A) White adipose tissue shows some expression of the XL-βGal fusion protein in blood vessels in *CMV-Cre*/+; +/*XLlacZGT* mice in whole mount staining for XGal. Scale bar 500 μm

(B) Brown adipose tissue showing XL-βGal fusion protein in blood vessels of *Nestin-Cre*/+; +/*XLlacZGT* neonatal mice in 7 μm paraffin sections. 20 μm scale bar.

(C) +/+; +/*XLlacZGT* white adipose tissue in neonates shows no XL-βGal fusion protein expression with XGal staining in whole mount tissues. Scale bar 500 μm.

Red arrows indicate blood vessel staining;

5.3.4. XL-βGAL EXPRESSION IN MUSCLES IS RESTRICTED TO NEONATAL TISSUE

XL-βGal expression was identified in other neonatal muscle tissues, including the intercostal muscles (Figure 5.4 A) and the tongue (Figure 5.4 B). Control XGal staining in *+/+*; +/*XLlacZGT* neonatal mice for the intercostal muscles and tongue indicated that this was genuine staining as no XGal staining was observed in these tissues (Figure 5.5). In adult *+/+*; +/*XLlacZGT* mice, no XGal staining was observed in either the intercostal muscles or the tongue (Figure 5.6 A and B).

In other tissues that had previously been described as *Gnasxl*-expressing using Northern blotting and RT-PCR (PLAGGE *et al.* 2004; XIE *et al.* 2006), including BAT (Figure 5.3 B), the stomach (Figure 5.4. C) and the heart (Figure 5.4. D), XL-βGal expression was observed to be limited to the blood vessels and no XGal staining was seen in the cells of the tissues themselves. In adult tissue this blood vessel expression was completely down-regulated (Figure 5.6 C).

To determine the localisation of the XL-βGal expression in the blood vessels double immunofluorescence was applied. This established that the expression of XL-βGal was limited to the alpha smooth muscle actin (αSMA) positive cells in the muscular walls of the blood vessels (Figure 5.7) and was not present in the endothelial cells of the blood vessels, as indicated by the endothelial marker von Willebrand Factor (vWF) (Figure 5.8).

5.3.5. ENDOGENOUS βGALACTOSIDASE-LIKE ACTIVITY WAS OBSERVED IN SOME TISSUES

Using immunofluorescence, XL-βGal expression was observed in the growth plates of neonatal bones of CMV-*Cre*/+; +/*XLlacZGT* mice (Figure 5.9. A), however, control tissues (+/+; +/*XLlacZGT* mice) stained with the

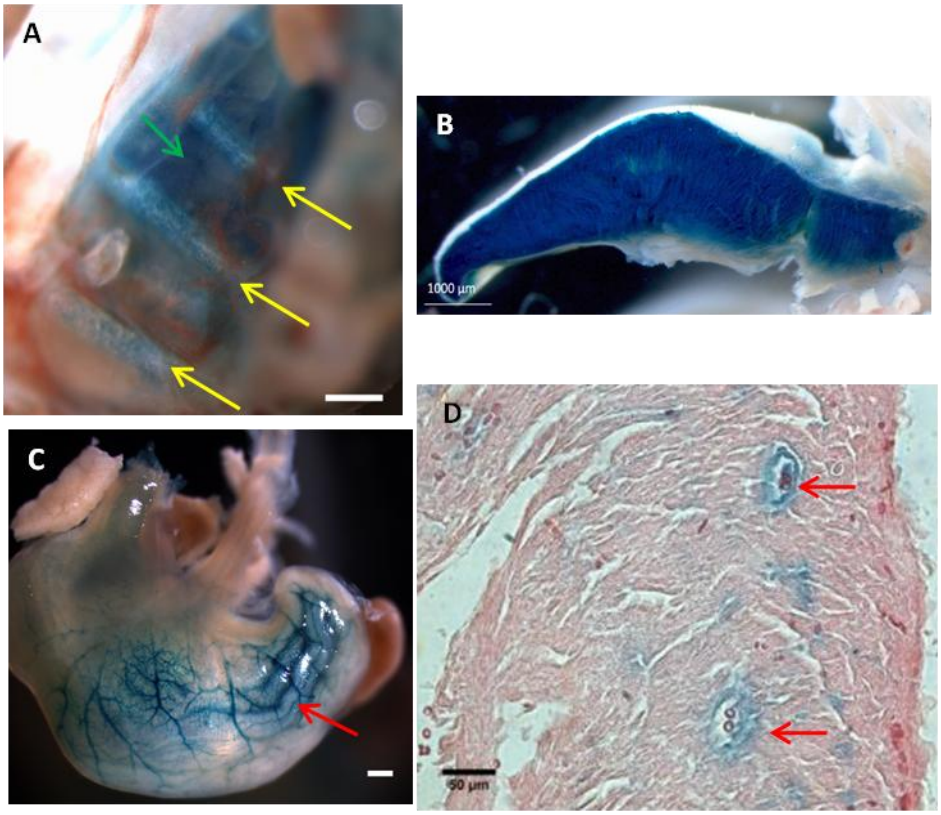

Figure 5.4. XGal staining of the various different muscles of neonatal *Cre/+; +/XLlacZGT* mice

(A) The intercostal muscle tissue surrounding the ribs (green arrow) stains for the fusion protein. Staining was also seen in the rib bones (yellow arrow). 500 µm scale bar

(B) Strong XL-βGal fusion protein staining in the muscle of the neonatal tongue (Staining performed by Stefan Krechowec). 1000 µm scale bar

(C) In stomach tissue of neonatal *CMV-Cre*/+; +/*XLlacZGT* mice XL-βGal fusion protein was confined to the blood vessels (red arrow). No staining was observed in the tissue of the stomach itself (Picture taken by Stefan Krechowec). 500 µm scale bar

(D) Neonatal heart in *Nestin-Cre*/+; +/*XLlacZGT* shows expression in the blood vessels (red arrows) but no staining in the muscle cells of the cardiac tissue. Counter-stained with Eosin. (Picture taken by Anna Newlaczyl). 50 µm scale bar; 7 µm paraffin section.

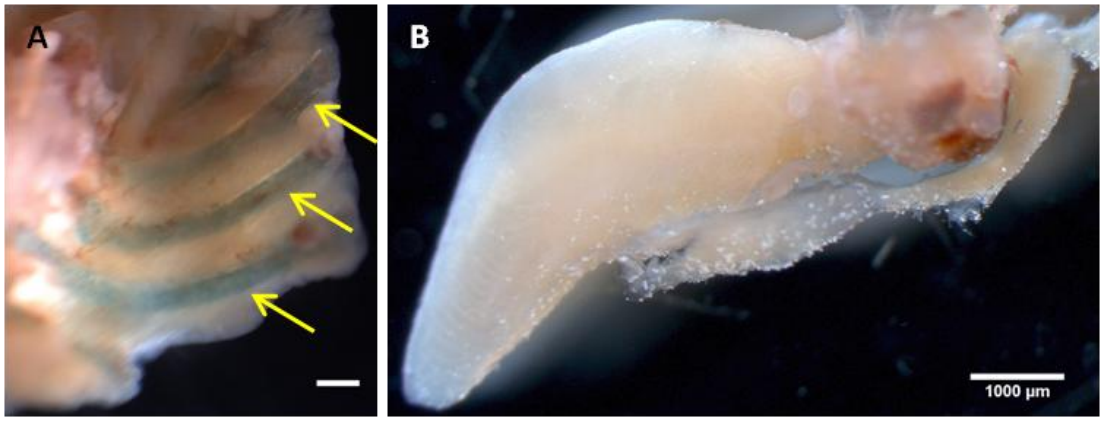

Figure 5.5. Muscle XGal staining in whole mount tissues of control +/+; +/*XLlacZGT* neonatal mice
(A) Control staining in the intercostal muscle +/+; +/*XLlacZGT* mice. There is staining in the rib bones detected indicating that it is endogenous βGalactosidase-like activity (Yellow arrows). XGal precipitate was not observed in the muscles.
(B) Whole mount staining of +/+; +/*XLlacZGT* neonatal tongue. None of the strong blue XGal precipitate is formed remains in this tissue.

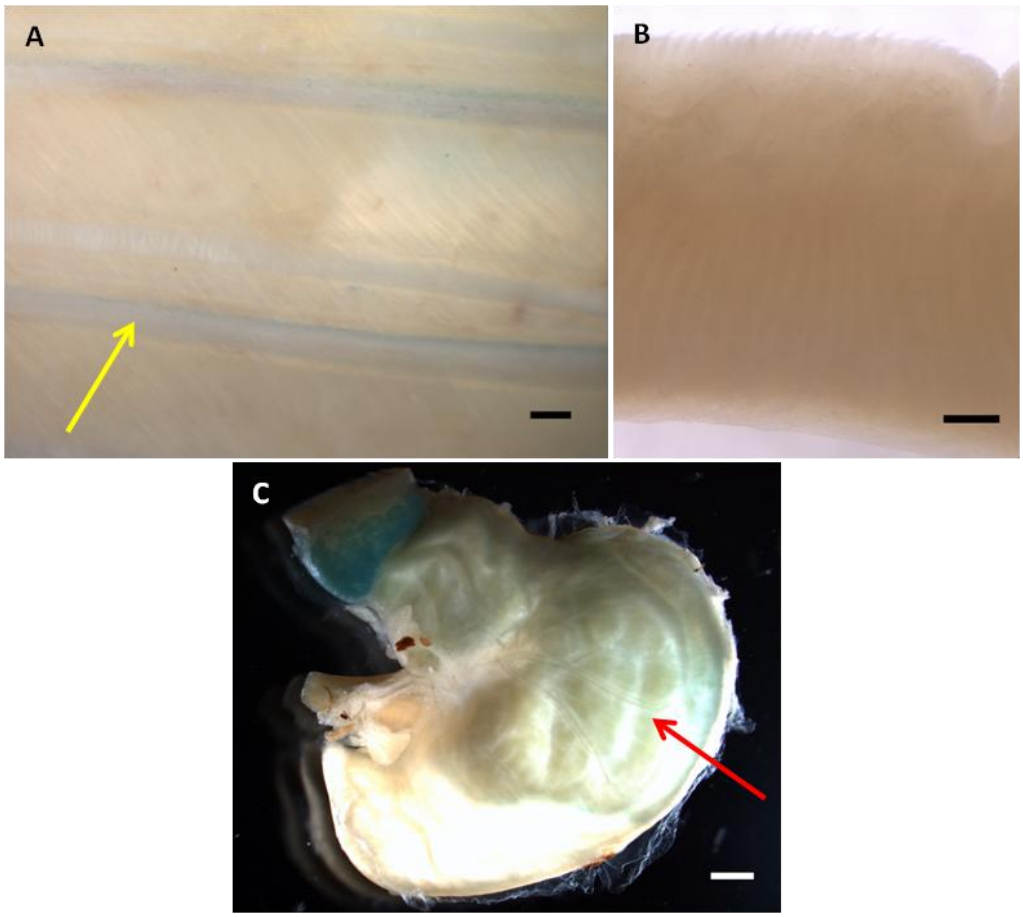

Figure 5.6. Whole mount XGal staining of adult peripheral tissues in *CMV-Cre*/+; +/*XLlacZGT* mice

(A) The strong blue XGal precipitate seen in neonates in lost in adult *CMV-Cre*/+; +/*XLlacZGT* mice. The endogenous βGalactosidase-like activity seen in bones is still observed (yellow arrows).

(B) XGal staining in the tongue of adult *CMV-Cre*/+; +/*XLlacZGT* mice showed no XL-βGal fusion protein expression

(C) XGal staining in whole mount stomach tissue indicated that XL-βGal fusion protein expression is lost in the blood vessels in adult *CMV-Cre*/+; +/*XLlacZGT* mice.

500 μm Scale bars

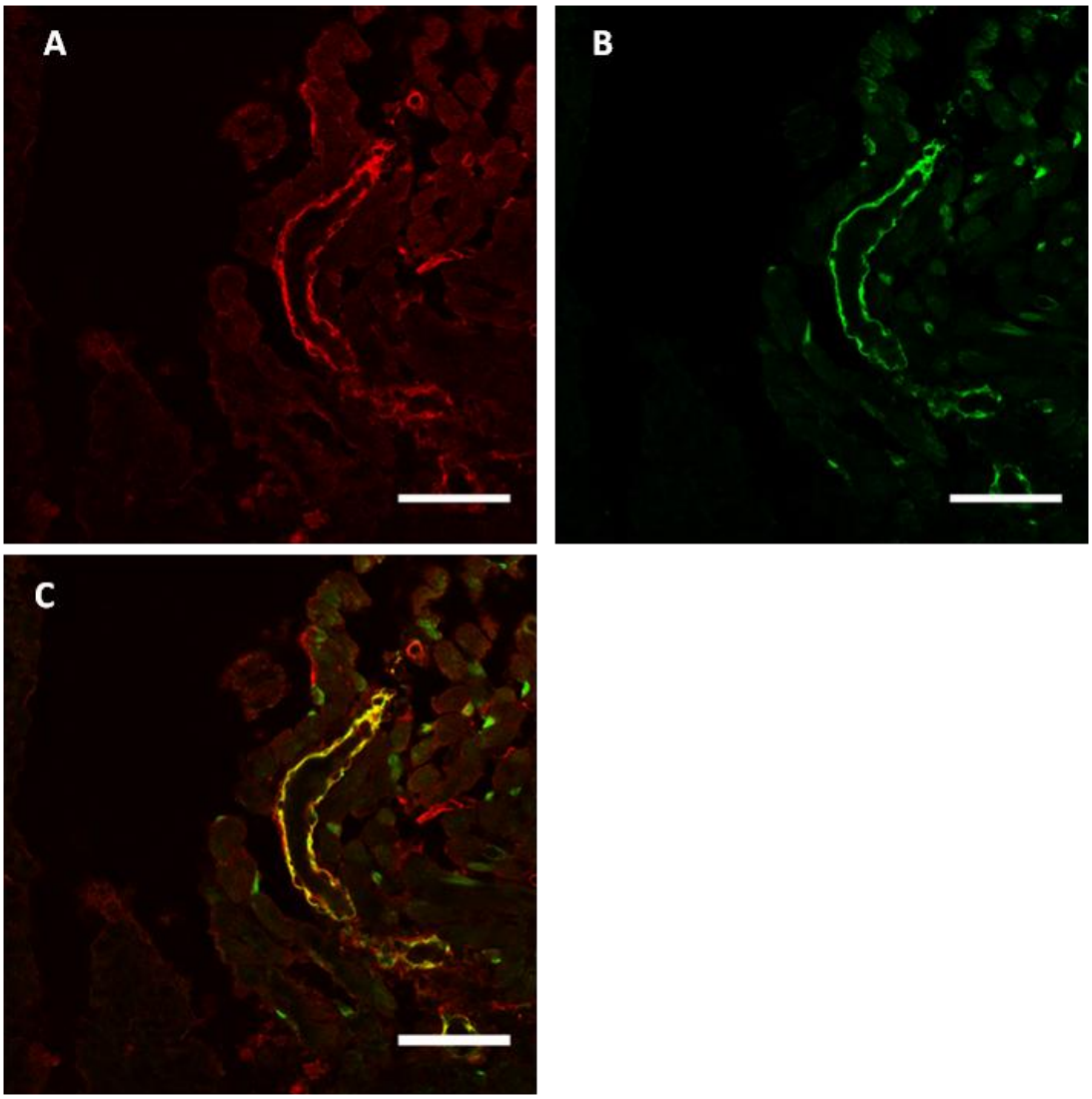

Figure 5.7. Confocal images of Colocalisation of XL-βGal fusion protein and alpha smooth muscle actin in neonatal blood vessels using immunofluorescence staining

(A) XL-βGal fusion protein staining in blood vessels with the anti-βGalactosidase antibody

(B) Alpha Smooth muscle actin staining in blood vessels with a directly labelled anti-alpha smooth muscle actin antibody

(C) Merged image of XL-βGal fusion protein and alpha smooth muscle actin in **(A)** and **(B)** respectively showing high level of colocalisation between the two proteins

50 μm scale bars; 14 μm cryostat sections

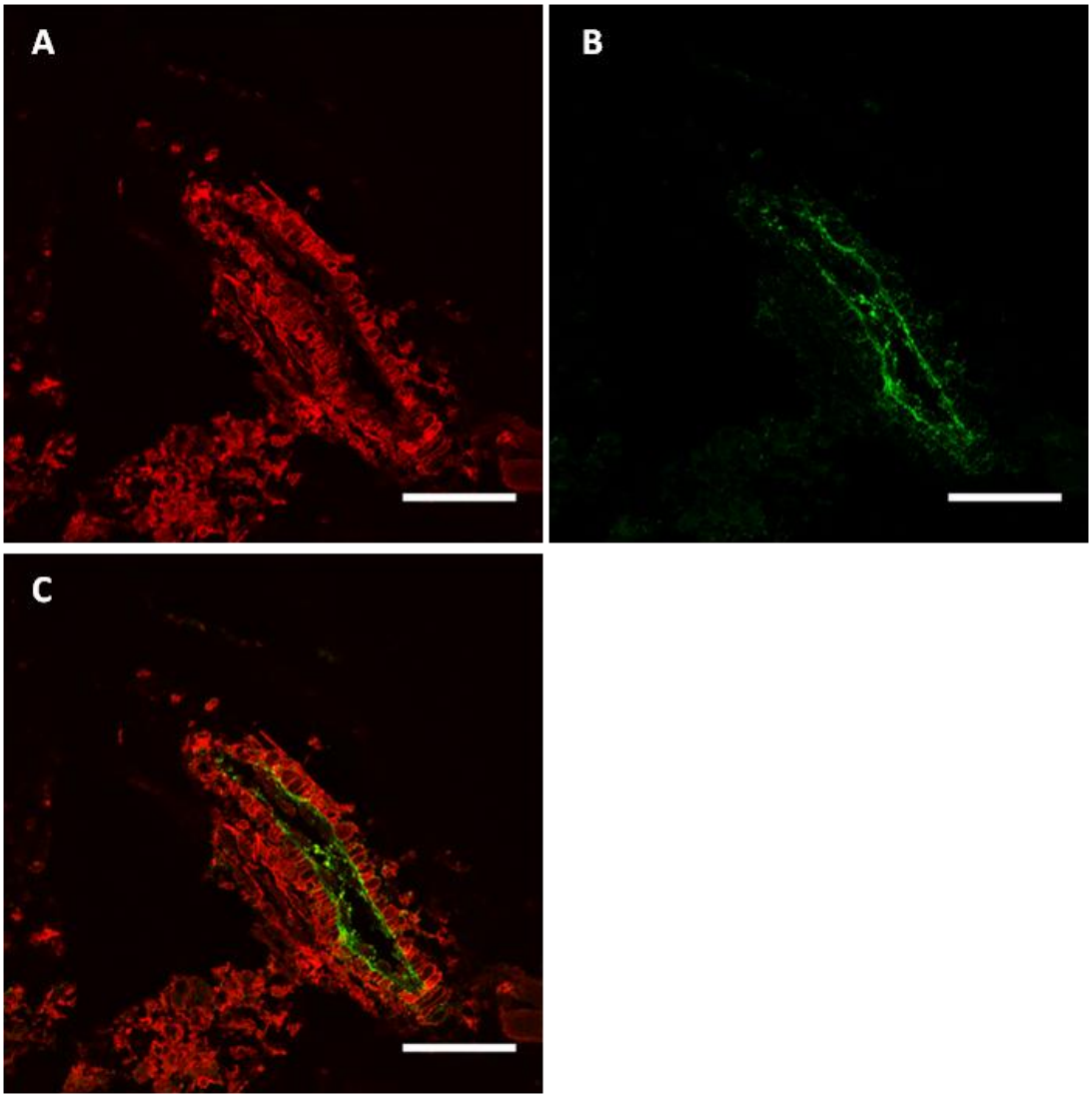

Figure 5.8. Confocal images of co-staining of XL-βGal fusion protein and von Willebrand Factor in neonatal blood vessels using immunofluorescence staining

(A) XL-βGal fusion protein staining in neonatal blood vessels of muscles

(B) von Willebrand Factor staining of neonatal blood vessels. This is a marker for endothelial cells in blood vessels.

(C) Merged image of XL-βGal fusion protein and von Willebrand Factor showed there was no overlap between XL-βGal fusion protein and von Willebrand Factor

50 μm scale bars; 14 μm cryostat sections

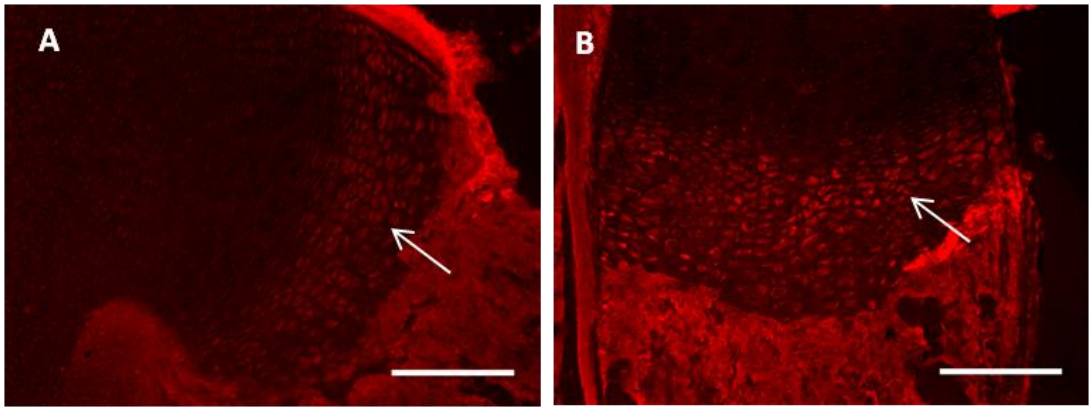

Figure 5.9. Neonatal immunofluorescence staining in the growth plates of neonatal limb bones is βGalactosidase-like activity

(A) βGalactosidase-like staining in the limb bones of *CMV-Cre*/+; +/*XLlacZGT* mice with the βGalactosidase antibody showed staining in the growth plates of neonatal mice

(B) There is βGalactosidase staining in the growth plates of +/+; +/*XLlacZGT* mice. This means there is βGalactosidase –like activity in the growth plates of bones.

500 μm scale bars; 25 μm cryostat sections

anti-βGalactosidase antibody showed the same pattern of staining with comparable strength (Figure 5.9. B). Negative controls showed little background staining could be attributed to the Dylight 594 secondary antibody. This endogenous βGalactosidase-like activity was also observed in bones of neonatal and adult mice using XGal staining (Figure 5.4. A; Figure 5.5. A; Figure 5.6. A) Endogenous βGalactosidase-like activity was also observed in the adult kidney medulla in +/+; +/*XLlacZGT* mice, in the sphincter of the stomach and the upper intestine of neonatal and adult mice (Figure 5.10).

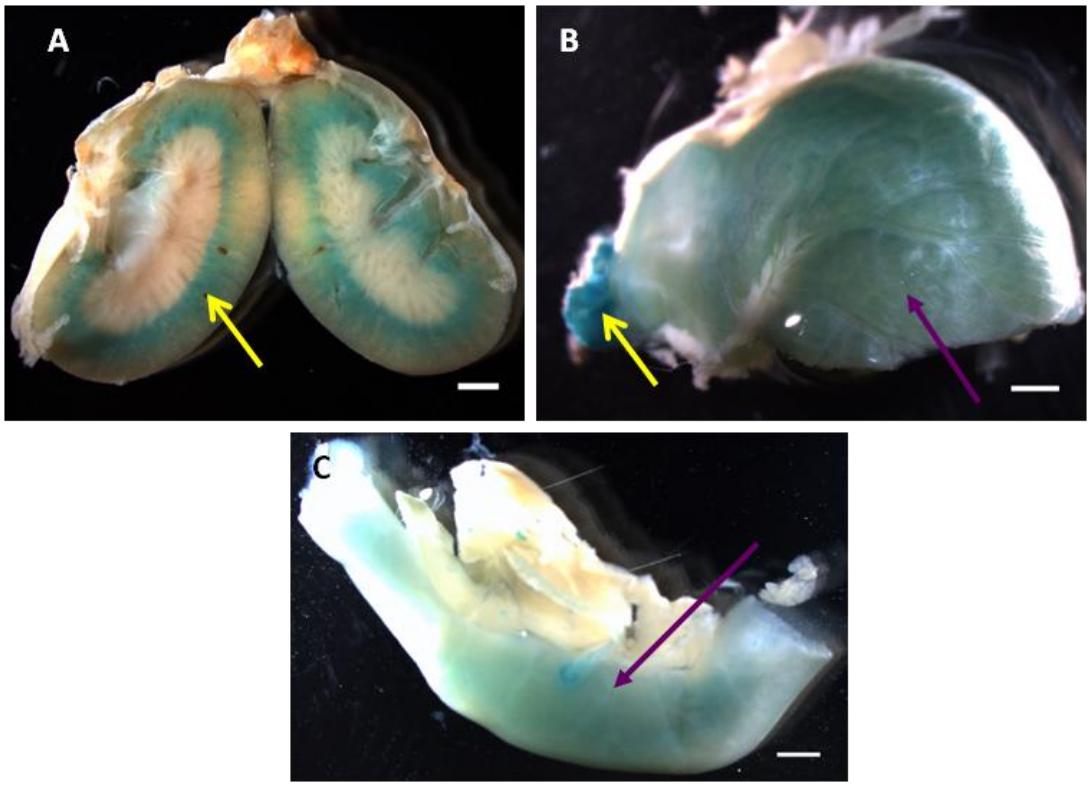

Figure 5.10. Whole mount control XGal staining in +/+; +/*XLlacZGT* adult mice showed endogenous βGalactosidase staining in some tissues

(A) Endogenous βGalactosidase-like staining in the medulla of the adult kidney.

(B) Endogenous βGalactosidase-like activity is seen in the sphincter of the stomach. The diffuse blue staining in the stomach is probably due to the gut flora of the mice

(C) In the upper gastrointestinal tract there was a diffuse staining in +/+; *+/XLlacZGT* mice which was attributed to the gut flora of mice. LacZ being a bacterial enzyme would result in a false positive staining in the gut.

500 μm scale bars; Yellow arrows indicate endogenous staining; Purple arrows indicate false positive staining in the gut caused my micro-flora found in the rodent gastrointestinal tract

5.4. DISCUSSION

5.4.1. PERIPHERAL *GNASXL* STAINING IN MUSCLES IS LIMITED TO NEONATES

Analysis of XL-βGal expression in neonatal peripheral tissues was previously confined to analysis of mRNA with Northern blots and RT-PCR (PLAGGE *et al.* 2004; XIE *et al.* 2006). These data indicated that there was neonatal *Gnasxl* expression in the heart, stomach, WAT and BAT (PLAGGE *et al.* 2004). Histology performed on these tissues in this project revealed that there was no XL-βGal expression in the cells of these tissue types and that the expression observed was from the blood vessels that ran through these tissues. Vascular tissue would have formed part of the Northern blot lysates previously analysed from these tissues but it would not have been possible to determine which cell types contributed to the detection of *Gnasxl.*

Further analysis of the XL-βGal expression in the neonatal blood vessels established that it was limited to the αSMA (as indicated by co-staining) in the muscular walls of the blood vessels. There was no staining in the endothelial cells of the vessels. This is consistent with other expression in the intercostal muscles and tongue. The very strong expression in the tongue of the neonates indicates it might be playing an important role in this area during development and this is obviously developing before birth. It is possible that the deletion of *Gnasxl* expression in these muscle tissues is a cause for the inertia observed in *Gnasxl* knock-out mouse pups (CATTANACH and KIRK 1985; KRECHOWEC and PLAGGE 2008; PLAGGE *et al.* 2004).

Analysis of adult muscle indicates that there is no expression of *Gnasxl* in any muscle tissues including the tongue, the intercostal muscles, or the blood vessels. These data concur with previous findings in rats and mice (PASOLLI *et al.*

2000). It is possible that this transient muscle expression during the neonatal period could be an explanation for the recovery of correct feeding behaviour (tongue and facial muscles) and activity levels (skeletal muscles) in adult knock-out mice (CATTANACH and KIRK 1985; KELLY *et al.* 2009; PLAGGE *et al.* 2004; XIE *et al.* 2006).

5.4.2. XL-βGAL FUSION PROTEIN EXPRESSION IN OTHER PERIPHERAL TISSUES

In the adrenal medulla and the pituitary XLαs expression had previously been identified with *in situ* hybridisation (PLAGGE *et al.* 2004). This data was replicated with XL-βGal staining and this expression pattern was maintained at adult stage. This is unsurprising as these tissues are derived from the neural tissues of the embryo and *Gnasxl* is highly expressed in neural tissues (PASOLLI and HUTTNER 2001).

5.4.3. ENDOGENOUS βGALACTOSIDASE-LIKE STAINING ACTIVITY

Endogenous βGalactosidase-like activity also detected in adult kidney medulla and in the gastrointestinal tracts of both neonates and adults. Mice have a large population of naturally occurring gut flora and as lacZ is an *E.Coli* derived enzyme it is likely that this is the cause of the staining seen in the gastrointestinal tissues.

The endogenous staining in all bones of neonatal and adult bones (regardless of genotype) might be due to staining in osteoclasts. This has been described previously (ODGREN *et al.* 2006).

CHAPTER 6. ANALYSIS OF METHYLATION IN THE *XLLACZGT* MOUSE LINE

6.1. INTRODUCTION

6.1.1. *XLLACZGT* CARRIER MICE EXHIBIT AN UNEXPECTED PHENOTYPE

Genotyping of the *XLlacZGT* pups from crosses of male gene trap carriers with female Cre-mice revealed that the genotypes were born in the expected Mendelian ratio. However, the phenotype of the +/+; +/*XLlacZGT* mice – which were expected to behave like and have the phenotype of wild type mice as the gene trap they carried would be inactive and should not have an effect on the expression of the XLαs protein – had the phenotype of *CMV-Cre*/+; +/*XLlacZGT* active gene trap carriers. In appearance they looked like *Gnasxl*$^{m+/p-}$ mice as well as showing the same neonatal mortality and growth retardation. In crosses of wild type females and *XLlacZGT* males, offspring showed the same phenotype when carrying the inactive gene trap. This unexpected phenotype of +/+; +/*XLlacZGT* pups led to the suspicion that *Gnasxl* expression might have become down-regulated by the insertion of the gene trap cassette in place of exon A20. Analysis of the expression levels by qPCR of *Gnasxl* in the Cre-negative gene trap carriers showed that there was a 90% reduction in expression levels of *Gnasxl* compared to wild type mice (KRECHOWEC *et al.* 2012).

To elucidate the cause of this reduction in mRNA expression levels the +/+; +/*XLlacZGT* mice were analysed for their methylation pattern at the *Nespas* and *Gnasxl* promoter with the wild type mice. *LacZ* cassette insertions can cause disruption to methylation. It has also recently been observed that the *Nespas-Gnasxl* DMR extends further along the locus than previously thought, and includes the A20 exon (SMALLWOOD and KELSEY 2011; TOMIZAWA *et al.* 2011). A gain of methylation on the paternal allele could cause silencing of the *Gnasxl* promoter.

6.1.2. AIMS

The aim of this experiment was to elucidate the methylation pattern at the differentially methylated proximal *Gnasxl* promoter and *Gnasxl* exon in *+/+*; +/*XLlacZGT* and wild type littermates produced from Cre x *XLlacZGT* crosses. The expected DNA fragments for each genotype had to be established and then the DNA from each genotype was analysed by Southern blot.

6.2. MATERIALS AND METHODS

6.2.1. TISSUE LYSIS FOR DNA EXTRACTION

Tissues were placed in tail lysis buffer at 55°C for 12-48 hours depending on the size of the tissue. If the tissue piece was large it was necessary to precipitate the DNA with an equal volume of isopropanol, remove the lysate and resuspend the DNA pellet with 500 μL 1 x TE buffer before performing the phenol/chloroform extraction described below.

6.2.2. GENOMIC DNA EXTRACTION AND PURIFICATION

Under the fume hood, an equal volume of phenol: chloroform: isoamyl alcohol (25:24:1; Sigma) was added to each sample and the sample was shaken until the solution was mixed thoroughly. The samples were centrifuged for 30 seconds and the aqueous layer was transferred to a fresh tube. It was important not to carry over any of the protein interphase layer. An equal volume of chloroform: isoamyl alcohol (24:1; Sigma) was added to the aqueous layer; the samples were mixed vigorously and then centrifuged for 30 seconds. The aqueous layer was again removed and transferred to a fresh tube. To this 0.1 volumes of 3 M sodium acetate (pH 5.0) and 2.5 volumes of 100% EtOH were added and mixed until white strings of DNA were observed. The samples were centrifuged for 1 minute and the supernatant removed; care was taken not to touch the DNA pellets. The DNA pellets were then washed with 70% EtOH and centrifuged for 1 minute. The EtOH was removed and the pellets were allowed to air-dry at 37°C for 10 minutes. Dry pellets were resuspended in an appropriate volume of 1 x TE.

6.2.3. RESTRICTION DIGESTS OF GENOMIC DNA

10-20 μg genomic DNA was digested with restriction enzymes overnight

at 37°C in a total volume of 50 µL containing one unit of restriction enzyme and 1 x concentration of restriction enzyme buffer. Digests were electrophoresed on 0.8-1.2% agarose gels made with TAE buffer and containing ethidium bromide for visualisation.

6.2.4. SOUTHERN BLOTTING AND DNA HYBRIDISATION

6.2.4.1. DIG PCR DNA probe labelling kit (Roche)

Primers were initially tested in Go Taq PCR reactions to make sure primer pairings produced bands of the expected size. 50 µL DIG-PCR reaction mix consisting of 160 ng/µl plasmid DNA; 1 x Buffer; 1 x DIG synthesis mix; 1 mM forward primer; 1 mM reverse primer; 1 U DIG polymerase was run on the thermocycler. The program consisted of a continuously heated lid at 111°C and a 2 minute hot start at 95°C followed by 30 cycles of: 30 seconds denaturing at 95°C, 30 seconds annealing at 56°C and 3 minutes extending at 72°C. The 30 cycles were followed by a final extension time of 7 minutes at 72°C and cooling to 10°C. 2 µL of the PCR product was run on a 2% agarose gel containing ethidium bromide to establish that the reaction worked. The labelled probes produced in the PCR reactions were heat denatured for 10 minutes at 100°C and then added to an appropriate volume of hybridisation solution to be used as DNA probes in hybridisation of blotted membranes.

6.2.4.2. Southern Blotting of Agarose Gels

Restriction digests of genomic DNA were run on agarose gels (0.8 or 1.2%) at a low voltage for several hours or overnight along with an appropriate DNA ladder. Gels were imaged in a gel dock along with a UV-sensitive ruler to allow confirmation of the band sizes detected on membranes after hybridisation and development. On completion of electrophoresis the gel was treated for 5 – 10 minutes in 0.25 M HCl, twice for 15 minutes with denaturing solution (0.5 M

NaOH; 1.5 M NaCl) and twice for 15 minutes with neutral solution (1 M NH_4 acetate). Gels were blotted with the bottom side exposed to a nylon membrane (GE Healthcare) for 24 – 48 hours to ensure complete transfer of DNA to the membrane. After cross-linking with UV light using a Stratagene Cross-linker to permanently bind the DNA to the membrane, the membranes were pre-hybridised with hybridisation buffer at 68°C for at least one hour. This solution was exchanged for the hybridisation buffer containing denatured DIG-labelled DNA probe and hybridised overnight at 68°C. Membranes were washed with 2 x SSC and 0.1% SDS, twice for 5 minutes at room temperature, then with two preheated stringent washes (0.2 x SSC and 0.1% SDS) for 20 minutes at 68°C. Equilibration was performed with DIG buffer 1 for several minutes prior to blocking the membrane with 1% blocking reagent (Roche) for 30 minutes at room temperature on a shaker. The membrane was incubated with 1% blocking reagent containing alkaline phosphatase-conjugated anti-DIG-Fab fragments (1:5000; Roche) for at least 30 minutes. Finally the membranes were washed twice for 15 minutes with DIG buffer 1 followed by equilibration in DIG buffer 3.

6.2.4.3. Membrane Development

A preparation of 45 µL NBT and 35 µL BCIP per 10 mL DIG buffer 3 was used for membrane development. The membrane was left floating in the development solution in the dark until a purple precipitate formed on the membrane (usually overnight) and the DNA fragments could be observed. Washing membranes in PBS stopped the reaction. Membranes were left to dry on Whatman™ 3MM paper in the dark, then stored in the dark.

6.3. RESULTS

6.3.1. SELECTION OF RESTRICTION ENZYMES

Using pDraw software, the *Gnasxl* promoter and exon were analysed for restriction site sequences of two types of restriction enzyme with specific properties. Firstly, a non-CpG methylation-sensitive enzyme was investigated; this needed to cut two or three times around the *Nespas-Gnasxl* DMR to create large DNA fragments, easily detectable by Southern blot, that could be cut into smaller fragments. The second enzyme was a methylation-sensitive restriction enzyme which would cut within the larger fragments created by the non-methylation-sensitive restriction enzyme. The two enzymes selected were NsiI (non-methylation-sensitive) and EagI (methylation-sensitive); these enzymes cut in each genotype differently with the sizes indicated in Table 6.1. For restriction site sequences of the restriction enzymes see Appendix 5.

6.3.2. DESIGN OF DIG-LABELLED DNA PROBES

Two probes were created to analyse the whole of the methylation region covering the *Gnasxl* promoter and exon 1. The first probe was created using the XL DIG Probe F1 and XL DIG Probe R1 primers (XL Dig probe F1/R1; Appendix 1). This would detect the methylation in the promoter and beginning of the *Gnasxl* exon (Figure 6.1). The second probe was created using the XL-F10 and XL-R5 primers (XL-F10/R5 probe; Appendix 1). This probe would detect the 687 bp fragment at the end of the *Gnasxl* exon 1 (Figure 6.1).

6.3.3. SOUTHERN BLOTTING OF DNA FROM *XLLACZGT* NEONATAL MICE

Brain tissue, dissected on neonatal day 1 (see Chapter 3), was prepared for genomic DNA extraction. DNA was collected from a +/+; +/*XLlacZGT* mice along with wild type littermates.

	+/+; +/XLlacZGT	**WT**	***CMV-Cre/+; +/+***
XL-DIG F1/R1 probe			
EagI/NsiI (EagI sites methylated)	(8.8 kbp) 5.8 kbp	5.8 kbp	5.8 kbp
EagI/NsiI (EagI sites unmethylated)	3.4 kbp	3.4 kbp	3.4 kbp
XL-F10/R5 Probe			
EagI/NsiI (EagI sites methylated)	(8.8 kbp) 5.8 kbp	5.8 kbp	5.8 kbp
EagI/NsiI (EagI sites unmethylated)	1.1 kbp	687 bp	687 bp

Table 6.1. Fragments detected by Southern blot probes. Brackets indicate the fragment size if the paternal allele were to have unexpected methylation.

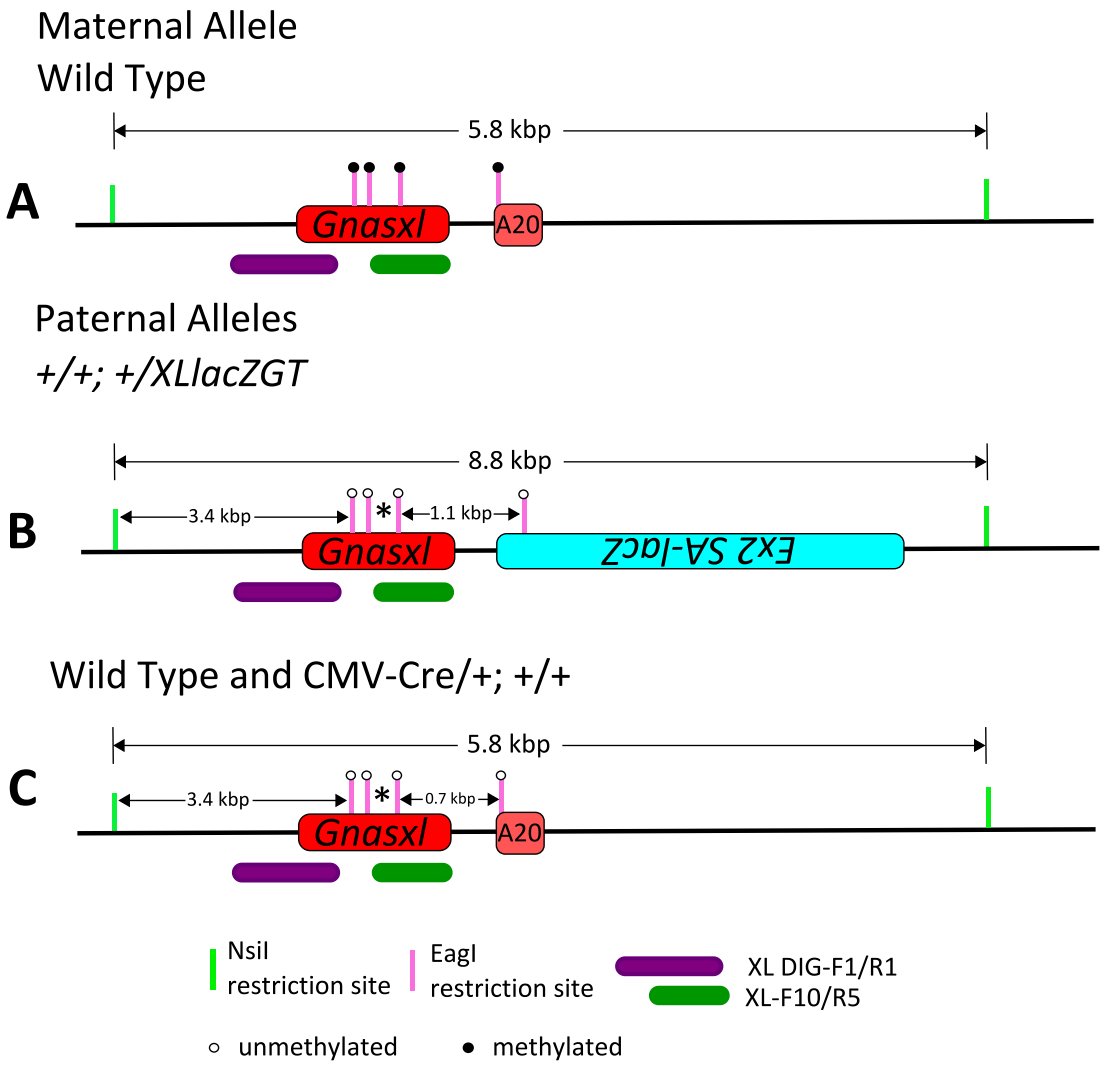

Figure 6.1. Schematic of Restriction Digest Patterns for Southern blotting of DNA from offspring of a *Cre* x *XLlacZGT* cross

(A) The maternal allele of each of the genotypes should be identical as it was inherited as a wild type allele from *Cre*-transgenic mice. As the maternal allele is methylated at the *Gnasxl* exon 1, it was expected that each probe would detect a 5.8 kbp DNA fragment.

(B) Carriers of the paternally inherited non-active gene trap, in the inverted position were expected to produce one detectable fragment for each probe that was used. The XL DIG-F1/R1 probe would detect a fragment of ~3.4 kbp while the XL-F10/R5 probe would detect a 1.1 kbp fragment if the paternal allele remained unmethylated (8.8 kbp if the paternal allele was methylated).

(C) Offspring that inherited a wild type paternal *Gnasxl* allele (with or without *Cre*) would produce the same size fragment as is detectable with the XL DIG-F1/R1 in gene trap carrying offspring of 3.4 kbp. The XL-F10/R5 would detect a 687 bp fragment.

* indicates a fragment of ~300 bp that is too small to be detected by XL-F10/R5 probe, open circles indicate no methylation at that position; closed circles indicate the presence of methylation at that position.

Although the hybridised blot only produced weak signals and had strong background, the XL Dig F1/R1 probe detected the maternal wild type allele fragment, which was expected to be methylated and contained no gene trap, at 5.8 kbp (Table 6.1; Figure 6.2). The paternal allele was also detected in all genotypes, producing a DNA fragment at 3.4 kb, which indicated an un-methylated allele (Table 6.1; Figure 6.2).

The XL-F10/R5 probe produced a different pattern of methylation depending on the genotype as these fragments were affected by an EagI restriction site within the *lacZ* cassette or the A20 exon (Table 6.1; Figure 6.1). The maternal wild type allele indicated that methylation was the same in all genotypes (5.8 kbp fragment; Figure 6.3). The paternal allele showed the expected 1.1 kbp fragment for the +/+; +/*XLlacZGT* DNA, and the 687 bp fragment for the wild type and *CMV-Cre*/+; +/+ (Figure 6.3).

Although these blots were not ideal and were performed on a tight timescale towards the end of the PhD project they showed that the methylation pattern of the mice carrying the inactive gene trap was as expected and not altered by the addition of the gene trap.

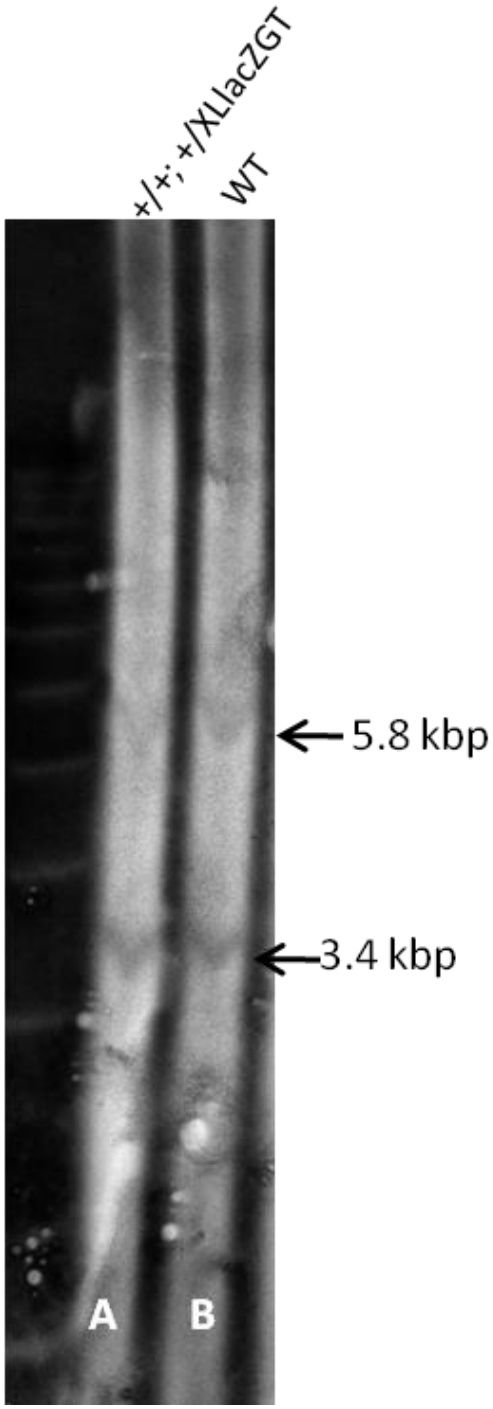

Figure 6.2. Southern Blot of neonatal brain with XL Dig-F1/R1 probe

(A) +/+; +/*XLlacZGT* DNA produced a fragment of 5.8 kbp this would be from the maternal allele and 3.4 kbp – this would be from the paternal allele. There is no detection of a larger 8.8 kbp fragment that would occur if methylation was present on the paternal allele and no reduction of the 3.4 kbp band which would disappear (or be reduced) if methylation occurred unexpectedly.

(B) The wild type DNA produces the same 5.8 kbp fragment from the maternal allele and a 3.4 kbp. fragment from the paternal allele.

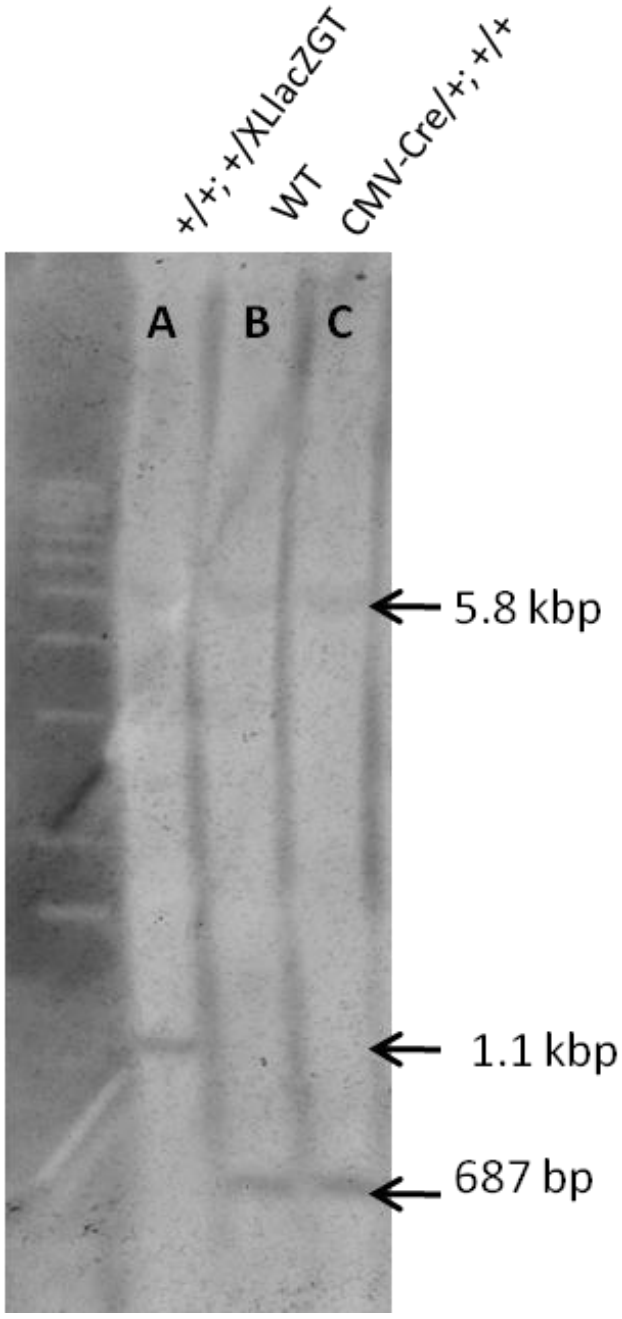

Figure 6.3. Southern Blot of Cre/*XLlacZGT* neonatal brain with XL-F10/R5 probe

(A) +/+; +/*XLlacZGT,* non-active gene trap carriers, produced the expected 5.8 kbp fragment from the maternal allele and the 1.1 kbp fragment that would be expected from the paternal allele if methylation was not present. This would suggest that the methylation is not altered.

(B) The wild type DNA produced fragments as expected. The methylated maternal allele appeared as expected along with the 687 bp fragment from the paternal allele that was expected.

(C) The *CMV-Cre*/+; +/+ mice appeared as wild type mice as expected.

6.4. DISCUSSION

The analysis by Southern blot revealed that there was no change in the methylation using either of the two probes. The maternal allele was detected as expected, with methylation still maintained in all of the genotypes. No unexpected methylation occurred in the *Gnasxl* exon region of the paternal alleles of the different genotypes. Given more time it would have been preferable to improve the Southern blot analysis and perhaps analyse the methylation using a more quantitative method (e.g. qPCR).

As there is no alteration in the methylation that could have been caused by the insertion of the gene trap, it is likely that inserting the gene trap in the position of exon A20 disrupted or deleted an important regulatory element, such as an enhancer. This would account for the reduced expression levels that are seen in both the *Cre*/+; +/*XLlacZGT* mice expressing the XL-βGal fusion protein and in the mice carrying the inactive gene trap (KRECHOWEC *et al.* 2012).

A new gene trap mouse line is in development in the laboratory. The gene trap uses td-tomato red fluorescent protein as the reporter instead of *lacZ*. The gene trap has been inserted further into the *Gnasxl* intron in a non-conserved region. This should not interfere with any enhancer elements that might be present around the exons.

CHAPTER 7. EXPLORATION OF POSSIBLE XLαS INVOLVEMENT IN NEUROPEPTIDE SIGNALLING IN THE BRAIN

7.1. INTRODUCTION

7.1.1. HYPOTHALAMIC REGULATION OF ENERGY HOMEOSTASIS

The hypothalamus is an important centre for food intake regulation and energy metabolism as previously discussed in Chapter 4. In this region of the brain there are many signalling neuropeptides that have been implicated in the control of energy homeostasis. These fall into one of two categories. Firstly, orexigenic peptides – those that increase food intake – and secondly, anorexigenic peptides – those that decrease food intake. Their effects on energy expenditure can differ regardless of their effects on food intake. Adult *Gnasxl*$^{m+/p-}$ mice have increased energy expenditure as well as increased food intake (an unusual combination), as it is normal that neuropeptides which increase food intake would reduce energy expenditure – although this is not always the case. *Gnasxl*$^{m+/p-}$ mice also have an increased leptin-sensitivity (Frontera *et al*. in prep) and insulin-sensitivity (XIE *et al.* 2006). These aspects of signalling are controlled (partially) in the hypothalamus and thus it was important to establish which pathways might be affected by the lack of XLαs.

7.1.2. OREXIN AND MELANIN-CONCENTRATING HORMONE INTERACT IN THE LH AND DMH TO REGULATE ENERGY HOMEOSTASIS

Orexin is an orexigenic peptide found in the LH and DMH. It is derived from the precursor pre-pro-orexin, a 130-residue polypeptide (SAKURAI *et al.* 1998). A product of a gene on mouse chromosome 2, the pre-pro-orexin amino acid sequence is conserved between species – human 83% identity to rat, mouse 95% identity to rat – with most of the differences between the sequences occurring in the C-terminal part of the precursor (DE LECEA *et al.* 1998; SAKURAI *et al.* 1998). This pre-pro-orexin gives rise to two separate peptides, orexin A and

orexin B, which show a large similarity to secretin (DE LECEA *et al.* 1998). Functional orexin appears in embryonic development and by the day of birth there are low levels expressed in the hypothalamus, reaching maximum expression by day 20 after birth (VAN DEN POL *et al.* 2001).

Orexin A is 33 amino acids in length and is C-terminally amidated. This molecule is highly conserved between species with bovine, rat, mouse and human orexin A being identical (SAKURAI *et al.* 1998). Orexin B is a 28 amino acid peptide, which is 46% identical to orexin A. Although this molecule is conserved between mouse and rat (DE LECEA *et al.* 1998; SAKURAI *et al.* 1998) there are two amino acid substitutes in the human form compared to the rodent form (SAKURAI *et al.* 1998). It also induces a transient increase in intracellular calcium in CHO/OX_1R cells in a dose dependent manner (DE LECEA *et al.* 1998; SAKURAI *et al.* 1998).

Two receptors have been discovered that can bind orexins: orexin receptor 1 (OX_1R) and orexin receptor 2 (OX_2R). These two G-protein-coupled receptors (GPCR) were discovered to have 64% identity and are more similar to each other than any other receptor (NAMBU *et al.* 1999; SAKURAI *et al.* 1998). They are conserved between species and are strongly expressed at neonatal stages. However, expression decreases towards adulthood (NAMBU *et al.* 1999; SAKURAI *et al.* 1998; VAN DEN POL *et al.* 2001).

Medium-sized orexin neurons constitute one of two types of neurons located in the LH of the brain (ABIZAID *et al.* 2006; DE LECEA *et al.* 1998; SAKURAI *et al.* 1998; VAN DEN POL *et al.* 2001). Immunofluorescence has shown that orexin is found in the cytoplasm of neurons (SAKURAI *et al.* 1998). When orexin A is applied to the LH there is a three-fold increase in food consumption within one

hour (SAKURAI *et al.* 1998; VAN DEN POL *et al.* 2001). These data suggest that orexins play some role in feeding regulation. Neurons in other areas of the brain involved in energy homeostasis do not express either isoform of orexin (DE LECEA *et al.* 1998; SAKURAI *et al.* 1998). However, orexin axons have a far-reaching effect with projections to the LDTg, NTS, the PVN, LC and the posterior hypothalamus (DE LECEA *et al.* 1998; NAMBU *et al.* 1999; VAN DEN POL *et al.* 2001). Withholding food for 48 hours results in a 2.4-fold increase in the production of pre-pro-orexin mRNA showing that orexin expression is responsive to nutritional status (SAKURAI *et al.* 1998).

In human patients with narcolepsy, a disorder that causes excessive drowsiness and sleep attacks, there is a deficiency of orexin. These patients have a decreased food intake but their BMI increases (SAKURAI 2007). It was also discovered that mice lacking orexin were hypophagic and developed late onset obesity due to decreased energy expenditure (SAKURAI 2007). There is a dense projection of orexin neurons to the Arc where orexins might act on NPY neurons while inhibiting POMC neurons in the same region (SAKURAI 2007). Reciprocal connections have also been observed indicated by NPY receptors being expressed in orexin-positive neurons (STANLEY *et al.* 2005). It is possible that orexins act upstream of the NPY system to regulate feeding behaviour and energy metabolism (ABIZAID *et al.* 2006). Decreases in food intake occur when anti-orexin A antibodies or OX_1R-selective antagonists are administered ICV (HAYNES *et al.* 2000; YAMADA *et al.* 2000) and when mice lack orexin (HARA *et al.* 2001; WILLIE *et al.* 2001). Administration of an OX_1R–selective antagonist decreases food intake in ob/ob leptin-deficient mice (HAYNES *et al.* 2002). Chronic administration of orexin A does not result in any change in body weight

(YAMANAKA *et al.* 1999).

It is essential that animals remain alert during the time they must spend searching for food and orexin seems to be an important factor in this response. If there is a scarcity of food then there is usually an increased "awake" period in order to facilitate further food searching. If orexin is not present then mice do not have this response (SAKURAI 2007). It has also been observed that orexins promote and maintain food anticipatory activity (FAA) (SAKURAI 2007). Food can be restricted to a specific period, when mice do not normally feed. This results in c-fos (a marker for neuronal activity) expression in orexin neurons during the restricted period when food was available rather than when the mice normally feed. Hence orexin neurons are active at the time when food is available and not when mice normally feed. This change in neuronal activation is not present in mice lacking orexin (SAKURAI 2007). Projections occur from neurons in the SCh to neurons which stimulate orexin, indicating an indirect role for orexin in circadian feeding behaviours (SAKURAI 2007). It may also provide a link between obesity and insomnia (ABIZAID *et al.* 2006).

Orexin stimulates sympathetic outflow which could be a reason for the increase in BMI in the orexin-ablated mice (SAKURAI 2007). It is possible that a decrease in orexin may produce decreased sympathetic tone and a decrease in energy expenditure (SAKURAI 2007). Food-seeking behaviours are known to be reinstated when ventral tegmental area infusions of orexin are administered (SAKURAI 2007).

ICV administration of orexin A strongly activates the CRH-expressing neurons in the limbic system, specifically in the central amygdala, and it would appear that there is a reciprocal activation (SAKURAI 2007). GABA, glucose, 5-HT,

NA and leptin are all known to inhibit orexin neurons while many peripheral humoral factors related to metabolism also influence them (SAKURAI 2007; STANLEY *et al.* 2005). Studies have also shown that orexin neurons are sensitive to the nutritional state of the body (BERTHOUD 2004; SAKURAI *et al.* 1998; YAMANAKA *et al.* 2003). In narcoleptic dogs it has been observed that food perception results in cataplexy (a sudden relaxation of muscle tone, often associated with an emotional state). This suggests that orexin is essential for the proper perception of food and some inadequacy in this system results in cataplexy (SAKURAI 2007). Orexin has been found to increase synaptic activity by increasing presynaptic release of glutamate and GABA (VAN DEN POL *et al.* 1998; VAN DEN POL *et al.* 2001). It has been established that orexin-expressing neurons act upon MCH neurons depolarising them and increasing synaptic transmission to these neurons (VAN DEN POL *et al.* 2004).

MCH is a 19 amino acid cyclic neuropeptide (BITTENCOURT *et al.* 1992) expressed primarily in the LH and ZI of the brain and derived from the *pmch* gene. These neurons are confined to a separate population than those expressing orexin. It has been shown to increase food intake and decrease energy expenditure (COLL *et al.* 2007; FUNATO *et al.* 2009; SHIMADA *et al.* 1998). MCH-expressing neurons have projections to many areas of the brain important for integration of nutrient-sensing and feeding behaviour. This makes their placement in the LH ideal for their signalling involvement in feeding regulation and energy expenditure (BITTENCOURT *et al.* 1992). MCH neurons have also been shown to partially co-express CART in the LH (F. BRISCHOUX 2001).

MCH-deficient mice have reduced body weight and are hypophagic despite having decreased plasma leptin levels and POMC mRNA, as well as

having an increased metabolism similar to the *Gnasxl*$^{m+/p-}$ mouse line (SHIMADA *et al.* 1998; XIE *et al.* 2006). Crosses of MCH knock-out mice with the leptin-deficient ob/ob obese mice produced less obese ob/ob offspring. This suggests that MCH has some opposing effect to leptin working downstream of leptin to regulate energy expenditure plus locomotor activity, and plays a significant role in the maintenance of energy balance (SEGAL-LIEBERMAN *et al.* 2003). MCH has also been found to depress the synaptic activity of its target cells (glutamate and GABA neurons) in rat hypothalamus (GAO and VAN DEN POL 2001).

MCH1R has been identified as a GPCR (originally discovered as an orphan GPCR and was named SLC-1 or GPR24) (LEMBO *et al.* 1999). MCH1R mRNA is localised to many areas of the brain, which also express XLαs including the Arc, Amy and DMH (SAITO *et al.* 2001). The MCH receptor 1 (MCH1R) knock-out might have more relevance to the *Gnasxl*$^{m+/p-}$ as they display a lean, hyperactive and hyperphagic phenotype more similar to the phenotype observed for the *Gnasxl*$^{m+/p-}$ mice (CHEN *et al.* 2002; MARSH *et al.* 2002; XIE *et al.* 2006).

7.1.3. CORTICOTROPIN-RELEASING HORMONE

CRH is a 41 amino-acid peptide. It is well described that CRH is located in the important SNS outflow centre, the PVN. CRH can also be found in the cerebral cortex, cerebellum and amygdalo-hippocampal complex (BITTENCOURT *et al.* 1999; SWANSON *et al.* 1983). It has other functions beside SNS mediation including neuroendocrine, autonomic and behavioural responses to stress as well as in controlling energy homeostasis. CRH has been shown to stimulate energy expenditure through BAT and reduce food intake (RICHARD *et al.* 2000).

This neuropeptide has two known receptors: CRHR1 and CRHR2 (PERRIN

and VALE 1999). These are both GPCRs (DAUTZENBERG and HAUGER 2002) which are known to couple the $G_s\alpha$ subunit for signalling (DAUTZENBERG *et al.* 2000). This $G_s\alpha$ coupling is involved in the Ca^{2+} transduction mediated by CRH receptors (BISHOP *et al.* 2000; CHALMERS *et al.* 1996; GUTKNECHT *et al.* 2009).

A deficiency of CRH is often related to neurodegenerative disorders such as Alzheimer's, Parkinson's and Huntingdon's (BEHAN *et al.* 1995; DE SOUZA 1995). If the opposite is induced (CRH is elevated) this has been associated with major depression (ARBORELIUS *et al.* 1999; MITCHELL 1998). CRH has also been implicated in eating disorders like anorexia nervosa.

7.1.4. CATECHOLAMINES IN THE HYPOTHALAMUS

Catecholamines are important neurotransmitters in the brain. XLαs is expressed in many regions of the brain which are catecholaminergic including the LC, the main noradrenergic centre in the brain. Tyrosine hydroxylase (TH) is the enzyme important in the production of catecholamines. It converts L-tyrosine to L-dihydroxyphenylanine (DOPA) using tetrahydrobiopterin as a co-enzyme and is the rate-limiting step in the production of noradrenaline and adrenaline. TH is found in the cytoplasm of catecholamine expressing cells (Figure 7.1).

Dopamine plays a role in food intake control as well as locomotion and emotional behaviours. Dopamine's control of energy homoeostasis is likely to be due to projections to the hypothalamus. Deficiency of the dopamine D2 receptor results in lean mice with decreased food intake. They have reduced plasma leptin with increased leptin sensitivity (KIM *et al.* 2010). It is thought that D2 receptors might have a role in the control of food intake by controlling signalling to the arcuate nucleus through leptin signalling (KIM *et al.* 2010).

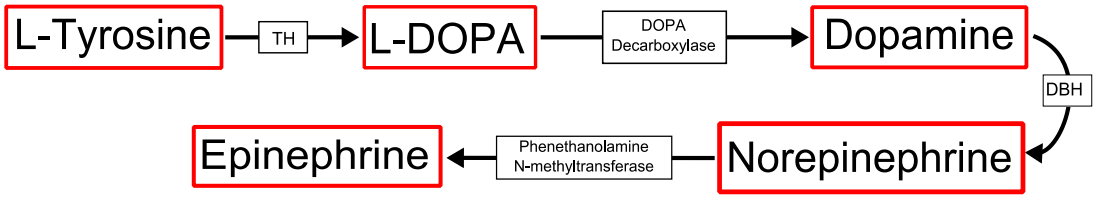

Figure 7.1. The production of Catecholamines.

L-Tyrosine is converted to L-DOPA by tyrosine hydroxylase (TH). L-DOPA is then converted to dopamine by DOPA decarboxylase. Dopamine is converted to norepinephrine this in turn is converted to epinephrine by phenethanolamine N-methyltransferase.

7.1.5. LEPTIN AND INSULIN SIGNALLING IN THE HYPOTHALAMUS

Leptin is secreted by adipocytes as a measure of adiposity and it is relayed to the brain to control food intake accordingly. The main centre for control of food intake and energy metabolism is in the hypothalamus. Here, the many signals that regulate energy homeostasis are integrated to regulate energy expenditure and food intake according to nutrient signals relayed from the peripheral tissues (i.e. the gut and adipose tissue). Leptin is known to increase energy expenditure and decrease food intake (CAMPFIELD *et al.* 1995; HALAAS *et al.* 1995; PELLEYMOUNTER *et al.* 1995; STEPHENS *et al.* 1995). Concurring with this finding, leptin-deficient ob/ob mice are obese and develop diabetes mellitus type 2 (INGALLS *et al.* 1950; ZHANG *et al.* 1994). The same effects are observed in mice (and humans) deficient in leptin receptor (LepR) (CLÉMENT *et al.* 1998; TARTAGLIA *et al.* 1995; ZHANG *et al.* 1994). Leptin has also been associated with other metabolic processes in bone homeostasis, reproduction, mood and emotions (BLÜHER and MANTZOROS 2007; KARSENTY 2006; LAM and LU 2007; LU 2007).

Gnasxl$^{m+/p-}$ mice have decreased plasma insulin and leptin as well as being insulin-sensitive (XIE *et al.* 2006) and leptin-sensitive (Frontera *et al.* in prep). Weight-reducing properties of leptin result from its inhibitory effect on orexigenic NPY/AgRP-expressing neurons in the Arc and its stimulatory effect on anorexigenic POMC neurons, reducing food intake and increasing energy expenditure (ELIAS *et al.* 1999). The leptin knock-out mouse line (ob/ob) or the knock-out of the leptin receptor (db/db) are obese and have poor fertility (HUMMEL *et al.* 1966; INGALLS *et al.* 1950). These mice have activated NPY/AgRP neurons that inhibit POMC neurons, which results in increased food intake and

decreased energy expenditure (ELIAS *et al.* 1999). In the Arc there are different populations of neurons of interest. The orexigenic NPY/AgRP neurons and the anorexigenic pro-opiomelanocortin (POMC) neurons are known to have opposing effects on controlling energy metabolism through leptin signalling (HAHN *et al.* 1998). Leptin stimulates POMC neurons resulting in a decrease in food intake and an increase in energy expenditure while producing an inhibitory effect on NPY/AgRP neurons (ELIAS *et al.* 1999). When leptin signalling is reduced these NPY/AgRP neurons are no longer inhibited by leptin, food intake is increased and energy expenditure is decreased (ELIAS *et al.* 1999). These neurons have inhibitory projections to POMC neurons, further reducing the restrictions on food intake (Figure 7.2). Both of these groups of neurons in the Arc have projections that exert their respective effects on MCH and orexin neurons in the LH (ELIAS *et al.* 1999).

POMC is the precursor for α-melanin-stimulating hormone (α-MSH). This activates melanocortin-3 and melanocortin-4 receptors (MC3R and MC4R). Deleting either of these receptors results in obesity and leptin resistance, whilst deletion of both results in an obesity phenotype more severe than their individual deletions (CHEN *et al.* 2000).

AgRP neurons release γ-aminobutyric acid (GABA). This release inhibits the neuronal activity of POMC neurons in the Arc (Figure 7.2) (COWLEY *et al.* 2001). Conversely, increased leptin inhibits the release of GABA from AgRP neurons and thus the inhibition of POMC neurons by AgRP is reduced (ELIAS *et al.* 1999).

When LepRs are restored in the Arc of LepR-deficient mice both hyperphagia and obesity are corrected (WALL *et al.* 2001). This indicates

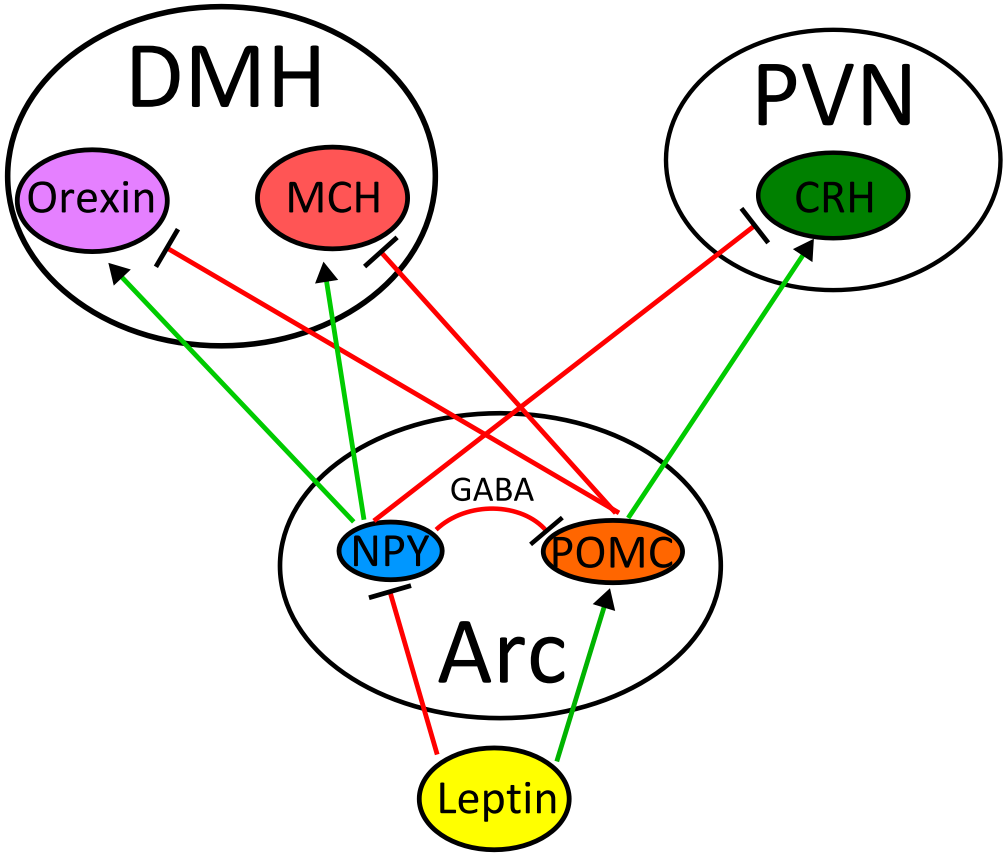

Figure 7.2. Schematic of the integration of nutrient sensing signals in the hypothalamus.
Leptin released from white adipose tissue inhibits neuropeptide Y expressing neurons which increase food intake and decrease energy expenditure and stimulates POMC neurons which decrease food intake and increase energy expenditure. NPY neurons inhibit POMC neurons by the release of GABA. NPY and POMC neurons have opposing effects on CRH in the PVN and on orexin and MCH in the DMH.
Green arrows indicate a stimulatory pathway. Red arrows indicate inhibitory pathway.

that neurons in this nucleus are essential for correct leptin signalling controlling food intake. LepR is not only expressed in the Arc but in many other regions of the brain including the PVH, DMH, LH and NTS (MORRIS AND RUI 2009).There is evidence that LepR in these different areas might act in parallel or synergistically (DONATO *et al.* 2011). It has been found that leptin and insulin act in parallel in anorexigenic POMC neurons to activate the PI3K pathway. However, in AgRP neurons these two molecules have opposing effects (XU *et al.* 2005). This implies that these two populations have different mechanisms for the mediation of these signals in the Arc (XU *et al.* 2005).

The mTOR-S6K pathway is essential for appropriate nutrient sensing in the hypothalamus (COTA *et al.* 2006; MORRIS and RUI 2009). mTOR signalling relevant to metabolism is known to occur in POMC and NPY/AgRP neurons in the Arc (COTA *et al.* 2006). This pathway is activated through signalling via the insulin receptor substrate (IRS). Both insulin and leptin are able to act via IRS, insulin directly and leptin in a triple complex with JAK2 and SH2B (Figure 7.3) (DUAN *et al.* 2004a; MORRIS and RUI 2009). SH2B is a ubiquitously expressed protein found in the cytoplasm of cells. It contains a pleckstrin homology (PH) and a src-homology-2 (SH2) domain along with many phosphorylation sites (RUI *et al.* 1997). SH2B has been shown to bind IRS and JAK2 at the same time resulting in leptin-stimulated PI3K signalling in cultured cells (DUAN *et al.* 2004a). Mice lacking SH2B ($SH2B^{-/-}$) have insulin resistance, glucose intolerance, leptin resistance, hyperphagia and obesity (DUAN *et al.* 2004b; REN *et al.* 2005). They also have increased energy expenditure gaining less weight than pair-fed wild type littermates despite hyperphagia, suggesting SH2B is involved in the control of both food intake and energy expenditure but could

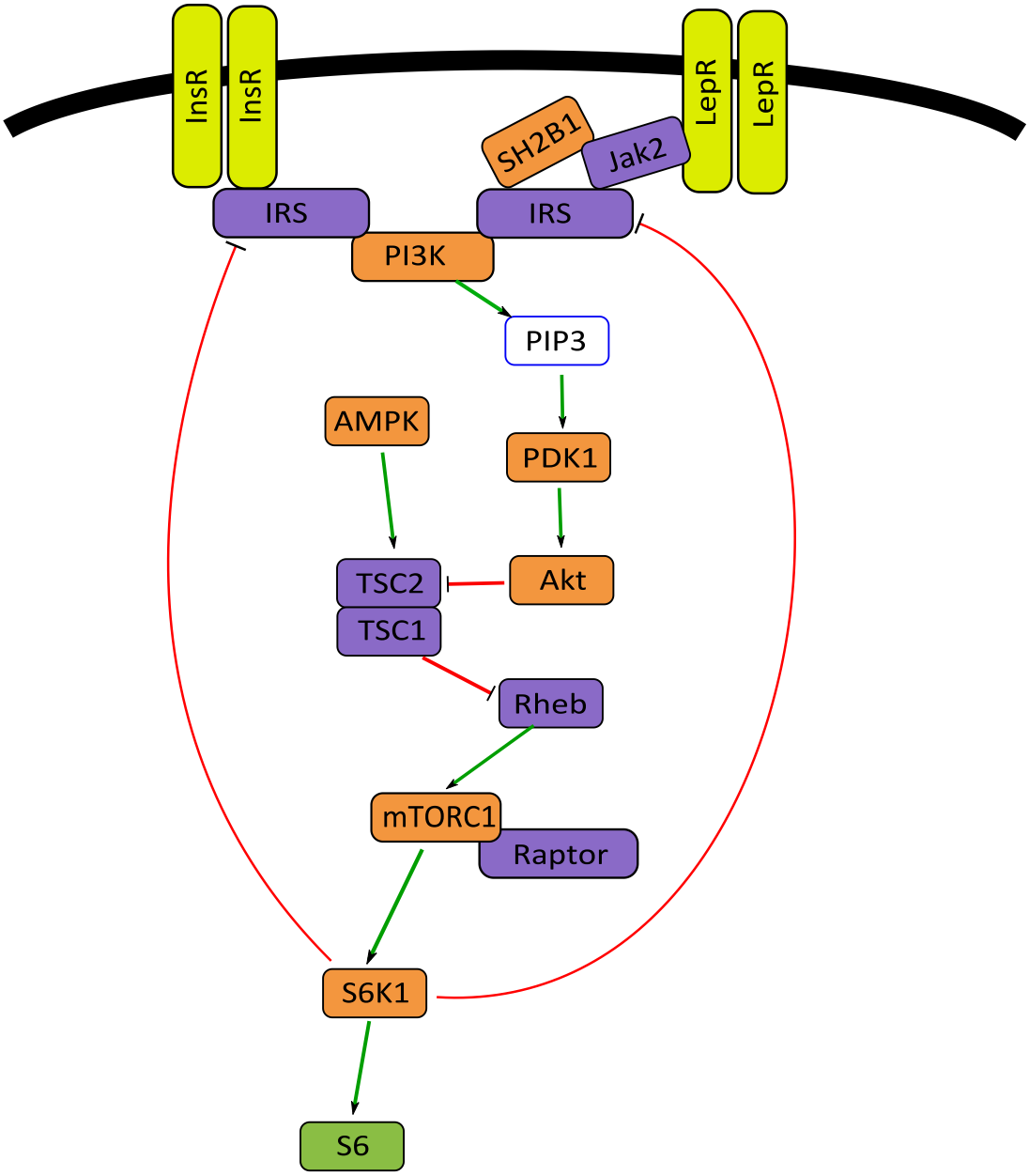

Figure 7.3. Schematic of insulin and leptin receptor signalling via the mTOR-S6K1 pathway.
Binding of insulin to the insulin receptor (InsR) results in activation of the insulin receptor substrate (IRS). This in turn activates the PI3K pathway, forming PIP3 activating PDK1 and Akt. Akt is an inhibitor of the tuberous sclerosis (TSC) protein 1/2 complex which in turn is an inhibitor of the mTORC1 complex. mTORC1 activates S6K1, resulting in the production of active S6 and the inhibition of IRS. This desensitises the receptor signalling and can cause insulin resistance.
It is also possible for leptin to activate this pathway. Leptin binds to the leptin receptor (LepR) this can activate IRS by the formation of a triple complex of Janus kinase 2 (JAK2), SH2B and IRS which can be bound by the leptin receptor and results in the activation of the PI3K pathway which continues as above.
It is possible for AMPK to stimulate the TSC complex which results in the inhibition of the mTOR-S6K pathway.

regulate them via separate neuronal pathways (REN *et al.* 2005). Interestingly, neuron-specific restoration of SH2B improves hyperphagia and reduces energy expenditure (REN *et al.* 2007).

Binding of IRS results in signalling via the mTOR-S6K1 pathway, after activation of the PI3K-Akt pathway. The activation of Akt results in the inhibition of the TSC1/TSC2 complex. This removes the inhibition that the TSC1/TSC2 complex imposes on mTOR and allows the activation of mTOR and S6K1. S6K1 is a major physiological substrate of mTOR in the hypothalamus (Figure 7.3) (CHENG *et al.* 2002). The activation of S6K1 results in a negative feedback loop onto IRS. This inhibits the whole pathway (Figure 7.3) (POLAK and HALL 2009). S6K1 activation produces active ribosomal protein S6 (rpS6) (Figure 7.3). This is a good histological marker for activation of the mTOR-S6K1 pathway.

Interestingly, the S6K1 knock-out mice are small with increased food intake, lypolysis, energy expenditure and insulin sensitivity with reduced body weight and adiposity, which is similar to the metabolic phenotype of the *Gnasxl*$^{m+/p-}$ mice (SHIMA *et al.* 1998; UM *et al.* 2004; XIE *et al.* 2006).

The leptin-mediated activation of mTOR signalling has important implications for weight management. It has also been shown that leptin induces a time- and dose-dependent phosphorylation of S6K1 in macrophages (MAYA-MONTEIRO *et al.* 2008).

7.1.6. GABAERGIC SIGNALLING IN THE HYPOTHALAMUS

$GABA_A$ neurons are central to the control of feeding behaviours (MIÑANO *et al.* 1992). It is thought that there are two opposing GABA-sensitive feeding centres that are present in the hypothalamus. If muscimol, the $GABA_A$ receptor

selective agonist, is applied to the medial nucleus of the hypothalamus then feeding is stimulated. However, if the same is applied to the lateral region of the hypothalamus then feeding is suppressed (MIÑANO *et al.* 1992).

Glutamate decarboxylase 67 kDa (Gad67) is a catalyst for the conversion of glutamate to GABA. Many GABA-expressing neurons act upon other neurons in an inhibitory manner (WATANABE *et al.* 2002). NPY neurons inhibit POMC through GABA release (Figure 7.2). XLαs has been shown to colocalise with NPY but not POMC neurons (Frontera *et al*. in prep).

A recent mouse line showed a very similar expression pattern of the vesicular GABA transporter (VGAT) in the brain to that of the *Gnasxl* expression identified in Chapter 4 (VONG *et al.* 2011).

7.1.7. GHRELIN

Ghrelin is a hunger hormone that is produced in the stomach and signals via the vagal nerve to the NTS (COLL *et al.* 2007). Its signalling increases food intake (COLL *et al.* 2007). Analysis of plasma from *Gnasxl*$^{m+/p-}$ mice has shown that there is a two-fold increase in plasma ghrelin in these mice (KRECHOWEC *et al.* 2012). This evidence supports another observation that injections of ghrelin in *Gnasxl*$^{m+/p-}$ mice produce a blunted response (i.e. a smaller increase in feeding) compared to wild type counterparts (Frontera *et al.* in prep).

It was discovered that ghrelin is the substrate for the previously known growth hormone secretagogue receptor (GHSR) (KOJIMA and KANGAWA 2008). There are ghrelin receptors on neurons in the Arc as well as in the brain stem. By binding to GHSR, ghrelin initiates a cascade of events culminating in the phosphorylation of AMPK (pAMPKα) which results is the inactivation of ACC (pACC) and thus a decreased production of malonlyl CoA which increases fatty

acid oxidation (Figure 7.4). AMPK is an activator of the TSC1/TSC2 complex which inhibits the mTOR-S6K1 pathway (Figure 7.3) (LAGE *et al.* 2008).

7.1.8. AIMS

The aim of this work was to investigate which pathways might be affected by the loss of XLαs. Pathways involved in the control of energy homeostasis were of particular interest, including the orexigenic peptides and pathways mediated by ghrelin and leptin signalling. This was analysed by immunofluorescence, immunohistochemistry and Western blotting.

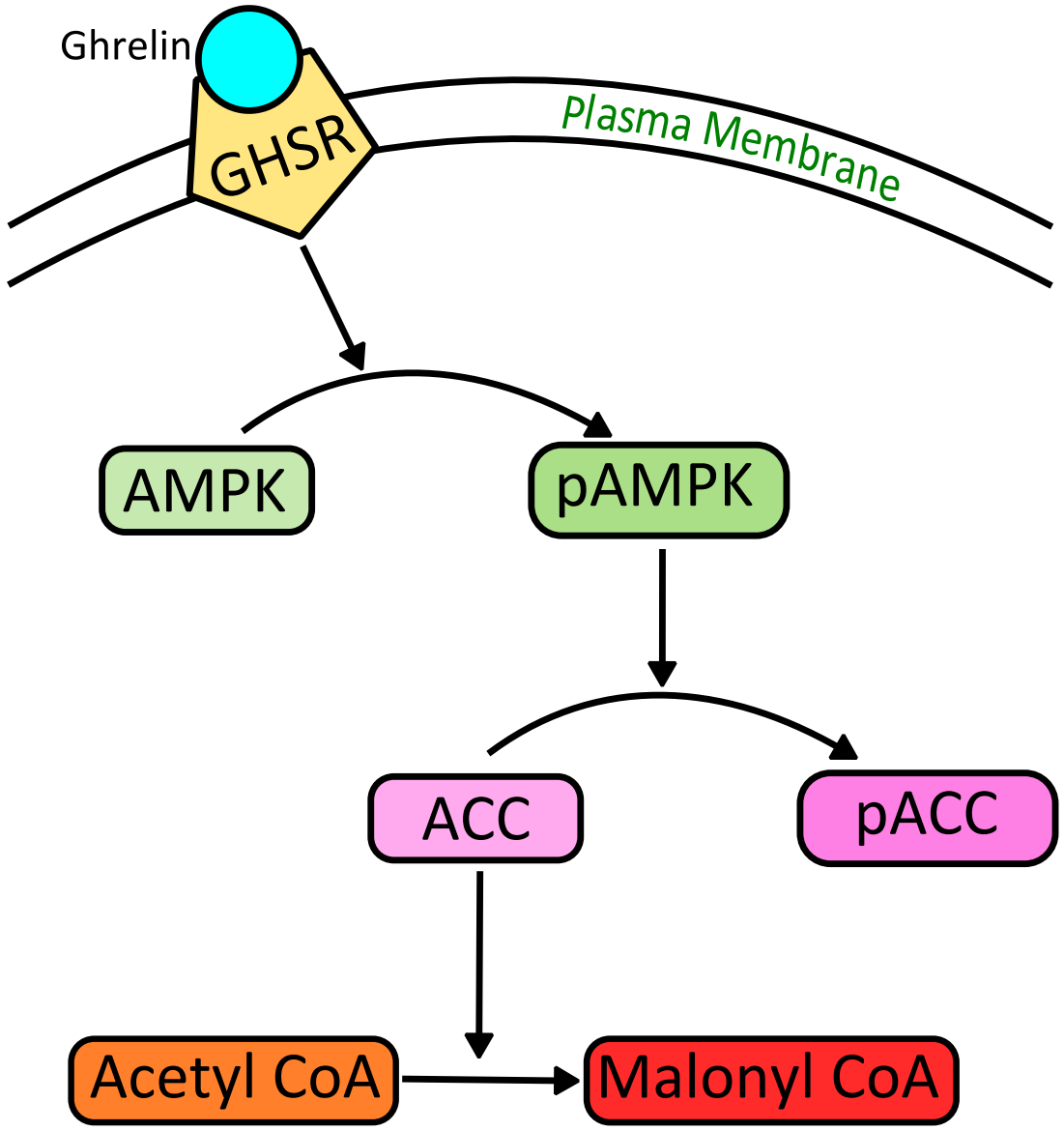

Figure 7.4. Ghrelin's Activation of AMPK.

Binding of ghrelin to the G-protein coupled growth hormone secretagogue receptor (GHSR) results in a cascade of events which finally results in the phosphorylation and activation of AMPK (pAMPK). This activation in turn results in the phosphorylation and inactivation of acetyl coenzyme A (ACC). The inactivation of ACC stops the conversion acetyl CoA into Malonyl CoA. A decrease in malonyl CoA results in the increased oxidation of cellular fatty acids.

7.2 MATERIALS AND METHODS

7.2.1. MICE AND TISSUE COLLECTION

Brains were collected from adult wild type and *Gnasxl*$^{m+/p-}$ mice. Tissues were collected and sectioned as in Chapter 4 for histology. Tissues to be used for Western blot analysis were collected by schedule one procedure, dissected out and frozen at -80°C until required for protein lysate preparation.

7.2.2 ANTIBODIES

7.2.2.1. Immunohistochemistry

The following primary antibodies were used: goat anti-XLαs (M14) (Santa Cruz; sc-18993; 1:200) and rabbit anti-MCH (Phoenix Pharmaceuticals; H-070-47; 1:500). Secondary antibodies used were: Vectastain Elite biotin-conjugated rabbit anti-goat (Vector laboratories; PK6105; 1:200), Vectastain Elite biotin-conjugated goat anti-rabbit (Vector laboratories; PK6101; 1:200), AffiniPure™ goat anti-rabbit HRP-conjugated (Jackson ImmunoResearch Laboratories; 703-035-155; 1:1000) and Affinipure™ donkey anti-goat Biotin conjugated (Jackson ImmunoResearch Laboratories; 705-065-147; 1:3000).

7.2.2.2. Immunofluorescence

The following primary antibodies were used: goat anti-XLαs (M14) (Santa Cruz; sc-18993; 1:200), rabbit anti-βGalactosidase (Cappel; 55976; 1:2000), rabbit anti-orexin A (Phoenix Pharmaceuticals; H-003-30; 1:500), rabbit anti-TH (Millipore; AB152; 1:200), rabbit anti-DBH (Santa Cruz; sc-15318; 1:100) and rabbit anti-pS6 (Cell Signalling Technology; #2211; 1:200). The following secondary antibodies were used: DAPI (Invitrogen; 1:1000), donkey anti-rabbit AF594 (Invitrogen; A21207; 1:1000) and donkey anti-goat AF488 (Invitrogen; A11055; 1:1000).

7.2.2.3. Primary antibodies tested and found to be unspecific in histology

Primary antibodies tested and found to be non-specific or that produced no staining included: rabbit anti-CRH (Abcam; ab8901), rabbit anti-CRH (Phoenix Pharmaceuticals; H-019-06) and rabbit anti-CRH (Lifespan Biosciences; LS-C50244).

7.2.2.4. Western blotting

Primary antibody concentrations used were*:* rabbit anti-pAMPKα (Cell Signaling Technology; #4188; 1:2000), rabbit anti-AMPKα (Cell Signaling Technology; #2603; 1:1000), rabbit anti-pACC (Cell Signaling Technology; 1:1000), rabbit anti-ACC (Cell Signaling Technology; #3662; 1:1000), monoclonal rabbit anti-pS6 (Cell Signalling Technology; #2211; 1:1000), monoclonal rabbit anti-S6 (Cell Signaling Technology; #2217; 1:1000), goat anti-XLαs (M14) (Santa Cruz; sc-18993; 1:500) and rabbit anti-GAPDH (Santa Cruz; sc-25778; 1:2000). Secondary antibodies were used in the following dilutions: AffiniPure™ donkey anti-goat horse radish peroxidase-(HRP-) conjugated (Jackson ImmunoResearch Laboratories; 703-035-147; 1:5000), AffiniPure™ goat anti-rabbit HRP-conjugated (Jackson ImmunoResearch Laboratories; 703-035-155; 1:10000).

7.2.3. IMMUNOHISTOCHEMISTRY DOUBLE STAINING

IHC was performed for XLαs as in the protocol described in Chapter 3. However, after incubation with the first colour substrate and washes, a 20 minute post-fix step with 4% PFA was applied, and the staining procedure was repeated as above using a different colour substrate (DAB without nickel chloride).

7.2.4. FLUORESCENCE ANALYSIS

Neuronal fluorescence intensity data for pS6 were analysed using ImageJ

software (RASBAND 1997-2011) on epifluorescence images. Individual cells were encircled. Their pixel intensity was measured and corrected for background intensity of the image from an average of nine 16 μm x 16 μm squares (100 x 100 pixels). Analysis of colocalisation was collected live on the epifluorescence microscope. Individual cells were deemed to be XLαs positive if they showed clear plasma membrane-associated staining. Staining of axons and punctuate non-specific staining were not included in cell counts.

7.2.5. WESTERN BLOTTING

7.2.5.1. Protein Lysate preparation

Individual hypothalami were homogenized and sonicated in 400 μL RIPA lysis buffer containing protease inhibitor cocktail (Sigma), PMSF (Sigma) and PhoSTOP (Roche). The first two inhibit the ability of proteases to break down proteins, and the latter protects against de-phosphorylation of proteins. Sonication disrupts the high molecular weight DNA. These samples were kept on ice then spun down for 10 minutes at 12000 g. Lysate supernatants were split into 100 μL aliquots and kept at -80°C allowing samples to be used for many experiments without fear of repeated freeze and thaw cycles damaging the proteins of interest. Protein concentration was determined using a Pierce® BCA Protein Assay kit (Thermo Scientific; 23227) following the manufacturer's directions.

7.2.5.2. Protein concentration analysis with Pierce® BCA Protein Assay kit

BSA protein standards were diluted from stocks provided with the kit and according to the manufacturer's instructions. Protein samples were diluted 1:10, then 100 μL of each sample and standard were pipetted into separate test tubes. Standards and samples were analysed in duplicate. To each test tube 2 mL working reagent was added and then incubated at 37°C for 30 minutes. The

tubes were allowed to cool to room temperature and then the OD_{562} measured for each. Average absorbencies of duplicate BSA standards produced a standard curve of protein concentration for the analysis. Protein lysate samples were compared to the standard curve and then the original 1:10 dilution was accounted for.

7.2.5.3. PAGE GELS

Gel cassettes (Sigma) were assembled and a resolving gel (see buffer list for composition) was poured into the cassette. The gel was overlayed with isobutanol and allowed to polymerise for 30 minutes. Polymerisation of the acrylamide was tested by checking that left over acrylamide had set in a 15 mL falcon. After polymerisation of this gel was complete the isobutanol was discarded and the gel front rinsed with ddH_2O. The gel front was dried carefully and the stacking gel (see buffer list for composition) was poured into the cassette, the comb inserted and the gel polymerised for 30 minutes. 20 µg of each lysate was mixed 1:1 with 2x Lamelli protein loading buffer (National Diagnostics) in a small volume, heat denatured for 3 minutes then loaded into the acrylamide gel along with a broad spectrum protein ladder (Fermentas). Any spare lanes were loaded with 1 x Lamelli protein loading buffer. The gel cassette was placed in the electrophoresis tank containing Tris-glycine running buffer and run at 10 mA through stacking gel then at 15 mA through the resolving gel until the bromphenol blue dye reached the bottom of the gel. It was important to keep the current constant to ensure expected migration of ions through the gel. The gel was removed from the glass plates and soaked for 10 minutes in transfer buffer ready to be placed in the blotting sandwich. Other components of the blot sandwich were prepared. Firstly, the sponge was soaked

in transfer buffer until any air bubbles trapped in it were removed. Then the Amersham Hybond™-P PVDF membrane (GE Healthcare) was soaked in MeOH for 10 seconds. The membrane was then soaked in ddH_2O for 5 minutes and in transfer buffer for 10 minutes. The Whatman-type™ 3MM filter paper was soaked for 20 minutes in transfer buffer. These components were layered onto the Western blot sandwich cassette, ensuring removal of any air bubbles between layers as they would disrupt transfer. Next the sponge was positioned in the cassette, then the gel (highest molecular weight bands towards the hinges), followed by the PVDF membrane and finally the filter paper. The cassette could then be folded over, clamped shut and placed into the transfer chamber with pre-cooled transfer buffer. This was allowed to equilibrate for 10 minutes with the magnetic stirrer before running the transfer at 30 V, 75 mA overnight. Transfer to the membrane was determined by checking for either the transfer of the coloured protein ladder to the membrane or by Ponceau staining.

7.2.5.4. Ponceau Staining:

To check that the transfer of the protein to the membrane had worked efficiently the membrane was submerged in Ponceau S solution for 5 minutes, destained in ddH_2O for 2 minutes then visualised. To completely destain the membrane for probing with antibodies it was washed in fresh ddH_2O for a further 10 minutes or until the red Ponceau S staining had disappeared.

7.2.5.5. Membrane Detection of Proteins:

Membranes were blocked with blocking solution (5% non-fat dried milk powder; 0.1% Tween20; TBS) for 1 hour at room temperature. They were then incubated with primary antibodies diluted in blocking solution overnight at 4°C. Membranes were washed four times for 10 minutes in TTBS and incubated with secondary antibodies diluted in blocking solution before being washed four

times with TTBS and incubated with Amersham™ ECL Plus Western Blotting Detection System (GE Healthcare), and exposed to film (Kodak). Films were developed in the dark and transferred through developer solution (Sigma) for 1 minute until bands of interest appeared, washed briefly in water and fixed for 1 minute in fixative solution (Sigma). Films were air-dried and stored at room temperature.

7.2.6. STATISTICAL ANALYSIS

pS6 intensity levels and Western blot data were analysed using ImageJ. Statistical tests were performed using MINITAB™ software. For pS6 fluorescence intensity data as well as Western blot analysis of pAMPKα, pACC and pS6, Student's t-tests were applied to the data. Cell counts for pS6 in the Arc were analysed by the non-parametric Wilcoxon matched-pairs signed-ranks test.

7.3. RESULTS

7.3.1. XLαS LOCALISATION IN THE LATERAL AND DORSOMEDIAL HYPOTHALAMIC AREAS

In the LH/DMH region of the brain are neurons expressing the orexigenic peptides orexin A and MCH. This area highly expresses XLαs as shown in Chapter 4. To assess the localisation of XLαs in comparison to orexin A, serial 14 µm, cryostat sections covering the entirety of the LH/DMH region of the brain were analysed in three rounds of staining (a total of 18 sections) to gain a representative overview of colocalisation for the two brains analysed. The data from sections across the whole area were pooled for each round of staining to achieve an average cell count for each individual. The percentage of colocalised cells was determined by dividing the number of colocalised cells by the number of orexin A positive cells or XLαs positive cells and standard error of the mean (SEM) was calculated. 23% of orexin A positive neurons in the DMH and LH coexpressed XLαs (n=2; 23.1 ± 5.22 %; Figure 7.5). 12 % of XLαs positive neurons also expressed orexin A (n=2; 11.7 ± 0.79 %; Figure 7.5).

A second population of neurons in the LH/DMH region of the hypothalamus, which is positive for MCH and separate from orexin A, did not express XLαs (Figure 7.6). Immunohistochemistry staining clearly indicated singly stained cells for each protein with no overlap of the two populations.

7.3.2. DOPAMINERGIC A12 NEURONS IN THE ARC CO-EXPRESS XLαS

There are dopaminergic neuron populations in the Arc (A12 group) and the ZI (A13 group), in the hypothalamic region of the brain. Both of these regions also express XLαs as shown in Chapter 4. To identify if the dopaminergic neurons are coexpressed with XLαs-expressing neurons in these areas

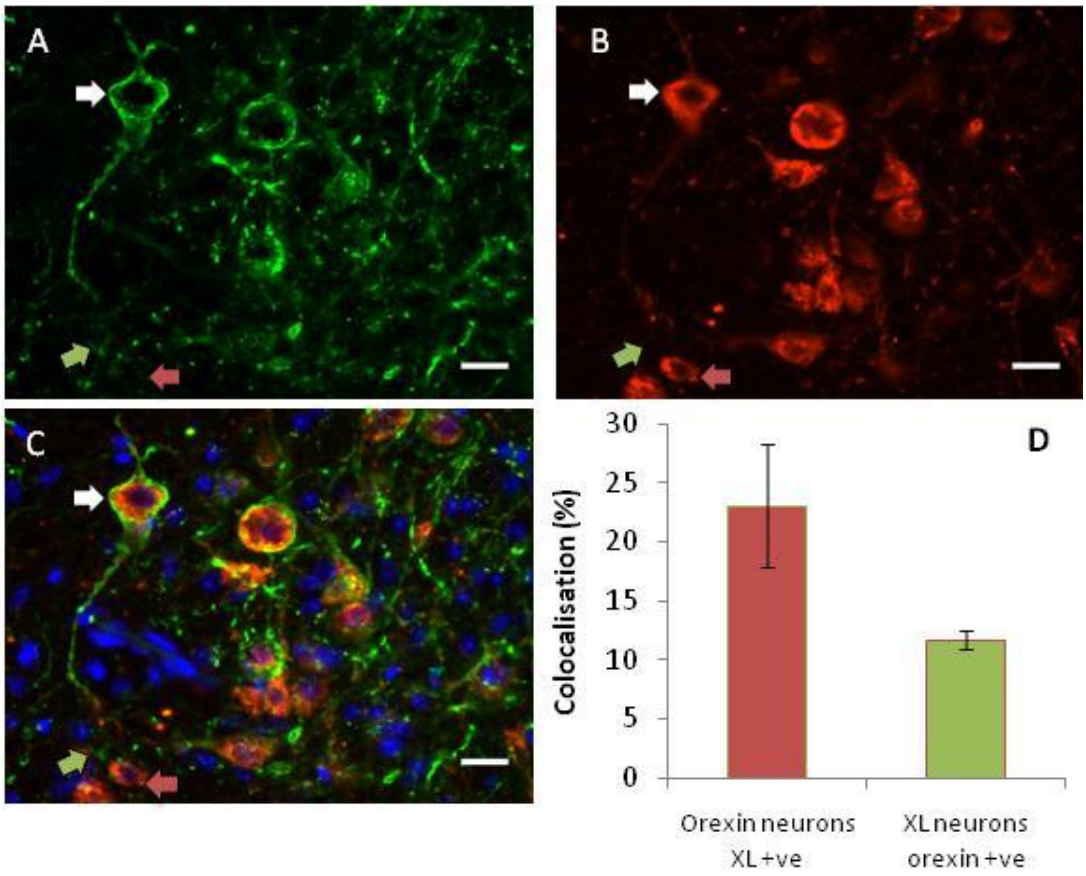

Figure 7.5. Immunofluorescence analysis of XLαs coexpression with orexin A in the lateral and dorsomedial hypothalami of adult wild type mice

(A) XLαs in the LH and DMH of adult wild type mice. This shows clear plasma membrane bound expression of this alternative G-protein alpha subunit. There is also clear fluorescent labelling of axonal projections from these neurons and throughout the tissue. An AF488-conjugated secondary antibody was used.

(B) Orexin A in the LH and DMH of adult wild type mice show that this food intake stimulating neuropeptide is located in the cytoplasm of neurons in these regions. An AF594-conjugated secondary antibody was used.

(C) A merge of the XLαs (green) and orexin A (red) images in **(A)** and **(B)** indicate that there is some colocalisation of the two proteins in this area. Nuclei are labelled with DAPI.

(D) Graphical representation of percentage colocalisation of orexin A positive neurons that also express XLαs (n=2; 23 ± 5.22 %) and XLαs positive neurons that also express orexin A (n=2; 12 ± 0.79 %). Cells expressing XLαs and/or orexin A were counted on an epifluorescence microscope.

White arrows indicate a double-labelled XLαs/orexin A labelled neuron, red arrows indicate an orexin A labelled neuron without XLαs and green arrows indicate a XLαs labelled neurons not expressing orexin A. Sections 14 μm; scale bars 20 μm.

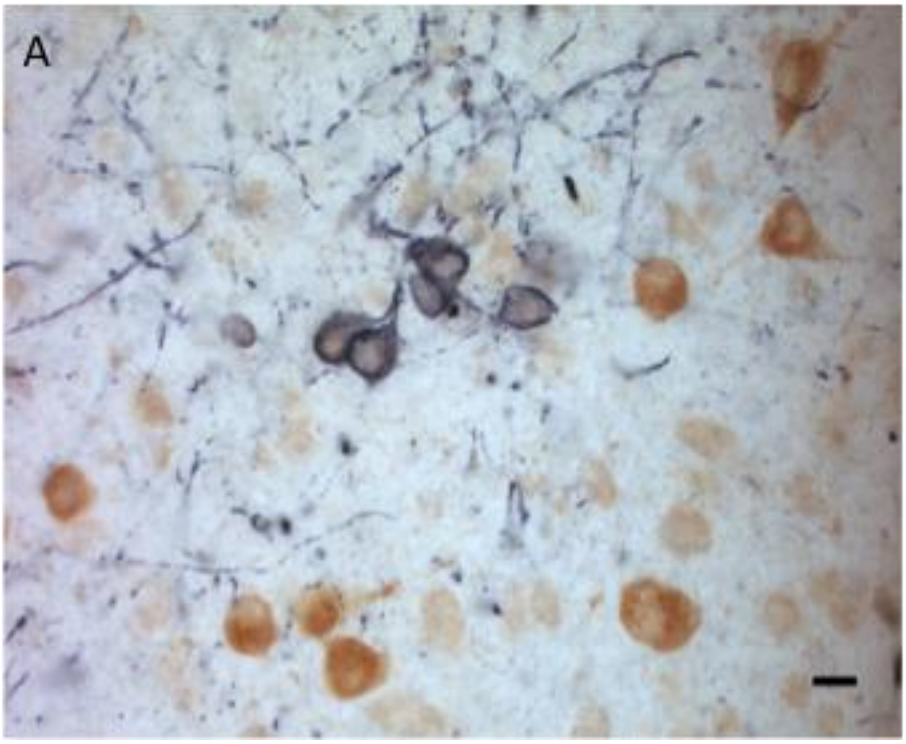

Figure 7.6. MCH localisation in the lateral and dorsomedial hypothalami does not overlap with XLαs staining in these areas.

(A) Double immunohistochemistry staining to analyse XLαs (purple) and MCH (brown) localisation in the LH and DMH indicates that the two proteins are expressed in different populations of neurons in these regions of the hypothalamus.

Sections 14 μm; scale bar 20 μm.

immunofluorescence was performed. TH is known to mediate the first step in the production of dopamine, norepinephrine and epinephrine. A TH antibody would only indicate that the neurons are catecholaminergic, thus it was necessary to determine if the neurons were dopaminergic or noradrenergic. DBH is an enzyme further down the adrenaline production pathway (Figure 7.1) and an antibody against this was used to distinguish between the types of neurons expressing XLαs in the Arc.

TH-expressing neurons showed some colocalisation with XLαs-positive neurons in the Arc. Interestingly colocalisation was confined to the A12 neurons in this region of the hypothalamus. Areas positive for TH in the dorsal regions (A13 population) were singly stained for TH (Figure 7.7). Arc colocalisation of TH-positive neurons also expressing XLαs was ~65% (n=2; 65 ± 17.2 %; Figure 7.7), while XLαs expressing neurons were also positive for TH in ~41% of counted cells (n=2; 41 ± 10.9 %; Figure 7.7).

Immunofluorescence staining in serial sections across the Arc indicated that the TH positive neurons seen in the A12/Arc region could only be defined as dopaminergic due to the lack of DBH positive neurons (Figure 7.8 A-C). Specificity of the second DBH antibody was tested in the LC, an area known to be noradrenergic, which clearly contained positive staining for DBH (Figure 7.8 D and E).

7.3.3. XLαs Does Not Colocalise with CRH in the PVN

In the PVN – a nucleus important for sympathetic outflow – CRH is expressed in many neurons. Initially double antibody staining was attempted, with IF and IHC. The antibodies available for CRH were found to be non-specific (see methods for tested antibodies). A double staining for CRH and XLαs was

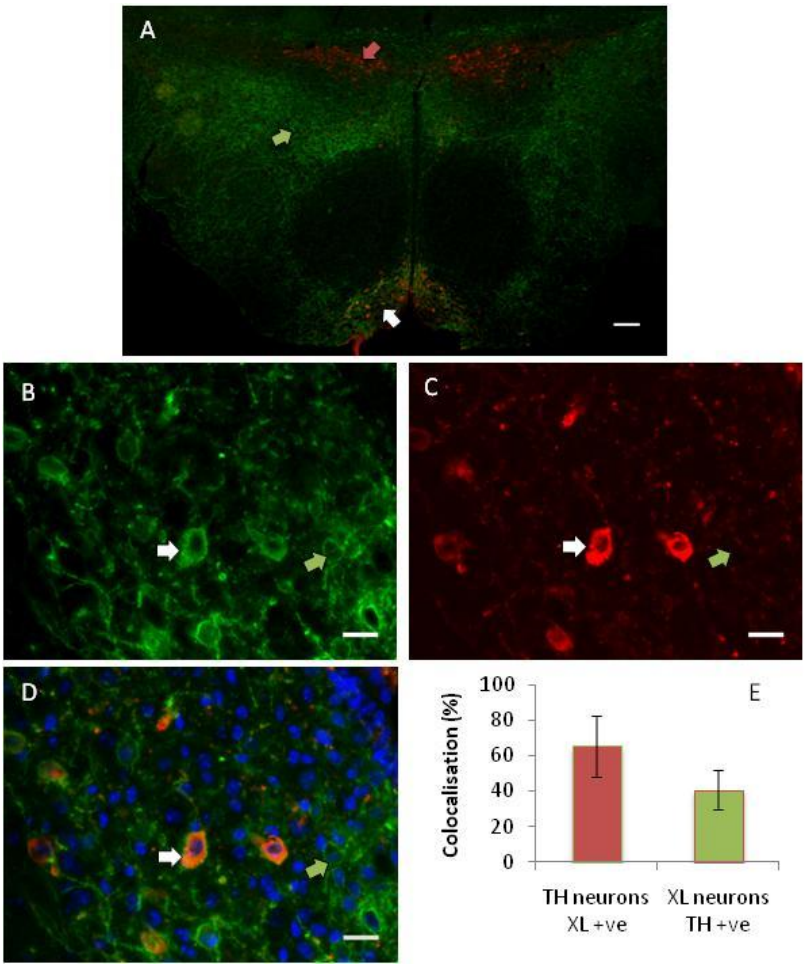

Figure 7.7. XLαs colocalisation with Tyrosine Hydroxylase (TH) in the Arc in adult wild type tissue

(A) Overview of XLαs and TH double staining in the hypothalamus. TH is observed in the Arc colocalised with XLαs (A12 neurons) but is not colocalised with XLαs in the A13 dopaminergic neurons of the ZI and XLαs stains the LH and DMH without TH.

(B) Staining of XLαs in the Arc of adult wild type mice show clear plasma membrane bound expression of this alternative G-protein alpha subunit. There is also clear fluorescent labelling of axonal projections from these cells. An AF488-conjugated secondary antibody was used.

(C) Staining of TH in the Arc of adult wild type mice shows that the neuropeptide is located in the cytoplasm of neurons in this area. An AF594-conjugated secondary antibody was used.

(D) A merge of the XLαs and TH images in (B) and (C) indicate that there is some colocalisation of the two proteins in this area. Nuclei are labelled with DAPI.

(E) Graphical representation of percentage colocalisation of TH positive neurons that also express XLαs (n=2 mice; 65 ± 17.2%) and XLαs positive neurons that also express TH (n=2 mice; 41 ± 10.9%) as counted on an epifluorescent microscope.

The white arrow indicates a double-labelled XLαs/TH area/neuron; the red arrow indicates a TH-labelled area without XLαs expression and the green arrow indicates an XLαs-labelled area/neuron not expressing TH. Sections 14 µm; (A) scale bar 200 µm; (B-D) scale bars 20 µm.

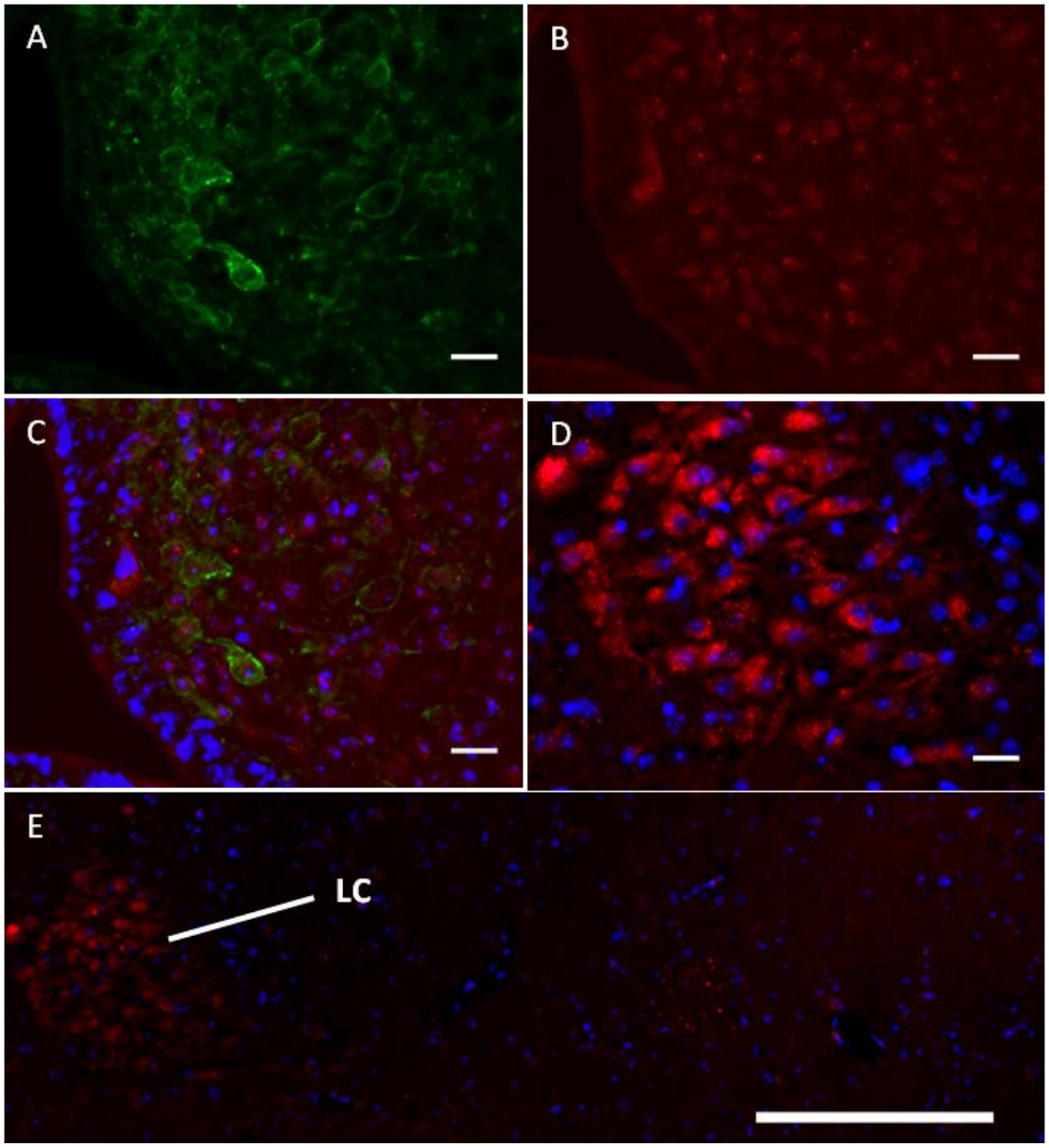

Figure 7.8. XLαs expressing neurons in the Arc do not co-express the norepinephrine marker, DBH

(A) XLαs expression in the Arc shows clear plasma membrane-bound staining of this alternative G-protein alpha subunit.

(B) DBH staining in the Arc. There is no clear staining that differs from background staining, indicating that they are dopaminergic not noradrenergic neurons in this region of the hypothalamus.

(C) Merged image of XLαs (A) and DBH (B) localisation in the Arc, there is no coexpression of XLαs and DBH in these cells.

(D) High magnification image of control DBH staining in the LC.

(E) Overview control staining of DBH in the LC shows the antibody is specific. There is no staining in other areas of the pons.

(A-D) Sections 14 µm thick; scale bars 20 µm

(E) Sections 14 µm thick; Scale bar 100 µm

attempted with an *in situ* hybridisation (ISH) for CRH mRNA, followed by an IHC staining for XLαs protein. Primers specific for CRH were used in RT-PCR to create a CRH specific cDNA. This was cloned into pSuperscript II SK plasmid using a ligation reaction. The plasmid was linearised and used in an in vitro transcription reaction to create a DIG-labelled RNA probe. This approach again proved unsuccessful. The ISH protocol detected the CRH mRNA in the PVN. Although the anti-XLαs antibody required a short heated antigen retrieval step, it was not possible to detect the XLαs protein after the overnight high temperature steps of the ISH protocol. In order to determine whether CRH might colocalise with XLαs in the PVN, ISH and IF protocols were carried out on adjacent sections from adult brain tissue. By staining separately for CRH and XLαs in this way it was possible to see that CRH positive cells were located in the centre of the PVN (Figure 7.9), while XLαs expressing cells were located around the periphery of the nucleus (Figure 7.9). This indicated that the XLαs was unlikely to co-localise with CRH in this region.

7.3.4. Analysis of mTOR-S6K activity in the Arc in *Gnasxl*$^{M+/P-}$ and Wild Type Sibling Mice

The mTOR-S6K pathway is important in insulin and leptin signalling. Its negative feedback loop onto IRS would result in sensitivity to both leptin and insulin. To assess changes in the mTOR-S6K pathway in the adult mouse Arc three aspects were investigated: colocalisation, pS6 positive cell number and pS6 fluorescence intensity. Colocalisation and cell number/fluorescence data were collected separately.

To assess colocalisation, two adult wild type mouse brains were cryosectioned at 14 μM and assessed for colocalisation of pS6 (a histological

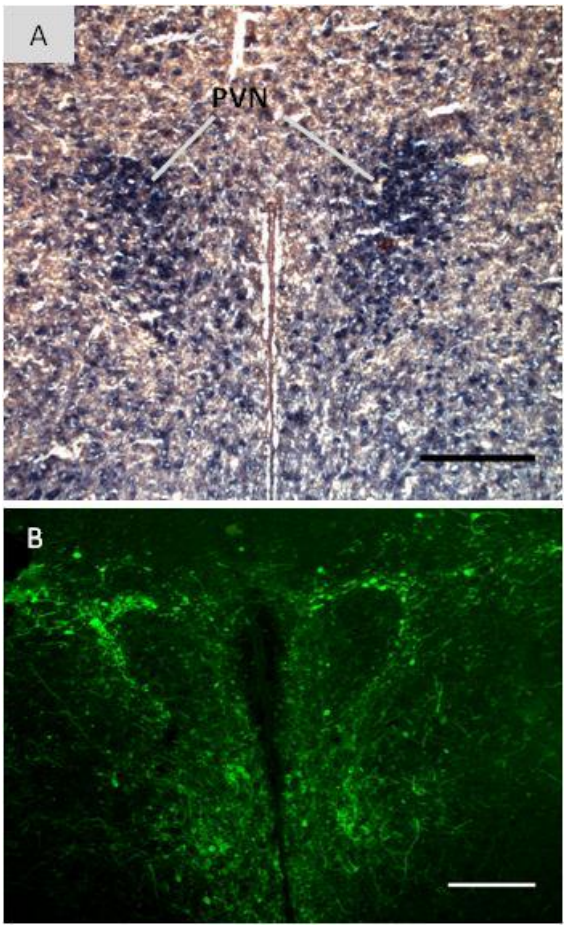

Figure 7.9. XLαs and CRH are located in different populations of neurons in the Paraventricular nucleus of the hypothalamus.

(A) *In situ* hybridisation probe for CRH in the paraventricular nucleus of the hypothalamus showing localisation to the central part of this nucleus.

(B) Immunofluorescence staining of XLαs in the peripheral neurons of the paraventricular nucleus of the hypothalamus, suggesting that XLαs and CRH do not colocalise in this nucleus of the brain.

Scale bars 200 μm; 14 μm sections

marker for mTOR-S6K activity) with XLαs. Analysis was carried out in three rounds of staining with pS6 and XLαs antibodies, on a range of serial cryostat sections across the Arc (18 sections). Data were pooled as for previous co-staining experiments and an average gained for each mouse. These pooled data were used in analysis allowing an overview to be obtained of the colocalisation across the entire nucleus. pS6 was found to colocalise with XLαs in the Arc. Approximately 19% of pS6 neurons expressed XLαs (n=2; 19 ± 7.4 %; Figure 7.10) and ~32% of XLαs neurons were also pS6 positive (n=2; 32 ± 8.9 %; Figure 7.10).

Analysis of cell number and fluorescence intensity of pS6-positive cells in the Arc was carried out in six wild type and six *Gnasxl*$^{m+/p-}$ mice. These were assessed as pairs of littermates that were perfused on the same day at approximately three months old. 14 μm cryostat brain sections from littermate pairs were stained simultaneously and images were taken at the same time to avoid differences in degradation in fluorescent secondaries over time.

pS6-positive cell number assessment in six wild type/*Gnasxl*$^{m+/p-}$ littermate pairs of mice indicated a decrease in the number of pS6-positive cells in *Gnasxl*$^{m+/p-}$ mice compared to their wild type siblings (n=6 per genotype; p=0.036; Figure 7.11).

Analysis of the fluorescence intensity of individual neurons in the Arc indicated there was no change in the pS6 protein expression level in neurons between wild type and *Gnasxl*$^{m+/p-}$ mice (n=6 per genotype; p=0.156; Figure 7.11), although a trend towards lower fluorescence intensity in the Arc of *Gnasxl*$^{m+/p-}$ mice was recognisable.

Analysis of whole hypothalamus protein lysates, using Western blotting

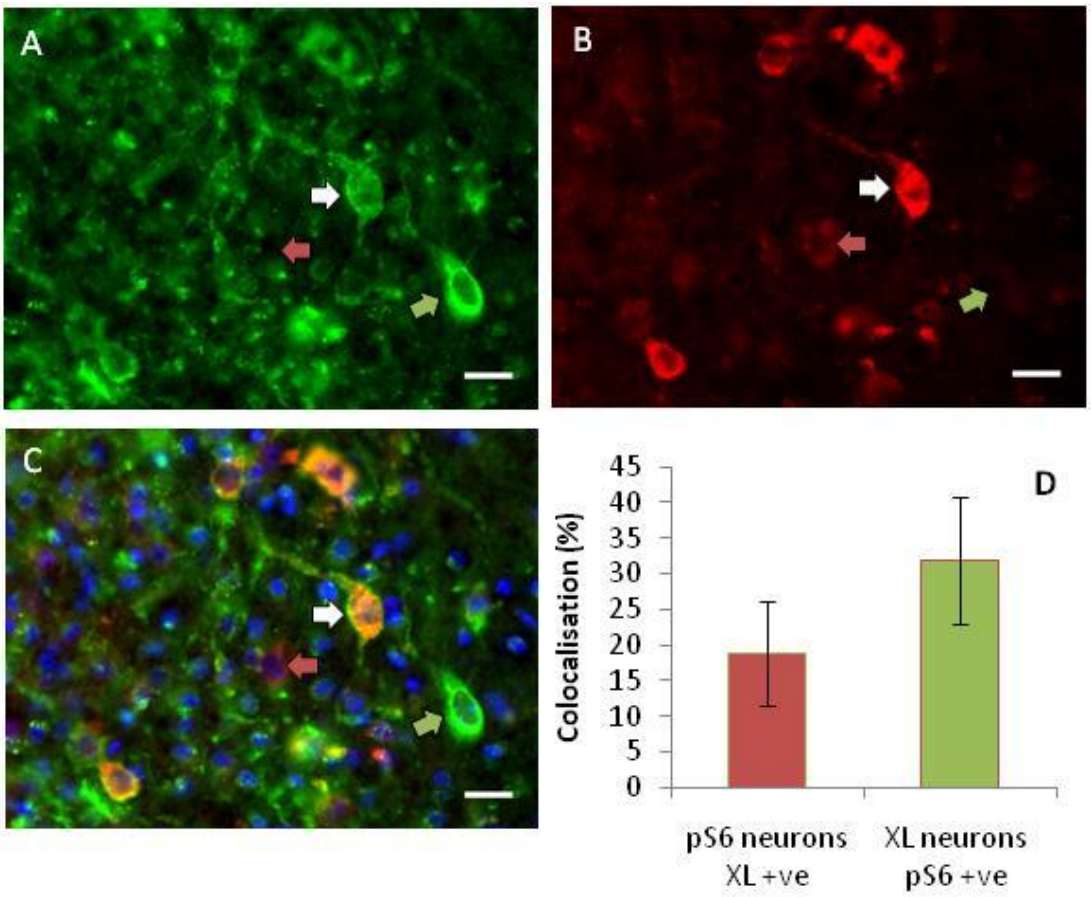

Figure 7.10. XLαs colocalisation with pS6 in the Arc of adult wild type mice

(A) XLαs in the Arc of adult wild type mice again shows clear plasma membrane bound expression of this alternative G-protein alpha subunit in this region. An AF488-conjugated secondary antibody was used to label these neurons.

(B) pS6 in the Arc in adult wild type mice show that this ribosomal protein is located in the cytoplasm of neurons in this area. An AF594-conjugated secondary antibody was used to label these neurons.

(C) A merge of the XLαs and pS6 images indicate that there is some colocalisation of the two proteins in this area. Nuclei are labelled with DAPI (blue).

(D) Graphical representation of percentage colocalisation of pS6 positive neurons that also express XLαs (n=2; 19 ± 7.4%) and XLαs positive neurons that also express pS6 (n=2; 32 ± 8.9%).

White arrows indicate an XLαs/pS6 double-labelled neuron, red arrows indicate a pS6-labelled neuron without XLαs expression and green arrows indicate a XLαs-labelled neurons not expressing pS6. Sections 14 µm, scale bars 20 µm, magnification x400.

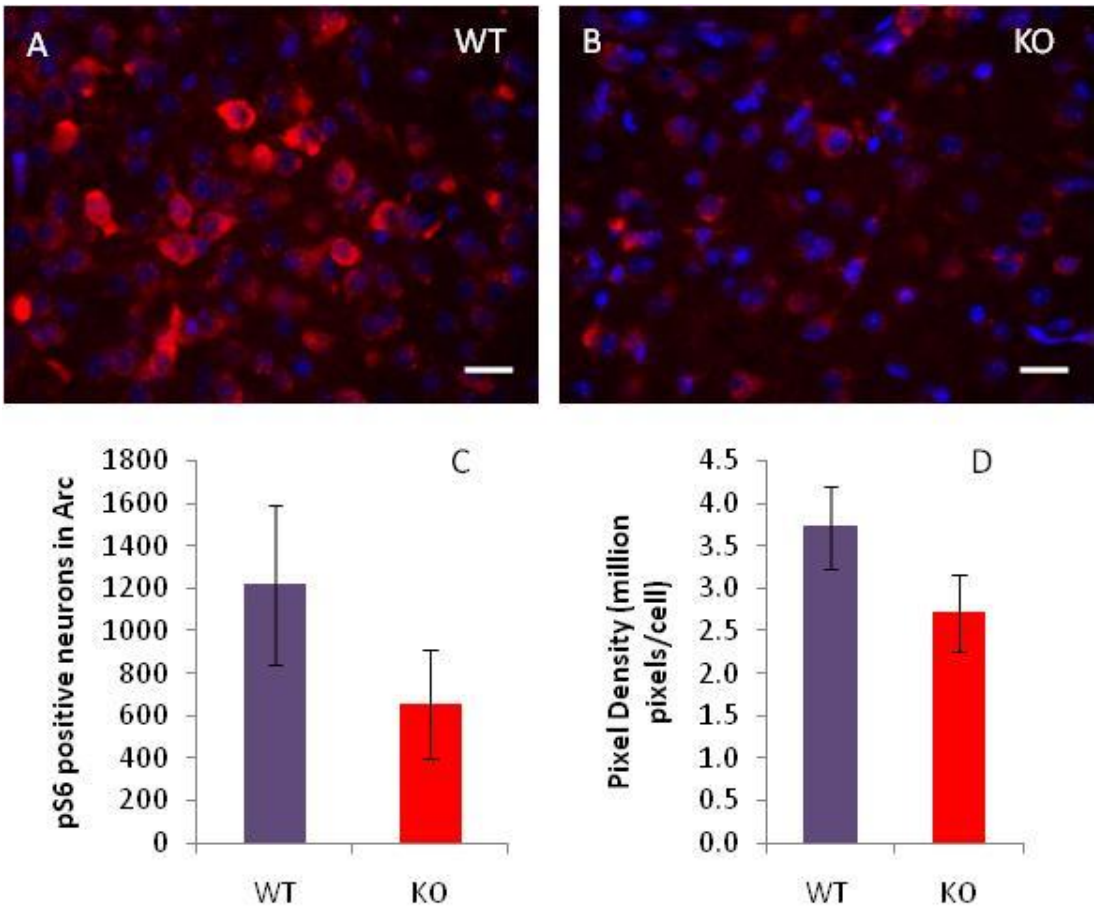

Figure 7.11. Comparison of pS6 expression in wild type and *Gnasxl*$^{m+/p-}$ mice

(A) Representative image of adult wild type expression of pS6 in the Arc. Mice used in this staining were approximately 2 months old.

(B) Representative image of pS6 in the Arc of *Gnasxl*$^{m+/p-}$ mice. This mouse was an littermate of the wild type in **(A)**. They were stained at the same time for pS6 and imaged on the same day.

(C) Graphical representation of pS6-positive neuron number in wild type and *Gnasxl*$^{m+/p-}$ mice. Data was analysed from sibling pairs. There were significantly less neurons expressing pS6 in *Gnasxl*$^{m+/p-}$ mice compared to their wild type siblings (n=6; p=0.036).

(D) Graphical representation of fluorescent intensity of pS6 in wild type and *Gnasxl*$^{m+/p-}$ mice. Data was analysed from sibling pairings but was not significantly different (n= 6; p=0.157).

(A) and (**B)** Scale bar 20 μm; 14 μm section.

for pS6 in wild type and *Gnasxl*$^{m+/p-}$ mice, revealed no significant difference in phosphorylation levels between genotypes (n=6 WT; n=8 *Gnasxl*$^{m+/p-}$; p=0.54; Figure 7.12). This could be due to the dilution of any changes in pS6 expression in specific areas of the hypothalamus (e.g. Arc) due to the use of whole hypothalamus lysates.

7.3.5. Markers For Ghrelin Signalling Do Not Appear To Change In *Gnasxl*$^{M+/P-}$ Mice.

The AMPK signalling pathway is an indicator of the activity in the ghrelin pathway. As plasma ghrelin was increased in *Gnasxl*$^{m+/p-}$ mice it was thought that perhaps an increase in ghrelin would result in an increase in AMPK activity and that it might be a cause of the increased food intake observed in *Gnasxl*$^{m+/p-}$ mice. Hypothalamic lysates from six wild type and eight *Gnasxl*$^{m+/p-}$ mice were prepared for protein detection by western blotting. pAMPKα was analysed in the context of the increased plasma ghrelin detected in the *Gnasxl*$^{m+/p-}$ mice (n=6 WT; n=8 KO; p=0.98; Figure 7.13) and as a second enzyme in the ghrelin pathway pACC (n=4 WT; n=5 KO; p=0.82; Figure 7.14) – these again proved to be non-significant between genotypes. Any changes seen would indicate the disregulation of the AMPK pathway and ghrelin signalling (Lage *et al.* 2008). Again, similar to the pS6 data, the lack of significance of the data might be due to the whole hypothalamus lysate diluting the changes of AMPK and ACC in a specific region of the hypothalamus.

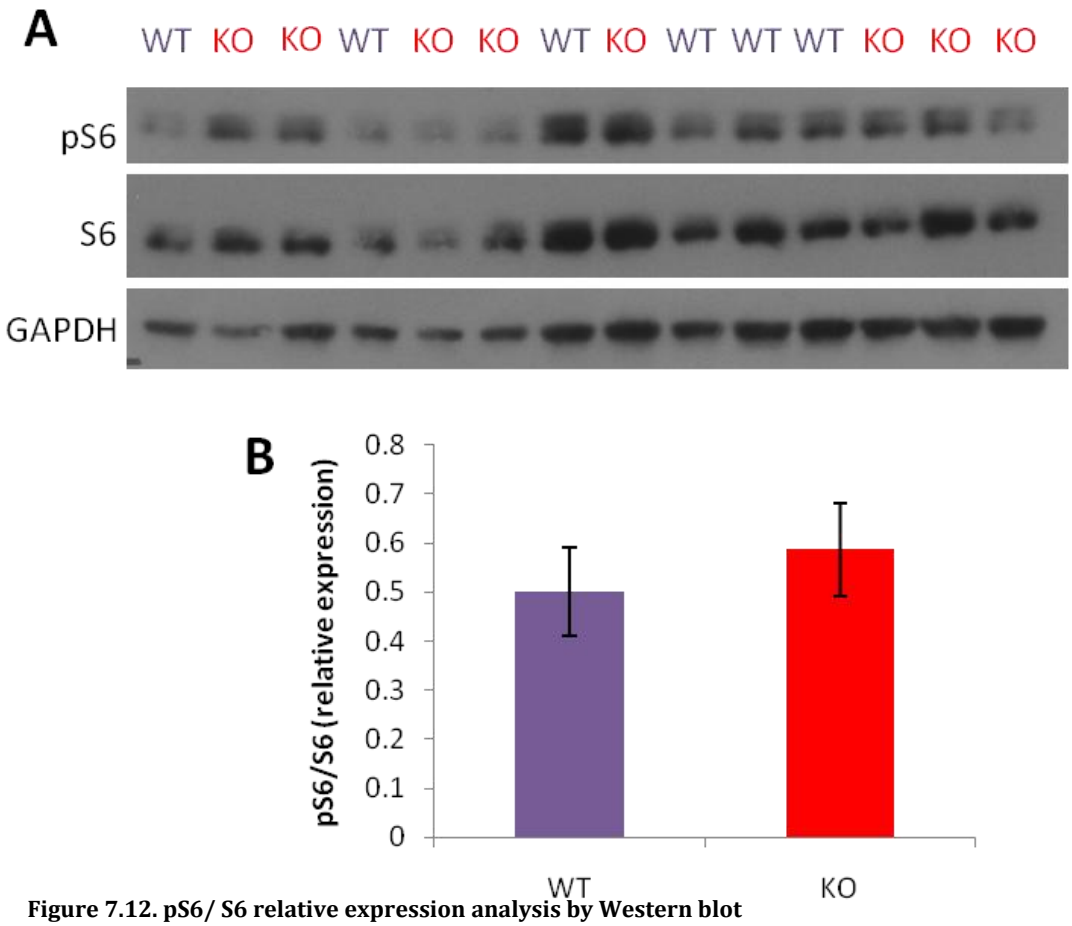

Figure 7.12. pS6/ S6 relative expression analysis by Western blot

(A) Western blots of phosphorylated S6 (pS6) were compared to total S6 (S6) from hypothalamic lysates of wild type (WT) and *Gnasxl*$^{m+/p-}$ (KO) littermate pairs. The membrane was probed for pS6 then stripped and reprobed with a total S6 antibody and then stripped again to probe for GAPDH. GAPDH was used as a house-keeper to have a second loading control. Mice were collected at 2 months of age for tissue extraction.

(B) Graphical representation of the quantitative analysis of the western blots showing no significant difference between the phosphorylated and total S6. Students t-test p=0.54.

WT n=6; KO n=8

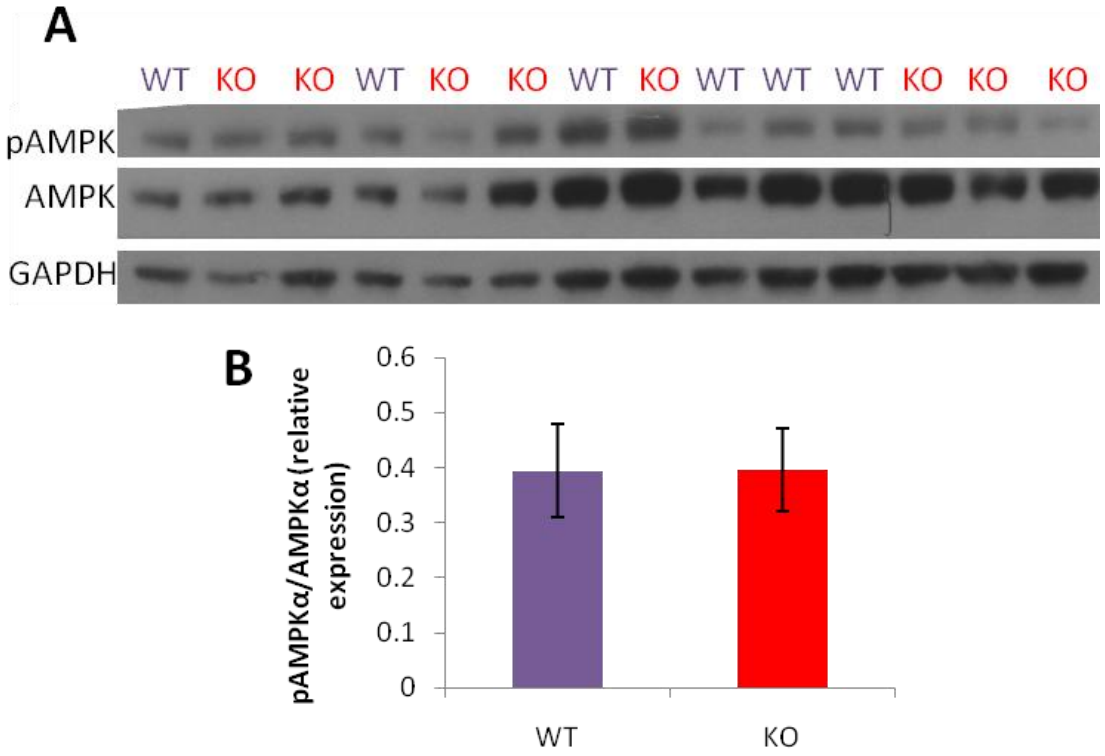

Figure 7.13. pAMPKα/AMPK relative expression analysis

(A) Western blots of phosphorylated AMPK (pAMPKα) were compared to total AMPKα (AMPK) from hypothalamic lysates from wild type (WT) and *Gnasxl*$^{m+/p-}$ (KO) age-matched sibling pairs. Mice were collected at 2 months of age for tissue extraction. GAPDH was used as a house-keeper to have a second loading control. Membranes were initially probed using an anti-pAMPKα antibody. These were then stripped and reprobed using an anti-total AMPKα antibody. GAPDH could be probed separately as there is large difference in the size of the GAPDH and AMPK proteins

(B) Graphical representation of the quantitative data analysed from the western blots showing no significant difference between the phosphorylated and total AMPK. Students t-test p=0.98.

WT n=6; KO n=8

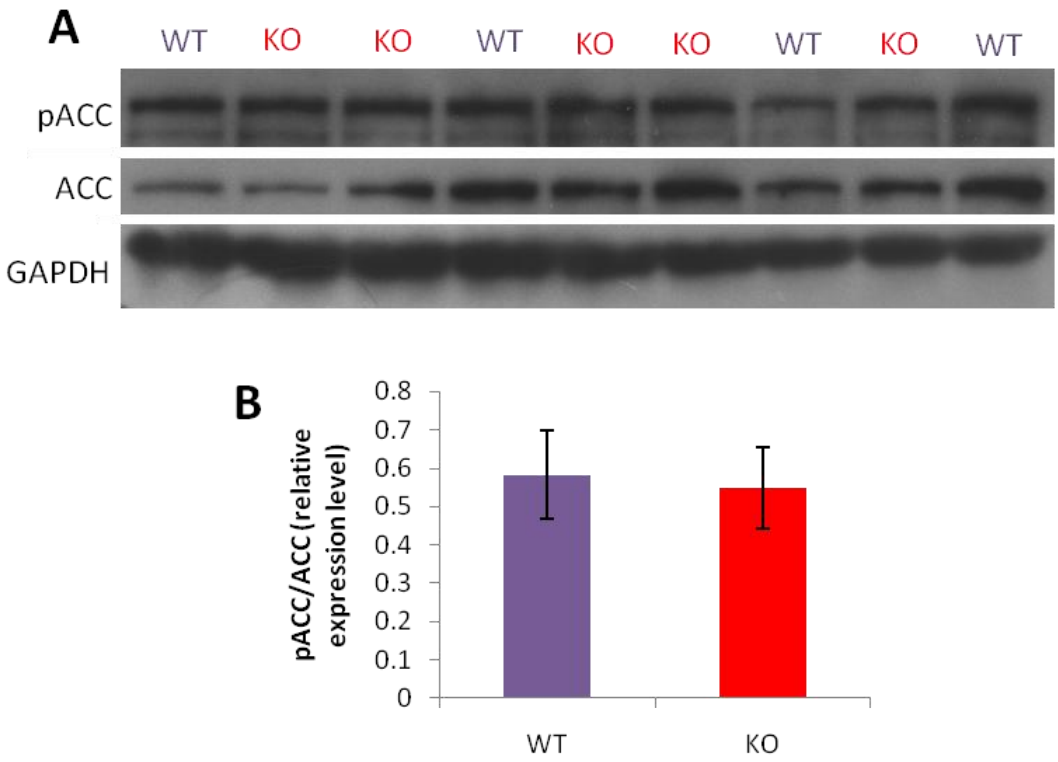

Figure 7.14. pACC/ACC relative expression.

(A) Western blots of phosphorylated ACC (pACC) were compared to total ACC (ACC) from hypothalamic lysates from wild type (WT) and *Gnasxl*$^{m+/p-}$ (KO) littermate pairs. Mice were collected at 2 months of age for tissue extraction. The house-keeper protein GAPDH was used as a second loading control for samples.

(B) Graphical representation of the data analysed from the western blots showing no significant difference between the phosphorylated and total ACC. Students t-test p=0.82.

WT n=4; KO n=5

7.4. DISCUSSION

7.4.1. XLAS IN OREXIGENIC PEPTIDE-EXPRESSING NEURONS

XLαs was found to co-express in a proportion of orexin A-positive neurons in the DMH. Orexin A, a peptide that increases energy expenditure and food intake, is also known to be involved in sleep and wakefulness (SAKURAI 2007; SAKURAI *et al.* 1998). If XLαs acts as an inhibitor of neuronal activity in these cells, then removal of XLαs in the *Gnasxl*$^{m+/p-}$ mice might cause an over-activity in these orexin cells, which could give rise to the increased food intake and energy expenditure that is seen in these mice (FUNATO *et al.* 2009; XIE *et al.* 2006). It is also possible that orexin, when disinhibited in these colocalised cells, is in part responsible for the increased energy expenditure in the XLαs-deficient mice. It would be interesting to investigate whether there is any change in the orexin expression in *Gnasxl*$^{m+/p-}$ mice with immunohistochemistry. Given that MCH and orexin have opposing effects on energy expenditure, it is unsurprising that XLαs is only found in one population.

7.4.2. CATECHOLAMINERGIC COLOCALISATION WITH XLAS

XLαs expression pattern overlaps with TH in a very specific way in the brain. XLαs is found in the LC (a noradrenergic nucleus) in the pons, where TH is highly expressed, but not in the substantia nigra or the ventral tegmental area (dopaminergic nuclei). The colocalisation in the hypothalamus was limited to the A12 dopaminergic neurons in the Arc with no colocalisation present in the A13 dopaminergic neurons. The A12 neurons are important for the production of prolactin from the pituitary gland (PHELPS 2004).

A D2-knock-out mouse line is hypermetabolic and lean, similar to the phenotype in *Gnasxl*$^{m+/p-}$ mice. They are also leptin sensitive. It is possible that

the dopamine-D2 receptors might play a role in controlling food intake in the arcuate nucleus through the control of leptin signalling (KIM *et al.* 2010).

7.4.3. mTOR-S6K PATHWAY

Gnasxl$^{m+/p-}$ mice exhibit a metabolic phenotype similar to that of a fasting state (hypoglycaemia, hypoinsulinaemia; hypoleptinaemia) and it has been shown that the mTOR-S6K pathway has reduced activity in mice under fasting conditions. The *Gnasxl*$^{m+/p-}$ mice also exhibit increased insulin and leptin sensitivity (Frontera *et al.* in prep) (XIE *et al.* 2006). mTOR-S6K negative feedback can desensitise the PI3K-Akt signalling pathway by inhibiting IRS with possible effects on hormone resistance (Figure 7.3).

The similarity between XLαs and S6K1 knock-out is interesting. These mouse models are both lean, hypermetabolic, and have increased food intake, lypolysis and insulin sensitivity (SHIMA *et al.* 1998; UM *et al.* 2004; XIE *et al.* 2006). It would be interesting to see if the loss or reduction of pS6-positive neurons specifically occurs in the neurons that have lost XLαs in the *Gnasxl*$^{m+/p-}$ mice. This could not be achieved with the current conditional knock-out due to the decreased expression levels of the XL-βGal fusion protein in the Arc, but it might be possible with the new targeting construct that is being prepared to create a new mouse line.

The full role of the mTOR-S6K pathway in the XLαs-deficient mice has yet to be elucidated. It is possible that alterations in this pathway may be a secondary factor, caused by the metabolic phenotype which is the result of some other disregulation from the ablation of XLαs. In order to confirm the reduction in expression of pS6 in the arcuate nucleus it would be necessary to perform Western blots on lysates created specifically from the Arc.

7.4.4. Phosphorylated Protein Changes Might be Masked in Whole Hypothalamic Lysates

The use of whole hypothalamic lysates for western blotting of S6, AMPK and ACC might be a reason for the lack of difference between wild type and *Gnasxl*$^{m+/p-}$ phosphorylated proteins. If there was a difference in a specific region of the hypothalamus, for example the Arc, but no difference in other regions, this might mask the difference in the small Arc region. This could be overcome by having a more specific dissection of the hypothalamic tissue. There is reason to believe that there would be a difference because the pS6 analysis by IF revealed a lower number of cells in the *Gnasxl*$^{m+/p-}$ mice compared to their wild type siblings.

It is also possible that the increased plasma ghrelin, previously observed (Krechowec *et al.* 2012), might be a secondary effect of the leanness described in the *Gnasxl*$^{m+/p-}$ mice (Xie *et al.* 2006).

In order to fully analyse the changes in the arcuate nucleus of the hypothalamus it would be necessary to perform dissection of specific areas of the hypothalamus and use lysates from these to analyse the relative levels of expression of AMPK and ACC.

7.4.5. Antibody Specificity Problems

The specificity of antibodies is a problem that has been repeatedly encountered during these analyses. MCH1R, GHSR and Gad67 as well as the CRH antibodies that were purchased were found to be unspecific. The Gad67 antibody has now been replaced and this analysis is ongoing. The CRH problem with antibodies was overcome by using *in situ* hybridisation. It was not possible to perform co-localisation with XLαs and CRH but the individual ISH and IF

stainings for CRH and XLαs, respectively, indicated that the two did not colocalise. It might be an option to use double IF-ISH in cases where antibodies are not specific.

CHAPTER 8. FINAL RESULTS SUMMARY AND DISCUSSION

8.1. FINAL SUMMARY OF RESULTS

8.1.1. EXON A20 SPLICING IN *GNASXL* TRANSCRIPTS

Data collected for alternative splicing of *Gnasxl* transcripts revealed that in the XLN1 truncated protein the exon A20 is regularly spliced into the protein and Exon 3 is always spliced. In the full-length XLαs protein exon A20 was rarely detected. It was also found that inclusion of the exon A20 in splicing resulted in a frame-shift with a premature stop-codon in mice. This concurred with data that had previously described human splicing (HAYWARD *et al.* 1998a).

8.1.2. XLAS EXPRESSION PATTERN CHANGES FROM NEONATAL AND ADULT STAGES

Changes in the expression pattern of XLαs between neonatal and adult phases of development were observed using wild type and Cre/+; +/*XLlacZGT* mice (Table 4.1). The orofacial motor nuclei had a reduced expression of XLαs/XL-βGal towards adulthood, however the LDTg could not be detected with XGal staining or immunohistochemistry in adults. The changes observed in the orofacial motor nuclei and the LDTg could explain the neonatal-specific phenotype of lethargy and reduced suckling. The expression in skeletal muscles, which was confined to neonatal stages, could also be a contributing factor to the lethargic phenotype in *Gnasxl*$^{m+/p-}$ neonatal mice that is recovered in adults when muscle expression is no longer observed.

8.1.3. MAINTAINED AND EXPANDED XLAS EXPRESSION IN THE BRAIN

The XLαs expression pattern, which is maintained from neonatal to adult phases of development, was in areas relevant for food intake (LH/DMH, Arc, PVN). These areas are unlikely to contribute to the suckling phenotype of the

neonates since hypothalamic circuits only become fully functional during the late postnatal period. The phenotype of poor suckling also persists beyond day 4 when the hypothalamic nuclei strongly express XLαs in neonates (KRECHOWEC *et al.* 2012).

8.1.4. MUSCLE EXPRESSION OF *GNASXL* IS OBSERVED IN NEONATAL TISSUE BUT NOT ADULT

Blood vessel staining was found in many tissues, which had previously been associated with *Gnasxl* expression by Northern blotting (PLAGGE *et al.* 2004), including the heart, stomach and BAT. This expression was confined to alpha smooth muscle actin-expressing cells and was lost in adult tissue.

Muscle expression of XLαs varied. The neonatal tongue contained strong XLαs expression which was completely lost in adult mice. Other muscle staining in intercostal muscles were also strongly stained in neonates while limb skeletal muscle had weaker expression (KRECHOWEC *et al.* 2012). In both cases expression was lost in adults. The loss of XLαs expression in muscle tissue could contribute to the poor suckling ability of neonatal *Gnasxl*$^{m+/p-}$ mice as well as the lethargy which has been observed (CATTANACH and KIRK 1985).

8.1.5. *GNASXL* EXPRESSION IS MAINTAINED IN TISSUES DERIVED FROM NEURAL TISSUE

In the intermediate layer of the pituitary gland and in the adrenal medulla *Gnasxl* expression was found in both neonates and adults, confirming previous data (PLAGGE *et al.* 2004). These layers are derived from neural tissue and are considered to be part of the SNS. Both are important for secretion of hormones. This expression is unlikely to contribute to the changing phenotype between neonatal and adult stages of development as it is maintained

throughout life.

8.1.6. Possible Implications of *Gnasxl* Removal in Signalling Pathways Involved In Energy Homeostasis

XLαs was found to partially co-express with orexigenic peptides in the hypothalamus (orexin A). This concurred with the NPY co-expression with XLαs in other work (Frontera *et al*. in prep). XLαs did not appear to co-localise with either CRH or MCH. Other antibodies for markers of energy homeostasis in the hypothalamus were not specific and this work is being continued in the laboratory to further analyse markers in the brain, including Gad67, which is of particular interest following recent reports showing that GABA has an expression pattern similar to XLαs (Vong *et al.* 2011).

The partial colocalisation of pS6 with XLαs in the Arc of wild type mice, along with the reduced number of pS6-expressing cells in the Arc of *Gnasxl*$^{m+/p-}$ mice suggest a role of the mTOR-S6K pathway in the *Gnasxl*$^{m+/p-}$ phenotype. The similarity of the S6K1-deficient mouse line, which is lean and hypermetabolic, to the *Gnasxl*$^{m+/p-}$ supports this suggestion (Um *et al.* 2004).

The involvement of this pathway in leptin and insulin signalling could be a possible cause of the leptin and insulin sensitivity observed in the XLαs-deficient mice (Frontera *et al*. in prep; (Xie *et al.* 2006)).

The increased plasma ghrelin levels (Krechowec *et al.* 2012) prompted an investigation into the pathways ghrelin might influence. AMPK and ACC are under the influence of this system. No changes were observed but this might be due to whole hypothalamic lysates masking any differences which could be occurring in specific regions of the hypothalamus, such as the Arc. This could be further investigated by using punch dissection of specific regions or by laser

dissection, both of which are difficult to perform in the mouse brain.

8.1.7. METHYLATION ANALYSIS

Analysis of the expression levels of *Gnasxl* in the genotypes produced from the Cre crosses with the *XLlacZGT* mouse line showed that mice containing the inactive gene trap had an unexpected reduction in *Gnasxl* expression, leaving only 10% of normal full-length expression (KRECHOWEC *et al.* 2012). This could not be attributed to a change in methylation over the *Gnasxl* promoter and first exon (Figure 1.2). It is possible that an unknown enhancer or other important expression element was deleted with the placement of the gene trap cassette.

To address this problem a new gene trap construct has been developed. This will allow the testing of the specific deletion of XLαs in neuron populations (e.g. NPY/AgRP, POMC) and/or tissue types (e.g. muscle).

8.2. SPECULATIVE DISCUSSION

It is interesting that the facial muscles that control the mouth and tongue, and the areas of the brain which control these muscles (7N, 12N, Mo5) both express XLαs at the neonatal stage of development. All of these tissues lose their expression of XLαs in adult mice.

Given that XLαs is expressed only from the paternal allele (being imprinted on the maternal allele) it would suggest that XLαs is important for the acquisition of nutrients from the mother during the period when the mother is the sole provider of resources. However, once the offspring are weaned and they no longer require resources from the mother it would appear that the expression of XLαs is lost in the aforementioned regions of the brain and the

muscles of the face. This is the time-point in development that the paternal genome would no longer need to influence nutrient acquisition.

These data fit the idea of parental-conflict theory. It would be necessary to determine the exact time-point in development when XLαs expression is lost in these regions. This would require further histological analysis of the expression pattern of XLαs in brain and muscle tissue in pre-weaning mice at several time-points in development.

APPENDICES

APPENDIX .1. OLIGONUCLEOTIDES

Oligo Name	Sequence
XL-FL1	5’-GGAAGCTGCTTCGGTCTATC-3’
XLN1-R6	5’-TCTAGTGGGGGTACTAGACT-3’
A20-F1	5’-AGCGACACTGAGGGTCGTTA-3’
Nesp2-F1	5’-GACTCCGTCCAGATTCTCCT-3’
Exon5-R1	5’-GTAGTCCACTCTGAACTT-3’
XL-F10	5’- GGAGCCAGGTCACTCTCAGC -3’
XL-R5	5’- CAGAAGCTGCCGCATTACCT-3’
XL DIG Probe-F1	5’- CGAGCAAGAACCTTTGGAAG-3’
XL Dig Probe-R1	5’-ATCCATTGCTTCAGGCTGG-3’
lacZ-F4	5’-TACGCCAATGTCGTTATCCA-3’
lacZ-R4	5’-GCGAATACCTGTTCCGTCAT-3’
Crh-F1A	5’-CCAAGGGAGGAGAAGAGAGC-3’
Crh-R1A	5’- AAGCGCAACATTTCATTTCC-3’
lacZ-R2	5’- TCGGGATAGTTTTCTTGC-3’
Cre-F1	5’- CATTTGGGCCAGCTAAACAT-3’
Cre-R1	5’- CCCGGCAAAACAGGTAGTTA-3’

Appendix Table 1. Oligonucleuotide primers used in PCR with their sequences

APPENDIX 2. CLONING VECTORS

pBLUESCRIPT SK

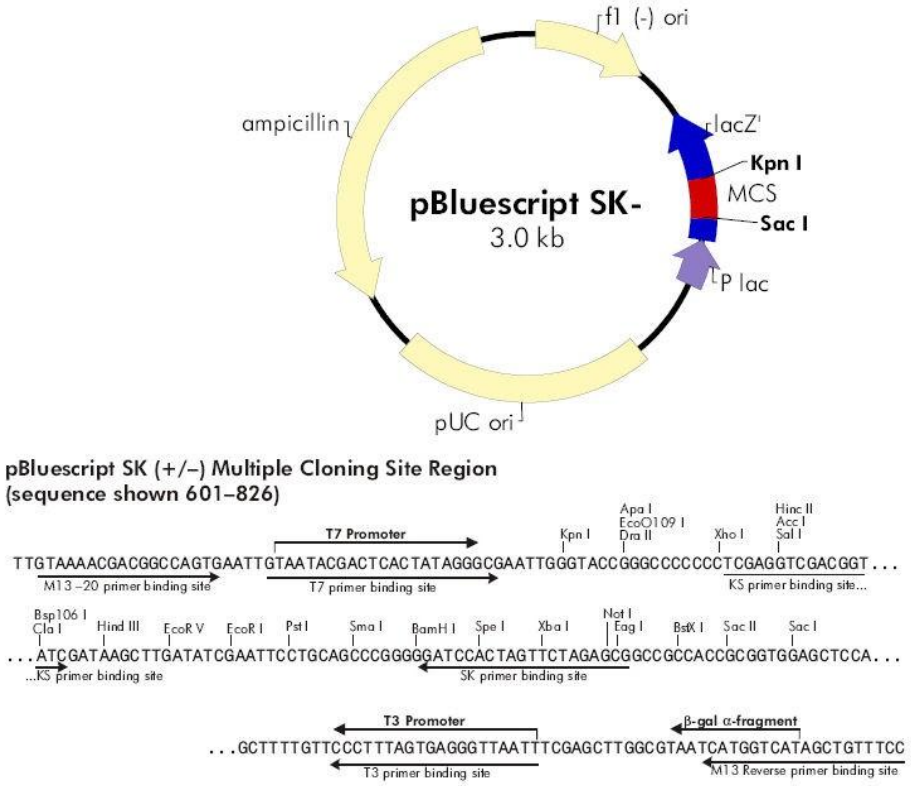

Appendix Figure 1. pBluescript SK vector schematic.

This indicates the layout of the pBluescript plasmid vector showing the resctriction sites and promoters.

pCR 2.1 CLONING VECTOR

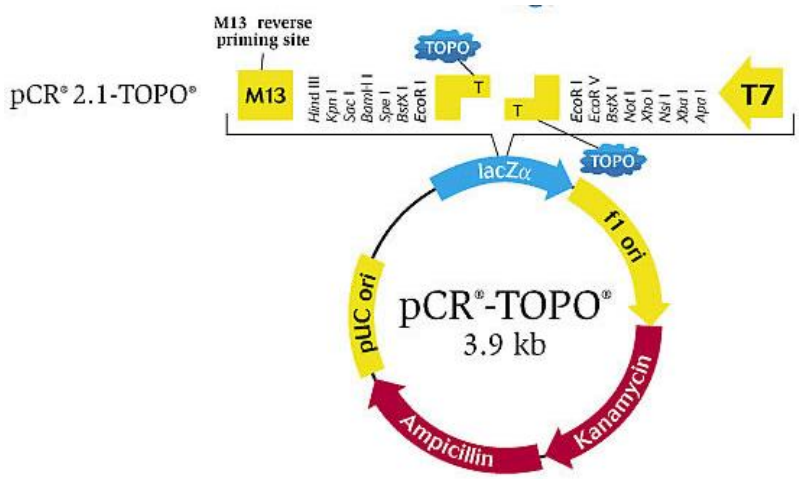

Appendix Figure 2. pCRTOPO cloning vector

The TOPO cloning vector used in the analysis of A20 alternative splicing. Showing at where the PCR product is inserted into the vector. This vector can only be sequenced in one direction using the T7.

APPENDIX 3. LOX VARIANTS

Appendix Table 2. Lox variants used in the production of the novel *Gnasxl* gene-targeting strategy in the XLlacZGT mouse line

Lox Variant	Sequence
LoxP	ATAACTTCGTATA **GCATACAT** TATACGAAGTTAT
Lox2272	ATAACTTCGTATA **GGATACTT** TATACGAAGTTAT

APPENDIX 4. VECTASTAIN ELITE KIT STAINING PRINCIPLE

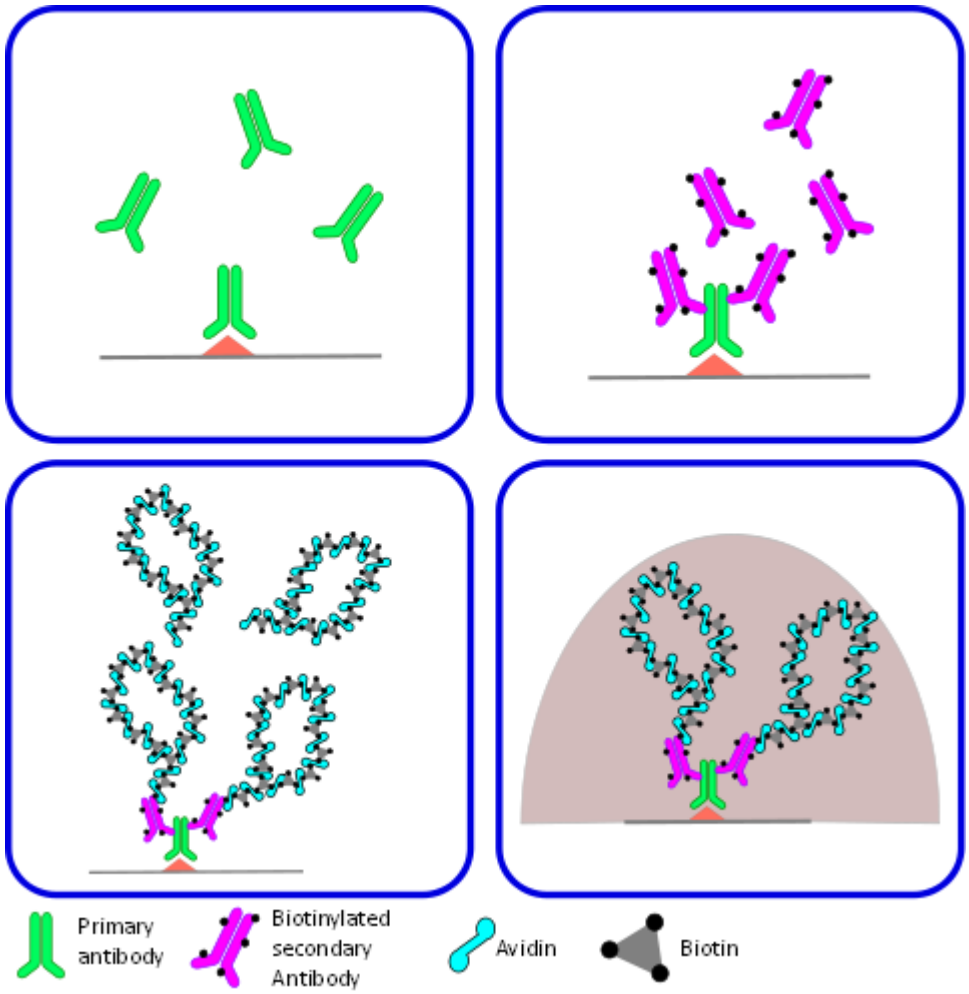

Appendix Figure 3.Vectastain Process

(A) The primary antibody is applied to the tissue section and binds to the antigen.

(B) After the excess primary antibody is washed off the biotinylated secondary is applied to the tissue and incubated. The biotin on the secondary allows more than one avidin molecule to bind to the primary antibody in the next step

(C) After the incubation with the secondary antibody and washing the avidin-biotin complex is applied to the tissue section.

(D) Finally the DAB:Ni colour substrate is added to the section.

APPENDIX 5. RESTRICTION ENZYMES

Restriction Enzyme	**Cut Sequence**
NsiI	ATGCA^T
EagI	C^GGCCG
EcoRI	G^AATTC
EcoRV	GAT^ATC

Appendix Table 3. Restriction enzymes used in all experiments indicating cut recognition sequence. Underlining indicates sensitivity to CpG methylation.

APPENDIX 6. ABSTRACTS AND PUBLICATIONS FROM THIS WORK

PUBLICATIONS

Krechowec, S. O., K. L. Burton, A. U. Newlaczyl, N. Nunn, N. Vlatkovic *et al.*, 2012 Postnatal changes in the expression pattern of the imprinted signalling protein XLalphas underlie the changing phenotype of deficient mice. PLoS ONE [Electronic Resource] **7:** e29753

POSTERS

1. A. Plagge, K. Burton, S. Krechowec, N. Nunn, A. Newlaczyl, R. Barrett-Jolley. **Postnatal changes in the expression pattern of *Gnasxl* correlate with changes in the phenotype of knock-out mice, hyperactivity of the sympathetic nervous system and elevated cardiovascular parameters.** Barcelona Imprinting Conference (2011).
2. A. Plagge, S. Krechowec, K. Burton, A. Newlaczyl, N. Nunn, R. Barrett-Jolley. **Postnatal changes in the expression pattern of the genomically imprinted *Gnasxl* transcript underlie the KO phenotype of neonatal failure-to-thrive and adult sympathetic nervous system hyperactivity.** GfG Conference (2011).
3. K. Burton, S. Krechowec, A. Newlaczyl and A. Plagge. **Expression pattern and signalling pathway alterations in the brain concur with the hypermetabolic phenotype of mice lacking *Gnasxl*/XLαs.** First author and presenter of a poster at the Physiological society main meeting, Oxford (11-14 July 2011).
4. K. Burton, N. Nunn, S. Krechowec, R. Barrett-Jolley and A. Plagge. **Hypothalamic expression pattern and molecular and physiological markers indicate elevated sympathetic stimulation of metabolism in XLα*s*-deficient mice**. Co-Author and co-presenter of a poster presented at the Physiological Society meeting for Metabolism and Endocrinology (24-26 March 2010).
5. K.L. Burton and A. Plagge **Comparative characterisation of *Gnasxl* (XLαs) expression in postnatal and adult mouse brain.** EMBO World Workshop 'Genomic Imprinting' Abstract and Poster (2008).

REFERENCES

ABIZAID, A., Q. GAO AND T. L. HORVATH, 2006 THOUGHTS FOR FOOD: BRAIN MECHANISMS AND PERIPHERAL ENERGY BALANCE. NEURON **51:** 691-702.

ALDES, L. D., M. E. CHAPMAN, R. B. CHRONISTER AND J. W. HAYCOCK, 1992 SOURCES OF NORADRENERGIC AFFERENTS TO THE HYPOGLOSSAL NUCLEUS IN THE RAT. BRAIN RES BULL **29:** 931-942.

ALON, T., L. ZHOU, C. A. PÉREZ, A. S. GARFIELD, J. M. FRIEDMAN *ET AL.*, 2009 TRANSGENIC MICE EXPRESSING GREEN FLUORESCENT PROTEIN UNDER THE CONTROL OF THE CORTICOTROPIN-RELEASING HORMONE PROMOTER. ENDOCRINOLOGY **150:** 5626-5632.

AMUNTS, K., O. KEDO, M. KINDLER, P. PIEPERHOFF, H. MOHLBERG *ET AL.*, 2005 CYTOARCHITECTONIC MAPPING OF THE HUMAN AMYGDALA, HIPPOCAMPAL REGION AND ENTORHINAL CORTEX: INTERSUBJECT VARIABILITY AND PROBABILITY MAPS. ANATOMY AND EMBRYOLOGY **210:** 343-352.

ARBORELIUS, L., M. J. OWENS, P. M. PLOTSKY AND C. B. NEMEROFF, 1999 THE ROLE OF CORTICOTROPIN-RELEASING FACTOR IN DEPRESSION AND ANXIETY DISORDERS. J ENDOCRINOL **160:** 1-12.

ARMSTRONG, W. E., 2004 CHAPTER 15 - HYPOTHALAMIC SUPRAOPTIC AND PARAVENTRICULAR NUCLEI, PP. 369-388 IN *THE RAT NERVOUS SYSTEM (THIRD EDITION)*, EDITED BY G. PAXINOS. ACADEMIC PRESS, BURLINGTON.

ASTON-JONES, G., 2004A CHAPTER 11 - LOCUS COERULEUS, A5 AND A7 NORADRENERGIC CELL GROUPS, PP. 259-294 IN *THE RAT NERVOUS SYSTEM (THIRD EDITION)*, EDITED BY P. GEORGE. ACADEMIC PRESS, BURLINGTON.

ASTON-JONES, G., 2004B LOCUS COERULEUS, A5 AND A7 NORADRENERGIC CELL GROUPS, PP. 259-294 IN *THE RAT NERVOUS SYSTEM*, EDITED BY G. PAXINOS. ELSEVIER ACADEMIC PRESS.

ASTON-JONES, G., AND F. E. BLOOM, 1981A ACTIVITY OF NOREPINEPHRINE-CONTAINING LOCUS COERULEUS NEURONS IN BEHAVING RATS ANTICIPATES FLUCTUATIONS IN THE SLEEP-WAKING CYCLE. J NEUROSCI **1:** 876-886.

ASTON-JONES, G., AND F. E. BLOOM, 1981B NOREPINEPHRINE-CONTAINING LOCUS COERULEUS NEURONS IN BEHAVING RATS EXHIBIT PRONOUNCED RESPONSES TO NON-NOXIOUS ENVIRONMENTAL STIMULI. J NEUROSCI **1:** 887-900.

ASTON-JONES, G., S. CHEN, Y. ZHU AND M. L. OSHINSKY, 2001 A NEURAL CIRCUIT FOR CIRCADIAN REGULATION OF AROUSAL. NAT NEUROSCI **4:** 732-738.

ASTON-JONES, G., M. ENNIS, V. A. PIERIBONE, W. T. NICKELL AND M. T. SHIPLEY, 1986 THE BRAIN NUCLEUS LOCUS COERULEUS: RESTRICTED AFFERENT CONTROL OF A BROAD EFFERENT NETWORK. SCIENCE **234:** 734-737.

BABAK, T., B. DEVEALE, C. ARMOUR, C. RAYMOND, M. A. CLEARY *ET AL.*, 2008 GLOBAL SURVEY OF GENOMIC IMPRINTING BY TRANSCRIPTOME SEQUENCING. CURRENT BIOLOGY **18:** 1735-1741.

BACON, S. J., AND A. D. SMITH, 1988 PREGANGLIONIC SYMPATHETIC NEURONES INNERVATING THE RAT ADRENAL MEDULLA: IMMUNOCYTOCHEMICAL EVIDENCE OF SYNAPTIC INPUT FROM NERVE TERMINALS CONTAINING SUBSTANCE P, GABA OR 5-HYDROXYTRYPTAMINE. J AUTON NERV SYST **24:** 97-122.

BACON, S. J., A. ZAGON AND A. D. SMITH, 1990 ELECTRON MICROSCOPIC EVIDENCE OF A MONOSYNAPTIC PATHWAY BETWEEN CELLS IN THE CAUDAL RAPHÉ NUCLEI AND SYMPATHETIC PREGANGLIONIC NEURONS IN THE RAT SPINAL CORD. EXP BRAIN RES **79:** 589-602.

BAMSHAD, M., C. K. SONG AND T. J. BARTNESS, 1999 CNS ORIGINS OF THE SYMPATHETIC NERVOUS SYSTEM OUTFLOW TO BROWN ADIPOSE TISSUE. AM J PHYSIOL **276:**

R1569-1578.

BASTEPE, M., Y. GUNES, B. PEREZ-VILLAMIL, J. HUNZELMAN, L. S. WEINSTEIN *ET AL.*, 2002 RECEPTOR-MEDIATED ADENYLYL CYCLASE ACTIVATION THROUGH XLALPHA(S), THE EXTRA-LARGE VARIANT OF THE STIMULATORY G PROTEIN ALPHA-SUBUNIT. MOLECULAR ENDOCRINOLOGY **16:** 1912-1919.

BEHAN, D. P., S. C. HEINRICHS, J. C. TRONCOSO, X. J. LIU, C. H. KAWAS *ET AL.*, 1995 DISPLACEMENT OF CORTICOTROPIN RELEASING FACTOR FROM ITS BINDING PROTEIN AS A POSSIBLE TREATMENT FOR ALZHEIMER'S DISEASE. NATURE **378:** 284-287.

BERNARDIS, L. L., AND L. L. BELLINGER, 1996 THE LATERAL HYPOTHALAMIC AREA REVISITED: INGESTIVE BEHAVIOR. NEUROSCI BIOBEHAV REV **20:** 189-287.

BERTHOUD, H. R., 2004 MIND VERSUS METABOLISM IN THE CONTROL OF FOOD INTAKE AND ENERGY BALANCE. PHYSIOLOGY & BEHAVIOR **81:** 781-793.

BERTON, O., AND E. J. NESTLER, 2006 NEW APPROACHES TO ANTIDEPRESSANT DRUG DISCOVERY: BEYOND MONOAMINES. NAT REV NEUROSCI **7:** 137-151.

BISHOP, G. A., C. M. SEELANDT AND J. S. KING, 2000 CELLULAR LOCALIZATION OF CORTICOTROPIN RELEASING FACTOR RECEPTORS IN THE ADULT MOUSE CEREBELLUM. NEUROSCIENCE **101:** 1083-1092.

BITTENCOURT, J. C., F. PRESSE, C. ARIAS, C. PETO, J. VAUGHAN *ET AL.*, 1992 THE MELANIN-CONCENTRATING HORMONE SYSTEM OF THE RAT BRAIN: AN IMMUNO- AND HYBRIDIZATION HISTOCHEMICAL CHARACTERIZATION. J COMP NEUROL **319:** 218-245.

BITTENCOURT, J. C., J. VAUGHAN, C. ARIAS, R. A. RISSMAN, W. W. VALE *ET AL.*, 1999 UROCORTIN EXPRESSION IN RAT BRAIN: EVIDENCE AGAINST A PERVASIVE RELATIONSHIP OF UROCORTIN-CONTAINING PROJECTIONS WITH TARGETS BEARING TYPE 2 CRF RECEPTORS. J COMP NEUROL **415:** 285-312.

BJÖRKLUND, A., R. Y. MOORE, A. NOBIN AND U. STENEVI, 1973 THE ORGANIZATION OF TUBERO-HYPOPHYSEAL AND RETICULO-INFUNDIBULAR CATECHOLAMINE NEURON SYSTEMS IN THE RAT BRAIN. BRAIN RES **51:** 171-191.

BLAHA, C. D., L. F. ALLEN, S. DAS, W. L. INGLIS, M. P. LATIMER *ET AL.*, 1996 MODULATION OF DOPAMINE EFFLUX IN THE NUCLEUS ACCUMBENS AFTER CHOLINERGIC STIMULATION OF THE VENTRAL TEGMENTAL AREA IN INTACT, PEDUNCULOPONTINE TEGMENTAL NUCLEUS-LESIONED, AND LATERODORSAL TEGMENTAL NUCLEUS-LESIONED RATS. J NEUROSCI **16:** 714-722.

BLÜHER, S., AND C. S. MANTZOROS, 2007 LEPTIN IN REPRODUCTION. CURR OPIN ENDOCRINOL DIABETES OBES **14:** 458-464.

BOULANT, J. A., AND J. D. HARDY, 1974 THE EFFECT OF SPINAL AND SKIN TEMPERATURES ON THE FIRING RATE AND THERMOSENSITIVITY OF PREOPTIC NEURONES. J PHYSIOL **240:** 639-660.

BOURET, S. G., S. J. DRAPER AND R. B. SIMERLY, 2004 TROPHIC ACTION OF LEPTIN ON HYPOTHALAMIC NEURONS THAT REGULATE FEEDING. SCIENCE **304:** 108-110.

BOURET, S. G., AND R. B. SIMERLY, 2004 MINIREVIEW: LEPTIN AND DEVELOPMENT OF HYPOTHALAMIC FEEDING CIRCUITS. ENDOCRINOLOGY **145:** 2621-2626.

BRANDEIS, M., M. ARIEL AND H. CEDAR, 1993 DYNAMICS OF DNA METHYLATION DURING DEVELOPMENT. BIOESSAYS **15:** 709-713.

BROADWELL, R. D., AND M. W. BRIGHTMAN, 1976 ENTRY OF PEROXIDASE INTO NEURONS OF THE CENTRAL AND PERIPHERAL NERVOUS SYSTEMS FROM EXTRACEREBRAL AND CEREBRAL BLOOD. J COMP NEUROL **166:** 257-283.

BROBERGER, C., J. JOHANSEN, C. JOHANSSON, M. SCHALLING AND T. HÖKFELT, 1998 THE

NEUROPEPTIDE Y/AGOUTI GENE-RELATED PROTEIN (AGRP) BRAIN CIRCUITRY IN NORMAL, ANORECTIC, AND MONOSODIUM GLUTAMATE-TREATED MICE. PROC NATL ACAD SCI U S A **95:** 15043-15048.

BURLET, S., C. J. TYLER AND C. S. LEONARD, 2002 DIRECT AND INDIRECT EXCITATION OF LATERODORSAL TEGMENTAL NEURONS BY HYPOCRETIN/OREXIN PEPTIDES: IMPLICATIONS FOR WAKEFULNESS AND NARCOLEPSY. J NEUROSCI **22:** 2862-2872.

CAMPBELL, N. A. R., J.B., 2002 *BIOLOGY*. BENJAMIN CUMMINGS.

CAMPFIELD, L. A., F. J. SMITH, Y. GUISEZ, R. DEVOS AND P. BURN, 1995 RECOMBINANT MOUSE OB PROTEIN: EVIDENCE FOR A PERIPHERAL SIGNAL LINKING ADIPOSITY AND CENTRAL NEURAL NETWORKS. SCIENCE **269:** 546-549.

CANNON, B., AND J. NEDERGAARD, 2004 BROWN ADIPOSE TISSUE: FUNCTION AND PHYSIOLOGICAL SIGNIFICANCE. PHYSIOL. REV. **84:** 277-359.

CASSIDY, S. B., M. FORSYTHE, S. HEEGER, R. D. NICHOLLS, N. SCHORK *ET AL.*, 1997 COMPARISON OF PHENOTYPE BETWEEN PATIENTS WITH PRADER-WILLI SYNDROME DUE TO DELETION 15Q AND UNIPARENTAL DISOMY 15. AMERICAN JOURNAL OF MEDICAL GENETICS **68:** 433-440.

CATTANACH, B. M., AND M. KIRK, 1985 DIFFERENTIAL ACTIVITY OF MATERNALLY AND PATERNALLY DERIVED CHROMOSOME REGIONS IN MICE. NATURE **315:** 496-498.

CATTANACH, B. M., J. PETERS, S. BALL AND C. RASBERRY, 2000 TWO IMPRINTED GENE MUTATIONS: THREE PHENOTYPES. HUM MOL GENET **9:** 2263-2273.

CECHETTO, D. F., D. G. STANDAERT AND C. B. SAPER, 1985 SPINAL AND TRIGEMINAL DORSAL HORN PROJECTIONS TO THE PARABRACHIAL NUCLEUS IN THE RAT. J COMP NEUROL **240:** 153-160.

CHALMERS, D. T., T. W. LOVENBERG, D. E. GRIGORIADIS, D. P. BEHAN AND E. B. DE SOUZA, 1996 CORTICOTROPHIN-RELEASING FACTOR RECEPTORS: FROM MOLECULAR BIOLOGY TO DRUG DESIGN. TRENDS PHARMACOL SCI **17:** 166-172.

CHARALAMBOUS, M., S. T. DA ROCHA AND A. C. FERGUSON-SMITH, 2007 GENOMIC IMPRINTING, GROWTH CONTROL AND THE ALLOCATION OF NUTRITIONAL RESOURCES: CONSEQUENCES FOR POSTNATAL LIFE. CURR OPIN ENDOCRINOL DIABETES OBES **14:** 3-12.

CHEN, A. S., D. J. MARSH, M. E. TRUMBAUER, E. G. FRAZIER, X. M. GUAN *ET AL.*, 2000 INACTIVATION OF THE MOUSE MELANOCORTIN-3 RECEPTOR RESULTS IN INCREASED FAT MASS AND REDUCED LEAN BODY MASS. NAT GENET **26:** 97-102.

CHEN, M., H. CHEN, A. NGUYEN, D. GUPTA, J. WANG *ET AL.*, 2010 G(S)ALPHA DEFICIENCY IN ADIPOSE TISSUE LEADS TO A LEAN PHENOTYPE WITH DIVERGENT EFFECTS ON COLD TOLERANCE AND DIET-INDUCED THERMOGENESIS. CELL METAB **11:** 320-330.

CHEN, M., H.-Z. FENG, D. GUPTA, J. KELLEHER, K. E. DICKERSON *ET AL.*, 2009A GS{ALPHA} DEFICIENCY IN SKELETAL MUSCLE LEADS TO REDUCED MUSCLE MASS, FIBER-TYPE SWITCHING, AND GLUCOSE INTOLERANCE WITHOUT INSULIN RESISTANCE OR DEFICIENCY. AM J PHYSIOL CELL PHYSIOL**:** 00443.02008.

CHEN, M., O. GAVRILOVA, J. LIU, T. XIE, C. DENG *ET AL.*, 2005 ALTERNATIVE GNAS GENE PRODUCTS HAVE OPPOSITE EFFECTS ON GLUCOSE AND LIPID METABOLISM. PROC NATL ACAD SCI U S A **102:** 7386-7391.

CHEN, M., J. WANG, K. E. DICKERSON, J. KELLEHER, T. XIE *ET AL.*, 2009B CENTRAL NERVOUS SYSTEM IMPRINTING OF THE G PROTEIN G(S)ALPHA AND ITS ROLE IN METABOLIC REGULATION. CELL METAB **9:** 548-555.

CHEN, Y., C. HU, C. K. HSU, Q. ZHANG, C. BI *ET AL.*, 2002 TARGETED DISRUPTION OF THE

MELANIN-CONCENTRATING HORMONE RECEPTOR-1 RESULTS IN HYPERPHAGIA AND RESISTANCE TO DIET-INDUCED OBESITY. ENDOCRINOLOGY **143:** 2469-2477.

CHENG, A., N. UETANI, P. D. SIMONCIC, V. P. CHAUBEY, A. LEE-LOY *ET AL.*, 2002 ATTENUATION OF LEPTIN ACTION AND REGULATION OF OBESITY BY PROTEIN TYROSINE PHOSPHATASE 1B. DEV CELL **2:** 497-503.

CHOTALIA, M., S. A. SMALLWOOD, N. RUF, C. DAWSON, D. LUCIFERO *ET AL.*, 2009 TRANSCRIPTION IS REQUIRED FOR ESTABLISHMENT OF GERMLINE METHYLATION MARKS AT IMPRINTED GENES. GENES & DEVELOPMENT **23:** 105-117.

CHRISTOPHE, J., 1998 IS THERE APPETITE AFTER GLP-1 AND PACAP? ANN N Y ACAD SCI **865:** 323-335.

CLAYTON, E. C., AND C. L. WILLIAMS, 2000 ADRENERGIC ACTIVATION OF THE NUCLEUS TRACTUS SOLITARIUS POTENTIATES AMYGDALA NOREPINEPHRINE RELEASE AND ENHANCES RETENTION PERFORMANCE IN EMOTIONALLY AROUSING AND SPATIAL MEMORY TASKS. BEHAV BRAIN RES **112:** 151-158.

CLÉMENT, K., C. VAISSE, N. LAHLOU, S. CABROL, V. PELLOUX *ET AL.*, 1998 A MUTATION IN THE HUMAN LEPTIN RECEPTOR GENE CAUSES OBESITY AND PITUITARY DYSFUNCTION. NATURE **392:** 398-401.

CLEMENTS, J. R., AND S. GRANT, 1990 GLUTAMATE-LIKE IMMUNOREACTIVITY IN NEURONS OF THE LATERODORSAL TEGMENTAL AND PEDUNCULOPONTINE NUCLEI IN THE RAT. NEUROSCI LETT **120:** 70-73.

COLL, A. P., I. S. FAROOQI AND S. O'RAHILLY, 2007 THE HORMONAL CONTROL OF FOOD INTAKE. CELL **129:** 251-262.

CONNAUGHTON, M., J. V. PRIESTLEY, M. V. SOFRONIEW, F. ECKENSTEIN AND A. C. CUELLO, 1986 INPUTS TO MOTONEURONES IN THE HYPOGLOSSAL NUCLEUS OF THE RAT: LIGHT AND ELECTRON MICROSCOPIC IMMUNOCYTOCHEMISTRY FOR CHOLINE ACETYLTRANSFERASE, SUBSTANCE P AND ENKEPHALINS USING MONOCLONAL ANTIBODIES. NEUROSCIENCE **17:** 205-224.

CONSTANCIA, M., G. KELSEY AND W. REIK, 2004 RESOURCEFUL IMPRINTING. NATURE **432:** 53-57.

CONSTANCIA, M., B. PICKARD, G. KELSEY AND W. REIK, 1998 IMPRINTING MECHANISMS. GENOME RESEARCH **8:** 881-900.

COTA, D., K. PROULX, K. A. SMITH, S. C. KOZMA, G. THOMAS *ET AL.*, 2006 HYPOTHALAMIC MTOR SIGNALING REGULATES FOOD INTAKE. SCIENCE **312:** 927-930.

COWLEY, M. A., J. L. SMART, M. RUBINSTEIN, M. G. CERDAN, S. DIANO *ET AL.*, 2001 LEPTIN ACTIVATES ANOREXIGENIC POMC NEURONS THROUGH A NEURAL NETWORK IN THE ARCUATE NUCLEUS. NATURE **411:** 480-484.

CRAWFORD, J. A., K. J. MUTCHLER, B. E. SULLIVAN, T. M. LANIGAN, M. S. CLARK *ET AL.*, 1993 NEURAL EXPRESSION OF A NOVEL ALTERNATIVELY SPLICED AND POLYADENYLATED GS ALPHA TRANSCRIPT. J BIOL CHEM **268:** 9879-9885.

CUNNINGHAM, E. T., AND P. E. SAWCHENKO, 1988 ANATOMICAL SPECIFICITY OF NORADRENERGIC INPUTS TO THE PARAVENTRICULAR AND SUPRAOPTIC NUCLEI OF THE RAT HYPOTHALAMUS. J COMP NEUROL **274:** 60-76.

CURLEY, J. P., S. B. PINNOCK, S. L. DICKSON, R. THRESHER, N. MIYOSHI *ET AL.*, 2005 INCREASED BODY FAT IN MICE WITH A TARGETED MUTATION OF THE PATERNALLY EXPRESSED IMPRINTED GENE PEG3. FASEB J **19:** 1302-1304.

DAUTZENBERG, F. M., AND R. L. HAUGER, 2002 THE CRF PEPTIDE FAMILY AND THEIR RECEPTORS: YET MORE PARTNERS DISCOVERED. TRENDS PHARMACOL SCI **23:** 71-

77.

DAUTZENBERG, F. M., J. HIGELIN AND U. TEICHERT, 2000 FUNCTIONAL CHARACTERIZATION OF CORTICOTROPIN-RELEASING FACTOR TYPE 1 RECEPTOR ENDOGENOUSLY EXPRESSED IN HUMAN EMBRYONIC KIDNEY 293 CELLS. EUROPEAN JOURNAL OF PHARMACOLOGY **390:** 51-59.

DE LECEA, L., T. S. KILDUFF, C. PEYRON, X. GAO, P. E. FOYE *ET AL.*, 1998 THE HYPOCRETINS: HYPOTHALAMUS-SPECIFIC PEPTIDES WITH NEUROEXCITATORY ACTIVITY. PROCEEDINGS OF THE NATIONAL ACADEMY OF SCIENCES OF THE UNITED STATES OF AMERICA **95:** 322-327.

DE SOUZA, E. B., 1995 CORTICOTROPIN-RELEASING FACTOR RECEPTORS: PHYSIOLOGY, PHARMACOLOGY, BIOCHEMISTRY AND ROLE IN CENTRAL NERVOUS SYSTEM AND IMMUNE DISORDERS. PSYCHONEUROENDOCRINOLOGY **20:** 789-819.

DONATO, J., JR., R. M. CRAVO, R. FRAZAO AND C. F. ELIAS, 2011 HYPOTHALAMIC SITES OF LEPTIN ACTION LINKING METABOLISM AND REPRODUCTION. NEUROENDOCRINOLOGY **93:** 9-18.

DUAN, C., M. LI AND L. RUI, 2004A SH2-B PROMOTES INSULIN RECEPTOR SUBSTRATE 1 (IRS1)- AND IRS2-MEDIATED ACTIVATION OF THE PHOSPHATIDYLINOSITOL 3-KINASE PATHWAY IN RESPONSE TO LEPTIN. J BIOL CHEM **279:** 43684-43691.

DUAN, C., H. YANG, M. F. WHITE AND L. RUI, 2004B DISRUPTION OF THE SH2-B GENE CAUSES AGE-DEPENDENT INSULIN RESISTANCE AND GLUCOSE INTOLERANCE. MOL CELL BIOL **24:** 7435-7443.

DUBOIS, N. C., D. HOFMANN, K. KALOULIS, J. M. BISHOP AND A. TRUMPP, 2006 NESTIN-CRE TRANSGENIC MOUSE LINE NES-CRE1 MEDIATES HIGHLY EFFICIENT CRE/LOXP MEDIATED RECOMBINATION IN THE NERVOUS SYSTEM, KIDNEY, AND SOMITE-DERIVED TISSUES. GENESIS **44:** 355-360.

EL MANSARI, M., K. SAKAI AND M. JOUVET, 1989 UNITARY CHARACTERISTICS OF PRESUMPTIVE CHOLINERGIC TEGMENTAL NEURONS DURING THE SLEEP-WAKING CYCLE IN FREELY MOVING CATS. EXP BRAIN RES **76:** 519-529.

ELIAS, C. F., C. ASCHKENASI, C. LEE, J. KELLY, R. S. AHIMA *ET AL.*, 1999 LEPTIN DIFFERENTIALLY REGULATES NPY AND POMC NEURONS PROJECTING TO THE LATERAL HYPOTHALAMIC AREA. NEURON **23:** 775-786.

ELIAS, C. F., C. LEE, J. KELLY, C. ASCHKENASI, R. S. AHIMA *ET AL.*, 1998 LEPTIN ACTIVATES HYPOTHALAMIC CART NEURONS PROJECTING TO THE SPINAL CORD. NEURON **21:** 1375-1385.

ELMQUIST, J. K., E. MARATOS-FLIER, C. B. SAPER AND J. S. FLIER, 1998 UNRAVELING THE CENTRAL NERVOUS SYSTEM PATHWAYS UNDERLYING RESPONSES TO LEPTIN. NAT NEUROSCI **1:** 445-450.

ENNIS, M., AND G. ASTON-JONES, 1989A GABA-MEDIATED INHIBITION OF LOCUS COERULEUS FROM THE DORSOMEDIAL ROSTRAL MEDULLA. J NEUROSCI **9:** 2973-2981.

ENNIS, M., AND G. ASTON-JONES, 1989B POTENT INHIBITORY INPUT TO LOCUS COERULEUS FROM THE NUCLEUS PREPOSITUS HYPOGLOSSI. BRAIN RES BULL **22:** 793-803.

ENNIS, M., M. BEHBEHANI, M. T. SHIPLEY, E. J. VAN BOCKSTAELE AND G. ASTON-JONES, 1991 PROJECTIONS FROM THE PERIAQUEDUCTAL GRAY TO THE ROSTROMEDIAL PERICOERULEAR REGION AND NUCLEUS LOCUS COERULEUS: ANATOMIC AND PHYSIOLOGIC STUDIES. J COMP NEUROL **306:** 480-494.

F. BRISCHOUX, D. F., P. Y. RISOLD,, 2001 ONTOGENETIC DEVELOPMENT OF THE DIENCEPHALIC MCH NEURONS: A HYPOTHALAMIC 'MCH AREA' HYPOTHESIS.

EUROPEAN JOURNAL OF NEUROSCIENCE **13:** 1733-1744.

FALKE, N., 1991 MODULATION OF OXYTOCIN AND VASOPRESSIN RELEASE AT THE LEVEL OF THE NEUROHYPOPHYSIS. PROG NEUROBIOL **36:** 465-484.

FALLON, J. H., AND R. Y. MOORE, 1978 CATECHOLAMINE INNERVATION OF THE BASAL FOREBRAIN. IV. TOPOGRAPHY OF THE DOPAMINE PROJECTION TO THE BASAL FOREBRAIN AND NEOSTRIATUM. J COMP NEUROL **180:** 545-580.

FAN, W., S. F. MORRISON, W. H. CAO AND P. YU, 2007 THERMOGENESIS ACTIVATED BY CENTRAL MELANOCORTIN SIGNALING IS DEPENDENT ON NEURONS IN THE ROSTRAL RAPHE PALLIDUS (RRPA) AREA. BRAIN RES **1179:** 61-69.

FERGUSON-SMITH, A. C., 2011 GENOMIC IMPRINTING: THE EMERGENCE OF AN EPIGENETIC PARADIGM. NATURE REVIEWS GENETICS **12:** 565-575.

FRITSCHY, J. M., AND R. GRZANNA, 1990 DEMONSTRATION OF TWO SEPARATE DESCENDING NORADRENERGIC PATHWAYS TO THE RAT SPINAL CORD: EVIDENCE FOR AN INTRAGRISEAL TRAJECTORY OF LOCUS COERULEUS AXONS IN THE SUPERFICIAL LAYERS OF THE DORSAL HORN. J COMP NEUROL **291:** 553-582.

FRONTERA, M., B. DICKINS, A. PLAGGE AND G. KELSEY, 2008 IMPRINTED GENES, POSTNATAL ADAPTATIONS AND ENDURING EFFECTS ON ENERGY HOMEOSTASIS. ADV EXP MED BIOL **626:** 41-61.

FUNATO, H., A. L. TSAI, J. T. WILLIE, Y. KISANUKI, S. C. WILLIAMS *ET AL.*, 2009 ENHANCED OREXIN RECEPTOR-2 SIGNALING PREVENTS DIET-INDUCED OBESITY AND IMPROVES LEPTIN SENSITIVITY. CELL METAB **9:** 64-76.

GAO, X. B., AND A. N. VAN DEN POL, 2001 MELANIN CONCENTRATING HORMONE DEPRESSES SYNAPTIC ACTIVITY OF GLUTAMATE AND GABA NEURONS FROM RAT LATERAL HYPOTHALAMUS. JOURNAL OF PHYSIOLOGY **533:** 237-252.

GARFIELD, A. S., M. COWLEY, F. M. SMITH, K. MOORWOOD, J. E. STEWART-COX *ET AL.*, 2011 DISTINCT PHYSIOLOGICAL AND BEHAVIOURAL FUNCTIONS FOR PARENTAL ALLELES OF IMPRINTED GRB10. NATURE **469:** 534-538.

GARTEN, L. L., M. V. SOFRONIEW AND R. E. DYBALL, 1989 A DIRECT CATECHOLAMINERGIC PROJECTION FROM THE BRAINSTEM TO THE NEUROHYPOPHYSIS OF THE RAT. NEUROSCIENCE **33:** 149-155.

GEORGIADES, P., M. WATKINS, G. J. BURTON AND A. C. FERGUSON-SMITH, 2001 ROLES FOR GENOMIC IMPRINTING AND THE ZYGOTIC GENOME IN PLACENTAL DEVELOPMENT. PROCEEDINGS OF THE NATIONAL ACADEMY OF SCIENCES OF THE UNITED STATES OF AMERICA **98:** 4522-4527.

GERMAIN-LEE, E. L., C. L. DING, Z. DENG, J. L. CRANE, M. SAJI *ET AL.*, 2002 PATERNAL IMPRINTING OF GALPHA(S) IN THE HUMAN THYROID AS THE BASIS OF TSH RESISTANCE IN PSEUDOHYPOPARATHYROIDISM TYPE 1A. BIOCHEM BIOPHYS RES COMMUN **296:** 67-72.

GERMAIN-LEE, E. L., W. SCHWINDINGER, J. L. CRANE, R. ZEWDU, L. S. ZWEIFEL *ET AL.*, 2005 A MOUSE MODEL OF ALBRIGHT HEREDITARY OSTEODYSTROPHY GENERATED BY TARGETED DISRUPTION OF EXON 1 OF THE GNAS GENE. ENDOCRINOLOGY **146:** 4697-4709.

GREGG, C., J. ZHANG, B. WEISSBOURD, S. LUO, G. P. SCHROTH *ET AL.*, 2010 HIGH-RESOLUTION ANALYSIS OF PARENT-OF-ORIGIN ALLELIC EXPRESSION IN THE MOUSE BRAIN. SCIENCE **329:** 643-648.

GRILL, H. J., 2006 DISTRIBUTED NEURAL CONTROL OF ENERGY BALANCE: CONTRIBUTIONS FROM HINDBRAIN AND HYPOTHALAMUS. OBESITY (SILVER SPRING) **14 SUPPL 5:** 216S-221S.

GRILL, H. J., AND M. R. HAYES, 2009 THE NUCLEUS TRACTUS SOLITARIUS: A PORTAL FOR

VISCERAL AFFERENT SIGNAL PROCESSING, ENERGY STATUS ASSESSMENT AND INTEGRATION OF THEIR COMBINED EFFECTS ON FOOD INTAKE. INT J OBES (LOND) **33 SUPPL 1:** S11-15.

GRILL, H. J., M. W. SCHWARTZ, J. M. KAPLAN, J. S. FOXHALL, J. BREININGER *ET AL.*, 2002 EVIDENCE THAT THE CAUDAL BRAINSTEM IS A TARGET FOR THE INHIBITORY EFFECT OF LEPTIN ON FOOD INTAKE. ENDOCRINOLOGY **143:** 239-246.

GRZANNA, R., W. K. CHEE AND E. W. AKEYSON, 1987 NORADRENERGIC PROJECTIONS TO BRAINSTEM NUCLEI: EVIDENCE FOR DIFFERENTIAL PROJECTIONS FROM NORADRENERGIC SUBGROUPS. J COMP NEUROL **263:** 76-91.

GUTKNECHT, E., I. VAN DER LINDEN, K. VAN KOLEN, K. F. VERHOEVEN, G. VAUQUELIN *ET AL.*, 2009 MOLECULAR MECHANISMS OF CORTICOTROPIN-RELEASING FACTOR RECEPTOR-INDUCED CALCIUM SIGNALING. MOL PHARMACOL **75:** 648-657.

HAGAN, J. J., R. A. LESLIE, S. PATEL, M. L. EVANS, T. A. WATTAM *ET AL.*, 1999 OREXIN A ACTIVATES LOCUS COERULEUS CELL FIRING AND INCREASES AROUSAL IN THE RAT. PROC NATL ACAD SCI U S A **96:** 10911-10916.

HAHN, T. M., J. F. BREININGER, D. G. BASKIN AND M. W. SCHWARTZ, 1998 COEXPRESSION OF AGRP AND NPY IN FASTING-ACTIVATED HYPOTHALAMIC NEURONS. NAT NEUROSCI **1:** 271-272.

HALAAS, J. L., K. S. GAJIWALA, M. MAFFEI, S. L. COHEN, B. T. CHAIT *ET AL.*, 1995 WEIGHT-REDUCING EFFECTS OF THE PLASMA PROTEIN ENCODED BY THE OBESE GENE. SCIENCE **269:** 543-546.

HAN, Z. S., AND G. JU, 1990 EFFECTS OF ELECTRICAL STIMULATION OF THE CENTRAL NUCLEUS OF THE AMYGDALA AND THE LATERAL HYPOTHALAMIC AREA ON THE OVAL NUCLEUS OF THE BED NUCLEI OF THE STRIA TERMINALIS AND ITS ADJACENT AREAS IN THE RAT. BRAIN RESEARCH **536:** 56-62.

HARA, J., C. T. BEUCKMANN, T. NAMBU, J. T. WILLIE, R. M. CHEMELLI *ET AL.*, 2001 GENETIC ABLATION OF OREXIN NEURONS IN MICE RESULTS IN NARCOLEPSY, HYPOPHAGIA, AND OBESITY. NEURON **30:** 345-354.

HAY-SCHMIDT, A., L. HELBOE AND P. J. LARSEN, 2001 LEPTIN RECEPTOR IMMUNOREACTIVITY IS PRESENT IN ASCENDING SEROTONERGIC AND CATECHOLAMINERGIC NEURONS OF THE RAT. NEUROENDOCRINOLOGY **73:** 215-226.

HAYES, M. R., AND M. COVASA, 2006 DORSAL HINDBRAIN 5-HT3 RECEPTORS PARTICIPATE IN CONTROL OF MEAL SIZE AND MEDIATE CCK-INDUCED SATIATION. BRAIN RES **1103:** 99-107.

HAYNES, A. C., H. CHAPMAN, C. TAYLOR, G. B. MOORE, M. A. CAWTHORNE *ET AL.*, 2002 ANORECTIC, THERMOGENIC AND ANTI-OBESITY ACTIVITY OF A SELECTIVE OREXIN-1 RECEPTOR ANTAGONIST IN OB/OB MICE. REGUL PEPT **104:** 153-159.

HAYNES, A. C., B. JACKSON, H. CHAPMAN, M. TADAYYON, A. JOHNS *ET AL.*, 2000 A SELECTIVE OREXIN-1 RECEPTOR ANTAGONIST REDUCES FOOD CONSUMPTION IN MALE AND FEMALE RATS. REGUL PEPT **96:** 45-51.

HAYWARD, B. E., A. BARLIER, M. KORBONITS, A. B. GROSSMAN, P. JACQUET *ET AL.*, 2001 IMPRINTING OF THE G(S)ALPHA GENE GNAS1 IN THE PATHOGENESIS OF ACROMEGALY. J CLIN INVEST **107:** R31-36.

HAYWARD, B. E., M. KAMIYA, L. STRAIN, V. MORAN, R. CAMPBELL *ET AL.*, 1998A THE HUMAN GNAS1 GENE IS IMPRINTED AND ENCODES DISTINCT PATERNALLY AND BIALLELICALLY EXPRESSED G PROTEINS. PROC NATL ACAD SCI U S A **95:** 10038-10043.

HAYWARD, B. E., V. MORAN, L. STRAIN AND D. T. BONTHRON, 1998B BIDIRECTIONAL

IMPRINTING OF A SINGLE GENE: GNAS1 ENCODES MATERNALLY, PATERNALLY, AND BIALLELICALLY DERIVED PROTEINS. PROC NATL ACAD SCI U S A **95:** 15475-15480.

HERMANN, D. M., P. H. LUPPI, C. PEYRON, P. HINCKEL AND M. JOUVET, 1997 AFFERENT PROJECTIONS TO THE RAT NUCLEI RAPHE MAGNUS, RAPHE PALLIDUS AND RETICULARIS GIGANTOCELLULARIS PARS ALPHA DEMONSTRATED BY IONTOPHORETIC APPLICATION OF CHOLERATOXIN (SUBUNIT B). J CHEM NEUROANAT **13:** 1-21.

HOLLAND, P. R., AND P. J. GOADSBY, 2009 CLUSTER HEADACHE, HYPOTHALAMUS, AND OREXIN. CURR PAIN HEADACHE REP **13:** 147-154.

HOLMES, R., C. WILLIAMSON, J. PETERS, P. DENNY, C. WELLS *ET AL.*, 2003 A COMPREHENSIVE TRANSCRIPT MAP OF THE MOUSE GNAS IMPRINTED COMPLEX. GENOME RES **13:** 1410-1415.

HORVATH, T. L., C. PEYRON, S. DIANO, A. IVANOV, G. ASTON-JONES *ET AL.*, 1999 HYPOCRETIN (OREXIN) ACTIVATION AND SYNAPTIC INNERVATION OF THE LOCUS COERULEUS NORADRENERGIC SYSTEM. J COMP NEUROL **415:** 145-159.

HOSOYA, Y., 1985 HYPOTHALAMIC PROJECTIONS TO THE VENTRAL MEDULLA OBLONGATA IN THE RAT, WITH SPECIAL REFERENCE TO THE NUCLEUS RAPHE PALLIDUS: A STUDY USING AUTORADIOGRAPHIC AND HRP TECHNIQUES. BRAIN RES **344:** 338-350.

HU, Y., B. T. BLOOMQUIST, L. J. CORNFIELD, L. B. DECARR, J. R. FLORES-RIVEROS *ET AL.*, 1996 IDENTIFICATION OF A NOVEL HYPOTHALAMIC NEUROPEPTIDE Y RECEPTOR ASSOCIATED WITH FEEDING BEHAVIOR. J BIOL CHEM **271:** 26315-26319.

HULL, D., AND M. M. SEGALL, 1966 DISTINCTION OF BROWN FROM WHITE ADIPOSE TISSUE. NATURE **212:** 469-472.

HUMMEL, K. P., M. M. DICKIE AND D. L. COLEMAN, 1966 DIABETES, A NEW MUTATION IN THE MOUSE. SCIENCE **153:** 1127-1128.

HUSO, D. L., S. EDIE, M. A. LEVINE, W. SCHWINDINGER, Y. WANG *ET AL.*, 2011 HETEROTOPIC OSSIFICATIONS IN A MOUSE MODEL OF ALBRIGHT HEREDITARY OSTEODYSTROPHY. PLOS ONE [ELECTRONIC RESOURCE] **6:** E21755.

INGALLS, A. M., M. M. DICKIE AND G. D. SNELL, 1950 OBESE, A NEW MUTATION IN THE HOUSE MOUSE. J HERED **41:** 317-318.

ISLES, A. R., W. DAVIES AND L. S. WILKINSON, 2006 GENOMIC IMPRINTING AND THE SOCIAL BRAIN. PHILOSOPHICAL TRANSACTIONS OF THE ROYAL SOCIETY OF LONDON - SERIES B: BIOLOGICAL SCIENCES **361:** 2229-2237.

IVANOV, A., AND G. ASTON-JONES, 2000 HYPOCRETIN/OREXIN DEPOLARIZES AND DECREASES POTASSIUM CONDUCTANCE IN LOCUS COERULEUS NEURONS. NEUROREPORT **11:** 1755-1758.

JÜPPNER, H., A. LINGLART, L. F. FRÖHLICH AND M. BASTEPE, 2006 AUTOSOMAL-DOMINANT PSEUDOHYPOPARATHYROIDISM TYPE IB IS CAUSED BY DIFFERENT MICRODELETIONS WITHIN OR UPSTREAM OF THE GNAS LOCUS. ANNALS OF THE NEW YORK ACADEMY OF SCIENCES **1068:** 250-255.

KAFRI, T., M. ARIEL, M. BRANDEIS, R. SHEMER, L. URVEN *ET AL.*, 1992 DEVELOPMENTAL PATTERN OF GENE-SPECIFIC DNA METHYLATION IN THE MOUSE EMBRYO AND GERM LINE. GENES DEV **6:** 705-714.

KARSENTY, G., 2006 CONVERGENCE BETWEEN BONE AND ENERGY HOMEOSTASES: LEPTIN REGULATION OF BONE MASS. CELL METAB **4:** 341-348.

KAWANO, H., AND S. DAIKOKU, 1987 FUNCTIONAL TOPOGRAPHY OF THE RAT HYPOTHALAMIC DOPAMINE NEURON SYSTEMS: RETROGRADE TRACING AND

IMMUNOHISTOCHEMICAL STUDY. J COMP NEUROL **265:** 242-253.

KAYAMA, Y., M. OHTA AND E. JODO, 1992 FIRING OF 'POSSIBLY' CHOLINERGIC NEURONS IN THE RAT LATERODORSAL TEGMENTAL NUCLEUS DURING SLEEP AND WAKEFULNESS. BRAIN RES **569:** 210-220.

KEHLENBACH, R. H., J. MATTHEY AND W. B. HUTTNER, 1994 XL ALPHA S IS A NEW TYPE OF G PROTEIN.[ERRATUM APPEARS IN NATURE 1995 MAY 18;375(6528):253]. NATURE **372:** 804-809.

KELLY, M. L., L. MOIR, L. JONES, E. WHITEHILL, Q. M. ANSTEE *ET AL.*, 2009 A MISSENSE MUTATION IN THE NON-NEURAL G-PROTEIN [ALPHA]-SUBUNIT ISOFORMS MODULATES SUSCEPTIBILITY TO OBESITY. INT J OBES **33:** 507-518.

KIM, K. S., Y. R. YOON, H. J. LEE, S. YOON, S. Y. KIM *ET AL.*, 2010 ENHANCED HYPOTHALAMIC LEPTIN SIGNALING IN MICE LACKING DOPAMINE D2 RECEPTORS. J BIOL CHEM **285:** 8905-8917.

KIMURA, T., L. SHARE, B. C. WANG AND J. T. CROFTON, 1981 CENTRAL EFFECTS OF DOPAMINE AND BROMOCRIPTINE ON VASOPRESSIN RELEASE AND BLOOD PRESSURE. NEUROENDOCRINOLOGY **33:** 347-351.

KLEMKE, M., H. A. PASOLLI, R. H. KEHLENBACH, S. OFFERMANNS, G. SCHULTZ *ET AL.*, 2000 CHARACTERIZATION OF THE EXTRA-LARGE G PROTEIN ALPHA-SUBUNIT XLALPHAS. II. SIGNAL TRANSDUCTION PROPERTIES. JOURNAL OF BIOLOGICAL CHEMISTRY **275:** 33633-33640.

KOJIMA, M., AND K. KANGAWA, 2008 STRUCTURE AND FUNCTION OF GHRELIN. RESULTS PROBL CELL DIFFER **46:** 89-115.

KOZASA, T., H. ITOH, T. TSUKAMOTO AND Y. KAZIRO, 1988 ISOLATION AND CHARACTERIZATION OF THE HUMAN GS ALPHA GENE. PROC NATL ACAD SCI U S A **85:** 2081-2085.

KOZLOV, S. V., J. W. BOGENPOHL, M. P. HOWELL, R. WEVRICK, S. PANDA *ET AL.*, 2007 THE IMPRINTED GENE MAGEL2 REGULATES NORMAL CIRCADIAN OUTPUT. NATURE GENETICS **39:** 1266-1272.

KRECHOWEC, S., AND A. PLAGGE, 2008 PHYSIOLOGICAL DYSFUNCTIONS ASSOCIATED WITH MUTATIONS OF THE IMPRINTED GNAS LOCUS. PHYSIOLOGY **23:** 221-229.

KRECHOWEC, S. O., K. L. BURTON, A. U. NEWLACZYL, N. NUNN, N. VLATKOVIC *ET AL.*, 2012 POSTNATAL CHANGES IN THE EXPRESSION PATTERN OF THE IMPRINTED SIGNALLING PROTEIN XLALPHAS UNDERLIE THE CHANGING PHENOTYPE OF DEFICIENT MICE. PLOS ONE [ELECTRONIC RESOURCE] **7:** E29753.

KRISTENSEN, P., M. E. JUDGE, L. THIM, U. RIBEL, K. N. CHRISTJANSEN *ET AL.*, 1998 HYPOTHALAMIC CART IS A NEW ANORECTIC PEPTIDE REGULATED BY LEPTIN. NATURE **393:** 72-76.

LAGE, R., C. DIEGUEZ, A. VIDAL-PUIG AND M. LOPEZ, 2008 AMPK: A METABOLIC GAUGE REGULATING WHOLE-BODY ENERGY HOMEOSTASIS. TRENDS MOL MED **14:** 539-549.

LAM, Q. L., AND L. LU, 2007 ROLE OF LEPTIN IN IMMUNITY. CELL MOL IMMUNOL **4:** 1-13.

LEDBETTER, D. H., V. M. RICCARDI, S. D. AIRHART, R. J. STROBEL, B. S. KEENAN *ET AL.*, 1981 DELETIONS OF CHROMOSOME 15 AS A CAUSE OF THE PRADER-WILLI SYNDROME. NEW ENGLAND JOURNAL OF MEDICINE **304:** 325-329.

LEI, L., Y. GU, J. G. MURPHY, P. YU, J. L. SMART *ET AL.*, 2008 BRAINSTEM RAPHE PALLIDUS AND THE ADJACENT AREA CONTAIN A NOVEL ACTION SITE IN THE MELANOCORTIN CIRCUITRY REGULATING ENERGY BALANCE. LIFE SCIENCE JOURNAL **VOL 5**.

LEMBO, P. M., E. GRAZZINI, J. CAO, D. A. HUBATSCH, M. PELLETIER *ET AL.*, 1999 THE RECEPTOR FOR THE OREXIGENIC PEPTIDE MELANIN-CONCENTRATING HORMONE IS A G-PROTEIN-COUPLED RECEPTOR. NAT CELL BIOL **1:** 267-271.

LEVINE, M. A., C. EIL, R. W. DOWNS, JR. AND A. M. SPIEGEL, 1983 DEFICIENT GUANINE NUCLEOTIDE REGULATORY UNIT ACTIVITY IN CULTURED FIBROBLAST MEMBRANES FROM PATIENTS WITH PSEUDOHYPOPARATHYROIDISM TYPE I. A CAUSE OF IMPAIRED SYNTHESIS OF 3',5'-CYCLIC AMP BY INTACT AND BROKEN CELLS. J CLIN INVEST **72:** 316-324.

LEVIS, M., AND H. BOURNE, 1992 ACTIVATION OF THE ALPHA SUBUNIT OF GS IN INTACT CELLS ALTERS ITS ABUNDANCE, RATE OF DEGRADATION, AND MEMBRANE AVIDITY. J. CELL BIOL. **119:** 1297-1307.

LEVITT, P., AND R. Y. MOORE, 1979 ORIGIN AND ORGANIZATION OF BRAINSTEM CATECHOLAMINE INNERVATION IN THE RAT. J COMP NEUROL **186:** 505-528.

LI, E., T. H. BESTOR AND R. JAENISCH, 1992 TARGETED MUTATION OF THE DNA METHYLTRANSFERASE GENE RESULTS IN EMBRYONIC LETHALITY. CELL **69:** 915-926.

LI, T., T. H. VU, Z. L. ZENG, B. T. NGUYEN, B. E. HAYWARD *ET AL.*, 2000 TISSUE-SPECIFIC EXPRESSION OF ANTISENSE AND SENSE TRANSCRIPTS AT THE IMPRINTED GNAS LOCUS. GENOMICS **69:** 295-304.

LIU, J., B. ERLICHMAN AND L. S. WEINSTEIN, 2003 THE STIMULATORY G PROTEIN ALPHA-SUBUNIT GS ALPHA IS IMPRINTED IN HUMAN THYROID GLANDS: IMPLICATIONS FOR THYROID FUNCTION IN PSEUDOHYPOPARATHYROIDISM TYPES 1A AND 1B. J CLIN ENDOCRINOL METAB **88:** 4336-4341.

LOEWY, A. D., AND S. MCKELLAR, 1981 SEROTONERGIC PROJECTIONS FROM THE VENTRAL MEDULLA TO THE INTERMEDIOLATERAL CELL COLUMN IN THE RAT. BRAIN RES **211:** 146-152.

LOEWY, A. D., J. H. WALLACH AND S. MCKELLAR, 1981 EFFERENT CONNECTIONS OF THE VENTRAL MEDULLA OBLONGATA IN THE RAT. BRAIN RES **228:** 63-80.

LU, J., M. A. GRECO, P. SHIROMANI AND C. B. SAPER, 2000 EFFECT OF LESIONS OF THE VENTROLATERAL PREOPTIC NUCLEUS ON NREM AND REM SLEEP. J NEUROSCI **20:** 3830-3842.

LU, X. Y., 2007 THE LEPTIN HYPOTHESIS OF DEPRESSION: A POTENTIAL LINK BETWEEN MOOD DISORDERS AND OBESITY? CURR OPIN PHARMACOL **7:** 648-652.

MANTOVANI, G., E. BALLARE, E. GIAMMONA, P. BECK-PECCOZ AND A. SPADA, 2002 THE GSALPHA GENE: PREDOMINANT MATERNAL ORIGIN OF TRANSCRIPTION IN HUMAN THYROID GLAND AND GONADS. J CLIN ENDOCRINOL METAB **87:** 4736-4740.

MANTOVANI, G., S. BONDIONI, A. LINGLART, M. MAGHNIE, M. CISTERNINO *ET AL.*, 2007 GENETIC ANALYSIS AND EVALUATION OF RESISTANCE TO THYROTROPIN AND GROWTH HORMONE-RELEASING HORMONE IN PSEUDOHYPOPARATHYROIDISM TYPE IB. J CLIN ENDOCRINOL METAB **92:** 3738-3742.

MANTYH, P. W., AND S. P. HUNT, 1984 NEUROPEPTIDES ARE PRESENT IN PROJECTION NEURONES AT ALL LEVELS IN VISCERAL AND TASTE PATHWAYS: FROM PERIPHERY TO SENSORY CORTEX. BRAIN RES **299:** 297-312.

MARSH, D. J., D. T. WEINGARTH, D. E. NOVI, H. Y. CHEN, M. E. TRUMBAUER *ET AL.*, 2002 MELANIN-CONCENTRATING HORMONE 1 RECEPTOR-DEFICIENT MICE ARE LEAN, HYPERACTIVE, AND HYPERPHAGIC AND HAVE ALTERED METABOLISM. PROC NATL ACAD SCI U S A **99:** 3240-3245.

MATTERA, R., M. P. GRAZIANO, A. YATANI, Z. ZHOU, R. GRAF *ET AL.*, 1989 SPLICE VARIANTS OF THE ALPHA SUBUNIT OF THE G PROTEIN GS ACTIVATE BOTH

ADENYLYL CYCLASE AND CALCIUM CHANNELS. SCIENCE **243:** 804-807.

MAYA-MONTEIRO, C. M., P. E. ALMEIDA, H. D'AVILA, A. S. MARTINS, A. P. REZENDE *ET AL.*, 2008 LEPTIN INDUCES MACROPHAGE LIPID BODY FORMATION BY A PHOSPHATIDYLINOSITOL 3-KINASE- AND MAMMALIAN TARGET OF RAPAMYCIN-DEPENDENT MECHANISM. J BIOL CHEM **283:** 2203-2210.

MCALLEN, R. M., 2004 PREOPTIC THERMOREGULATORY MECHANISMS IN DETAIL. AM J PHYSIOL REGUL INTEGR COMP PHYSIOL **287:** R272-273.

MERTINEIT, C., J. A. YODER, T. TAKETO, D. W. LAIRD, J. M. TRASLER *ET AL.*, 1998 SEX-SPECIFIC EXONS CONTROL DNA METHYLTRANSFERASE IN MAMMALIAN GERM CELLS. DEVELOPMENT **125:** 889-897.

MESULAM, M. M., E. J. MUFSON, B. H. WAINER AND A. I. LEVEY, 1983 CENTRAL CHOLINERGIC PATHWAYS IN THE RAT: AN OVERVIEW BASED ON AN ALTERNATIVE NOMENCLATURE (CH1-CH6). NEUROSCIENCE **10:** 1185-1201.

MEZEY, E., C. LÉRÁNTH, M. J. BROWNSTEIN, E. FRIEDMAN, D. T. KRIEGER *ET AL.*, 1984 ON THE ORIGIN OF THE SEROTONERGIC INPUT TO THE INTERMEDIATE LOBE OF THE RAT PITUITARY. BRAIN RES **294:** 231-237.

MIGUELEZ, M., C. H. BIELAJEW, M. DIOTTE AND R. SHIAO, 2001 DYNAMIC CHANGES IN CYTOCHROME OXIDASE ACTIVITY IN THE AMYGDALA FOLLOWING LESIONS OF REWARDING SITES IN THE LATERAL HYPOTHALAMUS. BEHAVIOURAL BRAIN RESEARCH **119:** 103-110.

MIÑANO, F. J., M. S. MENERES SANCHO, M. SANCIBRIÁN, P. SALINAS AND R. D. MYERS, 1992 GABAA RECEPTORS IN THE AMYGDALA: ROLE IN FEEDING IN FASTED AND SATIATED RATS. BRAIN RESEARCH **586:** 104-110.

MITCHELL, A. J., 1998 THE ROLE OF CORTICOTROPIN RELEASING FACTOR IN DEPRESSIVE ILLNESS: A CRITICAL REVIEW. NEUROSCI BIOBEHAV REV **22:** 635-651.

MORIN, S. M., N. LING, X. J. LIU, S. D. KAHL AND D. R. GEHLERT, 1999 DIFFERENTIAL DISTRIBUTION OF UROCORTIN- AND CORTICOTROPIN-RELEASING FACTOR-LIKE IMMUNOREACTIVITIES IN THE RAT BRAIN. NEUROSCIENCE **92:** 281-291.

MORRIS, D. L., AND L. RUI, 2009 RECENT ADVANCES IN UNDERSTANDING LEPTIN SIGNALING AND LEPTIN RESISTANCE. AM J PHYSIOL ENDOCRINOL METAB **297:** E1247-1259.

MORRISON, S. F., 2001A DIFFERENTIAL REGULATION OF BROWN ADIPOSE AND SPLANCHNIC SYMPATHETIC OUTFLOWS IN RAT: ROLES OF RAPHE AND ROSTRAL VENTROLATERAL MEDULLA NEURONS. CLIN EXP PHARMACOL PHYSIOL **28:** 138-143.

MORRISON, S. F., 2001B DIFFERENTIAL REGULATION OF SYMPATHETIC OUTFLOWS TO VASOCONSTRICTOR AND THERMOREGULATORY EFFECTORS. ANN N Y ACAD SCI **940:** 286-298.

MORRISON, S. F., AND W. H. CAO, 2000 DIFFERENT ADRENAL SYMPATHETIC PREGANGLIONIC NEURONS REGULATE EPINEPHRINE AND NOREPINEPHRINE SECRETION. AM J PHYSIOL REGUL INTEGR COMP PHYSIOL **279:** R1763-1775.

MORRISON, S. F., AND K. NAKAMURA, 2011 CENTRAL NEURAL PATHWAYS FOR THERMOREGULATION. FRONT BIOSCI **16:** 74-104.

MÜNZBERG, H., J. S. FLIER AND C. BJØRBAEK, 2004 REGION-SPECIFIC LEPTIN RESISTANCE WITHIN THE HYPOTHALAMUS OF DIET-INDUCED OBESE MICE. ENDOCRINOLOGY **145:** 4880-4889.

NAMBU, T., T. SAKURAI, K. MIZUKAMI, Y. HOSOYA, M. YANAGISAWA *ET AL.*, 1999 DISTRIBUTION OF OREXIN NEURONS IN THE ADULT RAT BRAIN. BRAIN RESEARCH **827:** 243-260.

NICHOLLS, R. D., 2000 THE IMPACT OF GENOMIC IMPRINTING FOR NEUROBEHAVIORAL AND DEVELOPMENTAL DISORDERS. J CLIN INVEST **105:** 413-418.

NIEUWENHUYS, A., J. R. PIJPERS, R. R. OUDEJANS AND F. C. BAKKER, 2008 THE INFLUENCE OF ANXIETY ON VISUAL ATTENTION IN CLIMBING. J SPORT EXERC PSYCHOL **30:** 171-185.

ODGREN, P. R., C. A. MACKAY, A. MASON-SAVAS, M. YANG, G. MAILHOT *ET AL.*, 2006 FALSE-POSITIVE BETA-GALACTOSIDASE STAINING IN OSTEOCLASTS BY ENDOGENOUS ENZYME: STUDIES IN NEONATAL AND MONTH-OLD WILD-TYPE MICE. CONNECT TISSUE RES **47:** 229-234.

PASOLLI, H. A., AND W. B. HUTTNER, 2001 EXPRESSION OF THE EXTRA-LARGE G PROTEIN ALPHA-SUBUNIT XLALPHAS IN NEUROEPITHELIAL CELLS AND YOUNG NEURONS DURING DEVELOPMENT OF THE RAT NERVOUS SYSTEM. NEUROSCIENCE LETTERS **301:** 119-122.

PASOLLI, H. A., M. KLEMKE, R. H. KEHLENBACH, Y. WANG AND W. B. HUTTNER, 2000 CHARACTERIZATION OF THE EXTRA-LARGE G PROTEIN ALPHA-SUBUNIT XLALPHAS. I. TISSUE DISTRIBUTION AND SUBCELLULAR LOCALIZATION. JOURNAL OF BIOLOGICAL CHEMISTRY **275:** 33622-33632.

PAVELKA, M., AND J. ROTH, 2010 WHITE ADIPOSE TISSUE

FUNCTIONAL ULTRASTRUCTURE, PP. 290-291. SPRINGER VIENNA.

PEEVER, J. H., A. NECAKOV AND J. DUFFIN, 2001 NUCLEUS RAPHÉ OBSCURUS MODULATES HYPOGLOSSAL OUTPUT OF NEONATAL RAT IN VITRO TRANSVERSE BRAIN STEM SLICES. J APPL PHYSIOL **90:** 269-279.

PELLEYMOUNTER, M. A., M. J. CULLEN, M. B. BAKER, R. HECHT, D. WINTERS *ET AL.*, 1995 EFFECTS OF THE OBESE GENE PRODUCT ON BODY WEIGHT REGULATION IN OB/OB MICE. SCIENCE **269:** 540-543.

PERELLO, M., R. C. STUART AND E. A. NILLNI, 2007 DIFFERENTIAL EFFECTS OF FASTING AND LEPTIN ON PROOPIOMELANOCORTIN PEPTIDES IN THE ARCUATE NUCLEUS AND IN THE NUCLEUS OF THE SOLITARY TRACT. AM J PHYSIOL ENDOCRINOL METAB **292:** E1348-1357.

PERRIN, M. H., AND W. W. VALE, 1999 CORTICOTROPIN RELEASING FACTOR RECEPTORS AND THEIR LIGAND FAMILY. ANNALS OF THE NEW YORK ACADEMY OF SCIENCES **885:** 312-328.

PETERS, J., AND C. BEECHEY, 2004 IDENTIFICATION AND CHARACTERISATION OF IMPRINTED GENES IN THE MOUSE. BRIEF FUNCT GENOMIC PROTEOMIC **2:** 320-333.

PEYRON, C., D. K. TIGHE, A. N. VAN DEN POL, L. DE LECEA, H. C. HELLER *ET AL.*, 1998 NEURONS CONTAINING HYPOCRETIN (OREXIN) PROJECT TO MULTIPLE NEURONAL SYSTEMS. JOURNAL OF NEUROSCIENCE **18:** 9996-10015.

PHELPS, C. J., 2004 POSTNATAL REGRESSION OF HYPOTHALAMIC DOPAMINERGIC NEURONS IN PROLACTIN-DEFICIENT SNELL DWARF MICE. ENDOCRINOLOGY **145:** 5656-5664.

PLAGGE, A., E. GORDON, W. DEAN, R. BOIANI, S. CINTI *ET AL.*, 2004 THE IMPRINTED SIGNALING PROTEIN XL ALPHA S IS REQUIRED FOR POSTNATAL ADAPTATION TO FEEDING. NAT GENET **36:** 818-826.

PLAGGE, A., G. KELSEY AND E. L. GERMAIN-LEE, 2008 PHYSIOLOGICAL FUNCTIONS OF THE IMPRINTED GNAS LOCUS AND ITS PROTEIN VARIANTS GALPHA(S) AND XLALPHA(S) IN HUMAN AND MOUSE. J ENDOCRINOL **196:** 193-214.

POLAK, P., AND M. N. HALL, 2009 MTOR AND THE CONTROL OF WHOLE BODY METABOLISM. CURR OPIN CELL BIOL **21:** 209-218.

RASBAND, W. S., 1997-2011 IMAGEJ, PP. U. S. NATIONAL INSTITUTES OF HEALTH.

REIK, W., 2007 STABILITY AND FLEXIBILITY OF EPIGENETIC GENE REGULATION IN MAMMALIAN DEVELOPMENT. NATURE **447:** 425-432.

REIK, W., AND J. WALTER, 2001 GENOMIC IMPRINTING: PARENTAL INFLUENCE ON THE GENOME. NAT REV GENET **2:** 21-32.

REN, D., M. LI, C. DUAN AND L. RUI, 2005 IDENTIFICATION OF SH2-B AS A KEY REGULATOR OF LEPTIN SENSITIVITY, ENERGY BALANCE, AND BODY WEIGHT IN MICE. CELL METAB **2:** 95-104.

REN, D., Y. ZHOU, D. MORRIS, M. LI, Z. LI *ET AL.*, 2007 NEURONAL SH2B1 IS ESSENTIAL FOR CONTROLLING ENERGY AND GLUCOSE HOMEOSTASIS. J CLIN INVEST **117:** 397-406.

RICHARD, D., Q. HUANG AND E. TIMOFEEVA, 2000 THE CORTICOTROPIN-RELEASING HORMONE SYSTEM IN THE REGULATION OF ENERGY BALANCE IN OBESITY. INT J OBES RELAT METAB DISORD **24 SUPPL 2:** S36-39.

RIZVI, T. A., M. ENNIS AND M. T. SHIPLEY, 1992 RECIPROCAL CONNECTIONS BETWEEN THE MEDIAL PREOPTIC AREA AND THE MIDBRAIN PERIAQUEDUCTAL GRAY IN RAT: A WGA-HRP AND PHA-L STUDY. J COMP NEUROL **315:** 1-15.

ROBERTSON, K. D., 2005 DNA METHYLATION AND HUMAN DISEASE. NATURE REVIEWS GENETICS **6:** 597-610.

RODRIGUEZ, C. I., F. BUCHHOLZ, J. GALLOWAY, R. SEQUERRA, J. KASPER *ET AL.*, 2000 HIGH-EFFICIENCY DELETER MICE SHOW THAT FLPE IS AN ALTERNATIVE TO CRE-LOXP. NAT GENET **25:** 139-140.

ROSSANT, J., 1993 IMMORTAL GERM CELLS? CURR BIOL **3:** 47-49.

RUI, L., L. S. MATHEWS, K. HOTTA, T. A. GUSTAFSON AND C. CARTER-SU, 1997 IDENTIFICATION OF SH2-BBETA AS A SUBSTRATE OF THE TYROSINE KINASE JAK2 INVOLVED IN GROWTH HORMONE SIGNALING. MOL CELL BIOL **17:** 6633-6644.

SAITO, Y., M. CHENG, F. M. LESLIE AND O. CIVELLI, 2001 EXPRESSION OF THE MELANIN-CONCENTRATING HORMONE (MCH) RECEPTOR MRNA IN THE RAT BRAIN. J COMP NEUROL **435:** 26-40.

SAKAMOTO, A., L. S. WEINSTEIN, A. PLAGGE, M. ECKHAUS AND G. KELSEY, 2009 GNAS HAPLOINSUFFICIENCY LEADS TO SUBCUTANEOUS TUMOR FORMATION WITH COLLAGEN AND ELASTIN DEPOSITION AND CALCIFICATION. ENDOCR RES **34:** 1-9.

SAKURAI, T., 2007 THE NEURAL CIRCUIT OF OREXIN (HYPOCRETIN): MAINTAINING SLEEP AND WAKEFULNESS. NAT REV NEUROSCI **8:** 171-181.

SAKURAI, T., A. AMEMIYA, M. ISHII, I. MATSUZAKI, R. M. CHEMELLI *ET AL.*, 1998 OREXINS AND OREXIN RECEPTORS: A FAMILY OF HYPOTHALAMIC NEUROPEPTIDES AND G PROTEIN-COUPLED RECEPTORS THAT REGULATE FEEDING BEHAVIOR.[SEE COMMENT]. CELL **92:** 573-585.

SCHWARTZ, G. J., 2002 NEURAL-IMMUNE GUT-BRAIN COMMUNICATION IN THE ANOREXIA OF DISEASE. NUTRITION **18:** 528-533.

SCHWENK, F., U. BARON AND K. RAJEWSKY, 1995 A CRE-TRANSGENIC MOUSE STRAIN FOR THE UBIQUITOUS DELETION OF LOXP-FLANKED GENE SEGMENTS INCLUDING DELETION IN GERM CELLS. NUCLEIC ACIDS RES **23:** 5080-5081.

SEGAL-LIEBERMAN, G., R. L. BRADLEY, E. KOKKOTOU, M. CARLSON, D. J. TROMBLY *ET AL.*, 2003 MELANIN-CONCENTRATING HORMONE IS A CRITICAL MEDIATOR OF THE LEPTIN-DEFICIENT PHENOTYPE. PROCEEDINGS OF THE NATIONAL ACADEMY OF SCIENCES OF THE UNITED STATES OF AMERICA **100:** 10085-10090.

SHIMA, H., M. PENDE, Y. CHEN, S. FUMAGALLI, G. THOMAS *ET AL.*, 1998 DISRUPTION OF THE P70(S6K)/P85(S6K) GENE REVEALS A SMALL MOUSE PHENOTYPE AND A

NEW FUNCTIONAL S6 KINASE. EMBO J **17:** 6649-6659.

SHIMADA, M., N. A. TRITOS, B. B. LOWELL, J. S. FLIER AND E. MARATOS-FLIER, 1998 MICE LACKING MELANIN-CONCENTRATING HORMONE ARE HYPOPHAGIC AND LEAN. NATURE **396:** 670-674.

SHUTE, C. C., AND P. R. LEWIS, 1967 THE ASCENDING CHOLINERGIC RETICULAR SYSTEM: NEOCORTICAL, OLFACTORY AND SUBCORTICAL PROJECTIONS. BRAIN **90:** 497-520.

SIMMONS, D. M., AND L. W. SWANSON, 2009 COMPARISON OF THE SPATIAL DISTRIBUTION OF SEVEN TYPES OF NEUROENDOCRINE NEURONS IN THE RAT PARAVENTRICULAR NUCLEUS: TOWARD A GLOBAL 3D MODEL. THE JOURNAL OF COMPARATIVE NEUROLOGY**:** 423-441.

SKINNER, J. A., B. M. CATTANACH AND J. PETERS, 2002 THE IMPRINTED OEDEMATOUS-SMALL MUTATION ON MOUSE CHROMOSOME 2 IDENTIFIES NEW ROLES FOR GNAS AND GNASXL IN DEVELOPMENT. GENOMICS **80:** 373-375.

SMALLWOOD, S. A., AND G. KELSEY, 2011 DE NOVO DNA METHYLATION: A GERM CELL PERSPECTIVE. TRENDS GENET.

SMITH, F. M., L. J. HOLT, A. S. GARFIELD, M. CHARALAMBOUS, F. KOUMANOV *ET AL.*, 2007 MICE WITH A DISRUPTION OF THE IMPRINTED GRB10 GENE EXHIBIT ALTERED BODY COMPOSITION, GLUCOSE HOMEOSTASIS, AND INSULIN SIGNALING DURING POSTNATAL LIFE. MOLECULAR AND CELLULAR BIOLOGY **27:** 5871-5886.

STANDAERT, D. G., S. J. WATSON, R. A. HOUGHTEN AND C. B. SAPER, 1986 OPIOID PEPTIDE IMMUNOREACTIVITY IN SPINAL AND TRIGEMINAL DORSAL HORN NEURONS PROJECTING TO THE PARABRACHIAL NUCLEUS IN THE RAT. J NEUROSCI **6:** 1220-1226.

STANLEY, S., K. WYNNE, B. MCGOWAN AND S. BLOOM, 2005 HORMONAL REGULATION OF FOOD INTAKE. PHYSIOLOGICAL REVIEWS **85:** 1131-1158.

STELLAR, E., R. HYMAN AND S. SAMET, 1954 GASTRIC FACTORS CONTROLLING WATER-AND-SALT-SOLUTION-DRINKING. J COMP PHYSIOL PSYCHOL **47:** 220-226.

STEPHENS, T. W., M. BASINSKI, P. K. BRISTOW, J. M. BUE-VALLESKEY, S. G. BURGETT *ET AL.*, 1995 THE ROLE OF NEUROPEPTIDE Y IN THE ANTIOBESITY ACTION OF THE OBESE GENE PRODUCT. NATURE **377:** 530-532.

STRUTZ, J., T. HAMMERICH AND R. AMEDEE, 1988 THE MOTOR INNERVATION OF THE SOFT PALATE. AN ANATOMICAL STUDY IN GUINEA PIGS AND MONKEYS. ARCH OTORHINOLARYNGOL **245:** 180-184.

SU, C. K., C. T. YEN, C. Y. CHAI AND J. S. KUO, 1991 NEURONS IN THE MEDULLARY GIGANTOCELLULAR RETICULAR NUCLEUS MEDIATE CARDIOINHIBITION IN CATS. CHIN J PHYSIOL **34:** 399-412.

SUNTER, D., I. MORGAN, C. M. EDWARDS, C. L. DAKIN, K. G. MURPHY *ET AL.*, 2001 OREXINS: EFFECTS ON BEHAVIOR AND LOCALISATION OF OREXIN RECEPTOR 2 MESSENGER RIBONUCLEIC ACID IN THE RAT BRAINSTEM. BRAIN RES **907:** 27-34.

SWANSON, L. W., P. E. SAWCHENKO, J. RIVIER AND W. W. VALE, 1983 ORGANIZATION OF OVINE CORTICOTROPIN-RELEASING FACTOR IMMUNOREACTIVE CELLS AND FIBERS IN THE RAT BRAIN: AN IMMUNOHISTOCHEMICAL STUDY. NEUROENDOCRINOLOGY **36:** 165-186.

TAPPAZ, M. L., M. WASSEF, W. H. OERTEL, L. PAUT AND J. F. PUJOL, 1983 LIGHT- AND ELECTRON-MICROSCOPIC IMMUNOCYTOCHEMISTRY OF GLUTAMIC ACID DECARBOXYLASE (GAD) IN THE BASAL HYPOTHALAMUS: MORPHOLOGICAL EVIDENCE FOR NEUROENDOCRINE GAMMA-AMINOBUTYRATE (GABA).

NEUROSCIENCE **9:** 271-287.

TARTAGLIA, L. A., M. DEMBSKI, X. WENG, N. DENG, J. CULPEPPER *ET AL.*, 1995 IDENTIFICATION AND EXPRESSION CLONING OF A LEPTIN RECEPTOR, OB-R. CELL **83:** 1263-1271.

TAYLOR, E. W., D. JORDAN AND J. H. COOTE, 1999 CENTRAL CONTROL OF THE CARDIOVASCULAR AND RESPIRATORY SYSTEMS AND THEIR INTERACTIONS IN VERTEBRATES. PHYSIOLOGICAL REVIEWS **79:** 855-916.

TOMIZAWA, S., H. KOBAYASHI, T. WATANABE, S. ANDREWS, K. HATA *ET AL.*, 2011 DYNAMIC STAGE-SPECIFIC CHANGES IN IMPRINTED DIFFERENTIALLY METHYLATED REGIONS DURING EARLY MAMMALIAN DEVELOPMENT AND PREVALENCE OF NON-CPG METHYLATION IN OOCYTES. DEVELOPMENT **138:** 811-820.

TORTORA, G. J., AND S. R. GRABOWSKI, 2003 THE ENDOCRINE SYSTEM, PP. 587-632 IN *PRINCIPLES OF ANATOMY AND PHYSIOLOGY*, EDITED BY B. ROESCH. JOHN WILEY AND SONS, UNITED STATES.

TRAVERS, J. B., 2004 CHAPTER 12 - OROMOTOR NUCLEI, PP. 295-319 IN *THE RAT NERVOUS SYSTEM (THIRD EDITION)*, EDITED BY G. PAXINOS. ACADEMIC PRESS, BURLINGTON.

TRONCHE, F., C. KELLENDONK, O. KRETZ, P. GASS, K. ANLAG *ET AL.*, 1999 DISRUPTION OF THE GLUCOCORTICOID RECEPTOR GENE IN THE NERVOUS SYSTEM RESULTS IN REDUCED ANXIETY. NAT GENET **23:** 99-103.

UGUR, O., AND T. L. Z. JONES, 2000 A PROLINE-RICH REGION AND NEARBY CYSTEINE RESIDUES TARGET XLALPHA S TO THE GOLGI COMPLEX REGION. MOL. BIOL. CELL **11:** 1421-1432.

UM, S. H., F. FRIGERIO, M. WATANABE, F. PICARD, M. JOAQUIN *ET AL.*, 2004 ABSENCE OF S6K1 PROTECTS AGAINST AGE- AND DIET-INDUCED OBESITY WHILE ENHANCING INSULIN SENSITIVITY. NATURE **431:** 200-205.

VAN BOCKSTAELE, E. J., E. E. COLAGO, P. CHENG, A. MORIWAKI, G. R. UHL *ET AL.*, 1996 ULTRASTRUCTURAL EVIDENCE FOR PROMINENT DISTRIBUTION OF THE MU-OPIOID RECEPTOR AT EXTRASYNAPTIC SITES ON NORADRENERGIC DENDRITES IN THE RAT NUCLEUS LOCUS COERULEUS. J NEUROSCI **16:** 5037-5048.

VAN DEN POL, A. N., C. ACUNA-GOYCOLEA, K. R. CLARK AND P. K. GHOSH, 2004 PHYSIOLOGICAL PROPERTIES OF HYPOTHALAMIC MCH NEURONS IDENTIFIED WITH SELECTIVE EXPRESSION OF REPORTER GENE AFTER RECOMBINANT VIRUS INFECTION. NEURON **42:** 635-652.

VAN DEN POL, A. N., X. B. GAO, K. OBRIETAN, T. S. KILDUFF AND A. B. BELOUSOV, 1998 PRESYNAPTIC AND POSTSYNAPTIC ACTIONS AND MODULATION OF NEUROENDOCRINE NEURONS BY A NEW HYPOTHALAMIC PEPTIDE, HYPOCRETIN/OREXIN. JOURNAL OF NEUROSCIENCE **18:** 7962-7971.

VAN DEN POL, A. N., P. R. PATRYLO, P. K. GHOSH AND X. B. GAO, 2001 LATERAL HYPOTHALAMUS: EARLY DEVELOPMENTAL EXPRESSION AND RESPONSE TO HYPOCRETIN (OREXIN). THE JOURNAL OF COMPARATIVE NEUROLOGY **433:** 349-363.

VONG, L., C. YE, Z. YANG, B. CHOI, S. CHUA *ET AL.*, 2011 LEPTIN ACTION ON GABAERGIC NEURONS PREVENTS OBESITY AND REDUCES INHIBITORY TONE TO POMC NEURONS. NEURON **71:** 142-154.

VORNOV, J. J., AND J. SUTIN, 1983 BRAINSTEM PROJECTIONS TO THE NORMAL AND NORADRENERGICALLY HYPERINNERVATED TRIGEMINAL MOTOR NUCLEUS. J COMP NEUROL **214:** 198-208.

VRANG, N., J. D. MIKKELSEN AND P. J. LARSEN, 1997 DIRECT LINK FROM THE

SUPRACHIASMATIC NUCLEUS TO HYPOTHALAMIC NEURONS PROJECTING TO THE SPINAL CORD: A COMBINED TRACING STUDY USING CHOLERA TOXIN SUBUNIT B AND PHASEOLUS VULGARIS-LEUCOAGGLUTININ. BRAIN RES BULL **44:** 671-680.

VRANG, N., C. B. PHIFER, M. M. CORKERN AND H. R. BERTHOUD, 2003 GASTRIC DISTENSION INDUCES C-FOS IN MEDULLARY GLP-1/2-CONTAINING NEURONS. AM J PHYSIOL REGUL INTEGR COMP PHYSIOL **285:** R470-478.

WALL, V. D., J. J. ALBERTS, D. J. MOORE, S. Y. NEWELL, M. PATTANAYEK *ET AL.*, 2001 THE EFFECT OF MERCURY AND PCBS ON ORGANISMS FROM LOWER TROPHIC LEVELS OF A GEORGIA SALT MARSH. ARCH ENVIRON CONTAM TOXICOL **40:** 10-17.

WALLACE, D. M., D. J. MAGNUSON AND T. S. GRAY, 1989 THE AMYGDALO-BRAINSTEM PATHWAY: SELECTIVE INNERVATION OF DOPAMINERGIC, NORADRENERGIC AND ADRENERGIC CELLS IN THE RAT. NEUROSCI LETT **97:** 252-258.

WALTER, J., AND M. PAULSEN, 2003 IMPRINTING AND DISEASE. SEMIN CELL DEV BIOL **14:** 101-110.

WANG, H. L., AND M. MORALES, 2009 PEDUNCULOPONTINE AND LATERODORSAL TEGMENTAL NUCLEI CONTAIN DISTINCT POPULATIONS OF CHOLINERGIC, GLUTAMATERGIC AND GABAERGIC NEURONS IN THE RAT. EUR J NEUROSCI **29:** 340-358.

WATANABE, M., K. MAEMURA, K. KANBARA, T. TAMAYAMA AND H. HAYASAKI, 2002 GABA AND GABA RECEPTORS IN THE CENTRAL NERVOUS SYSTEM AND OTHER ORGANS. INT REV CYTOL **213:** 1-47.

WEINSTEIN, L. S., S. YU, D. R. WARNER AND J. LIU, 2001 ENDOCRINE MANIFESTATIONS OF STIMULATORY G PROTEIN ALPHA-SUBUNIT MUTATIONS AND THE ROLE OF GENOMIC IMPRINTING. ENDOCR REV **22:** 675-705.

WILKINS, J. F., AND D. HAIG, 2003 WHAT GOOD IS GENOMIC IMPRINTING: THE FUNCTION OF PARENT-SPECIFIC GENE EXPRESSION. NATURE REVIEWS GENETICS **4:** 359-368.

WILKINSON, L. S., W. DAVIES AND A. R. ISLES, 2007 GENOMIC IMPRINTING EFFECTS ON BRAIN DEVELOPMENT AND FUNCTION. NAT REV NEUROSCI **8:** 832-843.

WILLIAMS, G., C. BING, X. J. CAI, J. A. HARROLD, P. J. KING *ET AL.*, 2001 THE HYPOTHALAMUS AND THE CONTROL OF ENERGY HOMEOSTASIS: DIFFERENT CIRCUITS, DIFFERENT PURPOSES. PHYSIOL BEHAV **74:** 683-701.

WILLIAMSON, C., C. V. BEECHEY, B. M. CATTANACH AND J. PETERS, 2011 MOUSEBOOK, PP.

WILLIAMSON, C. M., S. T. BALL, W. T. NOTTINGHAM, J. A. SKINNER, A. PLAGGE *ET AL.*, 2004 A CIS-ACTING CONTROL REGION IS REQUIRED EXCLUSIVELY FOR THE TISSUE-SPECIFIC IMPRINTING OF GNAS. NAT GENET **36:** 894-899.

WILLIAMSON, C. M., M. D. TURNER, S. T. BALL, W. T. NOTTINGHAM, P. GLENISTER *ET AL.*, 2006 IDENTIFICATION OF AN IMPRINTING CONTROL REGION AFFECTING THE EXPRESSION OF ALL TRANSCRIPTS IN THE GNAS CLUSTER. NAT GENET **38:** 350-355.

WILLIE, J. T., R. M. CHEMELLI, C. M. SINTON AND M. YANAGISAWA, 2001 TO EAT OR TO SLEEP? OREXIN IN THE REGULATION OF FEEDING AND WAKEFULNESS. ANNU REV NEUROSCI **24:** 429-458.

WILLING, A. E., AND H. R. BERTHOUD, 1997 GASTRIC DISTENSION-INDUCED C-FOS EXPRESSION IN CATECHOLAMINERGIC NEURONS OF RAT DORSAL VAGAL COMPLEX. AM J PHYSIOL **272:** R59-67.

WOLF, J., J. CHEVERUD, C. ROSEMAN AND R. HAGER, 2008 GENOME-WIDE ANALYSIS

REVEALS A COMPLEX PATTERN OF GENOMIC IMPRINTING IN MICE. PLOS GENET **4:** E1000091.

XIE, T., A. PLAGGE, O. GAVRILOVA, S. PACK, W. JOU *ET AL.*, 2006 THE ALTERNATIVE STIMULATORY G PROTEIN ALPHA-SUBUNIT XLALPHAS IS A CRITICAL REGULATOR OF ENERGY AND GLUCOSE METABOLISM AND SYMPATHETIC NERVE ACTIVITY IN ADULT MICE. J BIOL CHEM **281:** 18989-18999.

XU, A. W., C. B. KAELIN, K. TAKEDA, S. AKIRA, M. W. SCHWARTZ *ET AL.*, 2005 PI3K INTEGRATES THE ACTION OF INSULIN AND LEPTIN ON HYPOTHALAMIC NEURONS. J CLIN INVEST **115:** 951-958.

YAMADA, H., T. OKUMURA, W. MOTOMURA, Y. KOBAYASHI AND Y. KOHGO, 2000 INHIBITION OF FOOD INTAKE BY CENTRAL INJECTION OF ANTI-OREXIN ANTIBODY IN FASTED RATS. BIOCHEM BIOPHYS RES COMMUN **267:** 527-531.

YAMANAKA, A., Y. MURAKI, N. TSUJINO, K. GOTO AND T. SAKURAI, 2003 REGULATION OF OREXIN NEURONS BY THE MONOAMINERGIC AND CHOLINERGIC SYSTEMS. BIOCHEMICAL & BIOPHYSICAL RESEARCH COMMUNICATIONS **303:** 120-129.

YAMANAKA, A., T. SAKURAI, T. KATSUMOTO, M. YANAGISAWA AND K. GOTO, 1999 CHRONIC INTRACEREBROVENTRICULAR ADMINISTRATION OF OREXIN-A TO RATS INCREASES FOOD INTAKE IN DAYTIME, BUT HAS NO EFFECT ON BODY WEIGHT. BRAIN RESEARCH **849:** 248-252.

YODER, J. A., C. P. WALSH AND T. H. BESTOR, 1997 CYTOSINE METHYLATION AND THE ECOLOGY OF INTRAGENOMIC PARASITES. TRENDS GENET **13:** 335-340.

YOSHIDA, K., X. LI, G. CANO, M. LAZARUS AND C. B. SAPER, 2009 PARALLEL PREOPTIC PATHWAYS FOR THERMOREGULATION. J NEUROSCI **29:** 11954-11964.

YU, S., D. YU, E. LEE, M. ECKHAUS, R. LEE *ET AL.*, 1998 VARIABLE AND TISSUE-SPECIFIC HORMONE RESISTANCE IN HETEROTRIMERIC GS PROTEIN ALPHA-SUBUNIT (GSALPHA) KNOCKOUT MICE IS DUE TO TISSUE-SPECIFIC IMPRINTING OF THE GSALPHA GENE. PROC NATL ACAD SCI U S A **95:** 8715-8720.

ZAMUDIO, N., AND D. BOURC'HIS, 2010 TRANSPOSABLE ELEMENTS IN THE MAMMALIAN GERMLINE: A COMFORTABLE NICHE OR A DEADLY TRAP? HEREDITY **105:** 92-104.

ZARDETTO-SMITH, A. M., AND T. S. GRAY, 1990 ORGANIZATION OF PEPTIDERGIC AND CATECHOLAMINERGIC EFFERENTS FROM THE NUCLEUS OF THE SOLITARY TRACT TO THE RAT AMYGDALA. BRAIN RES BULL **25:** 875-887.

ZARDETTO-SMITH, A. M., AND T. S. GRAY, 1995 CATECHOLAMINE AND NPY EFFERENTS FROM THE VENTROLATERAL MEDULLA TO THE AMYGDALA IN THE RAT. BRAIN RES BULL **38:** 253-260.

ZHANG, Y., I. A. KERMAN, A. LAQUE, P. NGUYEN, M. FAOUZI *ET AL.*, 2011 LEPTIN-RECEPTOR-EXPRESSING NEURONS IN THE DORSOMEDIAL HYPOTHALAMUS AND MEDIAN PREOPTIC AREA REGULATE SYMPATHETIC BROWN ADIPOSE TISSUE CIRCUITS. J NEUROSCI **31:** 1873-1884.

ZHANG, Y., R. PROENCA, M. MAFFEI, M. BARONE, L. LEOPOLD *ET AL.*, 1994 POSITIONAL CLONING OF THE MOUSE OBESE GENE AND ITS HUMAN HOMOLOGUE. NATURE **372:** 425-432.

ZIGMAN, J. M., J. E. JONES, C. E. LEE, C. B. SAPER AND J. K. ELMQUIST, 2006 EXPRESSION OF GHRELIN RECEPTOR MRNA IN THE RAT AND THE MOUSE BRAIN. J COMP NEUROL **494:** 528-548.